ΠΑΝΕΠΙΣΤΗΜΙΟ ΙΩΑΝΝΙΝΩΝ
ΣΧΟΛΗ ΘΕΤΙΚΩΝ ΕΠΙΣΤΗΜΩΝ
ΤΜΗΜΑ ΧΗΜΕΙΑΣ

Σύνθεση β-D-γλυκοπυρανοζυλο-θειο-ημικαρβαζονών και συμπλόκων τους με μέταλλα μεταπτώσεως. Εφαρμογές ως αναστολείς της φωσφορυλάσης του γλυκογόνου και ως καταλύτες σε αντιδράσεις σύζευξης

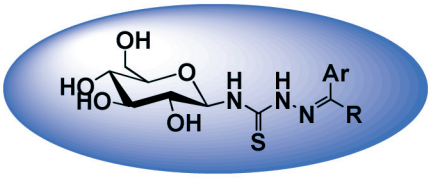

Alia - Cristina Tenchiu

ΔΙΔΑΚΤΟΡΙΚΗ ΔΙΑΤΡΙΒΗ

ΙΩΑΝΝΙΝΑ 2012

Ημερομηνία **αίτησης** της κ. TENCHIU ALIA-CRISTINA 12-06-2007

Ημερομηνία **ορισμού Τριμελούς Συμβουλευτικής Επιτροπής** Γ.Σ.Ε.Σ.: 672Α/15-06-07.

Μέλη Τριμελούς Συμβουλευτικής Επιτροπής:

Επιβλέπων:

Δήμητρα Κόβαλα-Δεμερτζή (Καθηγήτρια)

Μέλη:

Μαυρουδής Δεμερτζής (Επίκουρος Καθηγητής Πανεπιστημίου Ιωαννίνων)

Ιωάννης Κώστας (Δ/ντης Ερευνών ΙΟΦΧ/ΕΙΕ)

Ημερομηνία **ορισμού θέματος:** 15-06-07

Θέμα: «Σύνθεση β-D-γλυκοπυρανοζυλο-θειο-ημικαρβαζονών και συμπλόκων τους με μέταλλα μεταπτώσεως. Εφαρμογές ως αναστολείς της φωσφορυλάσης του γλυκογόνου και ως καταλύτες σε αντιδράσεις σύζευξης »

ΔΙΟΡΙΣΜΟΣ ΕΠΤΑΜΕΛΟΥΣ ΕΞΕΤΑΣΤΙΚΗΣ ΕΠΙΤΡΟΠΗΣ Γ.Σ.Ε.Σ.: 839^{A}/9-3-12

1. Δήμητρα Κόβαλα Δεμερτζή - (ως επιβλέπουσα) Καθηγήτρια Τμήματος Χημείας Πανεπιστημίου Ιωαννίνων (αυτοδίκαια αποχωπήσασα)

2. Μαυρουδής Δεμερτζής - Επίκ. Καθηγητής Τμήματος Χημείας Πανεπιστημίου Ιωαννίνων (αυτοδίκαια αποχωπήσασα)

3. Ιωάννης Κώστας - ΔιευΘυντής Ερευνών Εθνικού Ιδρύματος Ερευνών (επιβλέπων έρευνας)

4. Ιωάννης Πλακατούρας - Καθηγητής Τμήματος Χημείας Πανεπιστημίου Ιωαννίνων

5. Μαρία Λουλούδη - Καθηγήτρια Τμήματος Χημείας Πανεπιστημίου Ιωαννίνων

6. Νικόλαος Κουρκουμέλης Λέκτορας Ιατρικής Σχολής Πανεπιστημίου Ιωαννίνων

7. Δημήτριος Λεωνίδας - Αν. Καθηγητής Τμήματος Βιοχημείας και Βιοτεχνολογίας Πανεπιστημίου Θεσσαλίας

Έγκριση Διδακτορικής Διατριβής με βαθμό «Άριστα» στις 10-05-2012

ΠΑΝΕΠΙΣΤΗΜΙΟ ΙΩΑΝΝΙΝΩΝ
ΤΜΗΜΑ ΧΗΜΕΙΑΣ
ΤΟΜΕΑΣ ΑΝΟΡΓΑΝΗΣ ΚΑΙ ΑΝΑΛΥΤΙΚΗΣ ΧΗΜΕΙΑΣ
451 10 ΙΩΑΝΝΙΝΑ Τηλ.: ++30-26510- Fax: ++30-26510-08786

Ιωάννινα, 9-5-2012

Π ρ ο ς
το Τμήμα Χημείας
του Παν/μίου Ιωαννίνων

Θέμα: «Απόφαση επταμελούς εξεταστικής επιτροπής ενώπιον της οποίας η **Alia-Cristina Tenchiu** υποστήριξε τη διδακτορική της διατριβή»

Σήμερα 10/05/2012 και ώρα 15:00 μ.μ. έγινε δημόσια παρουσίαση της διδακτορικής διατριβής με θέμα: «**Σύνθεση β-d-Γλυκοπυρανοζυλο-Θειο-Ημικαρβαζονών και Συμπλόκων τους με Μέταλλα Μεταπτώσεως. Εφαρμογές ως Αναστολείς της Φωσφορυλάσης του Γλυκογόνου και ως Καταλύτες σε Αντιδράσεις Σύζευξης**», από την υποψήφια διδάκτορα Alia-Cristina Tenchiu. Η παρουσίαση έλαβε χώρα στην αίθουσα Φ2-145 του Τμήματος Χημείας, Πανεπιστημίου Ιωαννίνων, ενώπιον της κατά τον νόμο επταμελούς εξεταστικής επιτροπής.

Η Alia-Cristina Tenchiu ανέπτυξε επί μία ώρα τα κυριότερα αποτελέσματα της διατριβής της και στη συνέχεια απάντησε σε σειρά ερωτημάτων της εξεταστικής επιτροπής και του ακροατηρίου. Κατόπιν αποχώρησε η υποψήφια και το ακροατήριο και ακολούθησε σύσκεψη μεταξύ των μελών της επταμελούς επιτροπής. Η επιτροπή έκρινε ότι η Διατριβή είναι πρωτότυπη και συμβάλλει στην πρόοδο της επιστήμης. Προχώρησε δε στην έγκριση αυτής με βαθμό «**Αριστα**» και αποφάσισε την απονομή του Τίτλου της Διδάκτορος στην Alia-Cristina Tenchiu από το Τμήμα Χημείας του Πανεπιστημίου Ιωαννίνων.

Τα μέλη της εξεταστικής επιτροπής

Δ. Κόβαλα-Δεμερτζή, Καθηγήτρια (Επιβλέπουσα Καθηγήτρια)
Μαυρουδής Δεμερτζής, Μέλος της Τριμελούς Επιτροπής
Γιάννης Κώστας, Μέλος της Τριμελούς Επιτροπής
Ιωάννης Πλακατούρας, Καθηγητής
Μαρία Λουλούδη, Καθηγήτρια
Νικόλαος Κουρκουμέλης, Λέκτορας
Δημήτριος Λεωνίδας, Αναπληρωτής Καθηγητής

«I hope that the results of my lifelong efforts remain stable, of course not for centuries, but for a long time and after my approaaching death. Only two areas of lifelong efforts do I consider stable myself: my childrens and my scientific works.»
D. I. Mendeleev

«You cannot hope to build a better world without improving the individuals. To that end, each of us must work for our own improvement and, at the same time, share a general responsibility for all humanity, our particular duty being to aid those to whom we think we can be most useful.»
Marie Curie

«This thesis is dedicated to my parents and my sons, especially in memory of my father, whose spirits will inspire me forever»

«Αυτό το διακτορικό είναι αφιερωμένο στους γονείς μου και τους γιους μου, ειδικά στη μνήμη του πατέρα μου, του οποίου το πνεύμα θα με εμπνέει για πάντα»

CONTENTS

ACKNOWLEDGMENTS

The experimental part of this Thesis has been performed entirely at the Institute of Organic and Pharmaceutical Chemistry of the National Hellenic Research Foundation. I feel grateful to a number of people with whom I had the opportunity to work.

First of all, I would like to thank my esteemed teacher and supervisor **Dr. Ioannis D. Kostas** (member of the advisory and evaluation committee) for the excellent working conditions providing to me, many helpful suggestions and his great interest in pursuing this work during the period 2006-2010, and his suggestions in writing the Thesis.

I would like to thank **Prof. Dr. Dimitra Kovala-Demertzi** (member of the advisory and evaluation committee) from the Chemistry Department of the University of Ioannina for some suggestions in the synthetic part and for help in elucidating the crystal structures, **Assist. Prof. Dr. Mavroudis A. Demertzis** as a member of the Advisory Committee, and also the other members of the evaluation committee **Assoc. Prof. Dr. Demetres D. Leonidas**, **Prof. Dr. Ioannis Plakatouras**, **Prof. Dr. Maria Louloudi**, and **Lecturer Dr. Nikolaos Kourkoumelis** who contributed their suggestions in writing this Thesis. I also thank **Dr. Aris Terzis** from the Institute of Materials Science of the National Center for Scientific Research "Demokritos" who performed the crystallographic study for two of the glucopyranosyl-thiosemicarbazone derivatives, and **Assoc. Prof. Dr. John Markopoulos** from the Chemistry Department of the University of Athens for the magnetic measurements of the nickel complexes.

I thank **Kyra-Melinda Alexacou** and her supervisor **Dr. Demetres D. Leonidas**, **Dr. Evangelia D. Chrysina**, **Dr. Spyros E. Zografos**, and in particular **Dr. Nikos G. Oikonomakos** (passed away in 2008) for the enzyme kinetics and the crystallographic study of fifteen glycogen phosphorylase – glucopyranosyl thiosemicarbazone complexes, the diffraction data of which were collected at EMBL-Hamburg outstation, Daresbury Synchrotron Laboratory, UK and Max-Lab, Lund.

From my laboratory at the National Hellenic Research Foundation, I am grateful to **Dr. Ioannis Liratzis** for his unconditional help, insightful discussions and friendship. Many thanks to: **Dr. Constantinos G. Screttas**, **Dr. Maria-Micha Screttas**, **Dr. Barry R. Steele**, **Dr. Georgios A. Heropoulos**, **Dr. Claudine Patteux**, **Dr. Kalliopi Vallianatou**, **Dr. Carolina Vallalonga-Barber**, and to my best friend **Madalina Bucos**.

Finally, I would like to thank my teacher from the University of Bucharest in Romania, **Prof. Dr. Viorel Cîrcu**, who encouraged me to go further.

The work was supported by the **EU Marie Curie Early Stage Training (EST)** contract no MEST-CT-020575 "A European Research Training Site for the Design and Synthesis of Novel Neuroprotective and Hypoglycemic Agents through a Multi-disciplinary approach" (EURODESY).

ABREVIATIONS

Ac	acetyl
Acurea	*N*-acetyl-*N*'-β-D-glucopyranosyl
Ala	alanine residue
AMP	adenosine monophosphate
Ar	aryl
Arg	arginine residue
Asn	asparagine residue
Asp	aspartic residue
br	broad
Bu	butyl
Bza	benzaldehyde
Bzurea	*N*'-benzoyl-β-D-glucopyranosyl urea
t-Bu	tert butyl
*β*GluTSC	β-D-glucopyranosyl thiosemicarbazone
d	doublet
DIPAMP	Ethane-1,2-diylbis[(2-methoxyphenyl)phenylphosphane
DMF	*N,N*-dimethyl formamide
DMSO	dimethylsulfoxide
ee	enantiomeric excess
Et	ethyl
GC	gas cromatography
Glc	D-Glucose
GLP	glucagon-like peptide
Glu	glutamic residue
GP*b*	Glycogen phosphorylase *b*
His	histidine residue
m	multiplet(NMR)
Me	methyl
MS	mass spectrometry

NAG	*N*-(β-D-glucopyranosyl) 3-(2-naphtyl) propenoic acid amide
NMR	nuclear magnetic resonance
Phe	phenylalanine residue
PC	propylene carbonate
PLP	pyridoxal 5'-phosphate
rt	room temperature
RMGPb	rabbit muscle G
s	singlet
s.a.	specific activity
t	tripet(NMR)
Tf	trifluoromethanesulfonyl
Thr	threonine residue
TLC	thin layer chromatography
TON	turn over number
TOF	turn over frequency
TSc	thiosemicarbazone
TPPTS	3,3',3''-phosphinidynetris (benzenesulfonic acid)trisodium salt
UV	ultraviolet

I. PURPOSE

I. Purpose

Diabetes type 2 is a complex disease characterized by insulin resistance and abnormal insulin secretion, and it is the most common type of diabetes. It is estimated that the number of patients suffering from type 2 diabetes will reach 300 million by the year 2025. Glycogenphosphorylase (GP) catalyzes the first step of the intracellular degradation of glycogen, which is an important source of hepatic glucose production. Thus, inhibition of GP has emerged as potential therapeutic strategy for type 2 diabetes. Glucose derivatives are known to be selective and efficient catalytic inhibitors of human liver glycogen phosphorylase. On the other hand, thiosemicarbazones (TSCs) are a class of biochemically important compounds possessing a wide range of biological activity, and are very promising in the treatment of many diseases. So, it is very tempting the synthesis of new compounds bearing both the glucose and the thiosemicarbazone moieties in order to assess the inhibitory potential of these molecules to GP.

Transitional-metal homogeneous catalysis has become an essential tool for synthetic organic chemists and thus, there is a rapidly growing need for the development of new catalysts. In our laboratory at the National Hellenic Research Foundation in collaboration with the Chemistry Department of the University of Ioannina, the development of new metal complexes with thiosemicarbazones, which can serve as phosphane-free multidentate ligands, and their application in palladium-catalyzed coupling reactions has been an active area of research during the past years. In addition, carbohydrates are readily available and highly functionalised, they have widely been used as ligands in transitional-metal catalyzed reactions, and thus the evolution of glycopyranosyl-thiosemicarbazones in catalysis should be a subject of a great interest.

Taking into consideration the broad range of applications of glucose and also thiosemicarbazone derivatives provided in details in the introduction (chapter II), the aim of the present Thesis is to combine these two classes of molecules into a family bearing both moieties developing a general synthetic protocol for β-D-glucopyranosyl thiosemicarbazones and their evaluation on one hand in glycogen phsphorylase inhibition, and on the other hand as ligands in transitional-metal homogeneous catalysis.

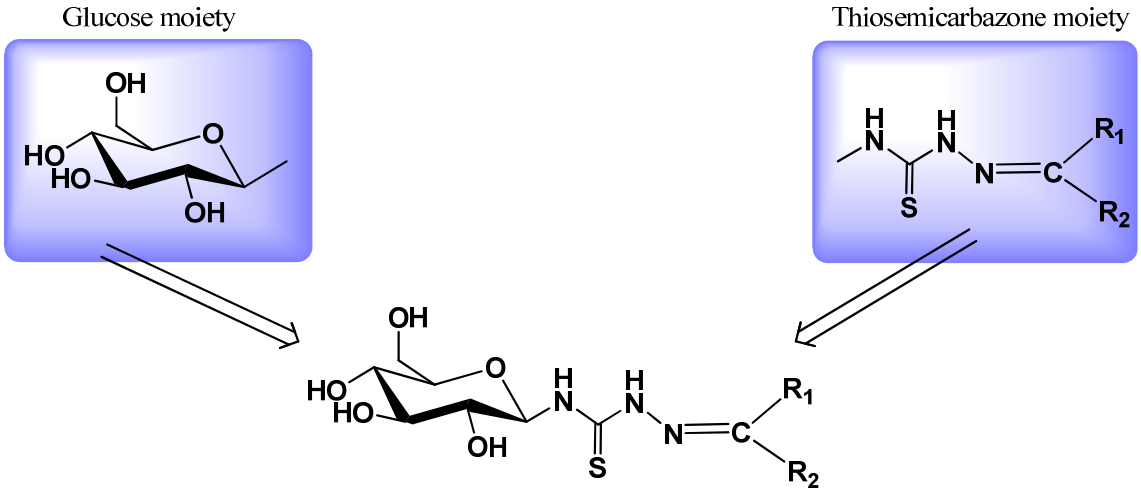

β-D-Glucopyranosyl thiosemicarbazones derivatives

II. INTRODUCTION

II.1. Introduction in carbohydrate chemistry

«Chemistry (from Egyptian kēme *(chem), meaning "*earth*") is the science concerned with the composition, structure, and properties of matter, as well as the changes it undergoes during chemical reactions».*

The study of carbohydrates began in late of nineteenth century. These organic molecules are aldehydes or ketones with several hydroxyl groups added, usually one on each carbon atom that is not part of the aldehyde or ketone functional group.

We know that many vital activities as diverse as healing, blood clotting, infection, preventior of infection, and fertilization all involve carbohydrates.

Carbohydrates are the main energy source for the human body. Chemically, carbohydrates are organic molecules in which carbon, hydrogen, and oxygen are bound together in the ratio: $C_x(H_2O)_y$, where ***x*** and ***y*** are whole numbers that differ depending on the specific carbohydrate to which we are referring. Humans and animals break down carbohydrates into glucose (blood sugar). The body uses this sugar for energy for cells, tissues and organs [1-3].

For example, the chemical metabolism of the sugar glucose is shown below:

$$C_6H_{12}O_6 + 6\ O2 \qquad 6\ CO_2 + 6\ H_2O + \text{energy}$$

These carbohydrates are manufactured by plants during the process of phtosynthesis. Plants harvest energy from sunlight to run the reaction just described in reverse:

$$CO_2 + 6\ H_2O + \text{energy (from sunlight)} \quad C_6H_{12}O_6 + 6\ O_2$$

The starting point is glucose, the most common on Earth - especially in the form of starch and cellulose - organic matter encountered. In addition to their solubility in water, their availability and the existing chirality constitute other important properties. Looking at the D-(+)-glucose, at

first glance seemingly is a simple formula $C_6H_{12}O_6$ but looking closer discovering a complex molecule [4].

There are two types of carbohydrates, the simple sugars and those carbohydrates that are made of long chains of sugars - the complex carbohydrates.

Carbohydrates play a major role in many recognition events. Recognition is the key to a variety of biological processes and the first step in numerous phenomena based on cell–cell interactions, such as fertilization, cell migration, organ formation, immune defense, microbial and viral infection, inflammation, and cancer metastasis [5]. Maillard in 1912 [6] identified the nonenzymatic reactions between amino acids and saccharides which are ubiquitors in nature. Maillard reaction involves the condensation of an amine with the carbonyl group of a reducing sugar, forming N-glycosylamine intermediates [7]. This intermediates then react via Amatory rearrangements, [8] forming a complicated and diverse network of chemistry that has been well characterized and represents important areas in both food science and medical research into aging.

Carbohydrates constitute the most abundant group of natural products. This fact is exemplified by the process of photosynthesis, which alone produce 4×10^{14} kg of carabohydrates each year.

Fischer, between 1884 and 1900, successfully determined the inner structure of the sugar group and thus gave to scientists the key to an understanding of other carbohydrates [9].

A vast literature on sugar derivatives has accumulated over the years and this subject continues to be a very active field in organic chemistry [10-14]. A main reason for this situation is obviously their diversity of reactions and their availability. It should be also noted that, carbohydrates are useful for structure-activity studies and for studies of enzymatic reactivity in connection with naturally occurring, biologically active derivatives.

Many alcohols (**1**), thiols (**2**), and amines (**3**) (Fig. 1) occur in nature as glycosides that are as *O*-, *S*-, or *N*-acetals at the anomeric posititon of glucose. The purpose of attaching these compounds to glucose is often to improve solubility or transports across membranes – to expel a toxin from the cell, for example. Sometimes glucose is attached in order to stabilize the compound so that glucose appears as nature's protecting group.

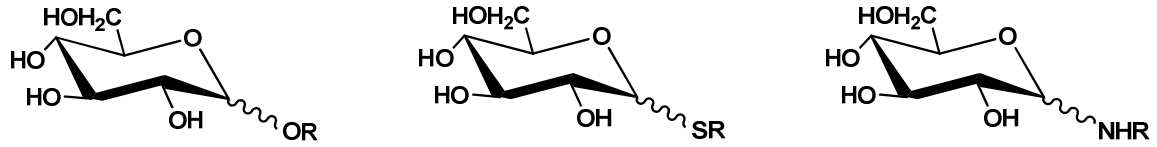

1 **2** **3**

Figure 1 Structure of compounds **1**, **2** and **3**

Spectinomycin, acarbose, sisomicin, kanamycin, neomycin are only few examples of drugs against infection, which contain a carbohydrate moiety residue [15].

The role of carbohydrate moiety includes enhancement of DNA sequence specificity and cell recognition [16]. Membrane permeability, water solubility, and chirality of chromophores or DNA damaging molecules are other properties of carbohydrates. Introduction of carbohydrate moieties into synthetic drugs should generate hybrid molecules of considerable interest.

Carbohydrates are a class of compounds possessing a wide spectrum of medical properties, are an important element in many natural antibiotics as chromophore, bleomycin [17, 18], and have been studied against cancer [19].

Yano et al. have investigate the in vivo activity of several palladium(II) complexes containing a sugar residue against P388 leukemia cells [20]. Most of Pd(II) complexes did not show any significant activity with the exception of compound **4** (Fig. 2). The low activity of the palladium(II) complexes [21] which were tested explained by their decomposition before entering the cell and reaching the cellular target due to their extremely high lability in biological fluids [16, 22].

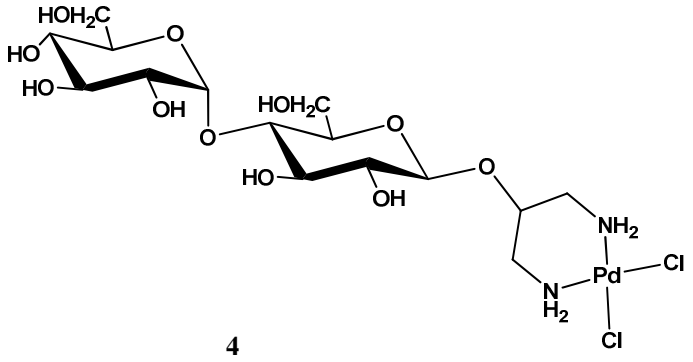

4

Figure 2 Stucture of Pd(II) complex containing a sugar unit

Glycosylamines can be used to form covalent bonds between the protein and the carbohydrate parts of *N*-glycoproteins [21, 23] and have been widely used in synthesis of *N*-nucleosides, glycosyl isothiocyanates, and glycosyl urea.

Glycosylamines (**5** and **6**; Fig. 3) are compounds of interest for the enzymology of carbohydrates, since they are considered as active-site-directed, reversible inhibitors of glycosidases [20, 24].

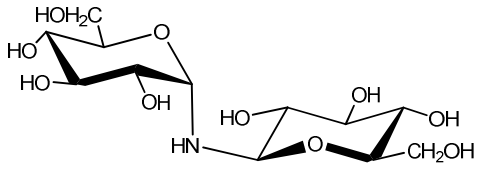

5

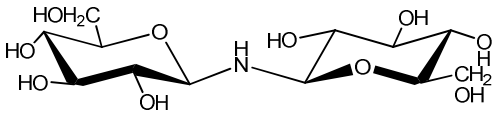

6

Figure 3 Glycosylamines

They usually bind more tightly with enzyme than their oxygen counterparts, provided that the basic character of their nitrogen atom is not diminished [25]. They have been used to study the specificity of β-D-glucosidase [26], and several pseudo glycosylamines, such as acarbose, are known as potent inhibitors of intestinal α-D-glycosidase.

However, the main drawback of glycosylamines is their propensity to rearrange in solution via immonium-ion intermediates, which lead to mutarotation and possible hydrolysis [27].

An alternative strategy for a convenient access for *N*-acylglycosylamines together with the micellar properties of these amphiphilic derivatives was reported by Lubineau et al. [28]. The treated sugar (glucose, galactose, cellobiose or manose) at 42°C for 36 h with a commercial aqueous solution of ammonia in the presence of one equivalent of ammonium hydrogen carbonate yielded quantitatively the corresponding glycosylamines (Scheme 1). Only in a few minutes, *N*-acylglycosylamines **8** could be obtained after lypophilization of the residue (i.e., the pure glycosylamines), which was dissolved in a mixture of ethanol and water and treated with acyl chlorides.

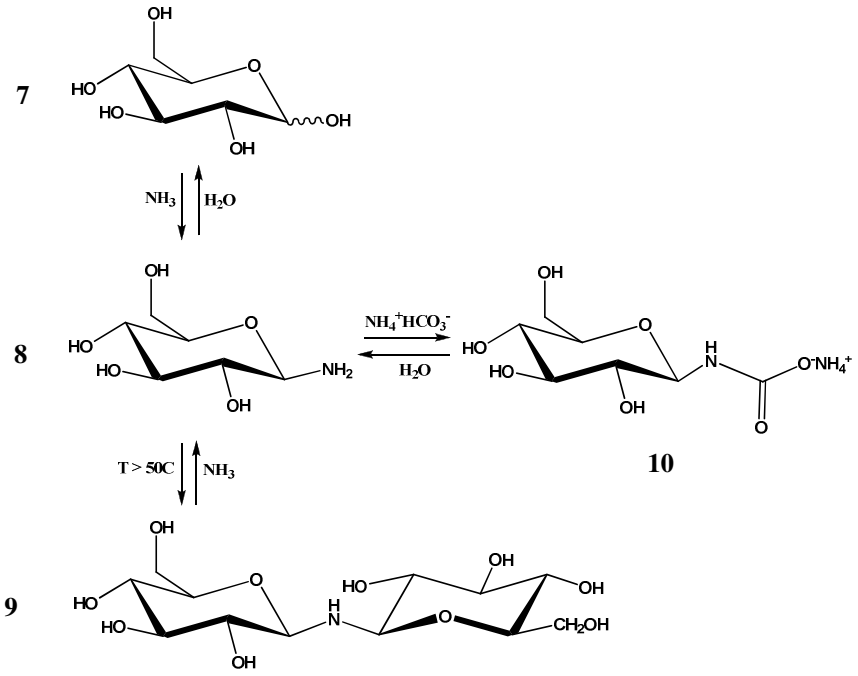

Scheme 1 Synthesis of glycosylamines

A series of glucopyranosylamide derivatives [29] were synthesized possessing C18 unsaturated hydrocarbons chains, which differ in the introductory position of a *cis* double bound, as building blocks for nanotube assemblies. Compound **11** has been proved to self-assemble in water to produce uniform nanotubes (Fig. 4) structure with significantly low diamenter dispersity of the other lipids.

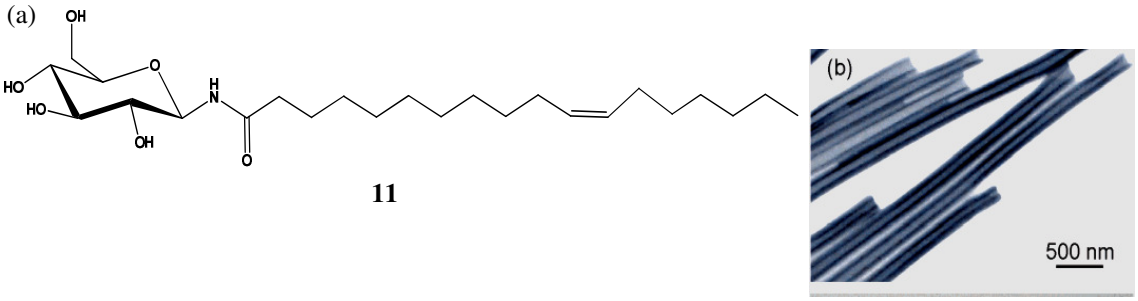

Figure 4 (a) *N*-(11-*cis*-Octadecenoyl)-*β*-D-glucopyranosylamine; (b) nanotubes [29]

They found that, the position of the cis double bond significantly influences the homogenity of the outer diameters as well as growth behavior of the self-assembled nanotube structures.

Cateni et al. studied and characterized a series of monoglycosyl diglycerides (**12**), which exhibit antimicrobial and antifungal activity [30]. It was observed that the antimicrobial activity in this

class of compounds is dependent on the nature of fatty acids; the octanoyl chain is the proper structural feature for the maximum activity (Fig. 5).

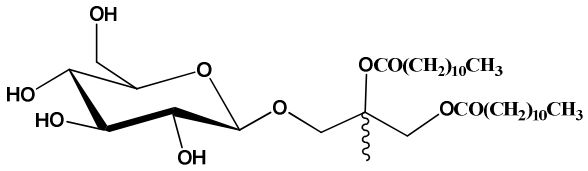

12

Figure 5 1,2-*O*-dilauroyl-3-O-(β-D-glucopyranosyl)-*rac*-glycerol

Glycosyl(thio)ureido sugar via carbodiimines (Fig. 6), which are found in the nature, a family of pseudooligosaccharides having an urea intersaccharide bridge, have been synthesized and reported for the first time by Ortiz Mellet et al. [31]. The procedures have been exploited in the development of an amine- isocyanate-free synthesis of urea- and thiourea-tethered pseudooligosaccharides via the corresponding glycosylcarbodiimines sugars. The fully unprotected compounds adopted preferentially, the (*Z,Z*) configuration at the pseudoamide bonds in water solution.

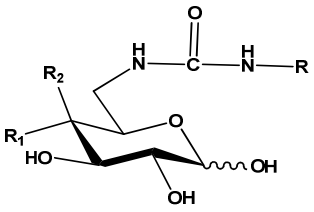

13

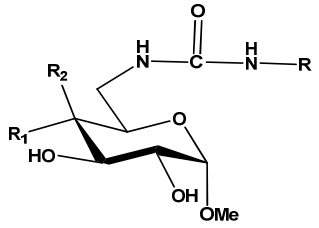

14

R =

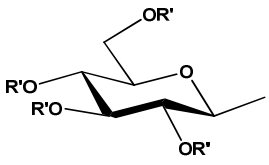

or

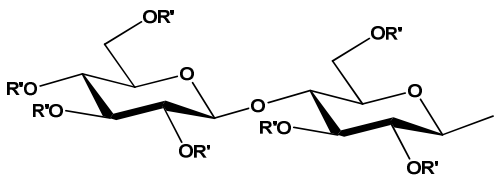

15 **16**

a = R_1 = OH
R_2 = H

b = R_1 = H
R_2 = OH

R'= OAc, H

Figure 6 Glycosyl(thio)ureido sugar derivatives

Allevi et al. reported the synthesis of thio analogues (**17**) and *N*-glucoside (**18**) of etoposide (Fig. 7) [32].

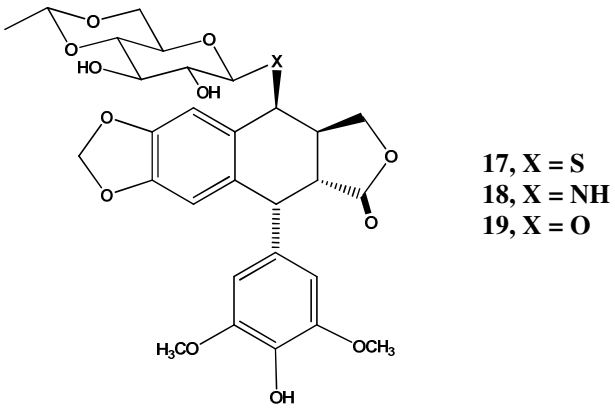

Figure 7 Etoposide and *S*- and *N*-analogues

An antitumor agent widely used in the treatment of leukemia, testicular cancers, and small cell lung cancer it is etoposide (**19**), which is an *O*-glycoside of 4'-demethylepipodophyllotoxin. It inhibits the enzyme topoisomerase II, which unwinds DNA, and by doing so causes DNA strands to break. Cancer cells are less able to repair this damage than healthy cells. Etoposide forms ternary complex with DNA and the topoisomerase II enzyme, preventing re-ligation of the DNA strands. This causes errors in DNA synthesis and promotes apoptosis of the cancer cells.

In addition, another example of glucopyranosyl which exhibit in vitro antineoplastic activities against leukemia and colon carginoma cells is 1'-β-D-glucopyranosyl-1,2,3-triazol-4,5-dimethanol-4,5-bis-(isopropylcarbamate) (**20**, Fig. 8) [33].

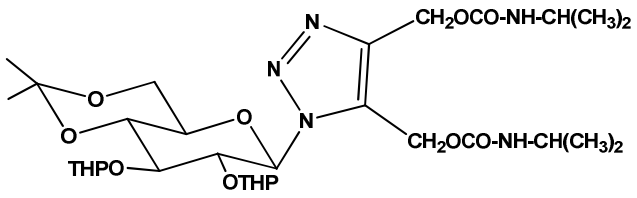

20

Figure 8 1'-β-D-glucopyranosyl-1,2,3-triazol-4,5-dimethanol-4,5-bis-(isopropylcarbamate)

Glycosidase are also anti-viral, anti-proliferative, and anti-diabetic agents. Many natural and synthetic glycosidase inhibitors mimic the charge buildup and/or the conformational distortion of the transitional state [34].

Glycosyl amines with a general stracture **21** or **22** (Fig. 9) inhibit a variety of glycosidases by positioning a positive charge in the active state site, which can interact with the carboxylate moieties [34-38].

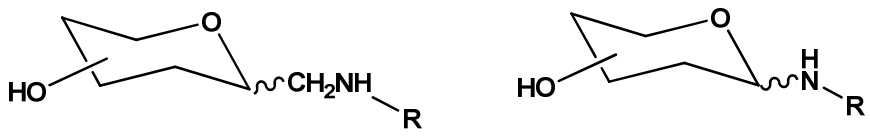

21 **22**

Figure 9 Alycone-modified glycosidase inhibitors

N-acetyl-β-D-glucopyranosylamine (**23**) was the first good glucose analog inhibitor of glycogenphosphorylase *b* (GP*b*) that binds at the catalytic site (with a Ki = 32 μM) opened a new class of compounds in this field [39]. This kind of inhibitors will be discussed in more details in chapter II.4.

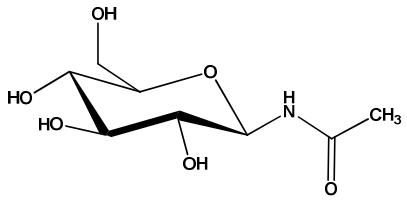

23

Figure 10 *N*-acetyl-β-D-glucopyranosylamine

In summary, carbohydrates can be considered as one of nature's better gift to the synthetic organic chemist because of their abundance and their endowment with unique stereochemical and functional features.

II.1.1. D-Glucose

The structure of glucose was discovered by Emil Fisher (Nobel Prize in 1902 in Chemistry). Glucose, a monosaccharide (or simple sugar), is an important carbohydrate in biology. The name comes from the Greek word ***glykys*** (γλυκύς), which means "sweet", plus the suffix "-ose" which denotes a sugar.

The living cells use as a source of energy and metabolic intermediate. Glucose is one of the main products of photosynthesis and starts cellular respiration in both prokaryotes and eukaryotes. Two steroisomers of the aldohexose sugars are known as glucose, only one of which (D-glucose) is biologically active. The mirror-image of the molecule, L-glucose, cannot be metabolized by cells in the biochemical process known as glycolysis [40].

By careful manipulation of protecting group such as acetals and reactions such as reduction and oxidation, it is possible to transform sugars into many different organic compounds retaining the natural optical activity of the sugar themselves. Glucose are also very cheap, it is ideal starting point for the synthesis of other compounds and widely used in this way, probably the cheapest available optically active compounds.

II.1.2. Structure

Pure carbohydrates contain carbon, hydrogen, and oxygen atoms, in a 1:2:1 molar ratio, giving the general formula $C_n(H_2O)_n$. (applies only to monosaccharides). However, many important "carbohydrates" deviate from this issue, such as deoxyribose and glycerol, although they are not, in the strict sense, carbohydrates. Sometimes, compounds containing other elements are also counted as carbohydrates (e.g. chitin, which contains nitrogen).

The simplest carbohydrates are monosaccharides, which are small straight-chain aldehydes and ketones with many hydroxyl groups added, usually one on each carbon except the functional group. Other carbohydrates are composed of monosaccharide units and break down under hydrolysis. These may be classified as disaccharides, oligosaccharides, or polysaccharides, depending on whether they have two, several, or many monosaccharide units.

Monosaccharides (or glyceraldehydes; e.g. glucose) can be linked together into what called polysaccharides (or oligosaccharides) in a large variety of ways. The carbohydrates may have one or more groups replaced or removed.

II.1.2.1. Structure of D-glucose

Glucose ($C_6H_{12}O_6$) contains six carbon atoms one of which is part of an aldehyde group and is therefore referred as an aldohexose. In solution, the glucose molecule can exist in an open-chain (acyclic) and ring (cyclic) form (in equilibrium), the latter being the result of a covalent bond between the aldehyde carbon atom and the C−5 hydroxyl group to form a six-membered cyclic hemiacetal (**a** and **b**; Fig.11) [41].

a **b**

Figure11 β-D-Glucose a) open-chain b) ring

When the cyclic hemiacetal is formed, the C−1 atom becomes a new stereogenic center and possesses either *R*- or *S*- configuration. At pH 7 the cyclic form is predominant. In the solid phase, glucose assumes the cyclic form. As the ring contains five carbon atoms and one oxygen atom, which resembles the structure of pyran, the cyclic form of glucose is also referred as glucopyranose.

II.1.3. Isomers

Aldohexose sugars have four chiral centers giving 2^4 = 16 stereoisomers. These are split into two groups, L and D, with 8 sugars in each. Glucose is one of these sugars, and *L* and D-glucose are two of the stereoisomers. Only seven of these are found in living organisms, of which D-glucose, D-galactose and D-mannose are the most important. These eight isomers (including glucose itself) are all diastereoisomers in relation to each other and all belong to the D-series.

An additional asymmetric center at C−1 (called *the anomeric carbon atom*), H−1(the anomeric proton) is created when glucose forms a ring, and two structures, so-called anomers, are formed — *α*-glucose and *β*-glucose. These anomers differ structurally with respect to the relative positioning of their hydroxyl group linked to C−1 and the group at C−6, which is termed the reference carbon (Fig. 12.) [15].

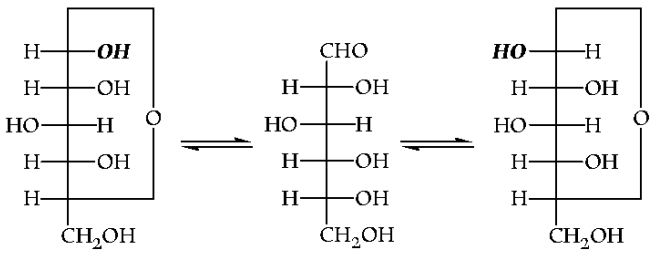

Figure 12 Howorth formulas - *α*-D-Glucose (left) and *β*-D-Glucose (right) in Haworth projection

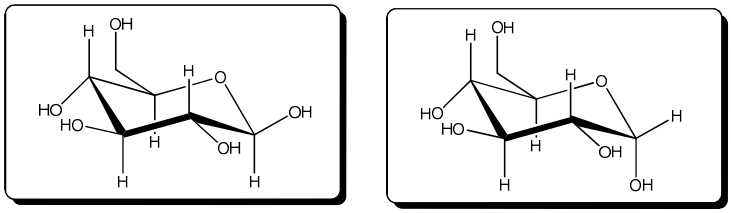

Figure 13 *α*-D-Glucose (left) and *β*-D-Glucose (right) conformations

When D-glucose is drawn as a Haworth projection in the standard chair conformation (fig. 3), the designation *α* means that the hydroxyl group attached to C−1 is positioned *trans* to the -CH_2OH group at C−5, while *β* means that it is *cis*. Another popular method of distinguishing *α* from *β* is

by observing whether the C−1 hydroxyl is below or above the plane of the ring (Fig. 14), respectively, but this method is an inaccurate definition and may fail if the glucose ring is drawn upside down or in an alternative chair conformation. The α and β forms interconvert over a timescale of hours in aqueous solution, to a final stable ratio α: β of 36:64, in a process called *mutarotation* [42].

Figure 14 Fisher projection - α-D-Gluose (left) and β-D-Glucose (right)

II.1.4. Chirality

Chirality is very important in biological systems as it is a fundamental component of molecular recognition (Fig. 15) [43-45].

In principle, there are three basic ways of obtaining enantiopure compounds [43-45]:

- from natural sources (where is produced only one enantiomer – *chiral pool*)
- separation of the two forms from a 50:50 mixture of enantiomers, so-called racemate
- asymmetric synthesis, including asynetric catalysis by selective preparation of one
- enantiomer of a chiral compound from achiral or prochiral starting material

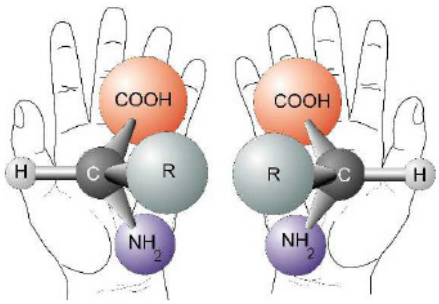

Figure 15 The two enantiomers of α-amino acids are non-superposable, as is the case with right and left hands

Whether due to the chirality of the molecules in water or in the solid form, D-glucose is dextrorotatory (rotate the direction of polarized light clockwise), and indeed the mirror-image isomer, L-glucose, is levorotatory (rotates polarized light counterclockwise) by the same amount.

The specific rotation of chemical compounds ([α]) is defined as the observed angle of optical rotation *a* when plane-polarized light is passed through a sample with a path length of 1 decimeter and a sample concentration of 1 gram per 1 deciliter. Specific rotation is calculated using these equations:

$$[\alpha]_D^{25} = \frac{observed\ rotation}{parthlenght(dm) \times concentration(\frac{g}{ml.})}$$

$[\alpha]_D^{25}$=*specific rotation*

II.2. Thiosemicarbazones

II.2.1. Introduction in Schiff bases

A *Schiff base* (or *azomethine*) contains a carbon-nitrogen double bound with the nitrogen atom attached to an aryl or alkyl group, and in contrast to imines nitrogen is not attached to a hydrogen. The general formula of a Schiff base is $R^1R^2C{=}NR^3$, where R^3 is an aryl or alkyl group. In the case that the R^3 is an aryl group, the compound is quite stable.

Schiff bases are relatively easily obtained by a condensation reaction of a carbonyl compound **24** and primary amines **25** by nucleophilic addition, usually in an alcoholic solution and sometimes refluxing (Scheme 3) [46]. The reaction is reversible, resulting in the intermediary carbinol-amine (hemiaminal, **26**), followed by a dehydration to generate an imine **27** containing an imine group (C = N) [47, 48]. Purity of the solvent in the condensation reaction is of primary importance and can considerably influence the Schiff base formation [49].

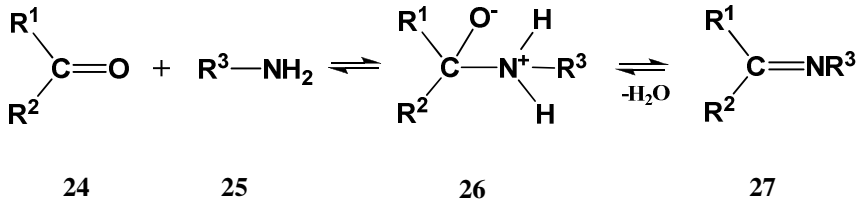

24 **25** **26** **27**

Scheme 3 Schiff base formation

II.2.2. Thiosemicarbazones

Thiosemicarbazones (hydrazine carbothioamides) are basically Schiff bases. They are a family of compounds with beneficial biological activity. One interesting thing is that the more pharmaceutically promising thiosemicarbazone derivatives possess additional functional groups that are not coordinated to their "primary" metal ion, suggesting that the biological activity may also depend on the non-coordinating groups [50].

II.2.2.1. Classification of thiosemicarbazones

Thiosemicarbazones are broadly classified as mono- and bis- thiosemicarbazones [50]. The basic mono-thiosemicarbazones (structure **28** and **29**, Fig. 16) have different, R^1, R^2, R^3 and R^4 substituents, and depending upon the substituents, various sub-classes of molecules are formed. Thiosemicarbazones based on an aldehyde have hydrogen atom as one of substituents (R^2) while R^1 may be an alkyl, an aryl or a heterocyclic group. Similary, substituents at N(3) nitrogen may be both hydrogen atoms, or one hydrogen, and a second alkyl, or aryl group, and finally N(3) may be a part of a ring. The secound category of mono- thiosemicarbazones depends upon the parent ketone group, and thus both substituents may be the same or different (alkyl or aryl group) [51]. The atom numberings shown in figure **16** is in accordance with the IUPAC system.

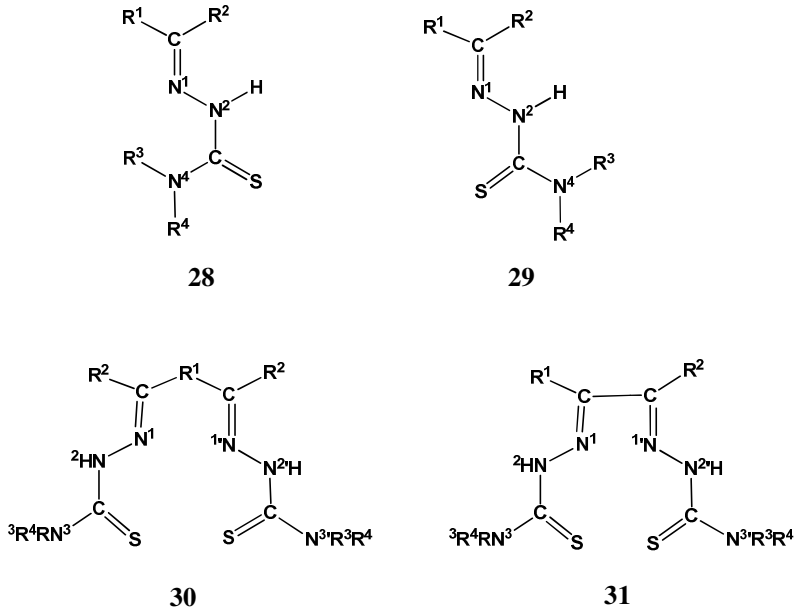

Figure 16 General structures of types of thiosemicarbazones

Bis-thiosemicarbazones have two arms connected via a ring, or a C-C bond. Examples are given in the figure above (**30** and **31**, fig. **16**).

II.2.2.2. Synthesis of thiosemicarbazones

Thiosemicarbazones are obtained by the condensation of an aldehyde or ketone with a thiosemicarbazide. Synthetic methods for thiosemicarbazones have been well presented by Klayman et al. [52, 53], Scovill [54], and Blanksma [55]. Klayman and co-workers [56] have outlined strategies for modifying thiosemicarbazones:

- exchange of the sulfur atom of the thiocarbonyl group by oxygen or selenium;
- changing the point of attachment of the thiosemicarbazone moiety in the parent aldehyde or ketone (particulary those containing additional potential coordinating sites);
- substitution on the terminal N(4) position;
- variation of the parent aldehyde or ketone.

II.2.2.3. Mechanism of a reaction between a carbonyl group and an amine

Looking at aldehydes and ketones, we learned that the characteristic pattern of many reactions of the carbonyl group begins with the formation of a bond between the carbonyl carbon and an attacking nucleophile. The nucleophile provides the electrons to form the new bond and the π bond of the carbonyl group is broken as it "gets out of the way." The electrons are moved from this π bond onto what was the carbonyl oxygen.

The idea which emerges from this is that a strong nucleophile can attack directly, without help from an acid catalyst. For a weak nucleophile, an acid catalyst is needed so that the carbonyl carbon is prepared to share a pair of electrons as a new covalent bond. The mechanism of reaction between an aldehyde and an amine provided in scheme 2 shows how these factors balance (scheme 4).

It is an experimental fact that this reaction – imine formation – is acid-catalyzed, which suggest that the unshared pair of electrons on amine nitrogen is not sufficiently nucleophilic to push the carbonyl π electrons "out of the way" without help from an H^+ which breaks that π bond in an earlier step. The weaker nucleophile would be more likely to need a little help from acid catalysis.

It is also an experimental fact that if we put in too much acid, the reaction stops. How do we make sense of this? The key is to remember that an amine is a base. Being a base means that an amine will react with an acid to form an ammonium ion.

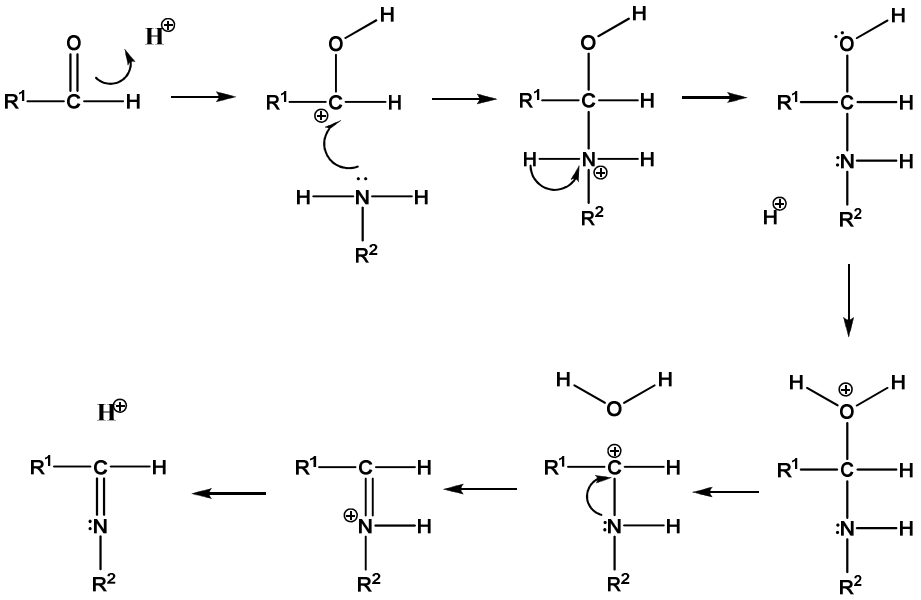

Scheme 4 Mechanism of a reaction between carbonyl group and an amine

II.2.2.4. Tautomerization of thiosemicarbazones

In solution, thiosemicarbazones probably exist in an equilibrium mixture of thione and thiol tautomers (**32** and **33**), and can bind to a metal in the neutral **32**, or the anionic forms **34** (Scheme 5). The anionic forms are generated after loss of N(2)(**32)** or SH(**33)** hydrogen ions. A number of bonding modes have been observed for the thiosemicarbazones in their neutral or anionic forms [50].

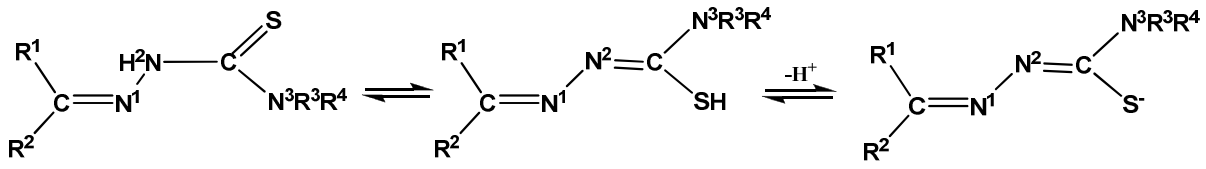

Scheme 5 Tautomerization of thiosemicarbazones

32 **33** **34**

II.2.2.5. Binding modes of thiosemicarbazones

Thiosemicarbazones represent a versatile type of ligands because of the number of donor atoms that they possess, among which sulfur is on a paramount impotance in the metal-ligand linkage; moreover, their configurational flexibility creates the possibility of a variety of coordination modes [57].

Thiosemicarbazone complexes reported so far involve predominantly the latter half of transition-metal ions, which reflect the central role played by sulfur coordination in these compounds and consequently their "soft acid-soft base" preference [50].

The thiosemicarbazone moiety (**35**; Fig. 17) without substituents attached to the thione sulfur coordinates as either a neutral or anionic NS bidentate ligand, depending on the method of complex preparation [58, 59]; a third coordinating atom often gives ONS (e.g.2-hydroxybenzaldehyde thiosemicarbazone, **36**; Fig. 18) [60] or NNS (e.g.2-actylpyridine thiosemicarbazone, **37**; Fig. 18) tridentate ligands.

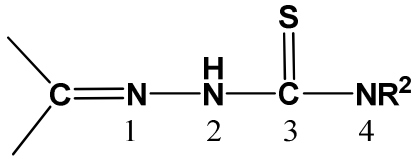

35

Figure 17 Thiosemicarbazone moiety

Nevertheless, a few examples of higher denticity including one or more thiosemicarbazone moieties, as well as monodentate coordination, have been reported [61]. If an additional coordinating functionality is present in the proximity of the donating centers, the ligand is bound in a tridentate manner. This occurs with either a neutral molecule [62] or the monobasic anion upon loss of hydrogen from N^2 [61].

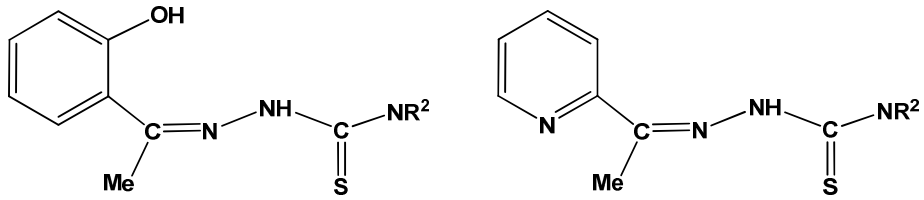

36 **37**

Figure 18 Chemical structure of 2-hydroxybenzaldehyde thiosemicarbazone(left) and 2-actylpyridine thiosemicarbazone(right)

When the additional functionality can also loose a proton (e.g. phenolic group), anions of greater negative charge are formed. When the heterocyclic atom and the azomethine nitrogen are involved in a bidentate coordination mode [63] and the sulfur atom is considered not to be coordinated, thiosemicarbazones are weakly coordinated to the same metal center, or they are coordinated to an adjacent metal center [61, 64].

II.2.2.6. Configuration of thiosemicarbazones

The presence of C=N makes thiosemicarbazones to exist as *E* and *Z* stereoisomers. Considering the thermodynamic stability, *E* isomer will predominate in the mixture [64].

In free unsubstitued thiosemicarbazones in solid state, the C=N-NH-CS-NH_2 backbone is usually almost planar, with S atom ***trans*** to the azomethine N (*E*-configuration; Scheme 6, **38**). A few thiosemicarbazones are excepted from this rule. Although there are several electronic and steric factors that may contribute to the adoption of this arrangament, the most important is probabily that the ***trans*** arrangement places the amine and the azomethine nitrogen atoms in relative positions suitable for intramolecular hydrogen bonding [65, 66]. In fact, thiosemicarbazones in which the amine group is fully substitued crystallize with the S atom ***cis*** to the azomethine N (*Z*-configuration; Scheme 6, **39**), Substitution of the hydrazinic H seems not to change the usual *E*-configuration of unsubstituted thiosemicarbazones. However, S-substituted thiosemicarbazones adopt the *Z* form (Scheme 6, **40**; X=S, R=alkyl).

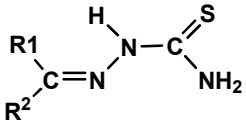

38

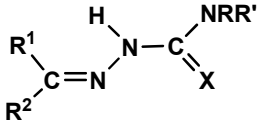

39

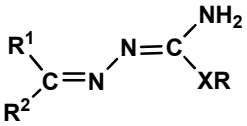

40

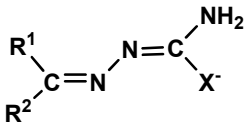

41

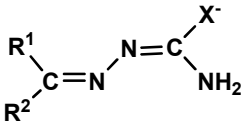

42

Scheme 6 Changing of thiosemicarbazones from *Z*-configuration into *E*-configuration

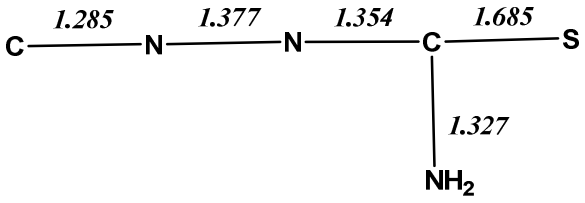

Scheme 7 Conventional single and double bonds

In Scheme 7, conventional single and double bonds are reprezented. Nevertheless, as was pointed out by Palenik et al. [67] on the basis of their pioneering work in the field, thiosemicarbazones are extensively delocalized system, especially when aromatic radicals are bound to the azomethine carbon atom. Scheme 7 indicates the mean bond lengths of the thiosemicarbazones (Cambridge Structural Database).

The C=S bond is close to the avarage for thioureas [68]. Thiosemicarbazones are versatile ligands in both neutral and anionic forms. Although the proton lost by the anions formally belongs to the hydrazinic –NH group, the anion is usually represented in the canonical form (Scheme 6, **40** and **41**) and usually *Z*-configuration; in the neutral molecules, the π-charge is actually delocalized.

II.2.2.7. Thiosemicarbazones and their metal complexes as bioactive molecules and pharmaceuticals: A summary

The recent literature shows that thiosemicarbazones exhibit a wide range of stereochemistry in complexation with transitional metal ions [69, 70].

Thiosemicarbazones is a class of biochemically important compounds possessing a wide range of biological activities, and is very promising in the treatment of many diseases, such as tuberculosis [71], E. coli [72], leukemia [73, 74], and have been of a great interest because of their reported antineoplastic action or as antioxidant and anti-dyslipidemic agents [75-77]. The hypozic selectivity of certain copper bis(thiosemicarbazones) and their use as vehicules for the delivery of radioactive copper isotopes to tumor [78] or leucocytes [79] has also attracted much attention [80]. The hypoxic selectivity is strongly dependent on the substituents on the carbon backbone.

In a recent paper, Holland et al. reported two new types of unsymmetrical bis(thiosemicarbazones) and their Zn(II) and Cu(II) (**43** and **44**; Fig. 19) complexes having conjugated water-soluble glucose, and they have recently been the subject of intense research because of their potential as

radiopharmaceuticals for the specific target of hypoxic tissue [81]. Hypoxia is a pathological condition that has been associated with stroke, heart disease, and certain types of cancer [82].

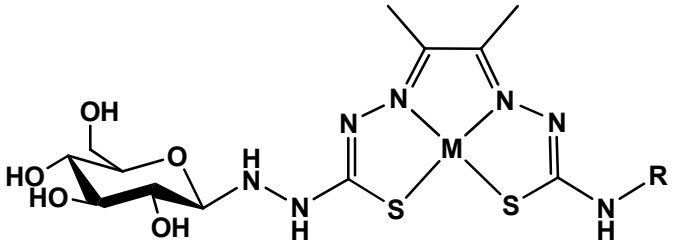

43, M = Zn, R = methyl, ethyl, allyl
44, M = Cu, R = methyl, ethyl, allyl

Figure 19 Glucose-functionalized zinc(II) and copper(II) bis(thiosemicarbazone) complexes

Many thiosemicarbazones such as marboran (**45**) [83] or triapine [84] (**46**) (Fig. 20) are already used in medical practice. Earlier studies on the biological properties of thiosemicarbazones and their metal complexes revealed that the biolocically active thiosemicarbazone molecules were planar and pyridine ring or a NNS tridentate system were present [85]. Furthermore, it is well understood that the biological activity depends on the parent aldehyde or ketone [50], and the presence of a bulky group at the terminal nitrogen considerably increases the activity [86]. Reports on N(4)-thiosemicarbazones have concluded that, an additional potential bonding site together with the presence of bulky groups at the N(4) position of the thiosemicarbazone moiety greatly enhances biological activity [87-89].

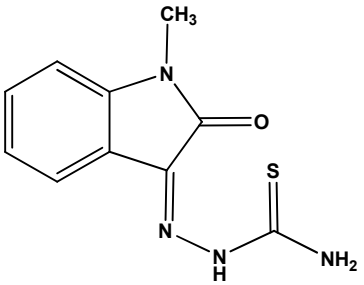

45

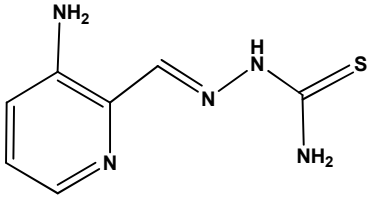

46

Figure 20 Chemical structure of marboran (**45**) and triapine (**46**)

One of the most potent known inhibitors of ribonucleoside diphosphate reductase is the family of thiosemicarbazones. The mechanism of their antitumor action is considered to involve either inhibition of the enzyme, ribonucleotide reductase, on obligatory enzyme in DNA synthesis or creation of lesions in DNA strands [90].

A major clinical challenge in successful treatment of cancer with anticancer drugs is that certain tumour cells develop a particular phenotype, called multi drug resistence (MDR), which makes these cells resistent to other classes of anticancer agents to which the tumour cells have not been treated previously [91]. Synthesis and characterization of a palladium complex of phenanthrenequinone thiosemicarbazone and evaluation of its antiproliferative properties in breast cancer and normal cells have been described [92]. The studies suggested that the complex is a potent antineoplastic agent that has selective activity against tumour cells and is effective against drug resistant breast cancer cells.

Platinum complex of 2-acetyl pyridine thiosemicarbazone has been synthesized in which intramolecular hydrogen bonds, π-π, Pt-Pt and Pt-π contacts lead to aggregation and to a two-dimensional supramolecular assembly. The complexes where found to have a completely lethal effect on Gram+ bacteria. Additionally, some of them showed effective antifungal activity towards yeast [93].

The effect of Pt(II) and Pd(II) complexes of 2-acetylpyridine thiosemicarbazone on sister chromatid exchange rates, human lymphocyte proliferation kinetics, and leukemia P388 have been investigated. Among these compounds, $[Pt(AcTsc)_2]\cdot H_2O$ and $[Pd(AcTsc)_2]$ were found to be the most effective in inducing antitumour and cytogenetic effects [94].

Antifungicial, antibacterial and antifertility activities of biologically active heterocyclic thiosemicarbazones and their coordination complexes with the dimethylsilicon moiety have been described. Some ligands and their corresponding dimethylsilicon(IV) complexes have been tested for their effects on several pathogenic fungi and bacteria. Two representative complexes have also been found to act as sterilizing agents by reducing the production of sperm in male mice [95].

A number of authors are interested in investigating the biological and medical properties of transitional metal complexes of thiosemicarbazones in recent years [59, 96]. New squere planar platinum complexes have been prepared. The ligands, in an anionic form, act as tridentate ligands which coordinate to the platinum (II) through the pyridinic nitrogen, the azomethine nitrogen (C=N), and the thiolato sulfur atom. Both the Schiff bases exhibit strong cytotoxicity effect towards A2780 cells (**47**; Fig. 21) lines and bladder cancer cell line (**48**; Fig. 21), respectively, the palladium(II) complexes being more active than *cis*-platinum [97, 98].

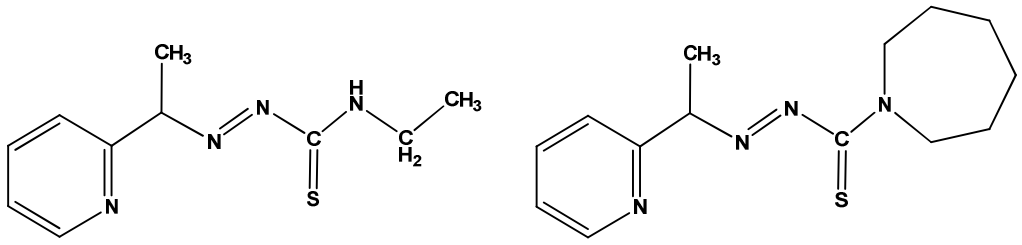

47 48

Figure 21 Molecular structures of the ligands **47** and **48**

Current biological and chemical research, therefore, has focused much attention on this ever-present and increasingly dangerous problem. Among the many types of compounds being investigated for antimicrobial properties, the thiosemicarbazones have a very important position. Many of these compounds (TSCs) have shown significant biological activities (antibacterial, antiviral, antifungial, antitumoural etc.), especially those containing heterocyclic and/or aromatic rings. Earlier works have also shown that transitional metal complexes of thiosemicarbazones often show even greater amount of bioactivity.

II.2.2.8. Other applications of thiosemicarbazones

Thiosemicarbazones have applications as analytical tools. Some thiosemicarbazones produce highly colored complexes with metal ions. These complexes have been proposed as analytical reagents that can be used in selective and sensitive determinations of metal ions [99, 100]. Ferrocene derivatives containing thiosemicarbazones in a side chain have been investigated by cyclic voltammetry and positron annihilation lifetime measurements. Positrons can form the positron-electron pair in molecular solids. Interest in the behaviour of the positron-electron pair is great because of the probability of its formation and its lifetime depends upon the physical and chemical properties of the solid. It has been shown that the redox and the electron capture processes took place on the Fe atom [101].

Cu(II), Co(II) and Fe(II) in pharmaceutical preparations could be determined using pre-column derivatization and solvent extraction with 2-acetylpyridine-4-phenyl-3-thiosemicarbazone as complexing reagent [102].

The inhibition of corrosion of aluminium in HCl solution by some derivatives of thiosemicarbazones has been studied using weight loss and hydrogen evolution techniques. The thiosemicarbazone derivatives used are 2-acetylpyridine-4-phenyl thiosemicarbazone, 2-

acetylpyridine-4-phenylisomethyl thiosemicarbazone and 2-acetylpyridine-4-phenylisoethyl thiosemicarbazone. The inhibition efficiency depends on the compound concentration [103].

The intrinsic fluorescence of Zn(II) bis(thiosemicarbazone) complexes has been used previously to measure cellular uptake and intracellular localization in a range of different cancer cell phenotypes [104].

In the recent years, thiosemicarbazones were successfully used for the **first time** as ligands in palladium-catalyzed coupling reactions (Heck and Suzuki) in air under conventional heating or a microwave irradiation by the research teams of Kostas and Kovala-Demertzi [105-107]; one of the catalyst is currently **commercially available**. This topic will be discussed in details in chapter II.3. Catalysis.

II.3. Diabetes mellitus

II.3.1. Introduction

Diabetes is among the largest contributors to global mortality through its long term complications. A dramatic increase in the number of diabetes patients was recorded at the end of the 20th century [108]. In particular, the past two decades have seen an explosive increase in the number of people diagnosed with diabetes [109, 110]. *Diabetes mellitus*, the most common hormonal deficiency disease, is characterized by hypoglycemia, insulin resistance, and defects in insulin secretion and is usually associated with dyslipidimia, hypertension, and obesity [111].

There are two forms of diabetes; *type 1* and *type 2*. In the *type 1* diabetes, the autoimmune-mediated destruction of pancreatic β-cell islets results in absolute insulin deficiency. *Type 2* diabetes mellitus, which accounts for 90-95% of cases, is characterized by insulin resistance and/or abnormal insulin secretion.

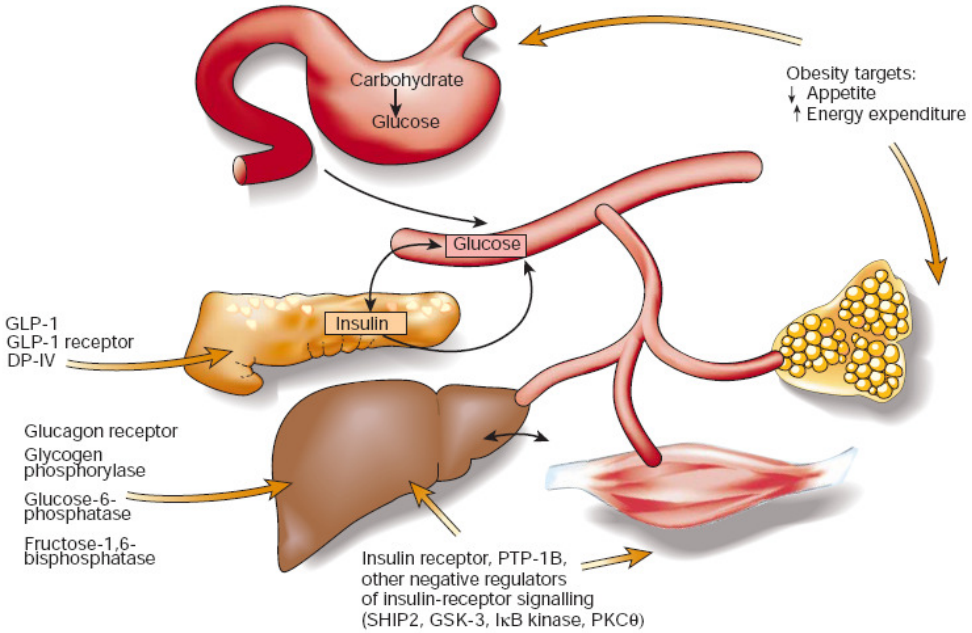

Figure 22 A better understanding of defects involving several key organ systems has led to new drug targets for *type 2* diabetes

Type 2 diabetes mellitus is currently estimated to affect more than 5% of the adult population in Western societies, and its incidence is expected to increase considerably in the future. Diabetes is a major cause of blindness and renal disease, and is known to significantly increase the risk of cardiovascular disease, leading to heart attack, stroke and amputation of the lower extremity(ies). Almost 90% of all diabetics are type 2 (T2D) and cannot be treated with exogenous insulin. Current preventative and therapeutic strategies do not achieve adequate control of blood glucose to prevent chronic morbidity, and there is a need to develop novel healthcare interventions to address this substantial biomedical challenge. The liver is largely responsible for unrestrained glucose production through increased rates of gluconeogenesis and glycogenolysis (Fig. 22). Potential drug targets that modulate these processes include the glucagon receptor (antagonists), glycogen phosphorylase (inhibitors), and other rate-controlling enzymes such as glucose 6-phosphatase and fructose-1,6-bisphosphatase (inhibitors). Defective glucose-stimulated insulin secretion by pancreatic islet β-cells could be alleviated with recombinant glucagon-like peptide 1 (GLP-1) or agonists of the GLP-1 receptor. Alternatively, decreased GLP-1 clearance can be achieved with inhibition of dipeptidylpeptidase IV (DP-IV). To reduce insulin resistance, enhanced insulin action in liver and muscle (and fat) might be achieved with small-molecule activators of the insulin receptor or inhibitors of protein tyrosine phosphatase (PTP)-1B. The development of anti-obesity agents that produce reduced appetite and/or increased energy expenditure will also lead to effective treatment (and prevention) of *type 2* diabetes [108].

At present, therapy for *type 2* diabetes relies on diet, exercise, hypoglycaemic drugs intended to reduce the hyperglycaemia (sulphonylureas or thiazolidinediones) and if this fail, insulin itself, which suppresses glucose production [112]. The current drugs have limited efficacy and tolerability and significant mechanism based side effects [108]. Thus, there is a continued interest in new therapeutic agents that can mimic the control of blood glucose concentrations, which is severely impaired in *type 2* diabetic patients.

T2D is characterized by excessive glucose production from the liver. One molecular approach aims to reduce this production, and involves inhibition of glycogen phosphorylase (GP). GP has a critical role in human carbohydrate catabolism (that is of special importance for the mobilisation of glycogen deposits) by catalysing the release of monomeric glucose from glycogen deposits. GP has been validated as a molecular target for therapeutic intervention in T2D by the discovery that a chloroindole carboxamide compound, an inhibitor of the enzyme, is highly effective in rodent models of diabetes.

II.3.2. Brief description of glycogen phosphorylase

Glycogen phosphorylase (GP) (Fig. 23), a key regulatory enzyme present in most mammals (muscle, brain and liver), located on human chromosomers 11, 20, and 14, respectively. GP-s are dimers of two identical subunits, each contain 841 amino acids and the essential cofactor pyridoxal phosphate (PLP, derived from vitamine B_6). GP is an allosteric enzyme that exists in two interconvertible forms, GP*b* (non-phosphorylated; low activity, low substrate affinity, predominantly T state) and GP*a* (phosphorylated; high activity, high substrate activity, predominantly R state) [109]. Both forms can exist in a less active T state and more active R state (Fig. 3) and the equilibrium between the two states is sensitive to concentrations of allosteric activators and inhibitors [113]. In the liver, the active form of the isoenzyme is not only responsible for the breakdown of glycogen storage material into glucose 1-phosphate, but it controls the activity of protein phosphatase, the enzyme responsible for the inactivation of GP*a* and the activation of glycogen synthesis. In the muscle, glucose-1-phosphate is utilized via glycolysis to generate metabolic energy. In the liver, it is mostly converted by phosphoglucomutase to glucose-6-phosphate and glucose, which is released for the benefit of other tissues. In the resting state glycogen phosphorylase exists in the inactive *b* form (GP*b*). In response to nervous or hormonal stimulation, GP*b* is converted to the phosphorylated form GP*a* through the phosphorylase kinase catalyzed addition of a phosphoryl group to a hydroxyl group of a specific serine (Ser14), as part of the cascade system initiated by cyclic AMP. The reverse process of dephosphorylation, stimulated by insulin, is catalyzed by protein phosphatase 1 (PP1). Allosteric activators, such as AMP or allosteric inhibitors such as ATP, glucose-6-phosphate, glucose and caffeine can alter the equilibrium between the two states, according to the Monod-Wyman-Changeux model for allosteric proteins. The T-state is stabilized by the binding of ATP, glucose-6-phosphate, glucose, and caffeine. The R-state is induced by AMP or IMP, substrates or certain substrate analogues. The T-state is a better substrate than the R-state for protein phosphatase 1. GP*a*, but not GP*b*, is a potent inhibitor of the phosphorylase action on glycogen synthase and it is only when GP has been dephosphorylated that the phosphatase is free to activate glycogen synthase, the rate limiting enzyme involved in glycogen synthesis. The phosphorylated form, GP*a*, is not longer dependent on AMP for activity, although the activity of GP*a* can be enhanced by AMP by about 10%.

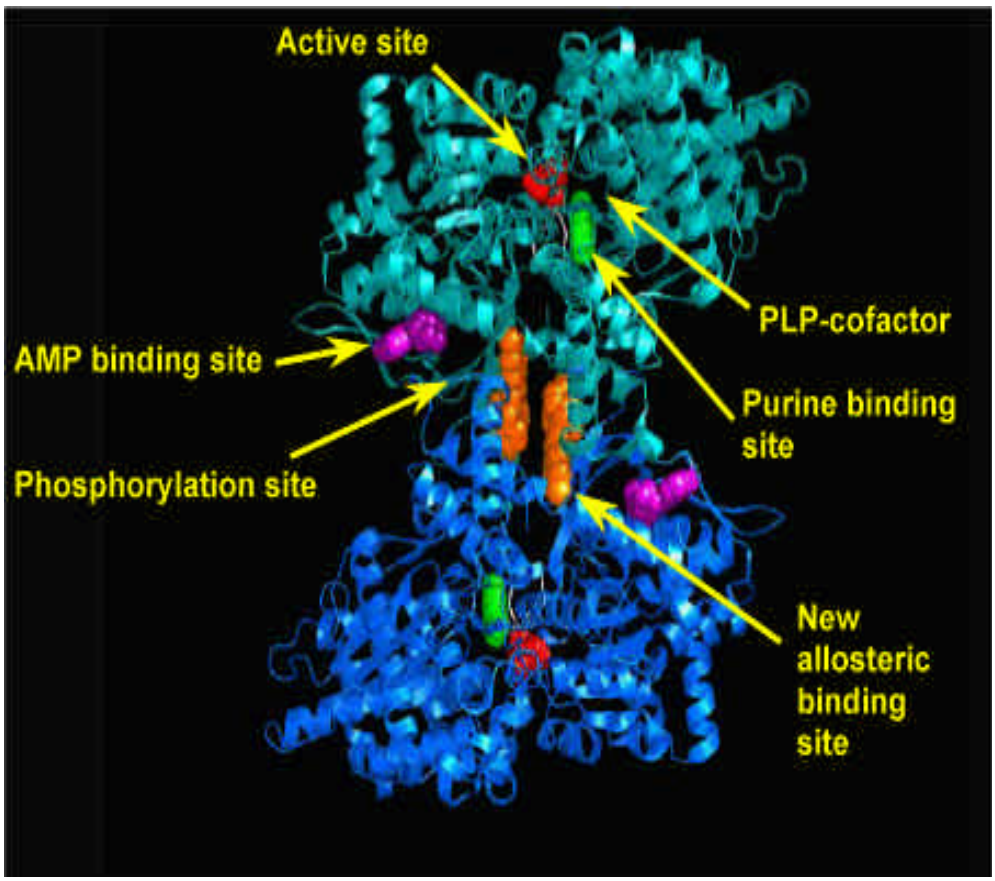

Figure 23 A schematic diagram of the muscle GP*b* dimeric molecule viewed downs the 2-fold. The positions are shown for the catalytic, allosteric, the inhibitor, and the new allosteric inhibitor sites. The catalytic site, which includes the essential cofactor pyridoxal 5'-phosphate (PLP, not shown), is buried at the centre of the subunit accessible to the bulk solvent through a 15 Å long channel. Glucose (shown in red), a competitive inhibitor of the enzyme that promotes the less active T state through stabilization of the closed position of the 280s loop (shown in white), binds at this site. The allosteric site, which binds the activator AMP, other phosphorylated compounds such as ATP, glucose-6-P, and the Bayer compound W1807 (shown in magenta), is situated at the subunit-subunit interface some 30 Å from the catalytic site. The inhibitor site, which binds purine compounds, such as caffeine, nucleosides or nucleotides at high concentrations, and flavopiridol (shown in green) is located on the surface of the enzyme some 12 Å from the catalytic site and, in the T state, obstructs the entrance to the catalytic site tunnel. The glycogen storage site (with bound maltopentaose, shown in orange) is on the surface of the molecule approximately 30 Å from the catalytic site, 40 Å from the original allosteric site, and 50 Å from the new allosteric site. The new allosteric inhibitor site, located inside the central cavity formed on association of the two subunits, binds CP320626 molecule (shown in yellow) and is some 15 Å from the allosteric effector site, 33 Å from the catalytic site and 37 Å from the inhibitor site [109]

The conversion of GP*a* to GP*b* relieves the allosteric inhibition that GP*a* exerts on the glycogen-associated PP1, which converts glycogen synthase D to the I form, thus allowing the phosphatase to stimulate the synthesis of glycogen. On the T to R transition the quaternary structural change is

represented by a 5° rotation of each subunit around an axis close to the interface between the cap´ region (residues 36´ to 47´, from the symmetry subunit) and helix a2 (Figure 24).

In the native T-state enzyme there is no access from the surface to the buried catalytic site. Access to this site is partly blocked by the 280s loop (residues 282 to 286). On the transition from the T-state to the R-state, the 280s loop becomes disordered and displaced, thus opening a channel that allows a crucial amino acid, Arg569, to enter the catalytic site in place of Asp283 and create the phosphate recognition site. This also provides access to glycogen substrate to reach the catalytic site. The shift and disordering of the 280s loop is associated with changes at the intersubunit contacts of the dimer that give rise to the allosteric effects [114].

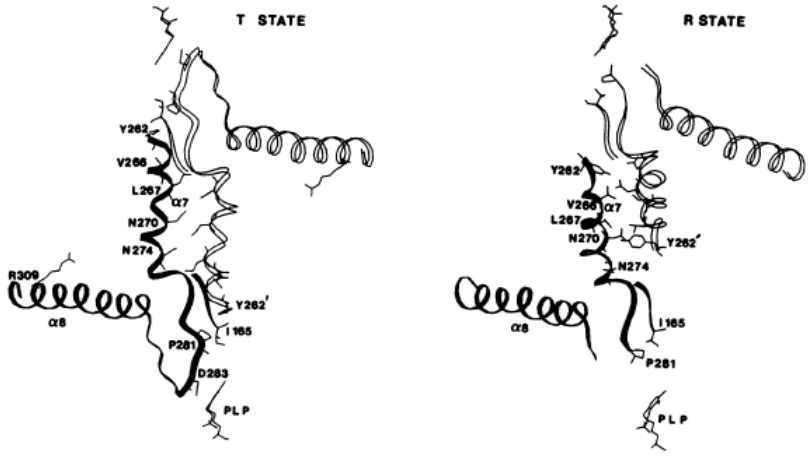

Figure 24 The change in the tower helices on the T to R activation of GPb. The view is down the twofold axis of symmetry [113]

In the last decade GP has been the target for inhibitor design [115-117] and many compounds have been reported. Several binding sites have been indentified in GP: the serine 14-phosphate recognition site, **the allosteric site** that binds the activator AMP and the inhibitor glucose 6-phosphate, **the catalytic site** that bind substrates glucose 1-phosphate and glycogen, and the physiological inhibitor glucose, **the inhibitor site**, which binds caffeine and related compounds, **the glycogen storage sit**e, and **the new allosteric site** that binds indole compounds [109, 113, 118]. The overall architecture of the native T-state muscle GP*b* with the active, the AMP, the phosphorylation, the purine, and new allosteric site is shown in Fig. 23, with the two subunits of the functionally active dimer related by a crystallographic 2-fold symmetry axis.

II.3.2.1. The GP binding sites

The catalytic site of GP is buried at the center of each monomer, and has been extensively investigated with glucose analogue inhibitors that bind at this site and promote the less active T state through stabilization of the closed position of the 280s loop, between helices α7 and α8, and blocks access of the substrate (glycogen) to the catalytic site [119]. This position prevents the crucial conformational changes that take place on activation of the enzyme that are critical for catalytic activity and create the phosphate recognition site.

The glycogen storage binding site of GP, which serves as a region through which the mammalian enzyme is attached to glycogen particles *in vivo*, is on the surface of the molecule, some 30 Å from the catalytic site. This site was identified from crystallographic binding studies with maltopentaose (G5) and matopentaose (G7) [120, 121].

The inhibitor binding site of GP is situated on the surface of the enzyme, at the entrance to the catalytic site (some 12 Å from it); it is a hydrophobic binding pocket and comprises residues from both domains 1 and 2. Occupation of this site stabilizes the T-state conformation of the enzyme and blocks access to the catalytic site, thereby inhibiting the enzyme. Inhibition of this site is generally synergistic with glucose, suggesting that inhibition could be regulated by blood glucose levels and would decrease as normoglycemia. This site has been probed with purines, nuclosides, nucleotides [109] and, more recently, flavopiridol [117].

The allosteric (or AMP) binding site of GP is situated at the subunit–subunit interface some 30 Å from the catalytic site; An inhibitor site, which binds purine compounds. The allosteric site, which binds the physiological allosteric activator AMP, and allosteric inhibitor glucose 6-phosphate, has been also shown to bind the Bayer compound W1807 (**49**; Fig. 25), the most potent inhibitor of GP known to date (Ki= 1.6 nM for GP*b* and Ki=10.8 nM for GP*a*) and several dihydropyridine diacid analogues [122-124].

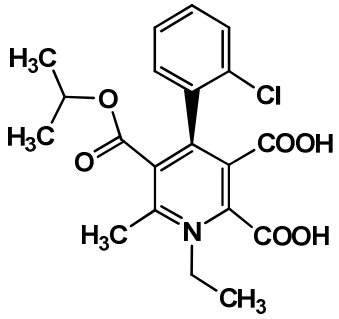

49(Bay W1807)

Figure 25 Chemical structure of Bay W1807 compound

Ligands occupying this site are able to inhibit GP by either direct inhibition of AMP binding and/or indirect inhibition of substrate binding through stabilization of the T- or T'-state conformation.

The new allosteric (or indole) binding site of GP, is located inside the central cavity of the dimeric enzyme, is formed on association of the two subunits. The allosteric site was discovered from crystallographic studies of the binding of indole-carboxamide (**50**; Fig. 26) and related synthetic counterparts like **51**, **52** [125], and **53** (Fig. 26) [126].

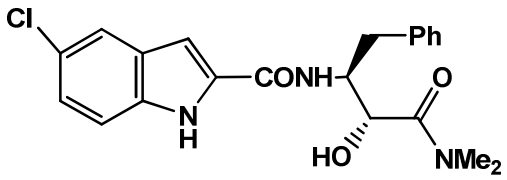

50

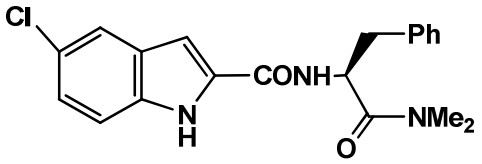

51

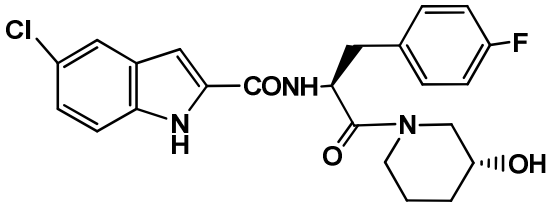

52

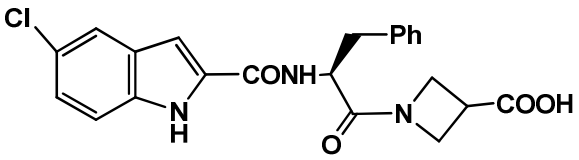

53

Figure 26 Chemical structure of compounds **2**, **3**, **4** and **5**

II.3.2.2. Glycogen metabolism

The liver is the predominant source of glucose. Hepatic glucose is produced in 2 pathways: *glycogenolysis* (the breakdown of glycogen), and *gluconeogenesis* (synthesis of glucose). Glycogenolysis is catalyzed in liver, muscle and brain by tissue specific isoforms of GP [127]. Hepatic glucose output is regulated by a complex system of enzyme, GP, and only the phosphorylate form (GP*a*) has the significant activity. GP*a* release glucose 1-phosphate from glycogen as show in Fig. 27 suggesting an important role for glycogenolysis in hepatic glucose production. Therefore the inhibition of hepatic GP could suppress glucose production arising from both glycogenolysis and glucogenolysis.

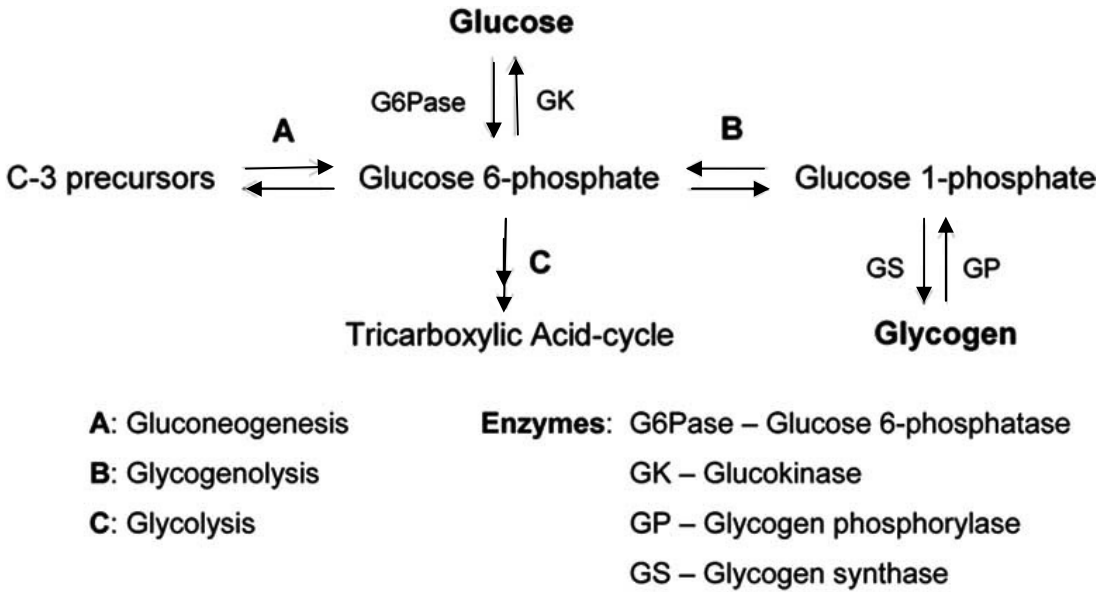

Figure 27 Overview of hepatic glycogenolysis and gluconeogenesis [127]

The conversion of GP*b* (inactive) to GP*a* (active) occurs through the phosphorylase kinase catalyzed addition of phosphoryl group to a hydroxyl group of a specific serine (Scheme 8). The reverse reaction of dephosphorylation that inactivates the enzyme is catalyzed by protein phosphatase 1, an enzyme that is regulated in response to insuline.

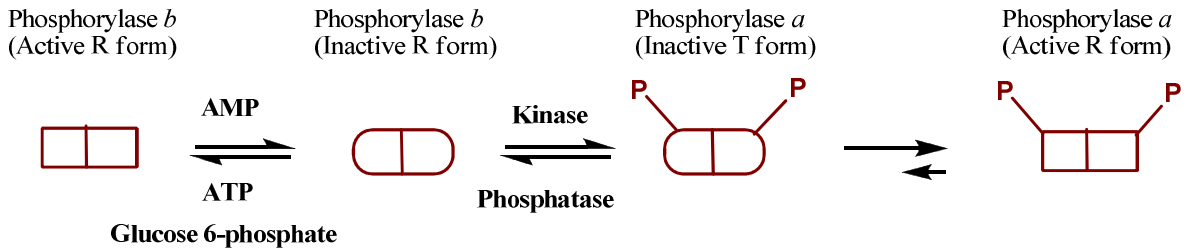

Scheme 8 The convertion of GP*b* in GP*a*

The conversion of GP*a* to GP*b* relieves the allosteric inhibition that GP*a* exerts on the glycogen-associated protein phosphatase 1, which converts glycogen synthesis, thus allowing the phosphatase to stimulate the synthesis of glycogen [128, 129].

GP, breaks up glycogen into glucose subunits (scheme 9).

Glycogen is a polymer of glucose residues linked mainly by α(1→4) glycosidic linkages. There are α(1→6) linkage at branch points. The chain and the branches are longer than shown. Glycogen is

left with one less glucose molecule, and the free glucose molecule is in the form of glucose 1-phosphate (**54**, Fig. 27).

Glycogen $_{(n\ residues)}$ + P_i → glycogen $_{(n-1\ residues)}$ + glucose-1-phosphate

Scheme 9 The break up of glycogen

In the liver, glucose 1-phosphate is mostly converted by phosphoglucomutase and glucose 6-phosphatae (**55**; Fig. 28) to glucose, which is relased for the benefit of other tissues [127], especially the central nervous system that relies on glucose as its majour source of fuel.

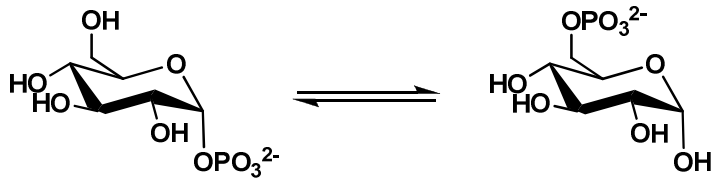

54 **55**

Figure 28 The conversion of glucose 1-phsphate in glucose 6-phosphate

Glycophosphorylase can only act on linear chain of glycogen (α(1→4) glycosidic linkage). Its work will imediately come to a half four residues away from α(1→6) branch (which are exceedingly common in glycogen). In these situation, a debranching enzyme is necessary, which will straighten out the chain in that area. Addditionally, an α(1→6) glucosidase enzyme is required to break the remaining α(1→6) residue that remains in the new linear chain. After all this is done, glycogen phosphorylase can continue.

II.3.3. Inhibitors of GP having a sugar moiety

In the last decade GP has been the target for inhibitor design [115] and many compounds have been reported to bind to five distinct sites, the catalytic, the glycogen storage, the allosteric, the new allosteric (or indole), and the inhibitor (or caffeine site) binding sites [109]. The efficacy of such inhibitors on blood glucose control and hepatic glycogen balance has been confirmed in *ex vivo* cell biology experiments and in animal models [115, 130].

Glucose is a physiological regulator of hepatic glycogen metabolism that promotes inactivation of glycogen phosphorylase and acts synergistically with insulin, leading to diminished glycogen degradation and enhanced glycogen synthesis [131]. Glucose inactivates phosphorylase *a* by competitive inhibition with substrate and by stabilization the T state (less active) form of the enzyme [132]. The knowledge of the tree-dimensional structure of T-state GP *b*-α-D-glucose complex has been used for the design of efficient inhibitors of GP that may prove beneficial in the regulation of glycogen metabolism in *type 2* diabetes [133]. Glucose is an effective allosteric inhibitor for both GP*a* and GP*b* with K_i values in the low mM range (for GP*a* K_i = 2.0mM and for GP*b* K_i = 1.7mM). Glucose binding at the catalytic site, promotes the less active T state. The binding of the catalytic site is dominated by the hydrogen bonds from each of the peripheral hydroxyl group to the protein atoms with the exception of only one charged group involved in polar contacts [134, 135].

N-acetyl-β-D-glucopyranosylamine (NAG) (**56**; Fig. 29) was the first efficient glucose analogue inhibitor of GP, which inhibited GP*b* activity with a K_i = 32 μM more than ~60 times lower than for the corresponding K_i of glucose [136].

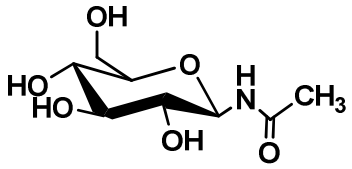

56

Figure 29 Chemical structure of NAG

The crystal structure of GP*b*-**56** complex at 1.9 Å resolution has shown that **56** fits neatly into the so-called β-pocket, a side channel from the catalytic site, lined by both polar and nonpolar groups and binding is stabilized through a strong hydrogen bond formed between the glycosidic amide nitrogen and the main chain carbonyl *O* of histidine (His 377) [137].

A large array of compounds with the NAG structure was synthesized, and tested. *N*-acetyl-*N*'-β-D-glucopyranosyl urea (**57**, Acurea; Fig. 30) and *N*-benzoyl-*N*'-β-D-glucopyranosyl urea (**58**, Bzurea; Fig. 30) with a K_i = 370 μM and K_i = 4.6 μM, respectivily [138].

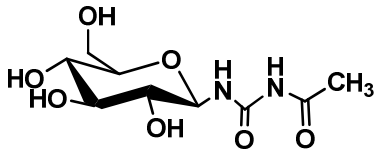

57

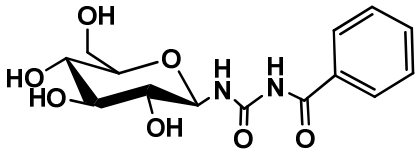

58

Figure 30 The chemical structure of Acurea(**57**) and Bzurea(**58**)

Acurea, binds at the catalytic site of GP*b* with essentially no disturbance of the structure, through noumerous hydrogen bonds and van der Waals interactions with residues at the active site of the enzyme. Bzurea binds tightly at the catalytic site and induces significant conformational changes in the vicinity of the site, promoting the less active T state through rearrangement and stabilization of the closed conformation of the 280s loop. The urea and benzoyl moieties fit tightly into the so-called β-pocket, a side channel from the catalytic side with no access to the bulk solvent. Furthermore, Acurea and Bzurea bind at the new allosteric site of GPb, which is highly specific for indole derivatives and currently a target for the development of hypoglycaemic drugs [119].

Introduction of a large hydrophobic group in the amide nitrogen of NAG led to more effective inhibitor *N*-(β-D-glucopyranosyl) 3-(2-naphtyl) propenoic acid amide (**59**; Fig. 31) (K_i = 4 μM). The strong binding of the 2-naphtyl derivative was attributed to its extensive interactions upon binding with the residues lining the so-called β-pocket of the catalytic channel of the enzyme [127, 138].

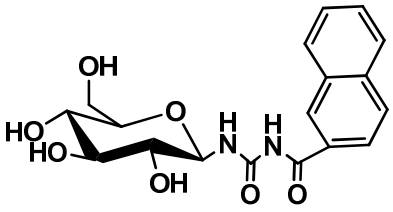

59

Figure 31 Chemical structure of N-(β-D-glucopyranosyl) 3-(2-naphtyl) propenoic acid aminde

The β-pocket is located next to the catalytic site of the enzyme in the direction of the β-anomeric substituent of bound D-glucose derivatives surrounded by both polar and apolar amino acid site chain [109]. The positions of water molecules occupied this site in the native GP*b*, provides insights for the design of new glucose analogues with substituents that would optimize the network of interactions with protein residues in close vicinity.

A very interesting peculiarity of these ureas is their ability to bind at the new allosteric site as well. This property has been demonstrated for the first time with the bezoyl urea **57** [139], and was also detected by X-ray crystallography.

However, even amide **60** (K_i = 3.5 μM) (Fig. 32) was also found bound at that binding site. Thus, new lead structures have been found to explore the properties of the new allosteric binding site [140].

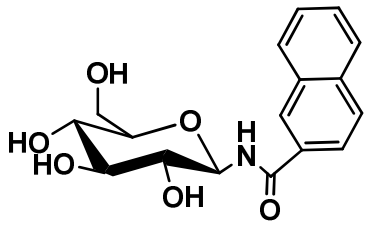

60

Figure 32 Chemical structure of N-(β-D-glucopyranosyl) 3-(2-naphtyl) propenoic acid aminde

It was shown that properly positioned and large enough hydrophobic groups attached to the amide moiety (as compound **60**) lead to increase of the inhibition potency by at least one order of magnitude than that of the best amide inhibitor known earlier (NAG) but they are still less efficient than the best known inhibitor of GP, urea **59**. Thus, it was concluded that the acyl urea moiety is essential for the strong inhibition.

Replacement of acyl group, in NAG, by an azidoacetyl group (compound **61**; Fig. 33), resulted in a decrease of the inhibitory potency (K_i = 48.7 μM) on GP*b*.

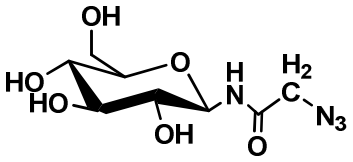

61

Figure 33 Chemical structure of azido-NAG

Structural studies have shown that azido-NAG (**61**), as compared to the NAG, on binding to the enzyme, forms additional contacts with the protein at the catalytic site which provide a rationale for the kinetic properties of the inhibitor [141].

However, other representative inhibitors of D-glucopyranosyl derivatives with triazole groups at the anomeric position (**62**, **63**, and **64**; Fig. 34) proved also micromolar inhibitors [142]. The α-D-glucopyranosyl derivatives **63** are generally significantly less efficient; compounds **64** are non-

inhibitory with a exception when R is 2-naphtyl which is a very weak inhibitor, from this series **62** compounds exhibit the strongest inhibition with some compounds (when R is CH_2OH and 2-naphtyl) in the low micromolar range. The weak inhibition of these compounds may reveal favorable polar/ionic contacts with the enzyme, however, does not break the general tendency that α-anomeric substituent's of the D-glucopyranosyl ring are not really efficient to make good inhibitor [143, 144].

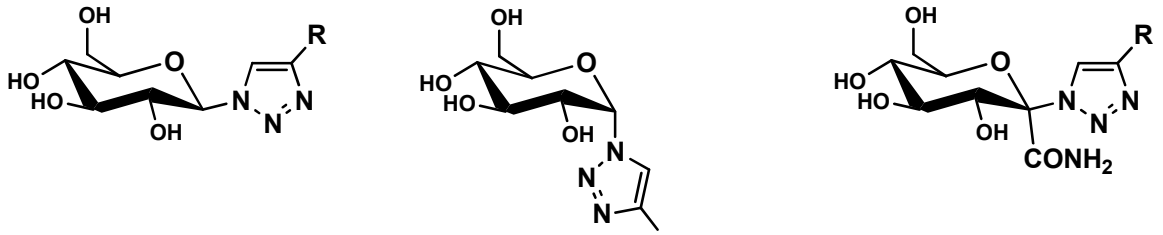

62 **63** **64**

Figure 34. Chemical structure of compounds **62**, **63** and **64**.

Following crystallographic analysis of the GPb-NAG complex, a large number of derivatives were synthesized and studied by X-ray crystallography with the objective to identify more potent inhibitors. Glucopyranosylidene spirothiohydantoin (**65**; Fig. 35) glucopyranosylidene spirohydantoin (**66**; Fig. 35), another class of compounds having a sugar moiety, has been identified as inhibitors of both muscle and liver GP*b* (K_i = 5.1 μM for **65** and K_i = 3.1 μM for **66**, respectively) and GP*a* showing to diminish liver GP*a* activity in *vitro*.

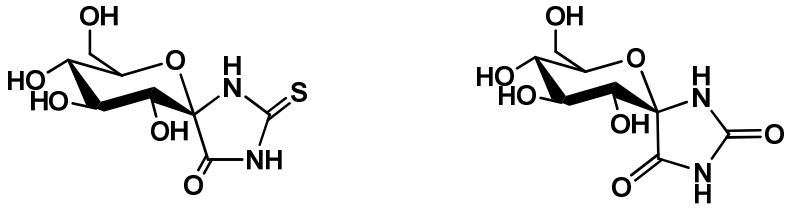

65 **66**

Figure 35 Chemical structures of compounds **65** and **66**

The structure of GP*b*-**65** complex revealed that the inhibitor was accommodated in the catalytic site of T state GP*b* with very little change of the tertiary structure, and provided a basis of understanding its potency and specificity. The glucopyranose moiety makes the standard hydrogen bonds and van der Waals contacts as observed in the glucose complex, while the rigid

thiohydantoin group is in a favorable electrostatic environment and makes additional polar contacts to the protein [145].

Crystallographic studies on the GP*b*-**66** complex relayed the structural features responsible for the tight binding of the catalytic center: i) hydrogen bonds between N(H) of the hydantoin and the main chain oxygen of His377 which also facilitates an optimal hydrogen bond between CH_2OH moiety in the glucose and the side chain of His377; ii) the rigid planar spyrohydantoin group undergoing little loss of conformational energy on binding; iii) the hydrogen bonding capability of the hydantoin polar groups exploiting existing water structure and creating additional water network to the protein, thereby providing additional enphalitic constributions [139, 146].

Amidocarbamate (**67**; Fig. 36) [147], the open chain of spirohydantoin (**66**; Fig. 35), is a very good inhibitor of GP*b*, with respect to glucose 1-phosphate, with a K_i = 16.5 μM. The crystallographic studies of GP-**67** complex have shown that amidocarbamate bind tightly at the catalytic site of T state GP*b*.

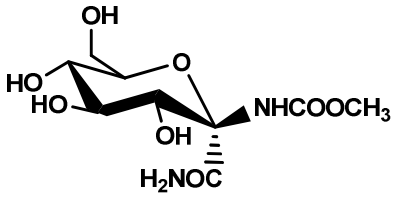

67

Figure 36 Chemical structure of compound **67**

Compounds with two sugar moieties attached to the terminal nitrogen of urea series (**68** and **69**; Fig. 37) showed very low inhibition of the enzyme activity (milimolar range) [148].

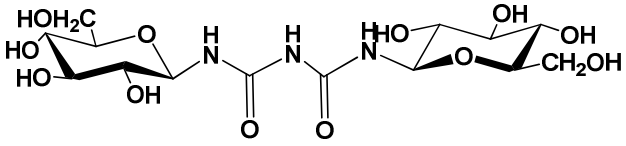

68

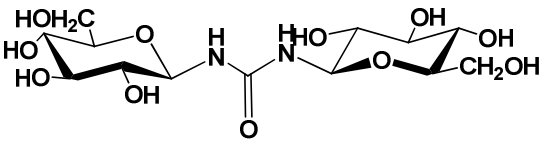

69

Figure 37 Chemical structure of compounds **68** and **69**

A number of β-D-glucose analogues were designed using the program GRID [149] (a program that calculates the nonbonded interaction energy between chemical functional group and the

macromolecule at a number of regularly spaced positions), which can predict energetically favorable substitutions and determine probable interaction sites between a functional group probe (e.g. hydroxyl, amino, methoxy) and the enzyme surface. These analogues were synthesized and tested for inhibition of, and binding to GP*b*. All the β-D-glucose analogues were competitive inhibitors with respect to the glucose 1-phosphate and bound at the catalytic site; they made similar interactions to those formed by α-D-glucose and the positions of the glucose core atoms as well as polar contacts to the peripheral hydroxyl groups of the glucopyranose ring were similar in all the compounds studied. The compounds exhibited a poorer inhibition constant (4.5-25.3; in a milimolar range) compared to the α-D-glucose, and it was argued that the observed increased in K_i is due to the loss of entropy on binding of the flexible β substituent [142].

Inhibition of GP has proven a promising approach in modulating the action of this enzyme which is the main regulator of blood glucose levels. This offers a new concept for fighting against type 2 diabetes an epidemically expanding metabolic disease. There are several binding sites in GP lending themselves to be targeted by various effectors.

II.4. Catalysis

II.4.1. Introduction in catalysis

«..the era of catalysis. *Catalysis* helps to make miraculous conversion with hydrogen, oxygen, nitrogen, or carbon monoxide possible at temperatures several hundred degrees lower than those conditions in which these gases reacted earlier. This chapter of catalysis is nearly unlimited...»
Emil Fisher *Stahl und Eisen* **1912**, 32, 1898.

Catalysis is the process in which the rate of chemical reaction is either increased or decreased by means of a chemical substance known as a *catalyst*. Unlike other reagents that participate in the chemical reaction, a catalyst is not consumed by the reaction itself. The catalyst may participate in multiple chemical transformations. Catalysts that speed the reaction are called *positive catalysts*, catalysts that slow down the reaction are called *negatives catalysts* or *inhibitors*. Substances that increase the activity of catalysts are called *promoters* and substances that deactivate catalysts are called *catalytic poisons*.

Over recent decades, there has been enormous progress in understanding the molecular mechanism leading to efficient catalytic reactions and this has had an explosive effect on developing new catalytic system. Since a large number of processes in the chemical industry now depend on catalysts to work efficiently, it is not surprising that catalysis is an extremely active research area.

Catalysis is a phenomenon of crucial importance not only for chemical and biochemical reactions occurring in nature, but also for chemical laboratories and industry. The production of a variety of chemicals involves catalytic reactions, as they consume less energy and generate less waste than stoichiometric ones.

Catalysts participate in chemical reactions by changing the kinetics, while the reaction results and the overall thermodynamics are the same (Fig. 38). The following factors can explain the effect of the catalyst on the reaction:

- Stabilization of the transition state:
- Decreasing the entropy of the reactants, by increasing that force their proximity and favorable spatial orientation;
- Selective enhancement of one specific pathway over the competing, undesired ones.

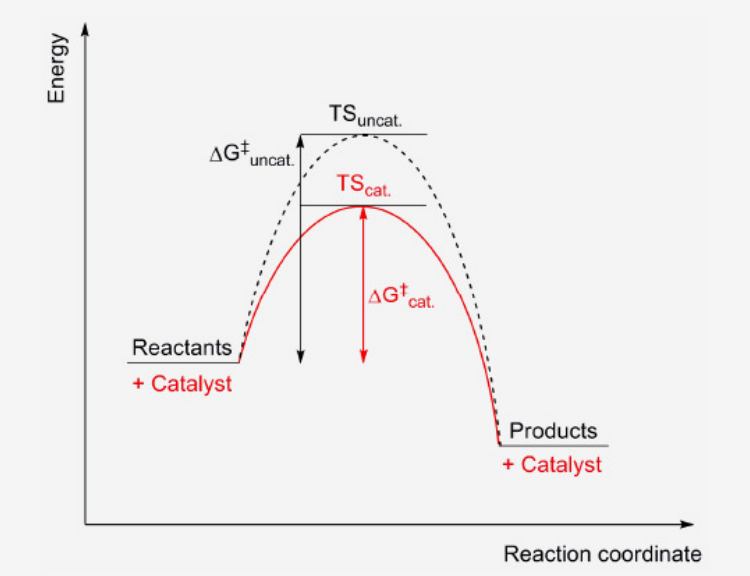

Figure 38 Effect on the catalyst on the reaction's Gibbs energy of activation

In a general sense, anything that increases the rate of a process is a catalyst, a term derived from the Greek "καταλύειν", meaning 'the annul', or 'to untie', or 'to pick up'. The term «catalysis» was first introduced by Jöns Jakob Berzeluis, who in 1835 noted that certain chemicals have the property of accelerating a reaction [150]. Later, Humphry Davy discovered that the oxidation of coal gas is catalyzed by platinum. In the 1880's, Wilhelm Ostwald at the Leipzig University gave the definition that a catalyst does not influence the thermodynamic equilibrium, but only affects the chemical rate of the reaction. For this work, Ostwald was awarded the **1909 Nobel Prize in Chemistry** [151].

Catalysis has not only advanced the level of efficiency but has also brought environmental benefits, as the higher selectivity of catalyzed reactions ensures a better usage of raw materials, less waste production and lower energy consumption. The production of the most industrially important chemicals involves catalysis. Similarly, most biochemically significant processed are catalyzed. Research into catalysis is a major field in applied science and involves many areas of chemistry e.g. organometallic chemistry, material science. Catalysis is a relevant to many aspects of environmental science, e.g. the catalytic convertor in automobiles and the dynamics of the ozone hole. Catalytic reactions are preferred in environmentally friendly green chemistry due to the reduced amount of waste generated [152], as opposed to stoichiometric reactions in which all reactants are consumed and more side products are formed. The most common catalyst is the proton (H+). Many transitional metals [153] and transitional metal complexes [154-157] are used in catalysis as well.

II.4.2. Applications of catalysis

The importance of catalysis and its applications in an academic and industrial level is obvious from the large number of Nobel Prizes already given in this topic. **Only in the first decade of the 21st century, four Nobel Prizes are dedicated to catalysis.**

2001: Knowles, Noyori and Sharpless for *asymmetric catalysis* (homogeneous).

2005: Chauvin, Grubss and Schrock for *metathesis* (homogeneous).

2007: Ertl for *chemical processes on solid surfaces* (heterogeneous).

2010: Heck, Negishi and Suzuki for *palladium-catalyzed coupling reactions* (homogeneous).

Catalysis plays an important role in many aspects of human progress: in the efficient manufacture of many kinds of materials, from fuels to plastics, in creating new energy sources and protecting the environment and in developing effective, safer medicines. More than 90% of industrial chemical products involve catalysis. It is given below only a few examples amongst a huge number of catalytic reactions with industrial applications.

A large variety of plastics are produced via polymerization.

Production of many drugs involves catalysis, and in particular asymmetric catalysis.

The annual world-wide production of aldehydes and their derivatives by hydroformylation is ca 8,000,000 tons.

Synthesis of ammonia from nitrogen, which employs an iron catalyst containing a small quantity of mixed oxide.

Millions of tones of benzene are hydrogenated each year to give cyclohexane, which is converted to nylon via adipic acid.

In addition, catalysis is a phenomenon of crucial importance not only for chemical and biochemical reactions occurring in nature, but also for chemical laboratories and industry. The production of a variety of chemicals involves catalytic reactions, as they consume less energy and generate less waste than stoichiometric ones. It is now accepted that in recent years homogeneous transitional metal catalysis, in particular carbon-carbon bond formation, had has a major impact in the modern organic chemistry. Academic and industrial research in this field is currently vibrant, and the output in research papers and books attest to this.

II.4.3. Catalysis-homogenous/heterogenous

II.4.3.1. Homogeneous catalysis

In chemistry, *homogeneous catalysis* is a sequence of reactions that involve a catalyst in the same phase as the reactants. Most commonly, a homogeneous catalyst is co-dissolved in a solvent with the reactants. In contrast to heterogeneous catalysis, the homogeneous catalyst remains in the same phase with the reactants involved in the chemical process. Some important advantages of homogeneous catalysis are the mild reaction conditions and the high activity and selectivity.
Homogeneous catalysis was established by the pioneering discovery of hydroformylation in 1938 by Otto Roelen in Ruhrchemie in Oberhausen (Fig. 1) [158]. Today, hydroformylation represents the largest volume industrial application of homogeneous catalysis employing organometallic catalysts, with an annual world-wide production of ca 8,000,000 tons, and has been recognized as the most effective method for the synthesis of aldehydes from olefins.
The pioneering work of G. Wilkinson [159] for alkene hydrogenation using a rhodium-based catalyst (**70**; Fig. 39) had a considerable impact on the development of homogeneous catalysis for the synthesis of organic compounds [160].

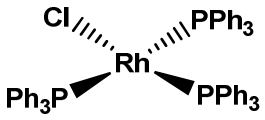

70

Figure 39 Chlorotris-(triphenylphosphine)rhodium, Wilkinson's catalyst for alkene hydrogenation

In nature, we also find some good examples of homogeneous catalysis, e.g. every moment the creation and destruction of ozone (O_3) is taking place. This is happening by oxygen ions. Oxygen molecules absorbing ultraviolet rays and splitting its own molecules into oxygen ions, these oxygen ions once again react with the ordinary oxygen molecules and creating ozone molecules. This may sound like any normal chemical reaction, but it has extreme significance for the survival of living creatures of this planet. By destructing and creating ozone with the help of ultraviolet light, homogeneous catalysis process preventing the penetration of ultraviolet rays to our atmosphere, and thus preventing many life threatening diseases. The hydrogen is the most pervasive homogeneous catalyst because water is the most common solvent. Water forms protons

by the process of self-ionization of water. In an illustrative case, acids accelerate (catalyze) the hydrolysis of ester:

$$CH_3CO_2CH_3 + H_2O \rightleftharpoons CH_3CO_2H + CH_3OH$$

In the absence of acid, aqueous solution of most esters do not hydrolyze at practical rates.

In the recent years, organocatalysis, which is also homogeneous catalysis, has attracted a huge interest. Enzymes are also homogeneous catalysts that are essential for life and also harnessed for industrial processes, but this topic is studied in a separate field of catalysis, so-called biocatalysis.

II.4.3.2. Heterogeneous catalysis

In contrast to homogeneous catalysis (**a**; Fig. 40) in *heterogeneous catalysis* the catalyst and the reactants are in different phase (**b**; Fig. 40). Heterogeneous catalysis offers the advantage that products are readily separated from the catalyst [161].

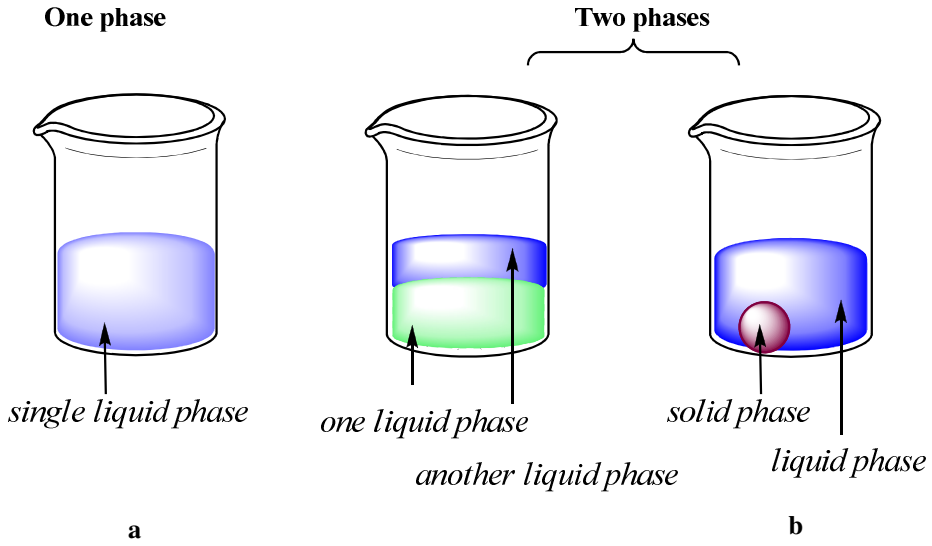

Figure 40 *a)* homogeneous catalysis; *b)* heterogeneous catalysis

Heterogeneous catalysis provides a medium (usually, a surface) on which the reaction may takes place [162].

In order the heterogeneous catalysis reaction to be occurred, one or more of the reactants must diffuse to the catalyst surface and absorb onto it. After reaction, the products must desorb from the

surface and diffuse away from the solid surface. Frequently, this transport of reactants and products from one phase to another plays a dominant role in limiting the reaction rate. Understanding these transport phenomena and surface chemistry such as dispersion is an important area of heterogeneous catalyst research. Catalyst surface area also is considered. Mesoporous silicates [163], for example, have found utility as catalysts because their surface areas may be in excess of 1000 m^2/g, which increase the probability that a reactant molecule in solution will come in contact with the catalyst surface and absorb. If diffusion rates are not taken into account, the reaction rate for various reactions on surfaces depends solely on the rate constants and reactant concentrations.

One example of heterogeneous catalysis is the hydrogenation of carbon–carbon double bond; the simplest example of this is the reaction between ethene and hydrogen in the presence of a nickel catalyst.

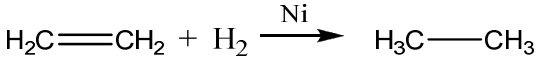

Another example can be carbon monoxide and various nitrogen oxides in car exhaust into more harmless molecules like carbon dioxide and nitrogen.

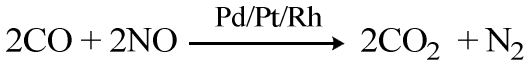

II.4.4. TON/TOF

Two of numerical terms that describe the activity of a catalytic system is the TON (turnover number) and TOF (turnover frequency) which is the catalytic activity of the system. The number of productivity is the catalytic system (catalyst productivity). TON is the total number of mol of product into a mol of the catalytic complex for each reaction [164]. TOF, determined by the average ratio of manufacturing the product, normalized by the initial mol of the catalyst added to the reaction. Based on the catalytic cycles are numerically the "times" that the catalytic cycle is completed within the time unit. The use of TOF number is practically useful for small scale reactions, since the calculation does not reflect important phenomena of the system. [164].

In more chemical fields, such as organometallic catalysis, turnover number is used with a slightly different meaning: the number of moles of substrate that a mole of catalyst can convert before becoming inactivated [164]. An ideal catalyst would have an infinite turnover number in this sense, because it wouldn't ever be consumed, but in actual practice one often sees turnover numbers which go from 100 to a million or more. The term **turnover frequency** (abbreviated TOF) is used to refer to the turnover per unit time, as in enzymology.

TON = fraction of product × substrate/Pd ratio.

II.4.5. Carbon-carbon coupling reactions

When two hydrocarbon fragments are coupled with the aid of a metal containing catalyst had place a *coupling reaction*. Coupling reaction should be divided into two main classes:

- Cross couplings- in which two different molecules react to form one new molecule.
- Homocoupling- in which two similar molecules react to form a new molecule.

An example of homocoupling reaction would be Ullman reaction [165], which is the reaction of copper metal with two molecules of an aryl halide (**71**) to form biaryl (**72**) [166] (Scheme 10).

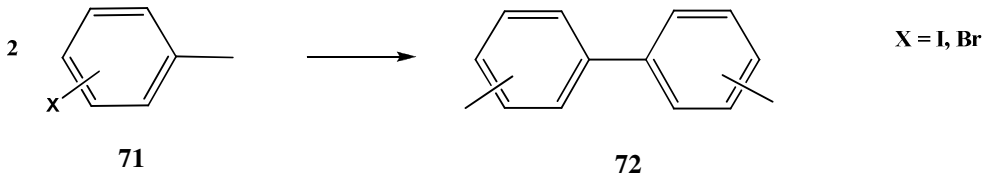

71 **72**

Scheme 10 Ullman reaction

The Ullman reaction often requires very high temperatures, and has partly been replaced in synthetic chemistry by palladium-catalyzed coupling reactions.

A common metal in this type of chemistry is palladium often added in the form of tetrakis(triphenylphosphine)palladium(0) [167]. This is an air-sensitive compound that is very efficient for coupling unsaturated halogen compounds with organometallics such as tributyltin hydride. While many coupling reactions involve reagents that are extremely susceptible to the presence of water and oxygen, but not all coupling reactions need to be performed with strict exclusion of water.

It is possible to perform palladium-based coupling reactions in aqueous solutions using a water-soluble triphenyl phosphine derivative [168]. In general, the oxygen in the air is more able to disrupt coupling reactions, because many of these reactions occur via unsaturated metal complexes that do not have 18 valence electrons. For example, in nickel and palladium-catalyzed cross-couplings, a zerovalent complex with two vacant sites (or labile ligands) reacts with the carbon halogen bond to form a metal halogen and a metal carbon bond. Such a zerovalent complex with labile ligands or empty coordination sites is normally very reactive toward oxygen.

II.4.5.1. Suzuki reaction (2010 Nobel Prize)

One of the most useful cross-coupling reactions between aryl halides and different reagents (alkenes, alkynes, amines, metallorganic compounds) has been the Suzuki–Miyaura reaction [169] that attracts a great attention by the researchers. There is no consensus on the nature of catalysis for this reaction [170]. Analysis of the literature for the last two years indicates that some researchers advance the hypothesis of a homogeneous catalysis mechanism [171-179] while the others suggest a heterogeneous mechanism [178-184]. It is worth mentioning that the most convincing evidence is for the homogeneous mechanism [171-175, 178, 179].
First published in 1979 by Akira Suzuki, the Suzuki reaction couples boronic acid (**75**)(containing an organic part) to halides (**73**)(Scheme 11) [185].

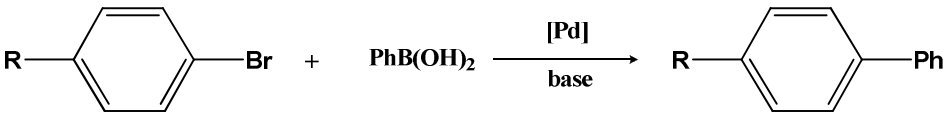

73 **74** **75**

R = H, OCH_3, NO_2, CN, etc.

Scheme 11 Suzuki reaction

The reaction relies on a palladium catalyst such as tetrakis(triphenylphosphine)palladium(0) to effect part of the transformation. The palladium catalyst (more strictly a pre-catalyst) is 4-coordinated, and usually involves phosphine supporting groups. In many publications this reaction also goes by the name *Suzuki–Miyaura reaction*. It is also referred as "Suzuki Coupling".

The palladium-catalyzed cross coupling reaction between organoboron compounds and organic halides or triflates provides a powerful and general method for the formation of carbon-carbon bonds [186, 187]. It is widely used to synthesize poly-olefines, styrenes, and substituted biphenyls, and has been extended to incorporate alkyl bromides [188]. Several reviews have been published [189, 190]. The Suzuki cross-coupling reaction has proven to be a powerful method for combining aryl halides and boronic acid (containing an organic part) to give a ready access to biaryl motifs [191, 192], which are found in a range of pharmaceutical, herbicides and natural products, as well as in conducting polymers and liquid crystalline materials.

A wide range of metal complexes have been used as catalysts in these coupling reactions, attention particulary being focused on palladium. Complexes bearing bulky phosphine [193], N-heterocyclic carbenes [194, 195] or palladacyclic complexes [196] have been found to be particulary active, and allow for the use of aryl chlorides as substrates rather than, with the majority of previous catalyst candidates, aryl bromides and iodides. Suzuki reaction requires the use of a base. This forms a more electron-rich intermediate with the boronic acid which is more reactive than than the original boronic acid towards attack of Pd(II) complexes. The use of water either as a solvent or additive helps with the solvation of these organic-insoluble materials. Also, as organoboron compounds are often quite stable to protolytic decomposition by water, there is significant potential for development of methodologies using water or aqueous media as solvents. When using neat water as a solvent, it is possible to perform the reaction using simple palladium salts such as $PdCl_2$ or $Pd(OAc)_2$ in air.

There are several advantages to this method:

- mild reaction condition;
- commercial availability of many boronic acid;
- the inorganic by-products are easily removed from the reaction mixture, making the reaction suitable for industrial processes;
- boronic acids are environmentally safer and much less toxic than organostannanes (Stille coupling);
- starting materials tolerate a wide variety of functional groups and they are unaffected by water;
- the coupling is generally stereo- and regioselective.

Some disadvantages are:

- generally halides react sluggishly;
- by-products such as self-coupling products are formed because of solvent-dissolved oxygen;
- coupling products of phosphine-bound aryl are often formed

II.4.5.1.1. Mechanism of Suzuki – Miyaura reaction

The catalytic cycle has four distinct steps (scheme 12):

- ✓ oxidative addition of an organic halide to the Pd(0)-species to form Pd(II);
- ✓ exchange of the anion attached to the palladium for the base (metathesis);
- ✓ transmetallation between Pd(II) and the alkylborate complex;
- ✓ the reductive elimination to form C-C sigma bond and regeneration Pd(0).

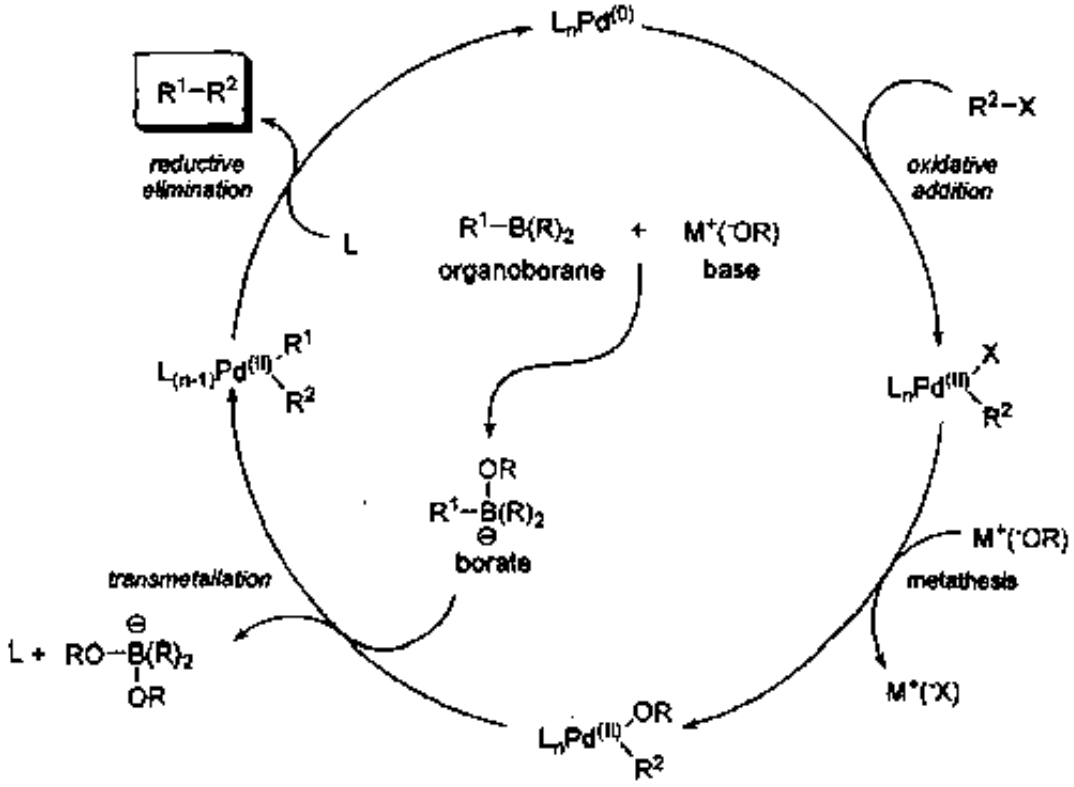

Scheme 12 The mechanism of Suzuki reaction

The reaction also works with pseudohalides, such as triflates (OTf), instead of halides, and also with boron-esters instead of boronic acids. The relative reactivity is: R_2-I > R_2-OTf > R_2-Br >> R_2-Cl.

II.4.5.2. Heck reaction (2010 Nobel Prize)

The palladium-catalyzed C-C coupling between aryl halides or vinyl halides and activated alkenes in the presence of a base is referred as the *Heck reaction*. The nature of the Heck reaction catalysis was discussed since the end of the 90ths [197, 198-205]. In the reviews published in 2006 [197, 200, 201, 206] the authors came to the conclusion on the higher probability of exclusive homogeneous catalysis.

The Heck reaction developed independently by Mizoroki and Heck in the early 1970's. Heck and co-workers reported the reaction under more opportune laboratory conditions by reacting organyl halides (**76**) with olefinic compounds (**77**) in the presence of hindered amine base and catalytic palladium to form substituted olefins (**78**) [207]. However, Mizoroki and co-workers reported the reaction with aryl iodides and potassium acetate in methanol at 120°C independently of Heck.

The Scheme 13 shows the general Heck reaction in which aryl, benzyl and styryl halides react with olefins at high temperatures in the presence of an amine base and a catalytic amount of Pd(0) to form substituted olefins.

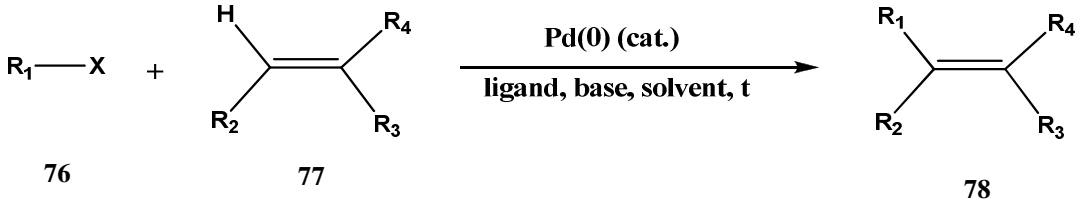

76 **77** **78**

Scheme 13 The Heck reaction

It has also been found that the reaction rate depends on the degree of substitution of the olefinic compound. Generally, more substituted olefins progress at a slower rate than the less substituted olefins. Also, the X group on the aryl or vinyl substituent has a large impact on the rate of the reaction. Typically the order of X group from fastest to slowest rate is I > Br ~ OTf >> Cl. It is typically difficult in catalysis to execute a coupling reaction with an aryl or vinyl chloride and remains a challenge to have it working as well or better than other halides. It is also worth noting that usually unsymmetrical olefins undergo substitution at the least substituted carbon [208].

The Heck reaction has become one of the most useful catalytic carbon-carbon bond forming processes in organic synthesis. Due to the Heck reaction being a reasonably simple way to synthesize substituted unsaturated compounds, its application is widely used in polymerization chemistry, UV screens, pharmaceuticals, preparation of hydrocarbons, and in advanced enantioselective synthesis of natural products [209].

II.4.5.4. Phosphane-free ligands used in coupling reactions

Coupling reactions are usually catalyzed by phosphorus ligands, and a large number of such ligands have been reported for the Suzuki [210-213] as well as the Heck reaction [214-217]. However, these catalysts are often water- and air-sensitive. Nevertheless, catalysis under phosphane-free conditions is a challege of high importance and a number of phosphine-free ligands have been reported for the Suzuki [106, 107] and the Heck reaction [218-221] in addition to ligand-free palladium catalysts [222].

In the recent years, for the **first time**, Kostas, Kovala-Demertzi and their co-workers used thiosemicarbazones as efficient ligands in the palladium-catalyzed Heck reaction of aryl bromides (from electron-rich to electron-poor) with styrene to afford stilbenes with a high selectivity towards the *trans*-stilbenes [105], and Suzuki reaction of aryl halides with phenylboronic acid to afford biphenyls in high yields under conventional heating [106] or a microwave irradiation [107]. The palladium complexes used as catalysts are shown in Fig. 41 (**79, 80** and **81**). Catalysis was performed in air with high turnover numbers. Palladium complex **80** is currently **commercially available** by ALDRICH (Product No.: 674125) and SANTA CRUZ (Product No.: sc-253529).

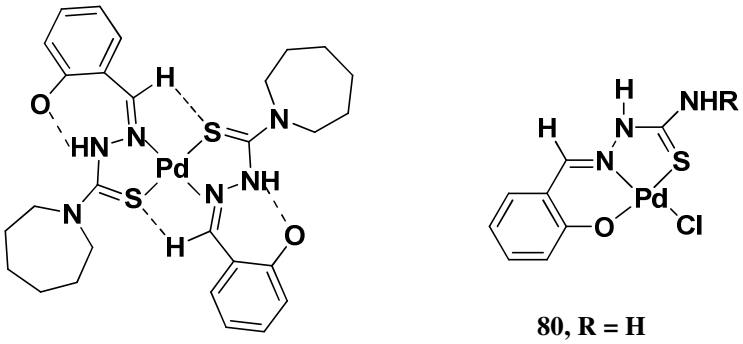

79

80, R = H
81, R = Et

Figure 41 The first Pd/thiosemicarbazones complexes used as catalysts in coupling reactions

Additionally, Kostas, Steele et al. synthesized palladium chelate complexes with S- or Se-containing substituted salicylaldehyde Schiff base derivatives (**82-85**, Fig. 42), which are thermally and air stable and efficiently catalyze the Suzuki-Miyaura cross-coupling of aryl bromides with phenylboronic acid in air [192].

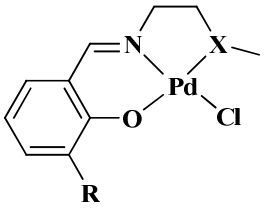

82, X = S, R = $CH(CH_2CH_3)_2$
83, X = S, R = H
84, X= Se, R = $CH(CH_2CH_3)_2$
85, X = Se, R = H

Figure 42 Palladium complexes with S- or Se-containing Schiff base ligands as catalysts for the Suzuki reaction in air

Nájera [223] have demonstrated that Suzuki coupling reaction of aryl chlorides with arylboronic acid in high conversion can be achieved by using the cyclopalladate dimino complex **86**, and Liu and co-worker found that complex **87** and **88** could act as a catalyst for the same reaction in aqueous medium [224]. (Scheme 16)

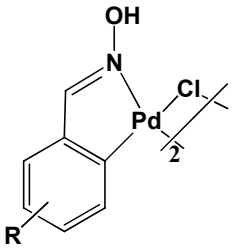

86

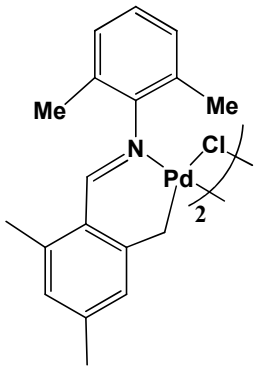

87

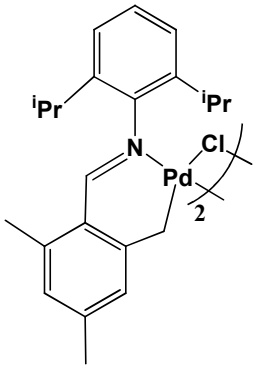

88

Scheme 16 Examples of palladium(II) cyclopalladate dimino complexes

II.4.6. Asymmetric catalysis (2001 Nobel Prize)

Asymmetric catalysis or more correct enantioselective catalysis in organic synthesis introduces one or more new and desired elements of chirality [225]. Asymmetric catalysis is recognized as a highly attractive strategy for the synthesis of chiral building blocks, which are indispensable for the synthesis of biologically active compounds.

The reactions can be promoted by small amounts of chiral or enantiomerically pure (or enriched) catalysts to lead the formation of enantiomerically pure or enriched products [226].

Asymmetric catalysis employs three different kinds of chiral catalysts:

- metal ligand complexes derived from chiral ligands
- chiral organocatalysts (small organic molecules)
- biocatalysts (enzymes)

One of the most important achievements in the field was the preparation, in 1975, of DIPAMP by Knowles et al. [227]. This chiral diphosphine combines the good properties of C_2–symetric chelating system with the simultaneous presence of two asymmetric phosphorus atoms. DIPAMP was efficient in asymmetric hydrogenation of dehydroaminoacids (ee's of up to 90–95%), allowing the preparation of (*L*)-DOPA (a drug useful in treating Parkinson disease), through rhodium-catalyzed asymmetric hydrogenation, (Scheme 17). Synthesis of L-DOPA (**90**) was the first industrial catalytic asymmetric synthesis [228].

89 **90**

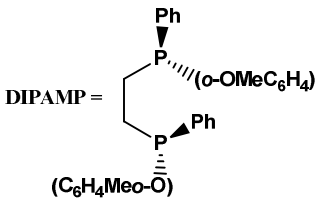

91

Scheme 17 Synthesis of L-DOPA and the chiral ligand used for the catalytic hydrogenation

The soluble metal-ligand complexes for asymmetric hydrogenation have started a new era in catalytic processes. Ryoji Noyori discovered the BINAP-ruthenium(II) complexes, which proved to be excellent catalysts in the asymmetric hydrogenation of various functionalized alkenes and ketones with very high enantioselectivities [229].

Parallel to the progress in catalytic asymmetric hydrogenation, Barry K. Sharpless developed chiral catalysts for asymmetric oxidation reactions [230]. For their work in the field of asymmetric

catalysis, W. Knowles, R. Noyori, B. K. Sharpless were awarded the 2001 Nobel Prize in Chemistry. Their discoveries have had a significant impact on academic and industrial efforts to obtain chiral compounds.

II.4.7. Carbohydrates in catalysis

Carbohydrates have been recognized as important tools in organic chemistry [231, 232], are readily available, higly functionalized, and have several stereogenic centers they have widely been used in transition-metal catalyzed asymmetric reaction [233]. A number of carbohydrate-based phosphines have been used, in conjunction with palladium acetate, as catalysts. Those ligands derived from halo- and amino-sugars forming glycoside [234] and glycosamine [235] based phosphines have received most attention (Fig. 43). They show higher activities than sodium triphenylphosphine-*m*-sulfonate (TPPMS) and *m*-trisulfonated triphenylphosphine (TPPTS) based analogues.

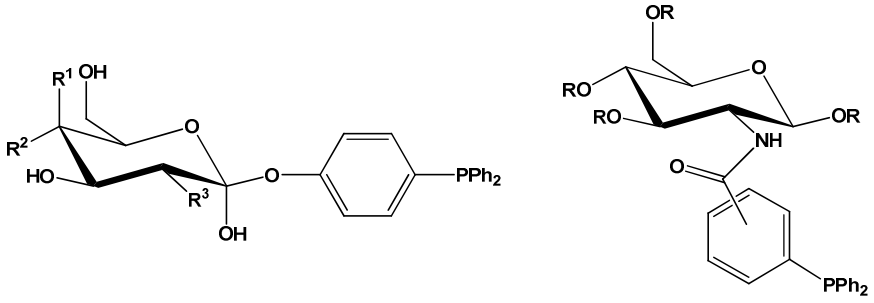

92 **93**

Figure 43 Two examples of glycoside and glycosamine derivatives

Phosphines (**94**, **97**; Fig. 44) also phosphinites (**95**; Fig. 44) [236, 237] and phosphites (**96,** Fig. 44) derived from sugars have already been developed [238, 239] and used successfully as ligands in asymmetric catalysis.

In particular, sugar derivatives which contain two elements with a different coordinating ability (e.g. **97**) were found to be efficient systems for palladium-catalyzed asymmetric allylic substitution [240-242].

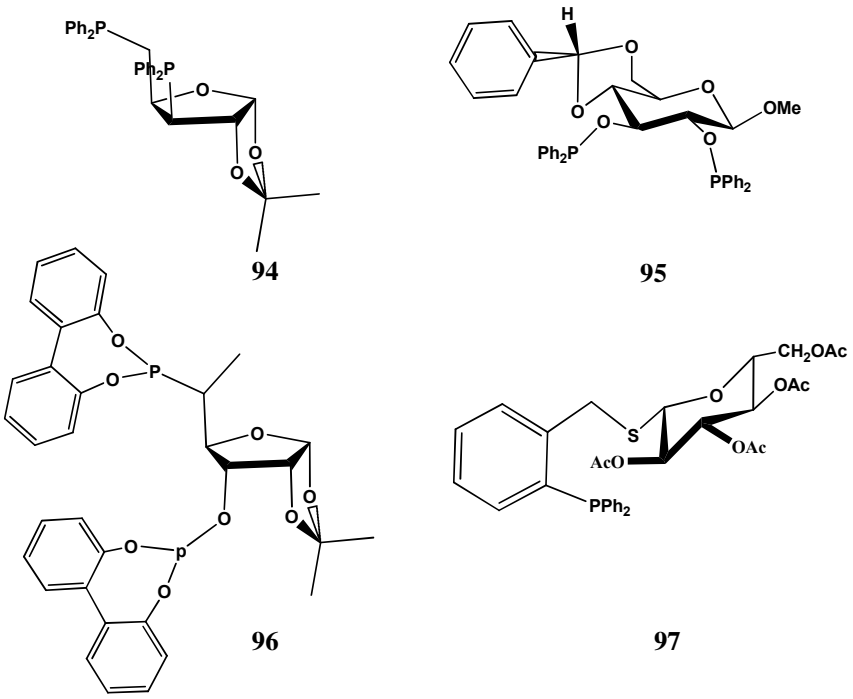

Figure 44 Examples of chiral ligands derived from saccharides

Sugars are used as building blocks in ligand synthesis, posses ~~a~~ chiral carbons but the water solubility of the compounds was not reached. A common problem is the air sensitivity of many of these compounds.

Meanwhile complexes of glucose are known, in which palladium(II) is coordinated with two adjacent deprotonated OH groups (**98**; Fig. 45) [243]. Compared to the previous examples, this substance has the advantage to be stable and soluble in an aqueous solution, at least at lower temperatures around 5°C. However, this compound did not display a catalytic activity.

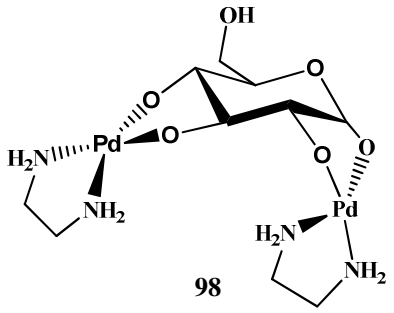

Figure 45 Chemical structure of Pd(II) complex **98**

Mannose and glucose analogues were also synthesized which form with platinum [244] and palladium [245] stable N, N-chelate ligands. An example **(99)** is shown in Fig. 46.

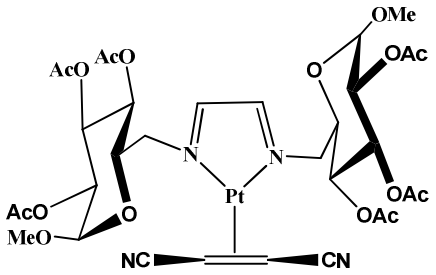

99

Figure 46 A example of platinum(0)-complex with a bidentate derivative of α-D-glucose

Beller et al. described the successful biphasic (xylene / ethylene glycol) Heck reaction [246], catalysed by a palladium complex with a carbohydrate-substituted triphenylphosphine (**100** and **101**; Fig. 47).

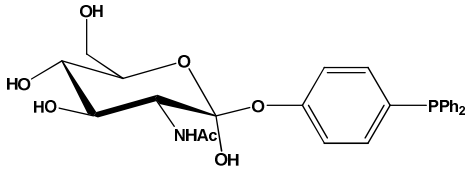

100

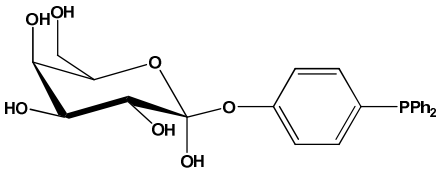

101

Figure 47 Two examples of carbohydrates-substituted triphenylphosphine

In the presence of the complex obtained from $[Pd(\eta^3\text{-}C_3H_5)Cl]_2$ and a chiral amphiphilic phosphinite-oxazoline, asymmetric allylic substitution of 1,3-diphenyl-2-propenyl acetate in water or in an aqueous/organic biphasic medium [247] has been performed and recycling of the catalyst (**104**) is possible (Scheme 18).

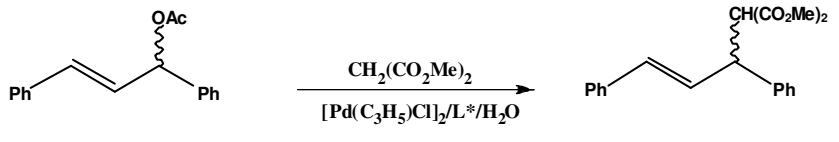

102 **103**

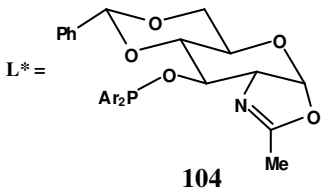

104

Ar = $C_6H_4CH_2N^+Et_2MeBF_4^-$ **ee = 82%**

Scheme 18. Allylic substitution reaction

It has been observed that, when the reaction is performed in presence of surfactant, the rate of palladium-catalyzed allylic alkylation in water is drastically enhanced [248]. However, when a chiral ligand such BINAP is used in the presence of centyltrimethylammonium hydrogen sulphate, enantioselectivity up to 92% is obtained in the reaction of dimethyl malonate with 1,3-diphenyl-2-propenyl acetate [249, 250].

III. Results and Discussion

III.1. Synthesis and characterization of aromatic aldehyde/ketone 4-(β-D-glucopyranosyl) thiosemicarbazones

After optimization of the synthetic pathways shown below for the target molecules, our synthetic protocol includes condensation of a glucose-thiosemicarbazide with the appropriate aldehyde or ketone.

III.1.2. Glucose–thiosemicarbazide (112)

In the past, only some sporadic papers have been published for the synthesis of the thiosemicarbazide **112** [251-258]. Two general protocols were investigated for its sytnhesis shown in route (*A*) and route (*B*) in the Scheme 19.

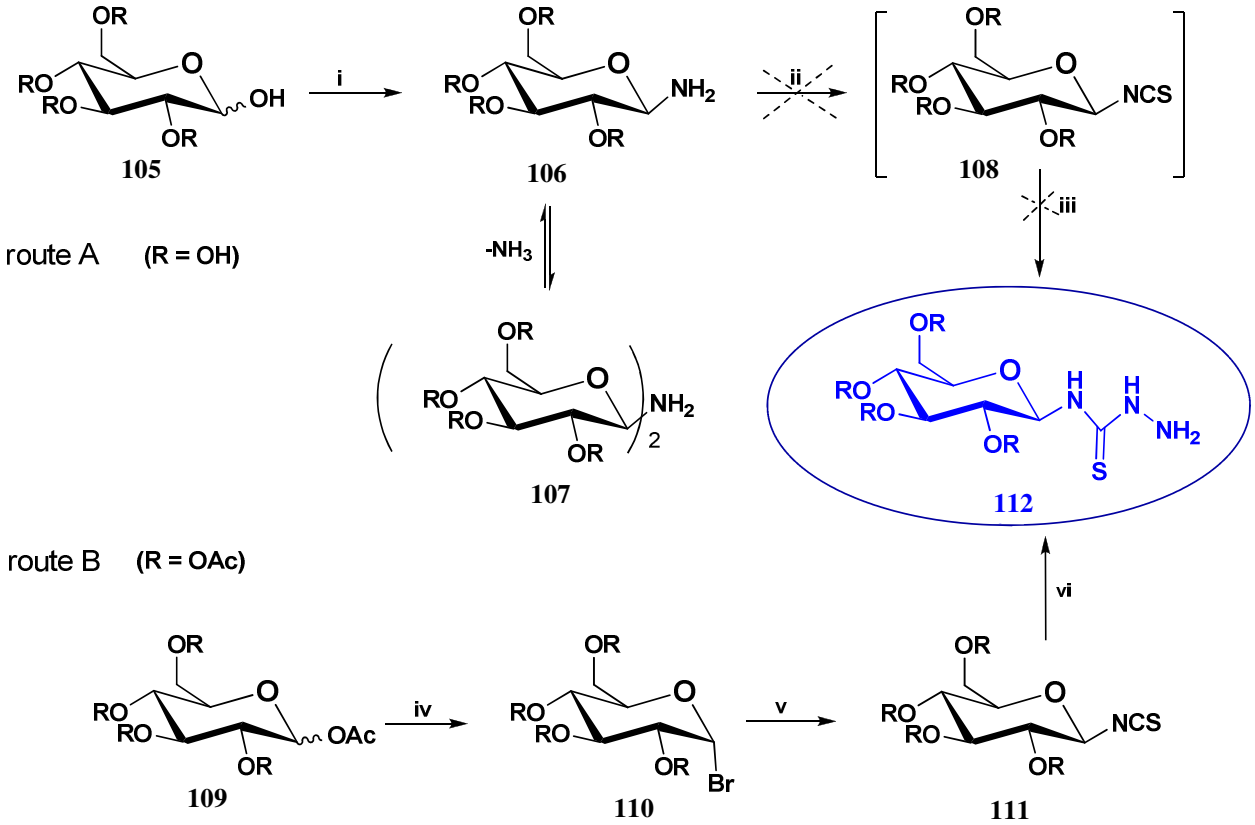

i:NH_2COONH_4, MeOH-NH_4OH, *N,N*-diisopropylethylamine, 37°C; ii:$CSCl_2$, pH8 ($NaHCO_3/CO_2$), 1:1 water/dioxane, −10°C, 30min; iii:N_2H_4, pH 9 $NaHCO_3/CO_2$), r.t. 2-5h; iv:HBr/CH_3COOH, Ac_2O; v: KSCN; vi: N_2H_4 dry, EtOH, ~5°C, 10min.

Scheme 19 Synthesis of β-D-glucose-thiosemicarbazide **112**

Route (A)

In order to obtain the thiosemicarbazide **112**, first of all we had to synthesise the glucopyranosyl amine **106**, which is not commercially available. Glucosylamine **106** can be obtained by two methods: *a*) a clasical method, based on the reaction of glucose with NH_3 [259] which requires a very long time for the reaction to be completed, or *b*) by treatment glucose with a mixture of ammonium carbamate and an aqueous NH_3 solution which involves a intermediate isolation of the salt of glucosylamine with carbamic acid, stable upon storage [260]. In order to avoid very long reaction times, we followed the second method in accordance to the literature information.

The ^{1}H-NMR spectrum of a D_2O solution of the compound **106** showed a signal at 4.08 ppm, characteristic of β-glycosylamine and another signal at 4.29 pmm indicated the presence of a small amount of di-β-glucosylamine **107**, as show in Fig. 50. Poor solubility of glucosylamine **106** in most solvents creates problems in its purification. The next steps invlolve treatment of **2** with $CSCl_2$ to yield the glucopyranosyl isothiocyanate **108**, and then its reaction with hydrazine to afford thiosemicarbazide **112** [261]. The reaction products were analyzed by ^{1}H NMR and showed that this procedure is not efficient enough for the preparation of pure **112** in high yield.

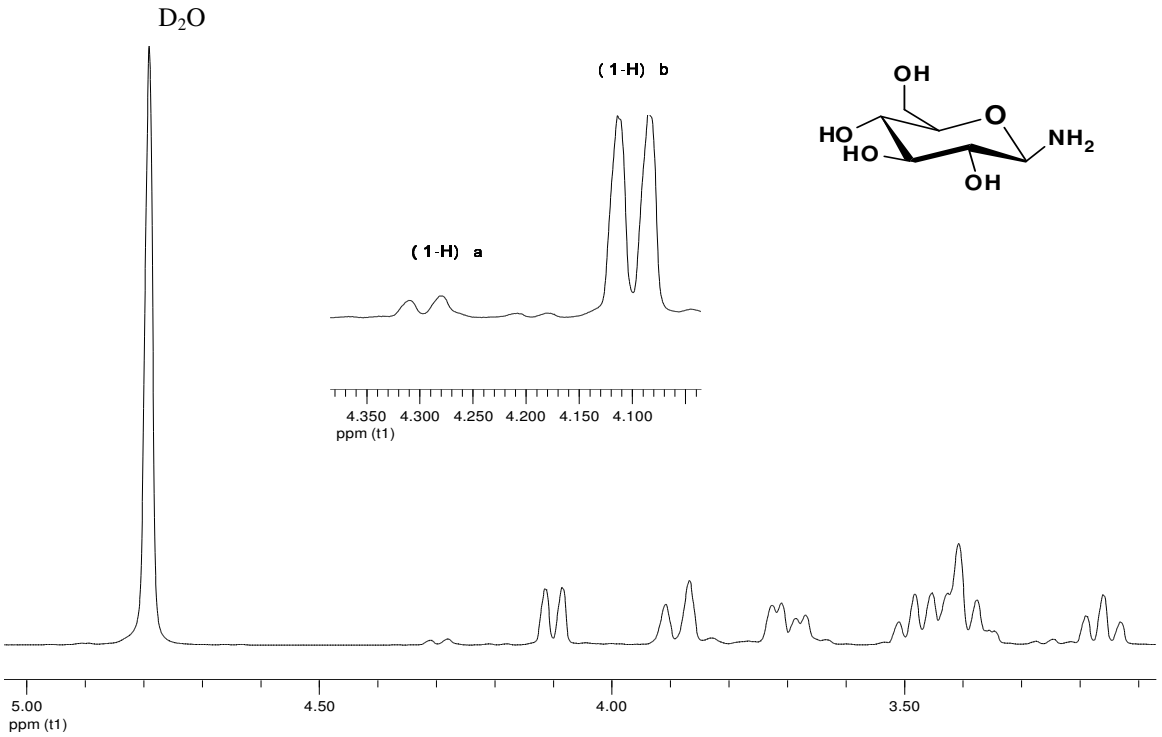

Figure 50 ^{1}H-NMR spectrum of glycosylamine **106**

Route (B)

In order to avoid solubility and purification problems by using D-glucose, we decided to start with D-glucose pentaacetate in which all hydroxyl groups are acetyl-protected. This route (Scheme 1) involves convertion of D-glucose pentaacetate **109** to the corresponding bromide **110**, replacement of the bromine group with isothiocyanate to yield **111**, and finally treatment of **111** with hydrazine. Details for each step are given below.

III.1.2.1. 2,3,4,6-tetra-*O*-acetyl-α-D-glucopyranosyl bromide (110)

To convert D-glucose pentaacetate (**109**) into α-acetobromo-D-glucose (**110**), suitable for the synthesis of the desired glucopyranosyl isothiocyanate (**111**), we first investigated the classical bromination method (Scheme 20). A number of reagents have been reported for the bromination of **109** such as BiX_3 [262], AcBr-AcOH [263], Ac_2O [264], or Br_2/red P [265]. In our case, we followed a straightforward approach using HBr in glacial acetic acid to replace the acetyl group by bromine in alpha position [266]. Purification of **110** was carried out by double recrystallization from freshly distilled ether, and monitored by TLC in a dark room using EtOAc/hexane (1:1) as eluent. Since **110** is sensitive to moisture and temperature, it must be kept in a fridge under –4°C, but not for a long time.

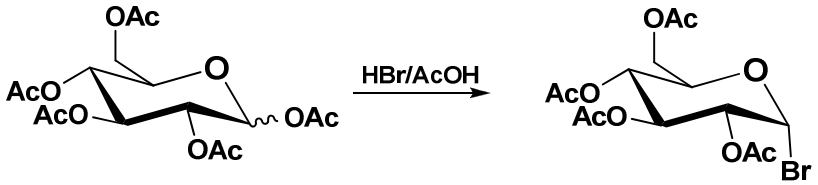

109 **110**

Scheme 20 Synthesis of 2,3,4,6-tetra-O-acetyl-α-D-glucopyranosyl bromide

The ^1H and ^{13}C NMR spectra (table 1) of compound **110** are in accordance with those previously reported [267]. The ^1H spectrum shows a doublet at 6.58 ppm corresponding to the anomeric proton with $^3J_{1\text{-H-2-H}}$ coupling 4.1 Hz, which confirmed the α- configuration of the sugar ring.

Table 1 *^{1}H and ^{13}C NMR chemical shift (in ppm) for the anomeric proton and carbon, in α-acetobromo-D-glucose* ***110***

	1-H	1-C
Compound **110**	6.58 ($^{3}J_{1\text{-H-2-H}}$ = 4.1 Hz)	86.5

III.1.2.2. 2,3,4,6-tetra-*O*-acetyl-β-D-glucopyranosyl isothiocyanate (111)

2,3,4,6-tetra-*O*-acetyl-β-D-glucopyranosyl isothiocyanate (**111**) was synthesized by the reaction of **110** with potassium thiocyanate in the melt in accordance to a known procedure [268]. The purity of this compound was checked by TLC and spectral analysis (Table 2). Compound **111** must also be kept in fridge (−4°C) but not for a long time.

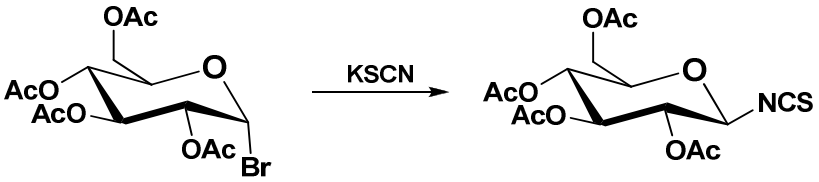

110 **111**

Scheme 21 Synthesis of 2,3,4,6-tetra-O-acetyl-β-D-glucopyranosyl isothiocyanate

The compound **111** was ready identified from the characteristic absorption bands in IR spectra at 2060-2120 cm^{-1} (-N=C=S) and at 1754 and 1230 cm^{-1} ($OCOCH_3$). The presence of isothiocyanate group was also confirmed by the characteristic ^{13}C resonance of the C=S group ($\delta_{C=S}$ 144.2 ppm) whereas the $^{4}C_1$ (D) conformation and β-anomeric configuration of the isothiocyanate substituent was evident from the $^{3}J_{H1\text{-}H2}$ Hz values around the pyranose ring.

Table 2 *^{1}H and ^{13}C NMR chemical shift (in ppm) for some representative proton and carbons of isothiocyanate* ***111***

	1-H	1-C	C=S
Compound **111**	5.01 ($^{3}J_{H1\text{-}H2}$ = 9.0 Hz)	83.4	144.2

III.1.2.3. *N*(4)-(2,3,4,6–Tetra-*O*-acetyl-β-D-glucopyranosyl)thiosemicarbazide(112)

Thiosemicarbazide **112** was prepared as a crystalline product in accordance to a known procedure by treatment of isothiocyanate **111** with dry hydrazine in ethanol [255]. The only modification in this procedure was the reaction temperature, which was kept at 5–10 °C in order to avoid the formation of a carbohydrate bearing diacylhydrazine framework (*N,N*'-bis{[(2,3,4,6-tetra-*O*-acetyl-β-D-glucopyranosyl)amino]thiocarbonyl} hydrazine) as a side product [269].

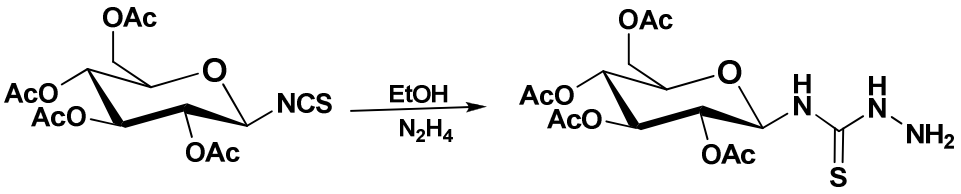

111 **112**

Scheme 22 Synthesis of *N*(4)-(2,3,4,6–Tetra-*O*-acetyl-β-D-glucopyranosyl)thiosemicarbazide

Two absorption bands at 3320-3450 cm^{-1}, which are related to the symmetrical and asymmetrical stretching vibrations of the amino group, are observed in the IR spectra of compound **112**. The ^{1}H NMR (DMSO-d_6, 25°C) spectrum of thiosemicarbazide (Fig. 51) showed singlets at ca. δ 9.27 ppm and δ 8.20 ppm for the $-N^{2}H$ and $-N^{4}H$, respectively, and a broad singlet at 4.60 ppm for $N^{1}H_2$ which indicated the absence of *N, N'*-Bis {[(2,3,4,6-tatre-*O*-acetyl-β-D-glucopyranosyl) amino]thiocarbonly}hydrazine [269]. A broad singlet was observed at δ 5.82 ppm for the anomeric proton.

The ^{13}C NMR (DMSO-d_6, 25°C) spectrum of thiosemicarbazide **112** showed a signal at δ 182.0 ppm assigned to thioamide (C=S) and a singlet at δ 81.0 ppm for the anomeric carbon.

Table 3 *^{1}H and ^{13}C NMR chemical shift (in ppm, in DMSO-d_6, 25°C) for some proton and carbons of thiosemicarbazide* ***112***

	1-H	1-C	C=S
Compound **112**	5.82	81.0	182.0

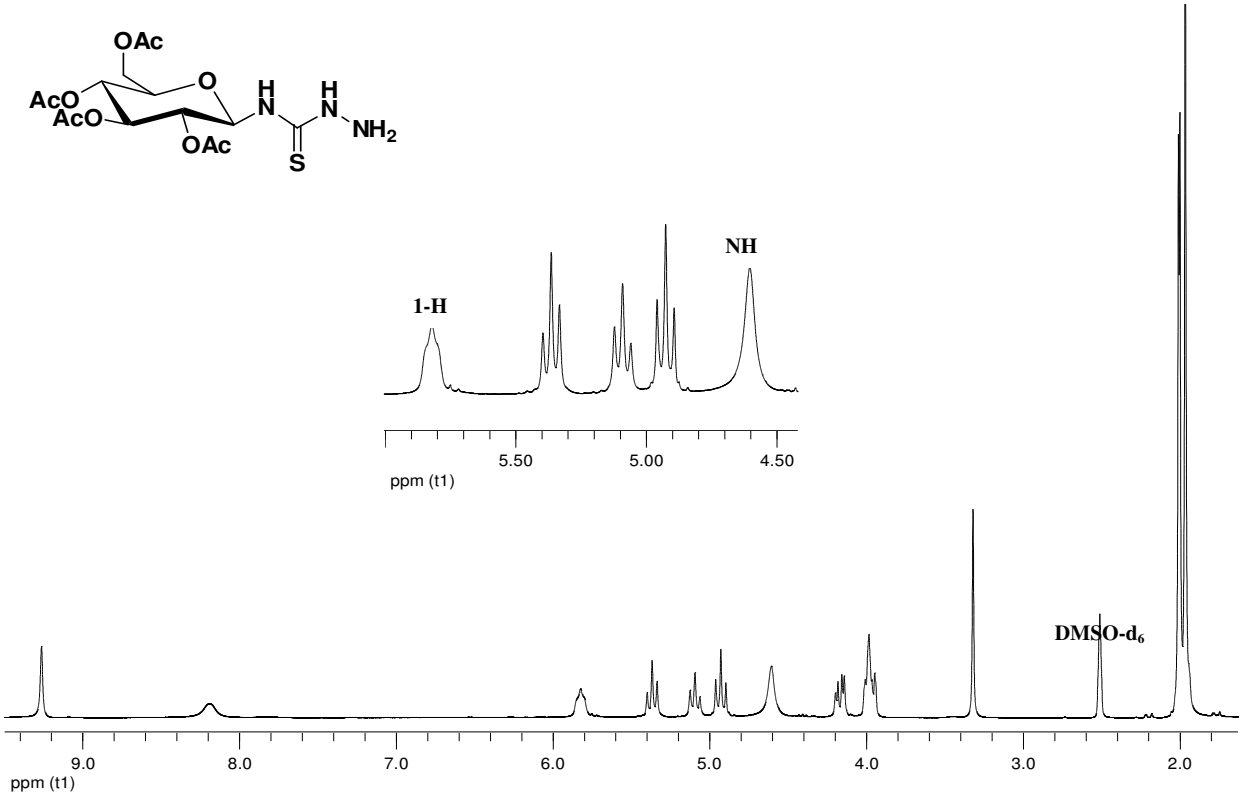

Figure 51 ^{1}H NMR spectrum in DMSO-d_6 of compound **112**

III.1.3. β-D-glucopyranosyl thiosemicarbazones

Condensation of the acetyl-protected β-D-glucose thiosemicarbazide (**112**) with a number of aldehydes or ketones in ethanol or methanol, adding a catalytic ammount of acetic acid at room temperature or refluxing in an oil bath leaded to the acetylated glucopyranosyl-thiosemicarbazones $\mathbf{L_{1\text{-}26}}$. The acetyl protective groups of $\mathbf{L_{1\text{-}26}}$ were removed by the Zemplén method in dry methanol in the presence of sodium methoxide, yielding the target molecules $\mathbf{L'_{1\text{-}26}}$. The synthesis of these molecules is outline in the scheme below.

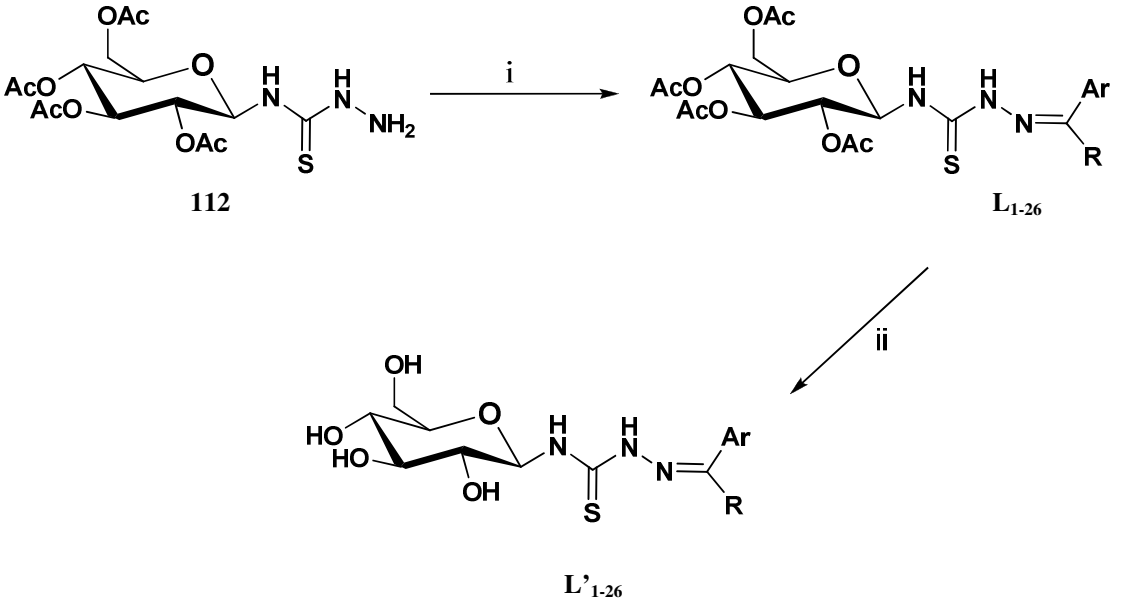

112 $\mathbf{L}_{1\text{-}26}$ $\mathbf{L'}_{1\text{-}26}$

Scheme 23 Reagents and conditions (i): ArC(R)=O, EtOH or MeOH, cat. AcOH, reflux; (ii) NaOMe. MeOH, r.t.

The compounds ($\mathbf{L}_{1\text{-}26}$ and $\mathbf{L'}_{1\text{-}26}$) were fully characterized by spectroscopic techniques, elemental analysis, and for two derivatives, one acetyl-protected and one with free hydroxyl groups, by X-ray analysis. A table list with the synthesized β-D-glucopyranosyl thiosemicarbazones ($\mathbf{L}_{1\text{-}26}$ and $\mathbf{L'}_{1\text{-}26}$) is given below.

***Table 4**: List of synthesized β-D-glucopyranosyl thiosemicarbazones:*

No.	Structure	No.	Structure
L_1	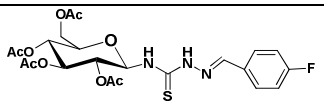	L'_1	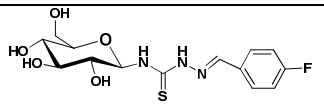
L_2	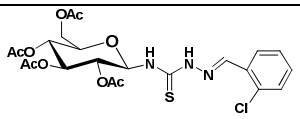	L'_2	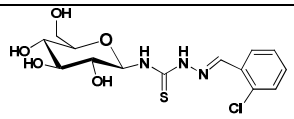
L_3	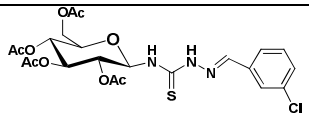	L'_3	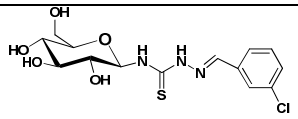
L_4	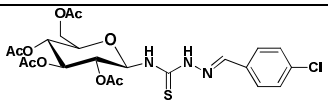	L'_4	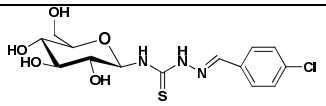
L_5	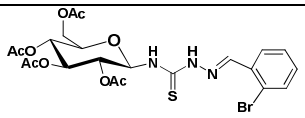	L'_5	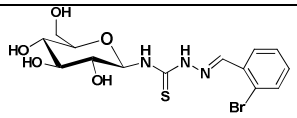
L_6	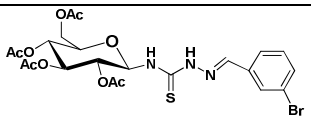	L'_6	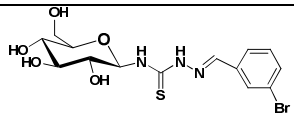
L_7	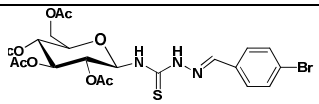	L'_7	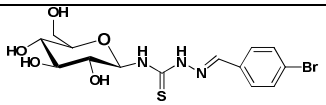
L_8	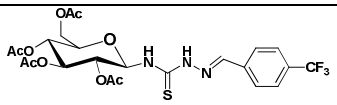	L'_8	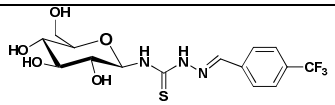
L_9	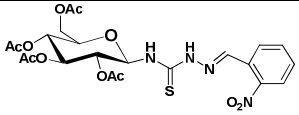	L'_9	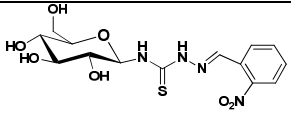
L_{10}	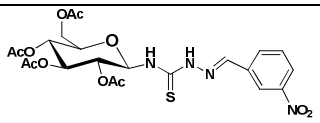	L'_{10}	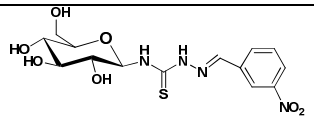
L_{11}	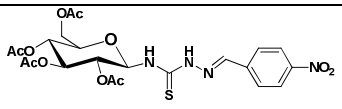	L'_{11}	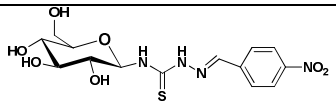
L_{12}	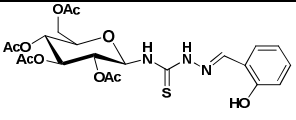	L'_{12}	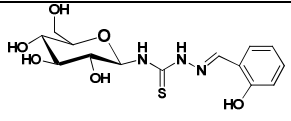
L_{13}	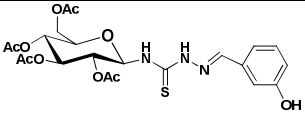	L'_{13}	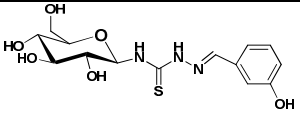

L_{14}	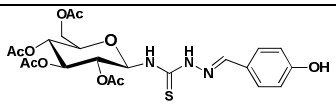	L'_{14}	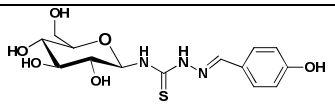
L_{15}	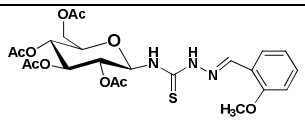	L'_{15}	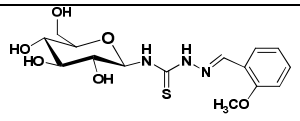
L_{16}	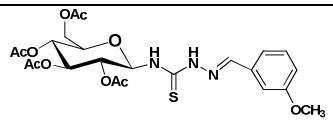	L'_{16}	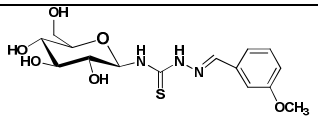
L_{17}	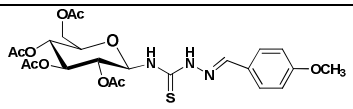	L'_{17}	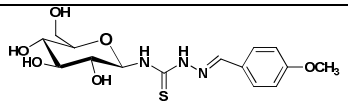
L_{18}	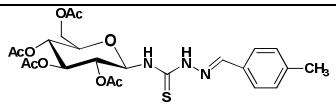	L'_{18}	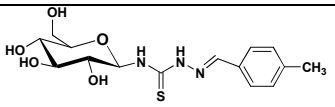
L_{19}	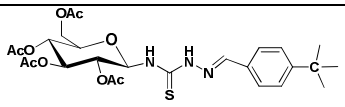	L'_{19}	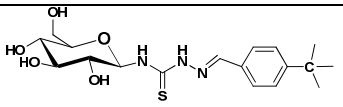
L_{20}	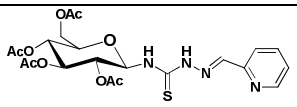	L'_{20}	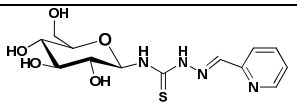
L_{21}	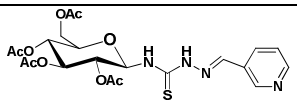	L'_{21}	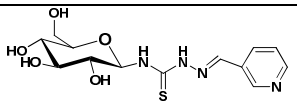
L_{22}	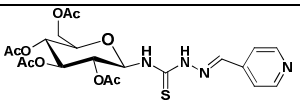	L'_{22}	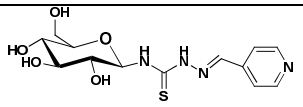
L_{23}	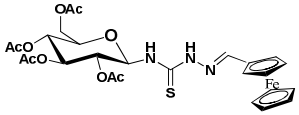	L'_{23}	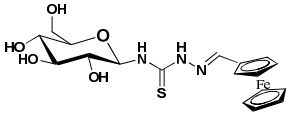
L_{24}	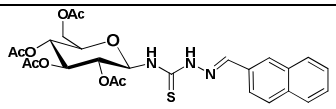	L'_{24}	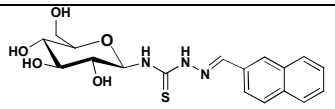
L_{25}	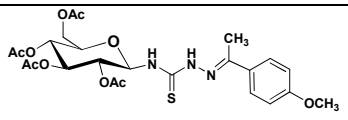	L'_{25}	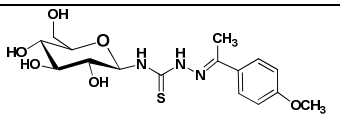
L_{26}	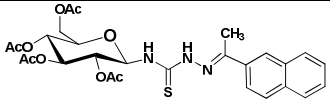	L'_{26}	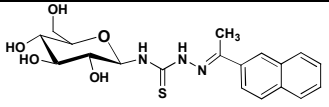

III.1.3.1. FT-IR spectral characterization

The β configuration of the aglycone in compounds **L** and **L'** is indicated by the absorption bands for the vibrations of the anomeric 1-C–H bond at 888-933 cm^{-1} in the FT-IR spectra [270, 271].

The existence of a strong band in the region 1031-1047 cm^{-1} ($\mathbf{L_{1-26}}$) for the acetylated compounds and 1018-1055 cm^{-1} for the deacetylated analogues ($\mathbf{L'_{1-26}}$), due to υ(C=S) and the absence of any band in the region 2500-2600 cm^{-1} due to υ(C-SH) suggest that the thiosemicarbazone moiety remains in the thione form [272, 273].

The IR spectra of compounds in which C=S group is attached to the nitrogen atom contain several bands in the region 1560-700 cm^{-1} due to the vibrations involving C=S and C-N stretching. The band in the region 820-839 cm^{-1} for $\mathbf{L_{1-26}}$ and 810-843 cm^{-1} for $\mathbf{L'_{1-26}}$ is also contributed to υ(C=S), the existence of this band very well defined in a narrow range [273, 274].

The characteristic bands at 1725–1753 cm^{-1} due to the C=O stretching vibration in compounds $\mathbf{L_{1-26}}$, vanish in the IR spectra of $\mathbf{L'_{1-26}}$, while broad absorption band of the hydroxyl group appears at 3203–3597 cm^{-1} for all deacetylated compounds $\mathbf{L'_{1-26}}$.

The full IR spectra for two representative compounds ($\mathbf{L_1}$, $\mathbf{L'_1}$, $\mathbf{L_{20}}$, and $\mathbf{L'_{20}}$) are given in the figures 52-55. In addition, the absortion bands at 1508-1549 cm^{-1} were attributed to the azomethine group υ(CH=N) stretch vibrations, in agreement with earlier reports of N(4)-substitued thiosemicarbazone [275, 276]. The amines ($\mathbf{L_{1-26}}$) showed additional sharp bands in the region 3310-3350cm^{-1} due to the υ(N-H) stretch.

However, in-plane and out-plan deformation vibrations characteristic of pyridine ring are observed respectively in the range 601–678 cm^{-1} for $\mathbf{L_{20-22}}$ and $\mathbf{L'_{20-22}}$ [277]. Some representative characteristic bands are given in tables 5 and 6, for $\mathbf{L_{1-26}}$ and $\mathbf{L'_{1-26}}$, respectively.

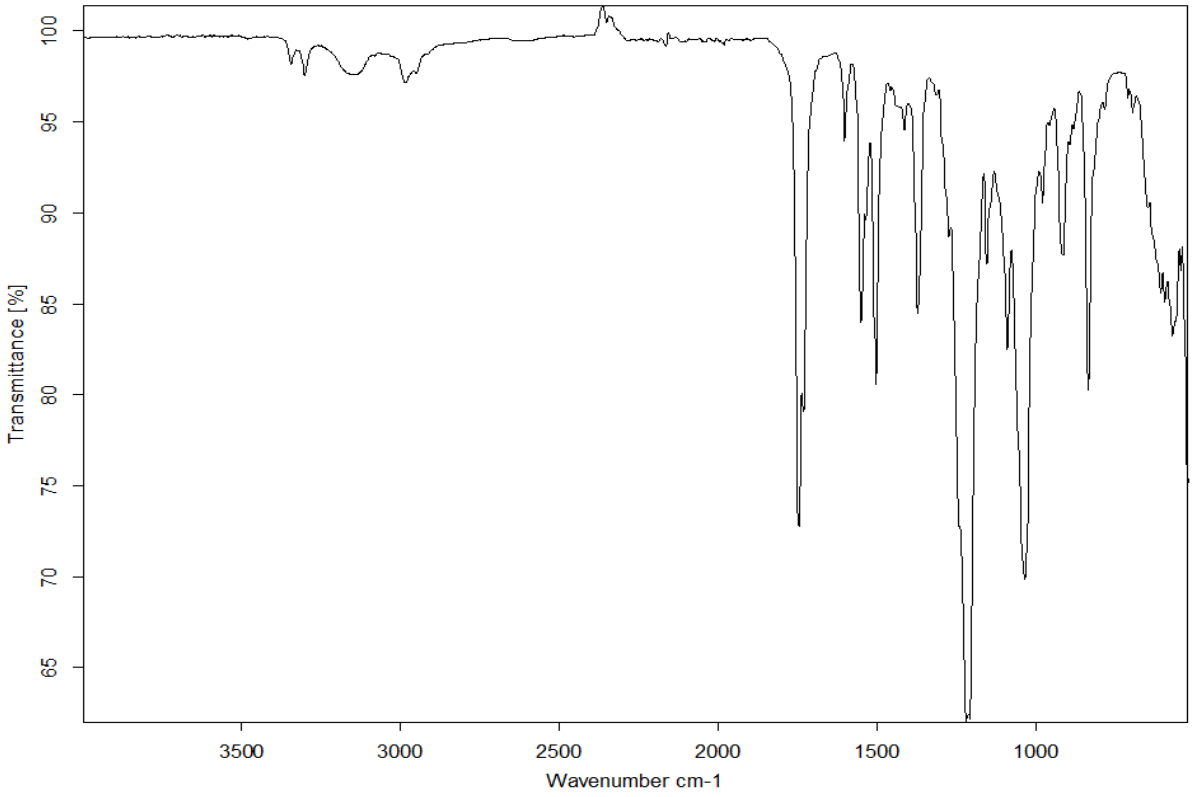

Figure 52 FT−IR spectrum of compound $\mathbf{L_1}$

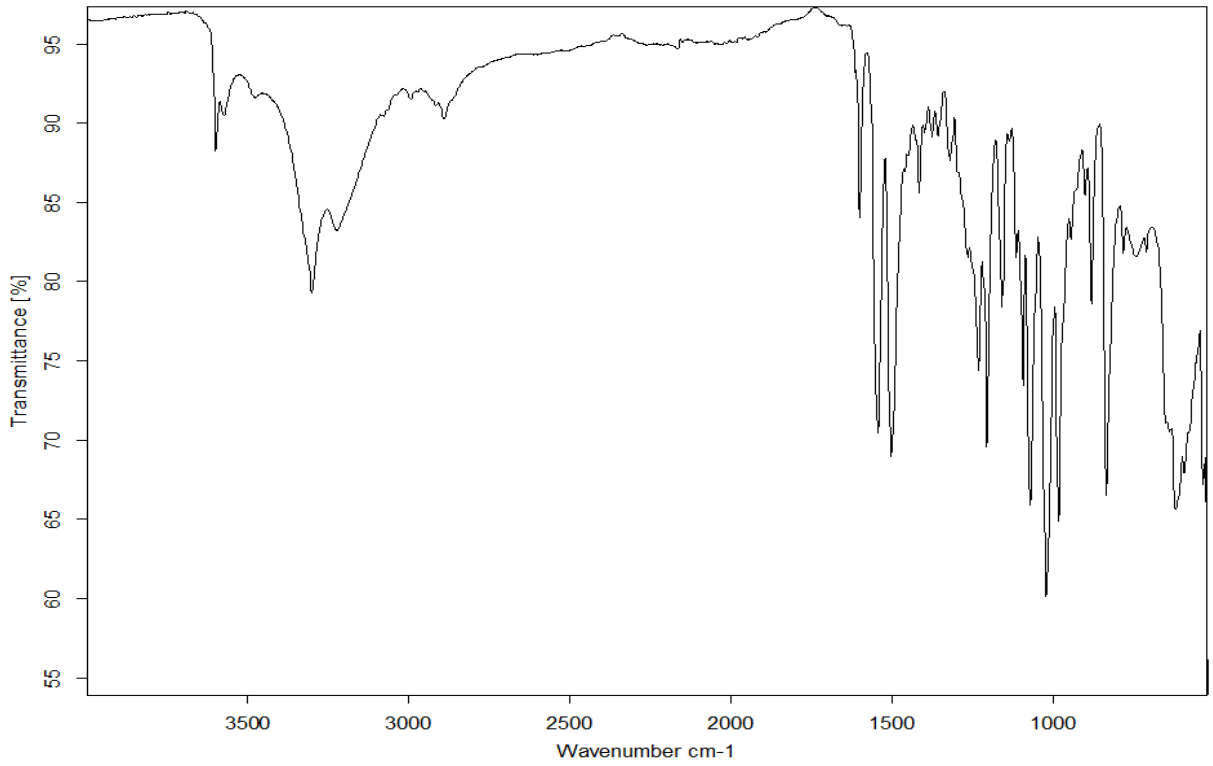

Figure 53 FT−IR spectrum of compound $\mathbf{L'_1}$

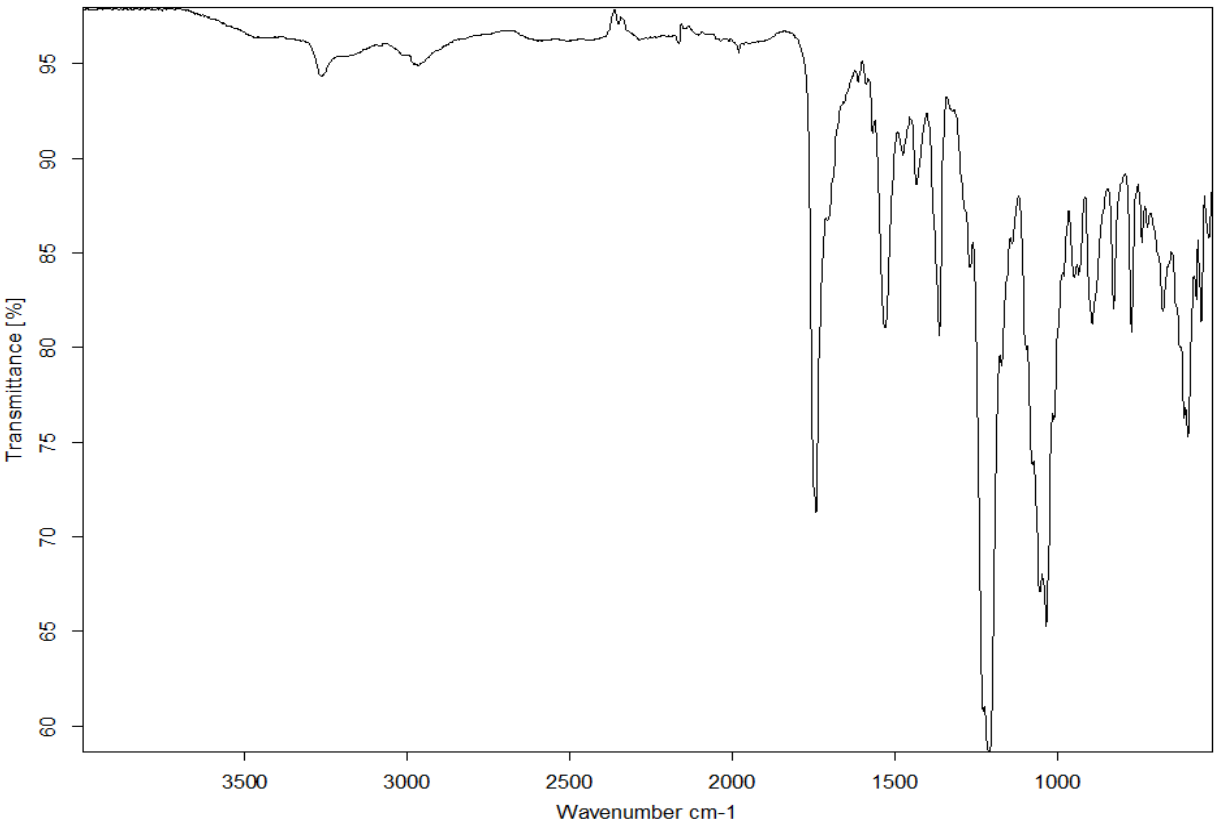

Figure 54 FT–IR spectrum of compound $\mathbf{L_{20}}$

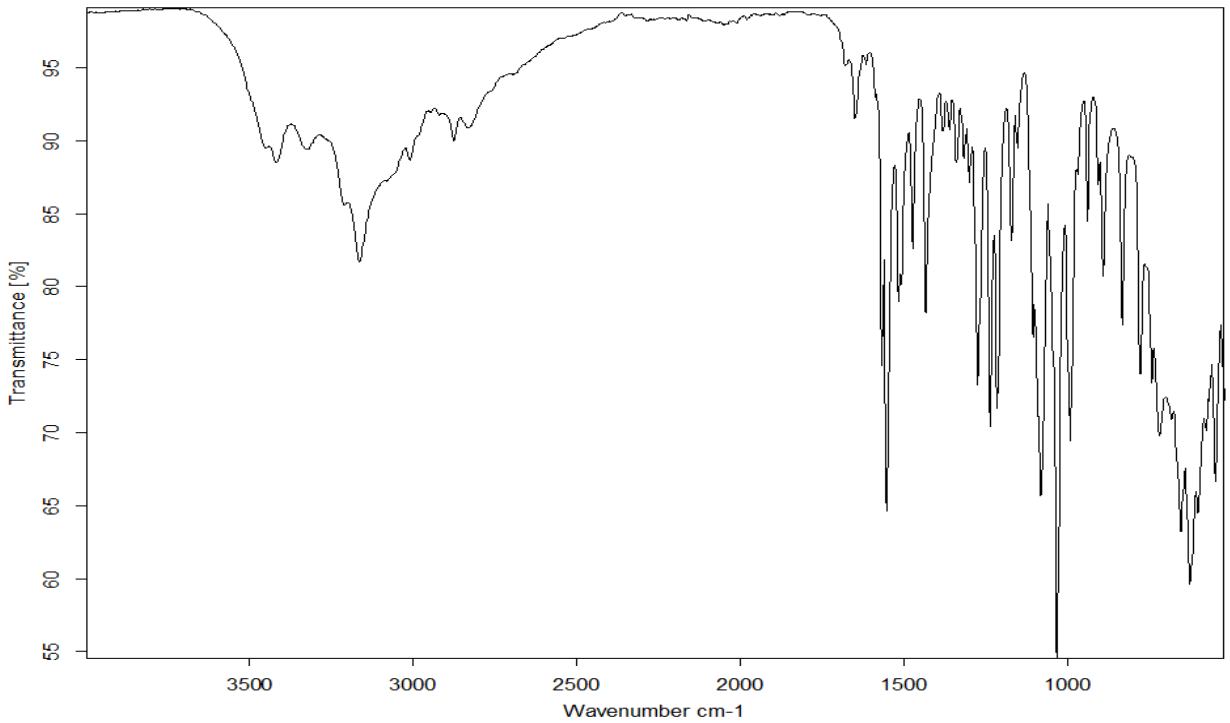

Figure 55 FT–IR spectrum of compound $\mathbf{L'_{20}}$

Table 5 *FT-IR for ligands* $\boldsymbol{L_1}$-$\boldsymbol{L_{26}}$

Ligand	υ(N−H)	υ(C=O)	υ(C=N)	(C=N-N)	υ(C=S)	(1-C−H)
$\mathbf{L_1}$	3146	1745	1553	1503	1039, 843	916
$\mathbf{L_2}$	3350	1745	1533	1503	1039, 822	920
$\mathbf{L_3}$	3324	1749	1549	1476	1043, 830	908
$\mathbf{L_4}$	3316	1745	1549	1492	1039, 835	912
$\mathbf{L_5}$	3134	1753	1529	1504	1039, 822	912
$\mathbf{L_6}$	3326	1737	1529	1490	1035, 843	900
$\mathbf{L_7}$	3134	1741	1545	1487	1035, 822	920
$\mathbf{L_8}$	3334	1749	1529	1487	1031, 830	912
$\mathbf{L_9}$	3320	1745	1525	1502	1035, 822	916
$\mathbf{L_{10}}$	3328	1737	1529	1510	1035, 820	920
$\mathbf{L_{11}}$	3314	1741	1525	1508	1031, 826	920
$\mathbf{L_{12}}$	3330	1745	1533	1460	1022, 830	920
$\mathbf{L_{13}}$	3320	1745	1537	1489	1035, 826	920
$\mathbf{L_{14}}$	3314	1741	1508	1514	1039, 835	920
$\mathbf{L_{15}}$	3328	1745	1529	1485	1039, 826	910
$\mathbf{L_{16}}$	3338	1737	1545	1505	1035, 830	912
$\mathbf{L_{17}}$	3312	1749	1541	1501	1035, 822	920
$\mathbf{L_{18}}$	3314	1741	1553	1500	1043, 830	933
$\mathbf{L_{19}}$	3326	1749	1533	1485	1047, 826	916
$\mathbf{L_{20}}$	3328	1741	1529	1495	1035, 839	888
$\mathbf{L_{21}}$	3320	1745	1533	1467	1031, 826	928
$\mathbf{L_{22}}$	3329	1737	1525	1518	1031, 830	896
$\mathbf{L_{23}}$	3322	1725	1525	1507	1035, 820	912
$\mathbf{L_{24}}$	3322	1753	1533	1500	1035, 830	904
$\mathbf{L_{25}}$	3330	1741	1529	1502	1035, 830	916
$\mathbf{L_{26}}$	3310	1741	1529	1489	1035, 835	916

Table 6 *FT-IR for ligands* ***L_1'-L_{26}'***

Ligand	υ(OH)	υ(C=N)	(C=N-N)	υ(C=S)	(1-C−H)
L_1'	3596	1545	1503	1022, 830	888
L_2'	3525	1537	1472	1039, 830	916
L_3'	3359	1537	1472	1035, 830	892
L_4'	3371	1537	1484	1031, 830	900
L_5'	3547	1545	1472	1026, 830	896
L_6'	3547	1533	1472	1031, 839	916
L_7'	3540	1553	1508	1035, 822	900
L_8'	3322	1541	1500	1035, 826	900
L_9'	3355	1537	1496	1035, 822	896
L_{10}'	3416	1545	1514	1035, 810	910
L_{11}'	3405	1537	1498	1035, 822	892
L_{12}'	3203	1553	1504	1035, 843	910
L_{13}'	3208	1553	1503	1031, 832	892
L_{14}'	3250	1521	1487	1018, 839	909
L_{15}'	3559	1537	1492	1026, 830	892
L_{16}'	3498	1557	1464	1031, 851	896
L_{17}'	3547	1549	1508	1031, 839	888
L_{18}'	3322	1553	1508	1035, 830	904
L_{19}'	3324	1541	1500	1018, 826	900
L_{20}'	3416	1557	1473	1039, 830	896
L_{21}'	3399	1537	1489	1043, 828	904
L_{22}'	3597	1541	1492	1035, 830	896
L_{23}'	3326	1534	1490	1024, 822	891
L_{24}'	3399	1525	1488	1055, 843	900
L_{25}'	3297	1510	1508	1018, 835	900
L_{26}'	3379	1562	1504	1018, 826	892

III.1.3.2. ^{1}H and ^{13}C NMR characterization

Peak assigments were based on ^{2}D NMR data (proton-proton correlated spectroscopy (^{1}H-^{1}H COSY), proton-carbond heteronuclear single-quantum coherence (^{1}H-^{13}C HSQC) and proton-carbon heteronuclear multiple-bond correlation (^{1}H-^{13}C HMBC).

The atom numbering used for the NMR data is as show in Fig. 56.

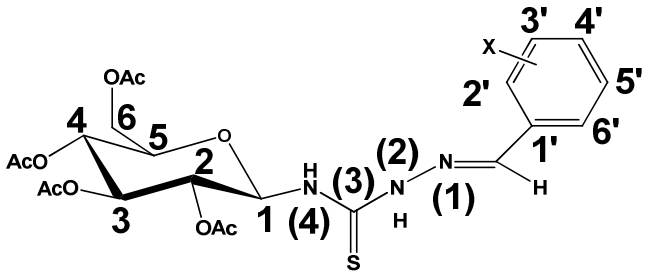

$\mathbf{L_x}$

Figure 56 Atom numbering used for the NMR data

In the ^{1}H NMR spectra of the βGluTSC acetyl-protected and deprotected derivatives, the anomeric proton 1-H is represented as a doublet of doublets at the range 5.95–5.61 ppm for the acetyl-protected derivatives (**L_{1-26}**), and 5.36–5.42 ppm for the deprotected derivatives (**L'_{1-26}**); this splitting is a consequence of spin-spin coupling of the anomeric proton with the protons attached to the N(4)H and the 2-H. The coupling constant $J_{1\text{-}H,2\text{-}H}$ (9.0–9.6 Hz) is an evidence which confirm the β configuration in compounds **L_{1-26}** and **L'_{1-26}** [271, 278]. The N(4)H proton appears as a doublet for the acetyl-protected compounds at 8.20-8.79 ppm and as a doublet or a broad singlet for the deacetylated analogues at 8.18-8.80 ppm. Furthermore, the N(2)H signal appeared in the region 8.81-11.93 ppm for the acetyl-protected and 10.47-12.03 ppm for the deacetylated analogues.

The expected signals from the phenyl rings of the thiosemicarbazone moiety are clearly observed in the range 6.89-8.81 ppm for the acetyl-protected compounds (**L_{1-26}**) and 6.78-8.62 ppm for the deprotected compounds (**L'_{1-26}**).

The singlet in ^{1}H NMR spectra in the range 7.70-8.90 ppm and 7.95-8.53 ppm is assigned to the azomethine proton for the acetyl-protected compounds (**L_{1-26}**) and the deprotected compounds (**L'_{1-26}**), respectively.

In the ^{13}C NMR spetra, the C=S resonance of the thiosemicarbazone moiety in all compounds is appeared at 177.0-179.6 ppm for the acetyl-protected compounds and at 177.5-179.2 ppm for the

deprotected analogues. In addition, other important singals in the ^{13}C NMR spetra of the thiosemicarbazone moiety is CH=N, which is appeared at 138.8-149.6 ppm for the acetylated compounds and at 138.0-149.1 ppm for the deprotected compounds.

For the anomeric proton, the 1-C is appeared at 81.4-82.5 ppm for the acetyl-protected derivatives and at 83.8-84.9 ppm for the deprotected derivatives. The acetyl signals observed in the spectrum of the protected compounds are missing in the $\mathbf{L'_{1\text{-}26}}$ compounds.

In ^{1}H NMR spectra of compounds $\mathbf{L_{23}}$ and $\mathbf{L'_{23}}$ the protons of the feroccenyl ring are appeared as a singlet at aproximatively δ 4.22 ppm. In both instances, two additional sets of signals and a multiplet are observed for $\mathbf{L_{23}}$ at about δ 4.84, 4.73, 4.49-4.45 ppm for the protons of the substituted cyclopentadienyl ring. Three additional sets of signals are observed for $\mathbf{L'_{23}}$ δ 4.81, 4.73, 4.44 ppm for the protons of substituted cyclopentadienyl ring; this is in accordance with literature [279].

The ^{1}H and ^{13}C NMR chemichal shift range of some characteristic protons (N(2)H, N(4)H, CH=N, anomeric 1-H) and carbons (C=S, 1-C) in compounds $\mathbf{L_{1\text{-}26}}$ and $\mathbf{L'_{1\text{-}26}}$ are presented in the tables 7 and 8, respectively.

Tabel 7 *^{1}H and ^{13}C NMR chemical shift (in ppm) for some characteristic proton and carbon atoms in* ***L_{1-26}***

Compound	N(2)H	N(4)H	CH=N	1-H	C=S	CH=N	1-C
		^{1}H				^{13}C	
L_1	11.93	8.80	8.07	5.95	178.9	142.4	82.3
L_2	9.76	8.29	8.26	5.72	178.5	139.7	81.5
L_3	9.64	8.35	7.74	5.67	179.1	141.7	82.4
L_4	9.40	8.30	7.72	5.69	178.9	142.7	82.3
L_5	9.61	8.26	8.21	5.66	179.2	142.4	82.3
L_6	10.18	8.35	7.92	5.66	178.9	142.0	82.3
L_7	9.32	8.30	7.69	5.68	179.5	140.5	82.4
L_8	10.14	8.38	7.84	5.67	179.0	141.9	82.2
L_9	9.69	8.30	8.43	5.73	179.3	138.8	82.3
L_{10}	10.07	8.43	8.57	5.65	179.2	140.5	82.4
L_{11}	10.11	8.42	7.90	5.65	179.2	140.4	82.4
L_{12}	9.81	7.81	8.90	5.68	177.7	148.3	82.5
L_{13}	9.87	8.23	7.74	5.71	178.3	144.3	81.5
L_{14}	9.84	8.20	7.69	5.74	177.8	144.3	81.5
L_{15}	9.43	8.25	8.21	5.78	178.8	139.8	82.3
L_{16}	10.22	8.30	7.77	5.61	178.4	143.5	82.4
L_{17}	9.78	8.26	7.70	5.72	178.3	143.9	82.2
L_{18}	9.73	8.25	7.77	5.72	178.1	140.2	81.4
L_{19}	10.26	8.29	7.85	5.71	178.7	143.9	82.2
L_{20}	10.14	8.45	7.96	5.72	179.4	140.5	82.2
L_{21}	10.49	8.34	7.89	5.68	179.1	140.3	82.2
L_{22}	10.56	8.39	7.81	5.64	179.4	140.7	82.2
L_{23}	11.72	8.38	7.93	5.87	177.0	145.0	81.2
L_{24}	10.41	8.38	7.82	5.72	178.9	144.3	82.2
L_{25}	8.81	8.38	--	5.76	179.1	149.6	81.4
L_{26}	9.18	8.50	--	5.76	179.6	148.0	82.3

In $CDCl_3$ for all compounds except **L_1**, **L_{13}**, **L_{16}** and **L_{23}**in DMSO-d_6.

Tabel 8 *NMR chemical shift (in ppm) for some characteristic proton and carbon atoms in* ***L'$_{1-26}$***

Compound	N(2)H	N(4)H	CH=N	1-H	C=S	CH=N	1-C
	^{1}H				^{13}C		
L'$_1$	11.75	8.60	8.10	5.39	178.6	141.8	84.0
L'$_2$	11.93	8.66	8.53	5.39	178.8	138.9	84.1
L'$_3$	11.82	8.75	8.08	5.40	178.8	141.4	84.1
L'$_4$	11.78	8.62	8.09	5.38	178.5	142.6	83.9
L'$_5$	11.95	8.69	8.50	5.38	179.2	141.8	84.5
L'$_6$	11.80	8.72	8.06	5.39	179.2	141.8	84.6
L'$_7$	11.80	8.62	8.06	5.36	179.2	144.8	84.7
L'$_8$	11.92	8.73	8.16	5.40	178.9	141.4	84.1
L'$_9$	12.03	8.69	8.53	5.39	179.0	138.0	84.1
L'$_{10}$	11.91	8.80	8.23	5.40	179.0	141.0	84.3
L'$_{11}$	11.97	8,79	8.20	5.40	179.0	140.3	84.1
L'$_{12}$	11.99	8.47	8.43	5.37	178.3	140.0	83.9
L'$_{13}$	11.69	8.44	8.02	5.37	178.7	144.3	84.2
L'$_{14}$	11.56	8.38	8.00	5.35	178.0	143.6	84.9
L'$_{15}$	11.73	8.51	8.47	5.37	178.4	138.6	84.9
L'$_{16}$	11.76	8.59	8.08	5.37	178.6	143.0	84.0
L'$_{17}$	11.63	8.46	8.06	5.37	178.2	143.0	84.0
L'$_{18}$	11.67	8.48	8.06	5.37	178.4	143.1	83.9
L'$_{19}$	11.71	8.48	8.09	5.38	178.5	143.1	84.0
L'$_{20}$	11.94	8.73	8.15	5.40	178.9	143.3	84.1
L'$_{21}$	11.86	8.69	8.11	5.37	178.8	140.1	84.1
L'$_{22}$	11.99	8.75	8.07	5.40	179.0	141.4	84.1
L'$_{23}$	11.49	8.18	7.95	5.39	177.5	144.3	84.7
L'$_{24}$	11.84	8.64	8.15	5.42	178.6	143.2	84.1
L'$_{25}$	10.47	8.35	--	--	178.0	149.1	83.8
L'$_{26}$	11.84	8.64	--	--	178.0	143.2	84.1

In DMSO-d_6.

Figures 57-60 show the ^{1}H NMR and the ^{13}C NMR spectra for the compounds **L$_8$** and **L'$_{14}$**.

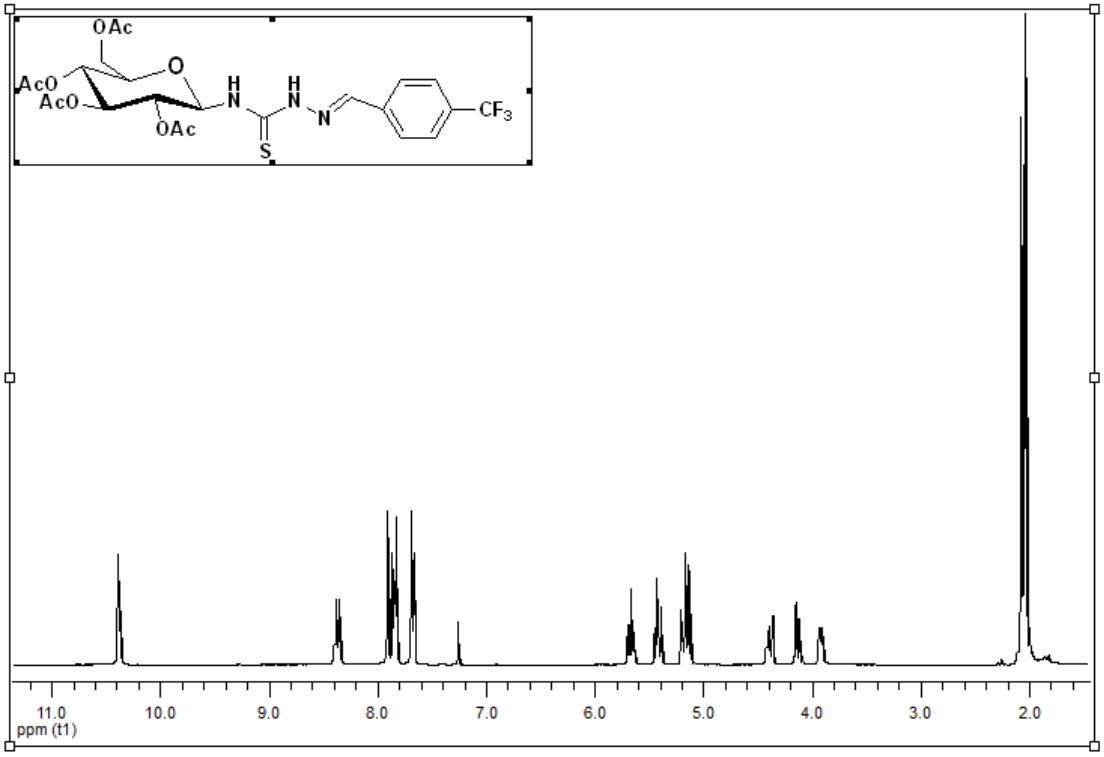

Figure 57 ^{1}H-NMR spectra in $CDCl_3$ (600MHz) for $\mathbf{L_8}$

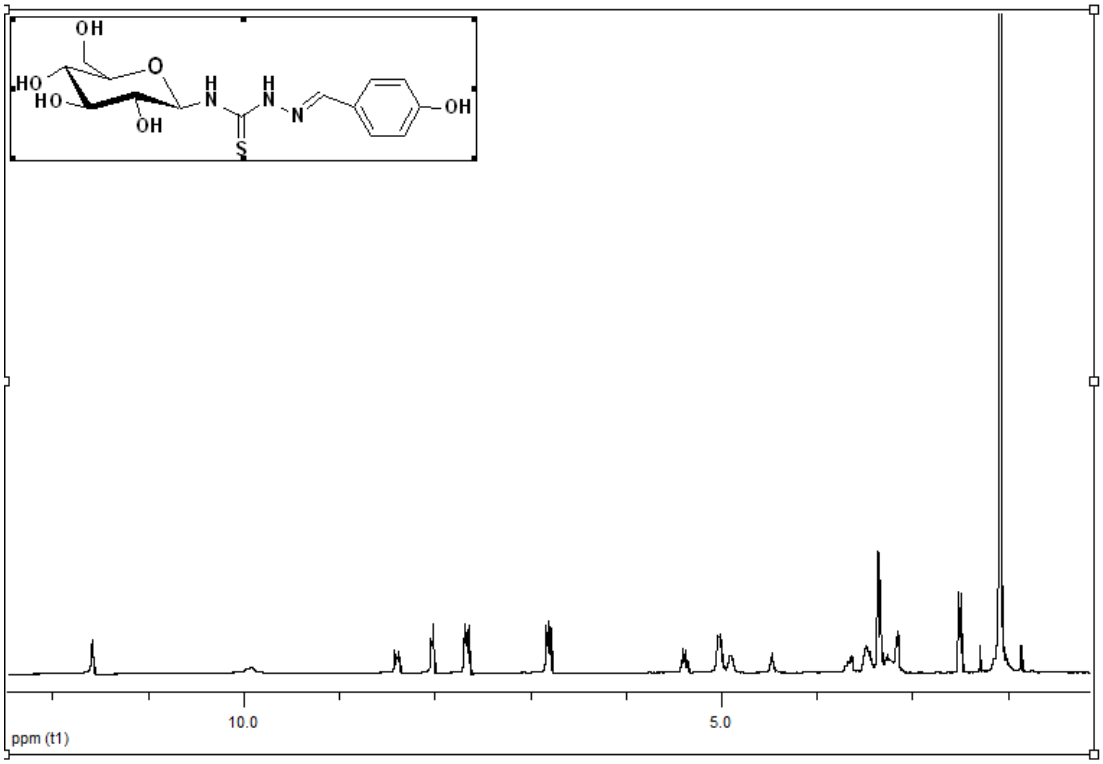

Figure 58 ^{1}H-NMR spectra in DMSO-d_6 (600MHz) for $\mathbf{L'_{14}}$

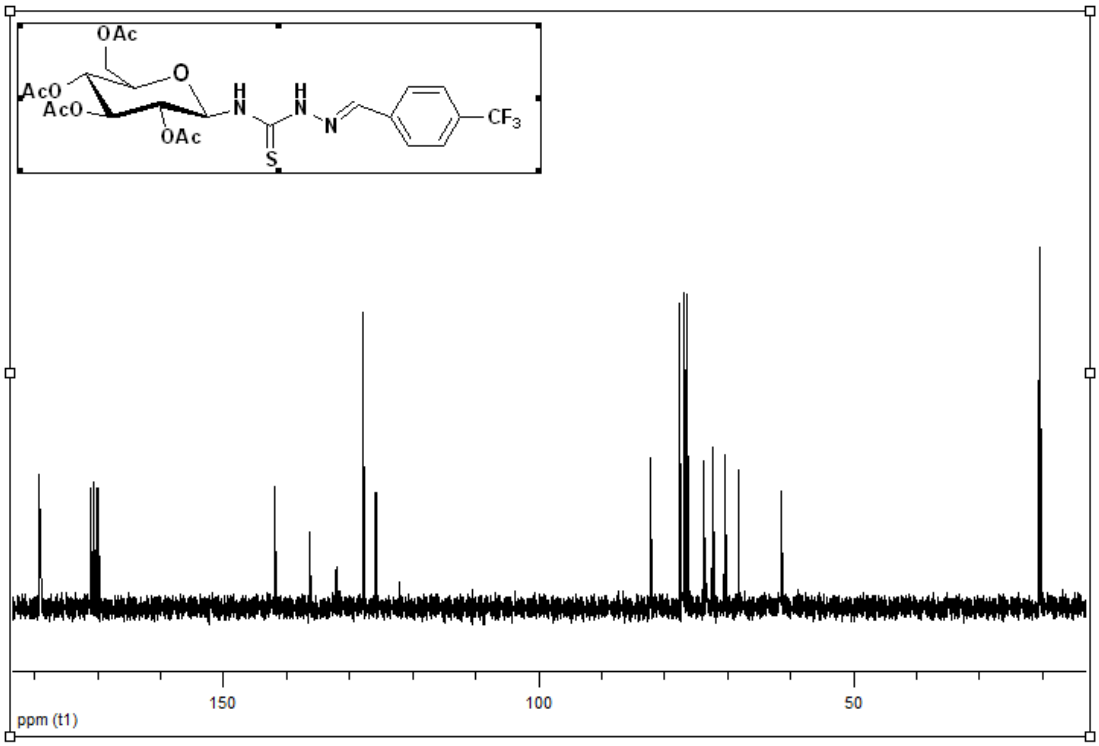

Figure 59 ^{13}C-NMR spectra in $CDCl_3$ (600MHz) for **L_8**

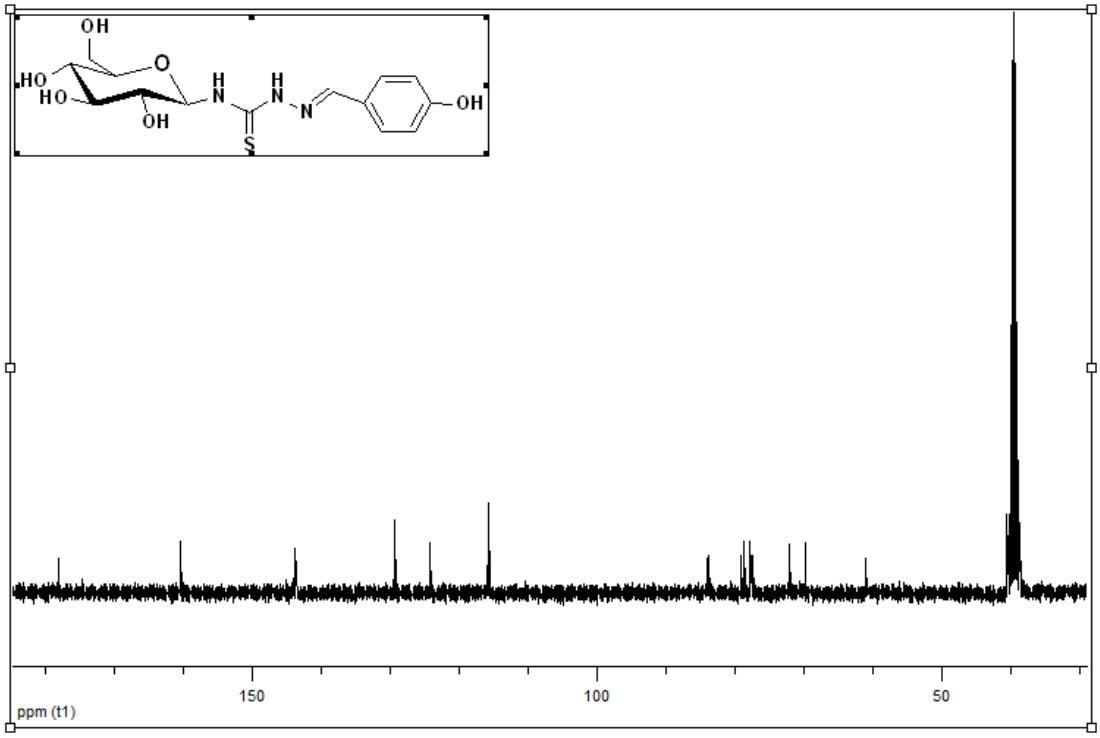

Figure 60 ^{13}C-NMR spectra in DMSO-d_6 (600MHz) for **L'_{14}**

III.1.3.3. E/Z isomers

It has previously been published that thiosemicarbazone derivatives pertaining the stereochemistry of the C=N bond, can exist in the *E*- or *Z*-form or as a mixture of *E/Z* isomers, usually with the *E*-form being the major isomer [272-284]. This may be due to the fact that, the *trans* arrangement places the amine and azomethine nitrogen atoms in relative positions more suitable for intramolecular hydrogen bonding.

By the ^{1}H-NMR spectroscopy, on the basic of data previously reported in several works concerning N-heteroaromatic thiosemicarbazones, it was possible to assign the correct conformation to the different products [281, 282]. Variation in isomeric ratio is dependent on the substituents on the thiosemicarbazones moiety and the solvent. The correct configuration can be determineted by ^{1}H-NMR spectroscopy, as the N(2)H appears at 9−12 ppm for the *E*-form, and 14−15 ppm for the *Z*-form [282]. In the ^{1}H-NMR spectra of freshly prepared solutions of protected or unprotected derivatives in $CDCl_3$ or DMSO-d_6, only one signal was observed for each hydrogen, indicating the presence of only one isomer (*E*), since the N(2)H resonace was assigned in the rage 8.64−12.03 ppm. However, a partial conversion of the *E* form into *Z*-form is possible for some compounds in solution after several hours. In figure 61, we present the ^{1}H-NMR spectra of **L_{20}** in $CDCl_3$ at different times. We also note that in DMSO-d_6 or CD_3OD at room temperature, we observed only one isomer for the acetylated compounds.

In a freshly prepared solution, only the *E* isomer exist(spectrum(a); Fig. 61), but after 24h, all signals are duplicated which indicates that both *E* and *Z* isomers (spectrum(b); Fig. 61). In the Z-form, an intramolecular hydrogen bond should be formed between N(2)H and the pyridine nitrogen [283, 284, 285]. After 48h, the equilibrium leads to the two forms in a ratio of about 1:1 (spectrum(c); Fig. 60). The most characteristic signals indicating the formatin of the two forms are those for N(2)H (10.14 ppm for *E*, 14.63 ppm for *Z*), N(4)H (8.45 ppm for *E*, 8.33 ppm for *Z*), the azometine hydrogen CH=N (7.96 ppm for *E*, 7.15 ppm for *Z*), and the anomeric proton 1- H (5.72 ppm for *E*, 5.86 ppn for *Z*). ^{13}C-NMR spectra could also provide information for the geometry of the molecules [286, 287]. The most significant resonance for the geometry determination is that of the azomethine carbon CH=N, presented as only one signal at 14.35 ppm in a short time ^{13}C-NMR experiment (H-decoupling) of a freshly prepared solution of **L_{20}** in $CDCl_3$, indicating the presence of only one isomer.

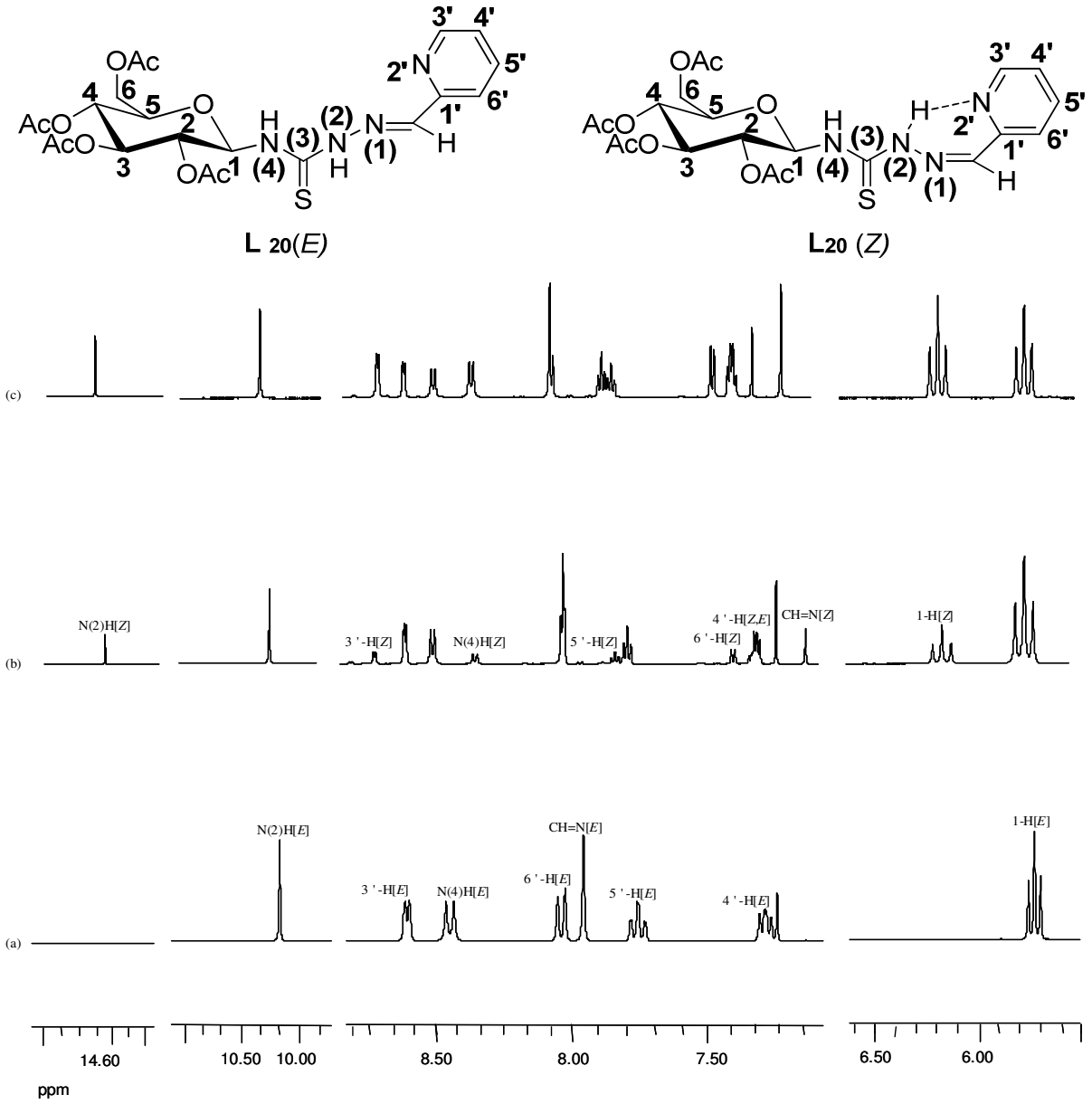

Figure 61 Part of ^{1}H-NMR spectra (600MHz) for $\mathbf{L_{20}}$ (E/Z isomers) in CDCl3 at diferent times: *a)* 5 min; *b)* 24h; *c)* 48h

However, in an overnight ^{13}C-NMR experiment (H-coupling), the signal is duplicated as an evidence that both *E* and *Z* forms coexist in solution. In the addition to the above-mentionated signal with $^{1}J_{C,H}$ value of 167.0 Hz, the azomethine carbon resonance of the other isomer is appeared at 137.5 ppm ($^{1}J_{C,H}$ 164.4 Hz). The resonance in lower field is assigned to the *E*-form, and that at the higher field to the *Z*-form [274].

As a conclusion, the ^{1}H NMR of the derivatives $\mathbf{L_{1\text{-}26}}$ and $\mathbf{L'_{1\text{-}26}}$ in DMSO-d_6 solution showed that the formation of the *E*-isomer was preferable for all compounds as proved by the relative upfield

δ_{NH} shift (9-12 ppm) of the NH proton. The Z-isomer has rather downfield shift (14-16 ppm) and only in some solvents such as $CDCl_3$ could be appeared after several hours [287, 288].

III.1.3.4. X-Ray crystallographic data of the ligands L_8 and L'_{14}

Colorless crystals of the acetylated derivative **L_8** and the deacetylated product **L'_{14}** suitable for X-ray determination were obtained by slow crystallization from ethanol and methanol, respectively. The molecular structure of **L_8** and **L'_{14}** are given in Fig. 62.

Selected interatomic distances, bond angles and torsion angles are collected in Table 9.

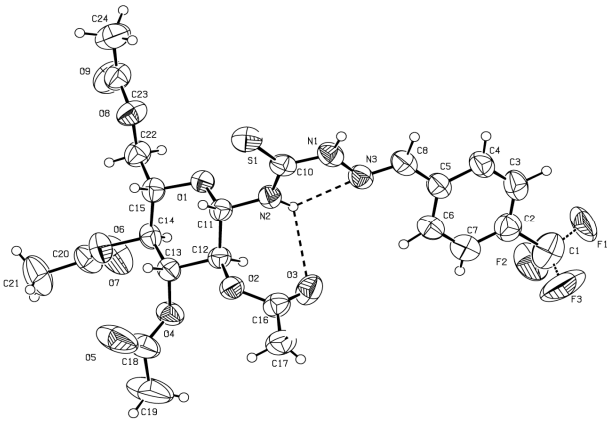

a

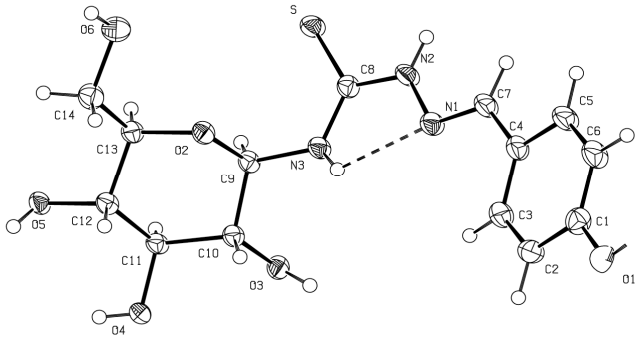

b

Figure 62 Labelled ORTEP diagram of **L_8** ((a), top) and **L'_{14}** ((b), bottom) with 40% probability ellipsoids

Tabel 9 *Selected geometric parameters in compounds* L_8 *and* L'_{14}

L_8		L'_{14}	
a) Bond distances (Å)			
O(1)–C(15)	1.422(3)	O(2)–C(13)	1.425(2)
O(1)–C(11)	1.427(3)	O(2)–C(9)	1.426(2)
N(2)–C(11)	1.435(3)	N(3)–C(9)	1.432(2)
N(2)–C(10)	1.336(4)	N(3)–C(8)	1.346(2)
S(1)–C(10)	1.668(3)	S–C(8)	1.704(2)
N(1)–C(10)	1.359(4)	N(2)–C(8)	1.335(2)
N(1)–N(3)	1.374(4)	N(1)–N(2)	1.389(2)
N(3)–C(8)	1.274(4)	N(1)–C(7)	1.284(2)
F(1)–C(1)	1.278(6)	O(1)–C(1)	1.350(2)
b) Bond angles (°)			
C(11)–O(1)–C(15)	113.0(2)	C(9)–O(2)–C(13)	112.0(2)
O(1)–C(11)–N(2)	107.2(2)	O(2)–C(9)–N(3)	107.3(2)
N(2)–C(11)–C(12)	109.8(2)	N(3)–C(9)–C(10)	113.0(2)
C(10)–N(2)–C(11)	124.2(2)	C(8)–N(3)–C(9)	121.8(2)
S(1)–C(10)–N(2)	125.8(2)	S–C(8)–N(3)	106.6(2)
S(1)–C(10)–N(1)	120.3(2)	S–C(8)–N(2)	121.2(2)
N(1)–C(10)–N(2)	114.0(3)	N(2)–C(8)–N(3)	116.2(2)
N(3)–N(1)–C(10)	120.2(3)	N(1)–N(2)–C(8)	119.3(2)
N(1)–N(3)–C(8)	117.2(3)	N(2)–N(1)–C(7)	114.1(2)
N(3)–C(8)–C(5)	121.2(3)	N(1)–C(7)–C(4)	122.5(2)
c) Torsion angle (°)			
O(1)–C(15)–C(22)–O(8)	-74.5(3)	2)–C(13)–C(14)–O(6)	61.7(2)
O(1)–C(15)–C(14)–C(13)	-65.2(3)	O(2)–C(13)–C(12)–C(11)	-51.8(2)
C(15)–C(14)–C(13)–C(12)	-56.0(3)	C(13)–C(12)–C(11)–C(10)	48.9(2)
C(14)–C(13)–C(12)–C(11)	53.9(3)	C(12)–C(11)–C(10)–C(9)	-52.8(2)
C(13)–C(12)–C(11)–O(1)	-55.5(3)	C(11)–C(10)–C(9)–O(2)	61.3(2)
C(12)–C(11)–O(1)–C(15)	63.0(3)	C(10)–C(9)–O(2)–C(13	-69.1(2)
N(2)–C(11)–O(1)–C(15)	-178.1(2)	N(3)–C(9)–O(2)–C(13)	168.6(2)
N(2)–C(11)–C(12)–C(13)	-172.8(2	N(3)–C(9)–C(10)–C(11)	-180.0(2)
C(11)–N(2)–C(10)–S(1)	7.9(4)	C(9)–N(3)–C(8)–S	-15.1(2)
C(11)–N(2)–C(10)–N(1)	-172.9(3	C(9)–N(3)–C(8)–N(2)	165.8(2)
N(2)–C(10)–N(1)–N(3)	-2.1(4)	N(3)–C(8)–N(2)–N(1)	-5.2(2)
C(10)–N(1)–N(3)–C(8)	174.2(3	C(8)–N(2)–N(1)–C(7)	-174.6(20)
N(1)–N(3)–C(8)–C(5)	177.4(3)	N(2)–N(1)–C(7)–C(4)	176.7(20)

In compound **L_8**, the three F atoms are disordered. The pyranosyl ring adopt a chair conformation, with the values of the puckering parameters being Q = 0.590(3) Å, θ = 176.6(3)°, φ = 138(4) ° (**L_8**), and Q = 0.586(2) Å, θ = 9.1(2) °, φ = 42(7) ° (**L'_{14}**). In **L_8**, the atoms C(11) and C(14) deviate on opposite sides from the mean plane formed by the others atoms C(12), C(13), C(15) and O(1)) by 0.232(2) and -0.241(3)Å, respectively. In a similar way in **L'_{14}**, the atoms C(9) and C(12) deviate by 0.287(2) and -0.184(1)Å, respectively, from the mean plane though the other atoms C(10), C(11), C(13) and O(2)).

For both compounds, the aglycone occupies an equatorial position (in **L_8**, the torsion angle N(2)–C(11)–C(12)–C(13) is -172.8(2) °; in **L'_{14}**, the torsion angle N(3)–C(9)–C(10)–C(11) is -180.0(2), which is assumed to the most stable form, and thus indicated the β-configuration. As in other β-pyranoses [289], the orientation of the primary alcohol group in **L'_{14}** is *gauche*, with the torsion angle O(2)–C(13)–C(14)–O(6) being 61.7(2) °. The dihedral angle between the phenyl ring and the pyranosyl ring is 65.5(2) and 67.6(2) ° for **L_8** and **L'_{14}**, respectively. The compound **L_8** exhibit *E*,*Z* configuration in relation to the C(8)–N(3) and N(1)–C(10) bond, respectively, and compound **L'_{14}** exhibit the same configuration in relation to the C(7)–N(1) and N(2)–C(8) bond, respectively.

In both molecules, the thiosemicarbazone moiety, is almost planar, due to the C=N double bond. Meanwhile, in **L_8**, atoms N(2) and N(3) are involved in an intramolecular N(2)–H···N(3) interaction, and in **L'_{14}**, atom N(3) and N(1) are involved in N(3)–H···N(1) interaction, which also contributes to the planarity of the thiosemicarbazone group. The formation of these hydrogen bond was favorated by the *Z* configuration in relation to the N(1)–C(10) and N(2)–C(8) bond **L_8** and **L'_{14}**, respectively. In both compounds, the S–C and the azomethine C–N bond distance exhibit increased double bond character. The N–N and both thioamide C–N bond distance indicate a considerable double bond character. This is indicative of the greater conjugation and more delocalized electron density of the thiosemicarbazone moiety [290, 291].

The two molecules are stabilized by intra- and intermolecular interaction. The packing diagrams of **L_8** and **L'_{14}** are presented in Fig. 63, and the intra and inte-rmolecular contacts are collected in Tabel 10.

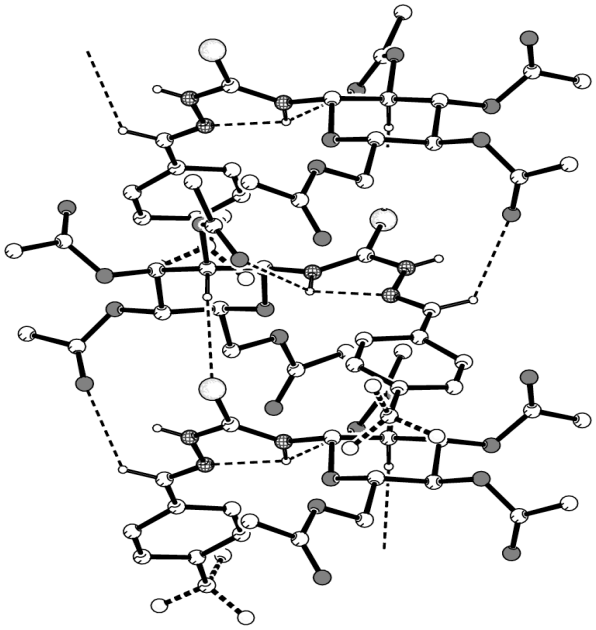

a

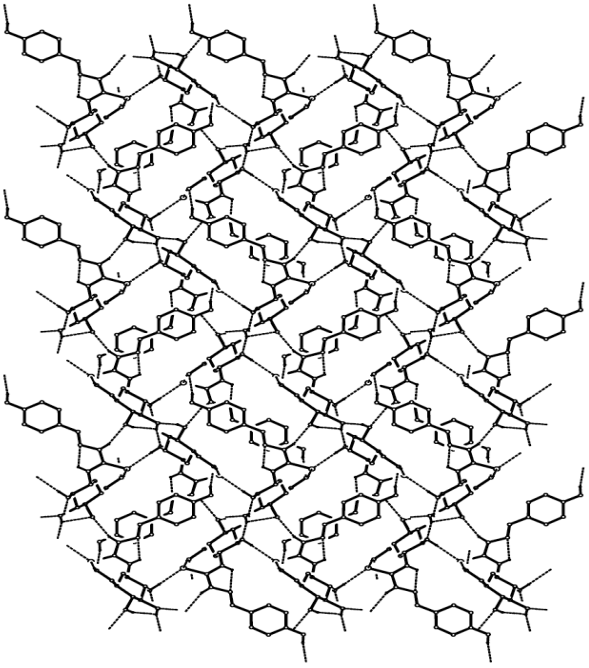

b

Figure 63 Packing diagram of $\mathbf{L_8}$ (*(a)*, left) and $\mathbf{L'_{14}}$(*(b)*, right) along the *c*- and *a*-axies, respectively

Tabel 10 *Inter and intra-molecular contacts (Å) for* ***L_8*** *and* ***L'_{14}***

Donor (D)		Acceptor(A)[a]	D···A	H···A	D···H···A
		L_8			
C(8)	H(C8)	O(7)^{i}	3.207(4)	2.53(3)	124(2)
C(12)	H(C12)	S(1)^{ii}	3.765(3)	2.78(3)	165.(2)
N(2)	H(N2)	O(3)	3.018(3)	2.55(3)	114(2)
N(2)	H(N2)	N(3)	2.592(3)	2.14(3)	111(2)
C(11)	H(C11)	S(1)	3.127(3)	2.69(2)	108(2)
C(12)	H(C12)	O(3)	2.696(3)	2.33(2)	100(2)
C(13)	H(C13)	O(5)	2.683(4)	2.30(2)	105(2)
C(14)	H(C14)	O(7)	2.688(4)	2.24(3)	109(2)
		L'_{14}			
O(1)	H(O1)	O(6)^{iii}	2.817(2)	2.08(3)	156(3)
N(2)	H(N2)	O(5)^{iv}	3.038(2)	2.23(2)	161(3)
O(3)	H(O3)	S^{v}	168(2)	2.32(2)	17692)
O(4)	H(O4)	O(3)^{iii}	2.730(2)	1.97(2)	160(2)
O(5)	H(O5)	O(4)^{iv}	2.643(2)	1.87(2)	164(2)
O(6)	H(O6)	S^{vii}	3.260(2)	2.48(3)	174(2)
C(6)	H(C6)	O(2)^{iii}	3.203(2)	2.36(2)	152(2)
C(7)	H(C7)	O(5)iv	3.354(2)	2.53(2)	146(2)
C(9)	H(C9)	S	3.043(2)	2.68(2)	103(2)
N(3)	H(N3)	N(1)	2.615(2)	2.20(2)	114(2)
O(4)	H(O4)	O(5)	2.917(2)	2.55(2)	110(2)

[a] Symetry codes: (i) 1 _ x, 1/2 + y, _7/2 _ z; (ii) 1 _ x, _1/2 + y, _7/2 _ z; (iii) 1/ 2 + x, 1/2 _ y, 2 _ z ; (iv) 3/2 _ x, 1 _ y, 1/2 + z; (v) 2 _ x, _1/2 + y, 3/2 _ z; (vi) _1/2 + x, 1/2 _ y, 1 _ z; (vii) _1 + x, y, z.

The monomers of **L_8** are linked by two intermolecular bonds C(8)–H(C8)···O(7) and C(12)–H(C12)···S(1). The monomers of **L'_{14}** are connected by strong and weak intermolecular hydrogen bonding interaction H–O···O, N–H···O, O–H···S, and C–H···O into a three-dimensional framework.

III.2. The binding of β-D-glucopyranosyl-thiosemicarbazones to glycogen phosphorylase: A new class of inhibitors

III.2.1. Overview

As mentioned in the introduction (chapter II.3), *N*'-benzoyl-β-D-glucopyranosyl urea which binds at the catalytic as well as the new allosteric site of glycogen phosphorylase (GP) is a potent GP inhibitor and a target for the development of hypoglycaemic drugs.

Using as lead *N*'-benzoyl-β-D-glucopyranosyl urea we have now assessed the inhibitory potential of a series of thiosemicarbazone derivatives of β-D-glucopyranosylamine [292] (**L'$_{1-26}$,** Table 11) to GP*b*. In these compounds the urea moiety of *N*'-benzoyl-β-D-glucopyranosyl urea is replaced by a thiosemicarbazone to:

- elongate the linker to the group that binds at the so called β-pocket of the catalytic site
- to test the contribution of the carbonyl oxygen of urea interactions to the inhibitory potency.

In addition, instead of the benzyl group of Bzurea, compounds **L'$_{1-26}$** have a benzyl ring with variety of groups attached at either *ortho*-, *meta*- or *para*- position with respect to the thiosemicarbazone moiety to investigate the ability of various groups to enhance the inhibitory potency of the benzyl-thiosemicarbazone derivatives [293]. On the other hand, thiosemicarbazones is a class of biochemically important compounds possessing a wide range of biological activity, and is very promising in the treatment of many diseases [294-297]. Compounds **L'$_1$**, **L'$_2$**, **L'$_3$**, **L'$_4$**, **L'$_6$**, **L'$_7$**, **L'$_8$**, **L'$_9$**, **L'$_{11}$**, **L'$_{12}$**, **L'$_{13}$**, **L'$_{14}$**, **L'$_{17}$**, **L'$_{18}$**, **L'$_{22}$** were found to be competitive inhibitors of GP*b* with respect to Glc-1-P with Ki values 3.4 - 314.6 μM. Crystallographic data show that these compounds bind at the catalytic site and, with the exception of compound **L'$_9$**, at the indole carboxamide site of GP*b* as well. Identification of the structural determinants contributing to inhibitor binding mode at the catalytic site should provide better understanding of the mechanism of inhibition of GP and aid the design of compounds with improved potency against GP.

III.2.2. Enzyme kinetics

The inhibitory efficiency of most of the thiosemicarbazone derivatives was tested in kinetic experiments with rabbit muscle glycogen phosphorylase *b* (RMGP*b*) and their inhibition constants are presented in Table 11. All compounds displayed competitive inhibition with respect to the substrate Glc-1-P, at constant concentrations of glycogen (0.2 % w/v) and AMP (1 mM) with IC_{50} values at the μM range. The most potent compound is compound **L'$_1$,** with a fluorine atom at the *para* position of the aromatic ring with IC_{50}= 5.7 μM while the least potent is compound **L'$_8$** (IC_{50}= 524.3 μM), with a -CF_3 group at the same position. Comparison of the ligands with *para* substitution (columns 1, 4, 6, 7, 9, 12, 13, and 14 in table 11) indicates that the inhibitory potency decreases with the increase in bulkiness of the substituent at this position. This is also evident when comparing the potency of compounds **L'$_{17}$** (methoxy) and **L'$_{18}$** (methyl), which have IC_{50} values of 406.5 μM and 192.4 μM, respectively or when comparing the potency of **L'$_1$** with that of **L'$_{18}$**. The only exception to this observation is the nitro compound **L'$_{11}$**, which is among the best inhibitors of the enzyme. This exception indicates that the chemical properties of the substituent are also affect significantly the potency of the ligand. Comparing the position (*ortho*, *meta* or *para*) of the substituent at the phenyl ring reveals that within the compounds with chlorine atom (**L'$_2$**, **L'$_3$**, and **L'$_4$**) the order of potency is *para* ≈*meta* > *ortho* while for those with a hydroxyl (**L'$_{12}$**, **L'$_{13}$**, and **L'$_{14}$**) is *ortho* > *meta* > *para*. The potency of compounds **L'$_6$** and **L'$_7$** with bromine atom at *para* and *meta* position does not differ much (IC_{50} values 50.4 μM and 93.2 μM) while **L'$_9$** and **L'$_{11}$** with a nitro group at *ortho* and *para* position, show large differences in their potency with IC_{50} values of 484.2 μM and 25.7 μM, respectively. Therefore a general pattern with respect to the position of the substituent (i.e., *para* is better than *meta*) is not evident from the kinetics results. Thus, for halogens the best position is *meta*, for the nitro group the *para* and for the hydroxyl the *ortho* position. However, it seems that the inhibitory potency of the compounds depends mostly on the chemical and physical properties (size, charge, polarizability, etc.) of the decorating groups of the phenyl ring.

Compound **L'$_1$** (IC_{50}=5.7 μM), is almost equipotent with Bzurea (K_i=4.6 μM) [297] while the rest of the inhibitors are poor inhibitors compared to their lead molecule (Bzurea). However, compounds **L'$_3$**, **L'$_4$**, **L'$_6$**, **L'$_{11}$**, and **L'$_{12}$** are still considered as potent inhibitors with IC_{50} values less than 50 μM and could be exploited as improved leads for further optimization.

Table 11 *Inhibitory efficiency of the thiosemicarbazone derivatives of β-D-glucopyranoze and the atom numbering scheme using in crystal structure*

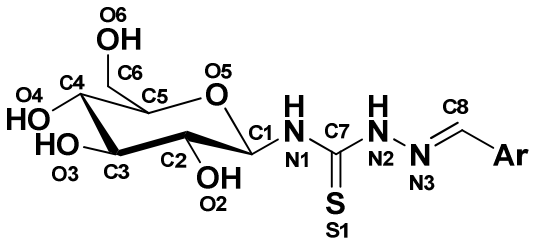

Column	Compound	Ar group	IC_{50}(μM)
1	**L'$_1$**	-C_6H_4-F-*p*	**5.7 ± 0.4**
2	**L'$_2$**	-C_6H_4-Cl-*o*	370 ± 9.7
3	**L'$_3$**	-C_6H_4-Cl-*m*	23.2 ± 0.5
4	**L'$_4$**	-C_6H_4-Cl-*p*	28.3 ± 1.7
5	**L'$_6$**	-C_6H_4-Br-*m*	50.4 ± 1.9
6	**L'$_7$**	-C_6H_4-Br-*p*	93.2 ± 5.1
7	**L'$_8$**	-C_6H_4-CF_3-*p*	524.3 ± 11.4
8	**L'$_9$**	-C_6H_4-NO_2-*o*	484.2 ± 23.3
9	**L'$_{11}$**	-C_6H_4-NO_2-*p*	25.7 ± 0.9
10	**L'$_{12}$**	-C_6H_4-OH-*o*	26.6 ± 3.3
11	**L'$_{13}$**	-C_6H_4-OH-*m*	180 ± 7.8
12	**L'$_{14}$**	-C_6H_4-OH-*p*	340.5 ± 21.7
13	**L'$_{17}$**	-C_6H_4- OMe-*p*	406.5 ± 40.6
14	**L'$_{18}$**	-C_6H_4- Me-*p*	192.4 ± 5.8
15	**L'$_{22}$**	-4-pyridyl	200 ± 17

III.2.3. Structural studies

In order to elucidate the structural basis of inhibition we have determined the crystal structure of GP*b* in complex with each of the 15 compounds presente in Table 11 (one example of GP*b* in complex with **L$_1$**; Fig. 64). The $2F_o$-F_c and F_o-F_c Fourier electron density maps calculated using the coordinates of the native structure indicated that all 15 compounds bound at *the catalytic* site and at the *new allosteric site* (with the exception of **L'$_9$** which was found bound only at the catalytic site). Electron density maps clearly defined the position of each atom of the inhibitors within the catalytic and the new allosteric site. In crystallographic experiments with a soak of 1 mM of each inhibitor for 3.5 hours, electron density maps suggested strong binding to the catalytic site, but partial occupancy of the new allosteric site by the ligand. It seems therefore that the new allosteric site is not the primary binding site for these inhibitors. A similar situation has been observed with Bzurea [138].

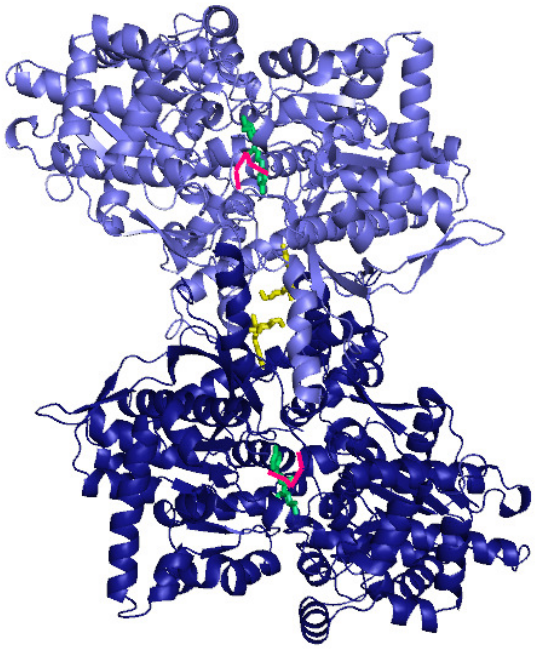

Figure 64 A schematic diagram of the GP*b* dimeric molecule viewed down the molecular dyan. One subunit is colored in dark blue and the other in light blue. The catalytic and the new allosteric site are marked by bound compound **L'$_1$** (in green and yellow respectively). Compound **L'$_1$**, on binding to the catalytic site, promotes the less active T state through stabilization of the closed position of the 280s loop (shown in pink and thicker) which blocks access for the substrate (glycogen) to the catalytic site

The structural results show that all inhibitors are bound with essentially no disturbance of the overall protein structure. The superimposition of the structures of native GP*b* and the GP*b* – inhibitor complexes over well defined residues (18-249, 262-312, 326-829) gave rmsd values 0.2-0.4 Å (Cα positions). However, upon binding to the catalytic site compounds **L'$_4$, L'$_7$, L'$_8$, L'$_{12}$, L'$_{17}$** and **L'$_{18}$**, trigger a significant shift of the 280s loop with concomitant changes in the adjacent imidazole of His571. Thus, the major rmsd between the structures of GP*b*-inhibitor and native GP*b* for main chain atoms are for the residues Asn282 (0.4-0.7 Å), Asp283, (0.7-1.0 Å), Asn284 (1.1-1.8 Å), Phe285 (0.8-0.9 Å), Phe286 (0.6-0.7 Å), and Glu287 (0.3-0.4 Å). In the native structure, the side chain atom NE2 of His571 forms a hydrogen bond with the side chain atom OD2 of Asp283. In the complex structures with compounds **L'$_4$, L'$_7$, L'$_8$, L'$_{12}$, L'$_{17}$** and **L'$_{18}$** the side chain of His571 is rotated ($\chi 1 \approx 20°$) to mainain this hydrogen bond with the side chain of Asp283 at the new position.

Furthermore, the conformational change of the 280s loop results in Asn284 being sandwiched between the side chains of Phe285 and Tyr613. These phenyl rings are the key components of the inhibitor site of GP*b*, a site that binds caffeine and a number of other fused ring compounds [109, 115, 298]. The insertion of Asn284 leads to the destruction of this site. This mimics the T to R allosteric transition, which also involves movement of the 280s loop [113]. However, a structural comparison between the present GP*b* complexes and maltodextrin phosphorylase [299, 300] where the 280s loop is held in an open conformation (in the R state GP*b* the 280s loop is disordered and its position ambiguous [301]) in the vicinity of the catalytic site has shown that the shifts of the 280s loop are not in the direction of the T to R allosteric transition. In addition, the new position of the 280s loop imposed by the binding of the present inhibitors still obstructs the entrance to the catalytic site of GP*b* and therefore all fifteen inhibitors can be classified as T state inhibitors. The mode of binding and the interactions that the glucopyranose moiety of all fifteen compounds makes with GP*b* residues at the catalytic site are almost identical with that of α-D-glucose [143, 308]. The benzaldehyde-derived thiosemicarbazone moiety is accommodated at the β-pocket of the catalytic site forming mainly van der Waals interactions with the protein. The sulfur group of thiosemicarbazone is hydrogen bonded either directly to Asp283 OD1 (compounds **L'$_1$**, **L'$_2$** and **L'$_{14}$**) or Leu136 N (compounds **L'$_4$**, **L'$_7$**, **L'$_8$**, **L'$_{17}$**, and **L'$_{18}$**), or to both (compounds **L'$_{11}$** and **L'$_{22}$**) or through a water molecule (compounds **L'$_3$, L'$_6$**, **L'$_9$, L'$_{12}$,** and **L'$_{13}$**) to the side chain of Asp283. Apart from these interactions the thiosemicarbazone moiety is not involved in any other hydrogen-bond interactions with neighbouring residues. The hydrogen bond between N1 of N-acetyl-β-D-glucopyranosylamine (NAG) and carbonyl O of His377, an interaction that has been observed in all

β-D-glucopyranosylamine analogues [109, 296] has not been observed in this complex similarly to the Bzurea complex [138]. At the new allosteric site the glyocopyranose moiety is engaged in hydrogen bond interactions with the side chain atoms of Glu190, and the main chain nitrogen of Ala192, while four water molecules mediate hydrogen bonds to side chain atoms of His57, Arg60, Asn187, and Tyr226. In addition, N1 from the thiosemicarbazone moiety forms a hydrogen bond with the carbonyl oxygen of Glu190 while N2 and N3 form hydrogen bonds with the side chain of Arg160. The interactions between **L'$_1$**, **L'$_3$**, **L'$_6$** and **L'$_{11}$** and the protein are shown in Fig. 65.

The glucopyranosyl-thiosemicarbazone derivatives studies (**L'$_1$**, **L'$_2$**, **L'$_3$**, **L'$_4$**, **L'$_6$**, **L'$_7$**, **L'$_8$**, **L'$_9$**, **L'$_{11}$**, **L'$_{12}$**, **L'$_{13}$**, **L'$_{14}$**, **L'$_{17}$**, **L'$_{18}$**, **L'$_{22}$**) have a benzaldehyde-derived group attached at the C8 position (Table 11), which has either a –Br or a –Cl or a –OH, or a –Me, or a OMe, or a –NO2, or a –F at *ortho*, *para* or *meta* positions instead of a benzaldehyde-derived group and there is a pyridinecarboxaldehyde-derived moiety. Since the conformation of the derivatives upon binding to the catalytic site and at the new allosteric site is very similar (Fig. 66), we describe below in more detail the interaction of the phenyl or pyridyl moiety of compounds **L'$_1$**, **L'$_2$**, **L'$_3$**, **L'$_4$**, **L'$_6$**, **L'$_7$**, **L'$_8$**, **L'$_9$**, **L'$_{11}$**, **L'$_{12}$**, **L'$_{13}$**, **L'$_{14}$**, **L'$_{17}$**, **L'$_{18}$**, **L'$_{22}$** with GP*b* in groups according to the substituent group of the aromatic ring of the inhibitors (Table 11).

The fifteen thiosemicarbazone β-D-glucopyranosylamine derivatives studied have a benzaldehyde group attached at the C8 position (Table 11) which has either a -Br or a -Cl or a -OH, or a -Me, or a -OMe or a –NO_2, or a -F at *ortho*, *para* or *meta* positions or instead of a benzaldehyde there is a pyridine. Since the conformation (Figure 66) and the protein-ligand interactions pattern of glucopyranosyl ring and the catalytic site is very similar, and the same applies for the inhibitors bound at the new allosteric site, we describe below in more detail the interactions of the phenyl or pyridyl moiety of compounds with GP*b* in groups according to the R group of the aromatic ring of the inhibitors.

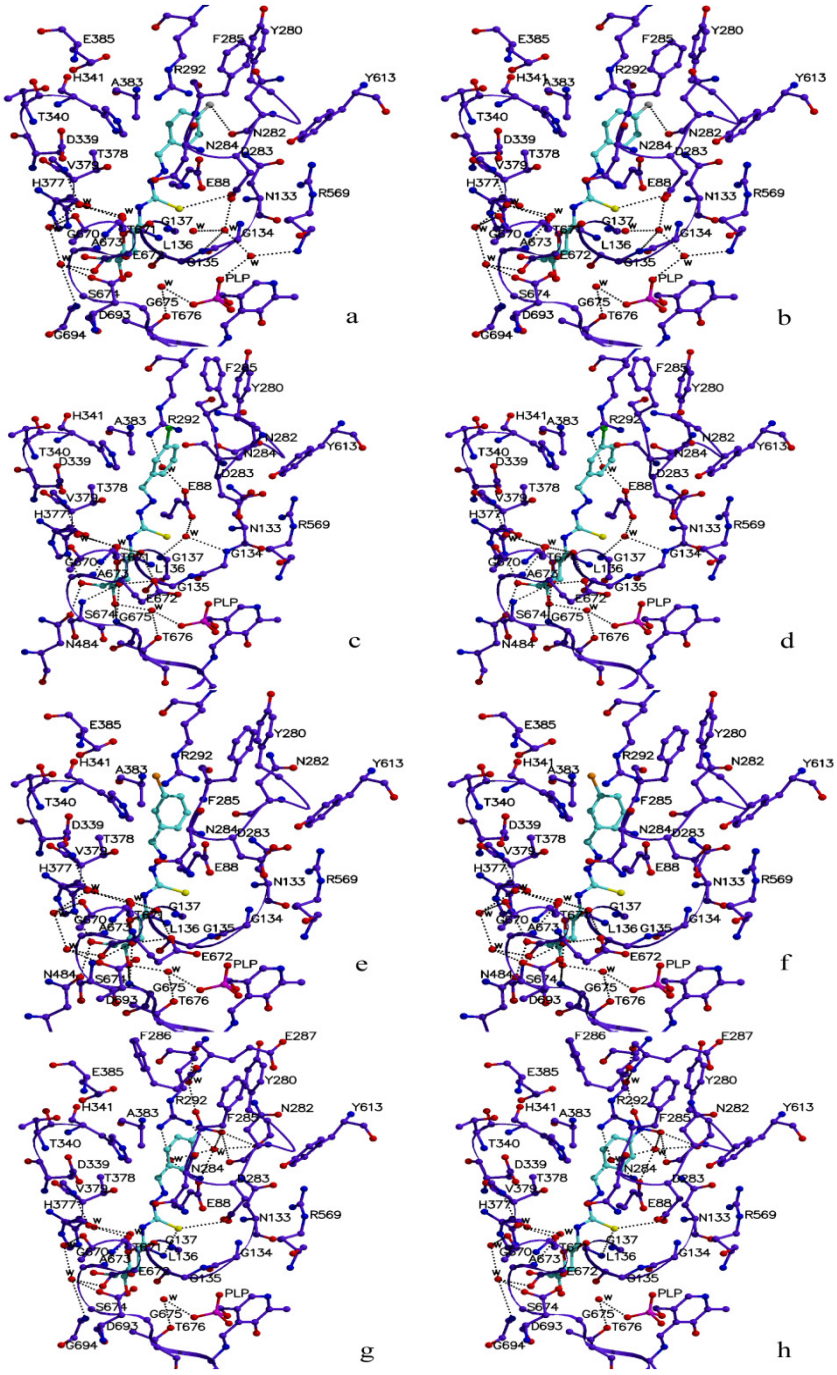

Figure 65 Schematic diagrams of the molecular interactions between GPb and inhibitors (**L'$_1$**, **L'$_3$**, **L'$_6$**, and **L'$_{11}$**, when bound at the catalytic site (a, c, e, g) and at the new allosteric site of GPb (b, d, f, h). The side chain of protein residues involved ligand binding is shown as ball-and-stick models. Hydrogen bond interactions between the inhibitors, protein residues and water molecules (w) are represented as dotted lines.

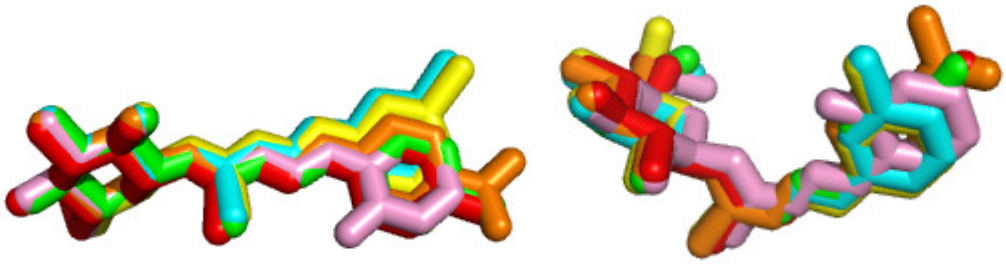

Figure 66 Structural comparision of the ligand molecules when bound at the catalytic new allosteric site (right) of GPb are shown in color; **L'$_1$** green, **L'$_6$** yellow, **L'$_3$** cyan, **L'$_{11}$** orange, **L'$_{12}$** pink and **L'$_{18}$** red

III.2.3.1. The halogen group

The conformation of the halogen inhibitors when bound at the catalytic site of GP*b* are very similar (Fig. 66). **L'$_1$** upon binding at the catalytic site of GP*b* forms 10 hydrogen bonds and 101 van der Waals interactions (Fig. 65), while inhibitor **L'$_8$** forms 11 hydrogen bonds and 95 van der Waals interactions with protein 330 residues. Compound **L'$_4$** form 9 hydrogen bonds, and 103 van der Waals interactions with the protein residues at the catalytic site, respectively while **L'$_7$** participates in 9 hydrogen-bonding interactions and 100 van der Waals interactions with residues of GP*b* at the same site.

Fluorine is a poorer hydrogen bond acceptor that oxygen (it cannot act as a donor) [304] and it affects significantly the hydrogen-bonding interactions between a ligand and residues of the catalytic site of GPb [304] that cannot donate a proton. In the **L'$_1$ –**GP*b* complex, fluorine forms a hydrogen bond [305] with Asn282 O whereas the fluorine atoms of the trifluoromethyl group of **L'$_8$** engage in hydrogen bond interactions with the side chain atoms of Arg292, the main chain oxygen and the side chain oxygen and the side chain OD1 of Asn282, and a water mediated interaction with side chain of Glu88. In **L'$_4$** the chloride group is involved only in 11 van der Waals interactions while **L'$_7$** bromine is involved in hydrogen bond interactions with Asn282 OD1 in addition to 10 van der Waals interactions (Table 12). Upon biding to the catalytic site of GP*b*, compounds **L'$_2$**, **L'$_3$**, **L'$_6$**, form 8, 8 and 9 hydrogen bonds, and 97, 86 and 100 van der Waals interactions with the protein residues, respectively (Fig. 65). The chloride group of **L'$_3$** forms two hydrogen bonds with the carbonyl oxygen atoms of Phe285 and Ala383 O and the chloro-phenyl ring engages in 4 van der Waals interactions. The bromide group of compound **L'$_6$** engages in a halogen bond interaction [306] with the carbonyl oxygen of Phe285 while the bromo-phenyl ring takes part in 7 van der Waals interactions with protein residues (Table 12). In the **L'$_2$–**GP*b*

complex the chloride group forms hydrogen bond with the main chain nitrogen of Phe285 and the chlorophenyl ring participates in 6 van der Waals interactions with GP*b* residues (Table 12).

Table 12 *Interactions of the aryl ring substituent of the inhibitors with GPb residues at the catalytic site.*

Compound	Hydrogen/halogen bonds	Number of Van der Waals interactions
L'$_1$	**Asn282 O**	**6**
L'$_2$	Phe285 N	6
L'$_3$	Phe285 O; Ala383 O	4
L'$_4$	--	11
L'$_6$	Phe285 O	7
L'$_7$	Asn282 OD1	10
L'$_8$	Asp339 OD2; Ala383 O	3
L'$_9$	Glu88 OE1	15
L'$_{11}$	Tyr280 O; Asn282 O	13
L'$_{12}$	Asp283 O	6
L'$_{13}$	Asn282 O	2
L'$_{14}$	Asn282 O	0
L'$_{17}$	--	15
L'$_{18}$	--	8
L'$_{21}$	Asp339 OD2; Ala383 O	3

The most interesting observation of the binding of the halogen compounds is that the binding of **L'$_4$**, **L'$_7$**, and **L'$_8$** causes a significant conformational change of the GP*b* residues of 280s loop and on average the Cα atoms of residues 282-287 are shifted by 1.0 Å from their positions at the native structure. The conformational change is less profound in the **L'$_1$**, **L'$_3$**, **L'$_6$** complexes where the average shift of all atoms of residues 282-287 is 0.3 Å while in the **L'$_2$** complexes this was not observed. Interestingly, the trifluoromethyl derivative triggers significant conformational changes to the 280s loop whereas the effect of the binding of fluoro-compound is less profound. Therefore, it seems that the *para* halogen substituents trigger a most significant conformational change than

those at *meta* or *ortho* position. The exception of **L'$_1$** might be attributed to the smaller size of the fluoride group as compared to those of the trifluoromethyl, chloride or bromide group.

Kinetic studies revealed that compound **L'$_1$** is the most potent of all fifteen compounds, almost 92 times more potent than compound **L'$_8$** and equipotent to Bzurea [138]. Structural composition of the **L'$_1$**– GP*b* complex with the GP*b*-Bzurea complex at the catalytic site (Fig. 67a) showed that the two inhibitors bind in a similar manner and this provides a structural basis to their equipotency. Therefore it seems that replacement of the urea moiety with thiosemicarbazone does not affect the potency of the inhibitor since Bzurea and **L'$_2$** are equipotent.

Kinetic studies revealed that **L'$_3$** and **L'$_4$** (*para* and *meta* position of chloride derivatives) have a significant better inhibitory effect on GP*b*, than the **L'$_2$** (*ortho*) derivative with IC_{50} values 16 and 13 times lower, respectively. The binding position of the chloro-phenyl ring is different in the three compounds. Its position in compound **L'$_3$** is 1.8 Å apart from its position in compounds **L'$_2$** and **L'$_4$**, and the angle between the planes of the benzyl ring in the two latter compounds is ~20°. The chloride group is engaged in halogen bond interactions with the carbonyl oxygen of Phe285 and Ala383 in compound **L'$_3$** and with the main chain nitrogen of Phe285 in compound **L'$_2$**, while in compound **L'$_3$** is involved only in van der Waals interactions (Table 12). However, the most interesting observation of the binding of the chloro-compounds is that compounds **L'$_3$** and **L'$_4$** induce the 280s loop conformational change described above whereas compound **L'$_2$** does not. This conformational change and the stabilization of the 280s loop seem to form the structural basis for the much higher potency of compounds **L'$_3$** and **L'$_4$** with respect to **L'$_2$**.

Kinetic experiments indicated that inhibitors **L'$_6$** and **L'$_7$** are almost equipotent (Tabel 11) and this is consistent with structural studies that show that both inhibitors bind very similarly to the catalytic site of GP*b* engaging in approximately the same number of interactions with protein residues (Table 12). Futhermore, on binding both compounds **L'$_6$** and **L'$_7$** displace five water molecules from the active site of the unliganded structure.

Upon binding to the new allosteric site of GP*b*, inhibitors **L'$_1$** and **L'$_8$** form 4 hydrogen bonds each and 111 and 77 van der Waals interactions, respectively (Fig. 66). The fluoro and fluoromethyl groups do not engage in any hydrogen bond interactions with protein residues. Structural comparison with the Bzurea binding revealed that the β-D-glucopyranose moiety in the two ligands is shifted to an opposite direction (Fig. 68b). Upon binding to the new allosteric site of GP*b*, compounds **L'$_2$**, **L'$_3$**, and **L'$_4$** form three hydrogen bonds each and exploit 64, 79, 85 van der Waals interactions, respectively (Fig. 65).

A structural comparison with Bzurea which also binds at the same site [138] revealed that the glucopyranose moiety once again shifts to opposite directions by approximately 93° with respect to the backbone. The binding of **L'$_2$**, **L'$_3$**, and **L'$_4$** at the new allosteric site does not promote any significant conformational change apart from the shift of the side chain of Arg60 which has been observed for all compounds that bind to this site. Inhibitors **L'$_6$** and **L'$_7$** were also found bound at the new allosteric site.

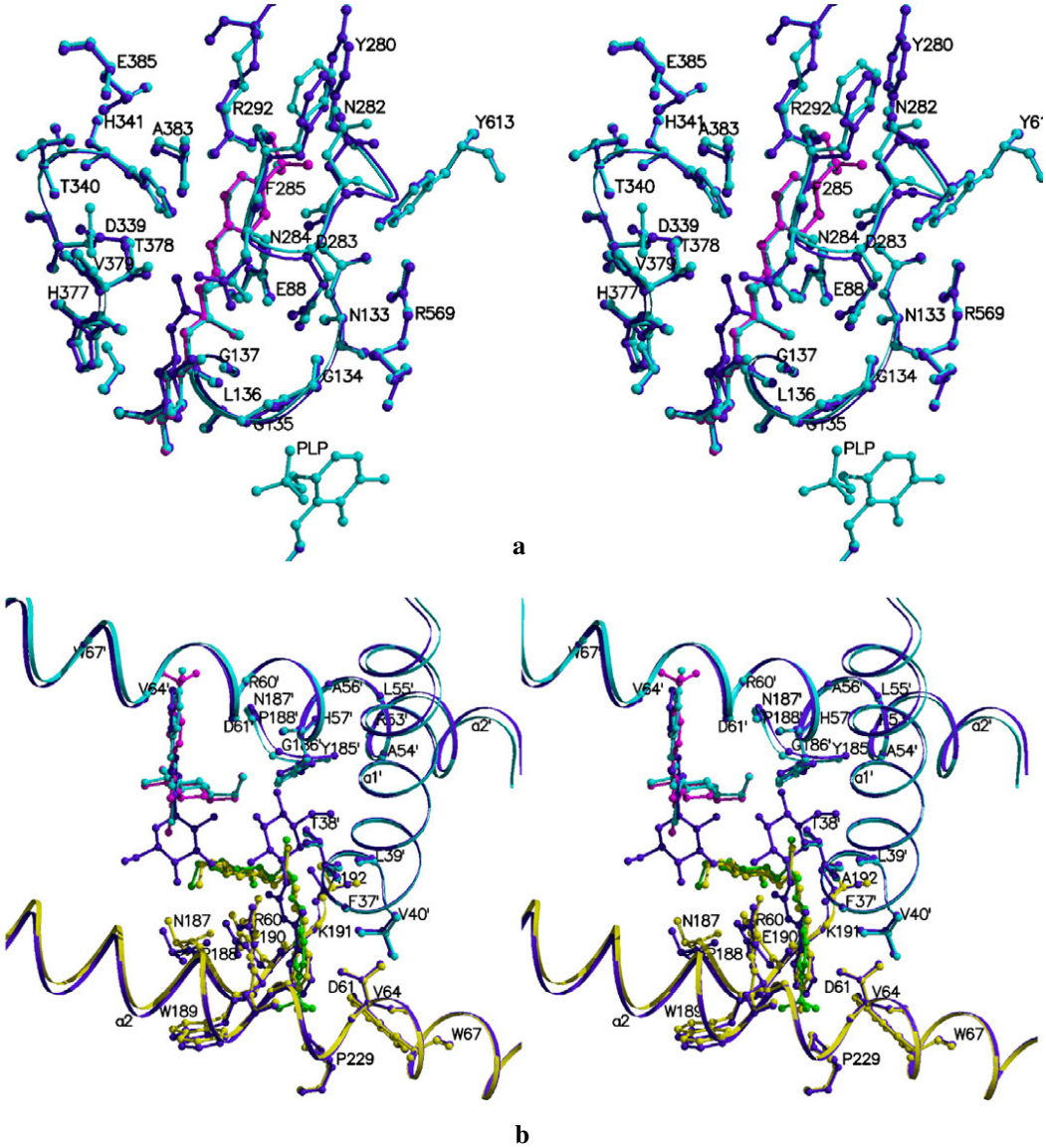

Figure 67 *(a)* Stereodiagrams of the structural comparision between GP*b* in complex with **L'$_1$** (cyan) and *N'*-benzoyl-*N*-β-D-glucopyranosly urea (magenta) at the catalytic site of GP*b* and *(b)* in the vicinity of the new allosteric site (*N'*-benzoyl-*N*-β-D-glucopyranosly urea-GP*b* complex, magenta) and GP*b*- **L'$_1$** complex (subunit 1, yellow and subunit 2, cyan) and GP*b*- **L'$_8$** complex (subunit 1, green and subunit 2, magenta)

Compound **L'$_6$** is bound at the new allosteric site with two alternative conformations in which the orientation of the bromo-benzyl moiety differs by 180°. Compound **L'$_7$** displays only one conformation at this site and both **L'$_6$** and **L'$_7$** form 7 hydrogen bonds and 34 van der Waals interactions with protein residues (Fig. 65). The most significant conformational change at this site upon binding of these inhibitors is the shift of the side chain of Arg60 by ~2.0 Å from its position at the native GPb structure, which is probably due to the stereochemical impediments imposed by the inhibitor molecule and has also been observed upon binding of Bzurea to the same site. A structural comparision with the binding of Bzurea at this site [208] revealed only minor conformational changes.

III.2.3.2. The nitro group

Inhibitors **L'$_9$** and **L'$_{11}$**, 2- and 4-nitro-benzaldehyde 4-(β-D-glucopyranosyl) thiosemicarbazone upon binding to the catalytic site of GP*b* take part in 11 and 14 hydrogen bond interactions with the protein while they exploit 114 and 129 van der Waals interactions with GP*b* residues (Fig. 65). Interestingly a structural comparison of the complexes with that of the free enzyme reveals that the binding of the two inhibitors does not cause any significant conformational changes including the 280s loop. The nitro group in compound **L'$_9$** participates in a hydrogen bond interaction with the side chain of Glu88 (Table 12) and water mediated hydrogen bonds with the main chain nitrogen of Gly134 and Gly137.

In compound **L'$_{11}$** the nitro group is involved in hydrogen bond interactions with the carbonyl oxygen of Tyr280 and Asn282 (Table 12) and a water mediated hydrogen bond with the carbonyl oxygen of Glu287 (Fig. 65). Kinetic studies revealed that inhibitor **L'$_{11}$** (*para* position) is almost 19 times more potent than **L'$_9$** (*ortho* position). This difference in their potency can (i) to the three additional hydrogen bond interactions of inhibitor **L'$_{11}$** with respect to those of **L'$_9$**, and (ii) to the hydrogen bonds of atom O7 of the nitro group of **L'$_{11}$** with main chain oxygen atoms of Tyr280 and Asn282 from 280s loop (unlike the nitro group of **L'$_9$** which does not form any interactions with residues of the 280s loop) that lead to further stabilization of its closed conformation.

Upon binding to the new allosteric site of GP*b*, inhibitor **L'$_{11}$** forms three direct and six water mediated hydrogen bonds and 79 van der Waals interactions with GPb residues (Fig. 64). Structural comparison with Bzurea bound at this site revealed that the glucopyranose moiety shifts to opposite directions by approximately 93° with respect to the backbone. Inhibitor **L'$_9$** was not found bound at the new allosteric site.

III.2.3 3. The hydroxyl group

The 2-, 3-, and 4-hydroxy-benzaldehyde 4-(β-D-glucopyranosyl) thiosemicarbazone (**L'$_{12}$**, **L'$_{13}$**, and **L'$_{14}$**) were found bound at the catalytic and the new allosteric site. The conformation of the three compounds upon binding at the catalytic site differs. Thus, in compound **L'$_{12}$** the torsion angle C8-N3-N2-C7 is 180° so that the conformation about the N2-N3 bond is *trans* geometry while in compounds **L'$_{13}$** and **L'$_{14}$** it is −180° (for atom numbering, see in Table 11). In addition, the hydroxyphenyl ring is coplanar with the thiosemicarbazone linker in compounds **L'$_{12}$** and **L'$_{14}$** whereas in **L'$_{13}$** is inclined by ~20°. Upon binding to the catalytic site of GPb, inhibitors **L'$_{12}$**, **L'$_{13}$** and **L'$_{14}$** form 15, 15 and 13 hydrogen bonds, and expoit 109, 125, and 97 van der Waals interactions, respectively (Fig. 68). The binding mode of hydroxyphenyl group differs between the three inhibitors. The hydroxyl group is bound deep in the so-called β-pocket involved in van der Waals interactions with protein residues dominated by polar-non polar contacts with Glu88, Asn282, Asp283, Phe285, Arg292, and His341. The binding of **L'$_{12}$** and **L'$_{14}$** but not **L'$_{13}$** triggers significant shifts of the main chain atoms from their position in the native GP*b* structure. The major rmsd values of the main chain atoms are for residues Asn282 (0.7Å), Asp283 (0.7Å), Asn282 (1.1Å), Phe285 (0.9Å), Phe286 (0.6Å). In the **L'$_{14}$** complex the hydroxyl group is hydrogen-bonded with the carbonyl oxygen of Asn282 and it is not involved in any van der Waals interactions (Table 12). Compound **L'$_{13}$** displays two alternative conformations for the hydroxylphenyl group 180° apart and the hydroxyl group takes part in hydrogen bond interactions with either the carbonyl oxygen of Ala383 and water mediated interactionswith side chain atoms of Glu88 and Arg292 or the carbonyl oxygen of Asn282 (Fig. 68, Table 12). The hydroxyl group in compound **L'$_{12}$** forms a hydrogen bond with the carbonyl oxygen of Asp283 (Table 12).

Kinetic studies revealed that **L'$_{12}$** (*ortho* position) has the best inhibitory effect on GP*b* with an IC_{50} value of 26.6 μM while inhibitors **L'$_{13}$** and **L'$_{14}$** (*meta* and *para* position) are less potent with IC_{50} values of 180 μM and 340.5 μM respectively. This difference in their inhibitory potency might be attributed to the number of the van der Waals interactions of the hydroxyl group with GPb residues in each inhibitor complex (Table 12). Thus, **L'$_{12}$** which displys 6 interactions is more potent than **L'$_{13}$** (2 interactions) which in turn is more potent than **L'$_{14}$** (no interactions).

On binding to the new allosteric site all three inhibitors have similar conformation which differs significantly from that observed in the catalytic.

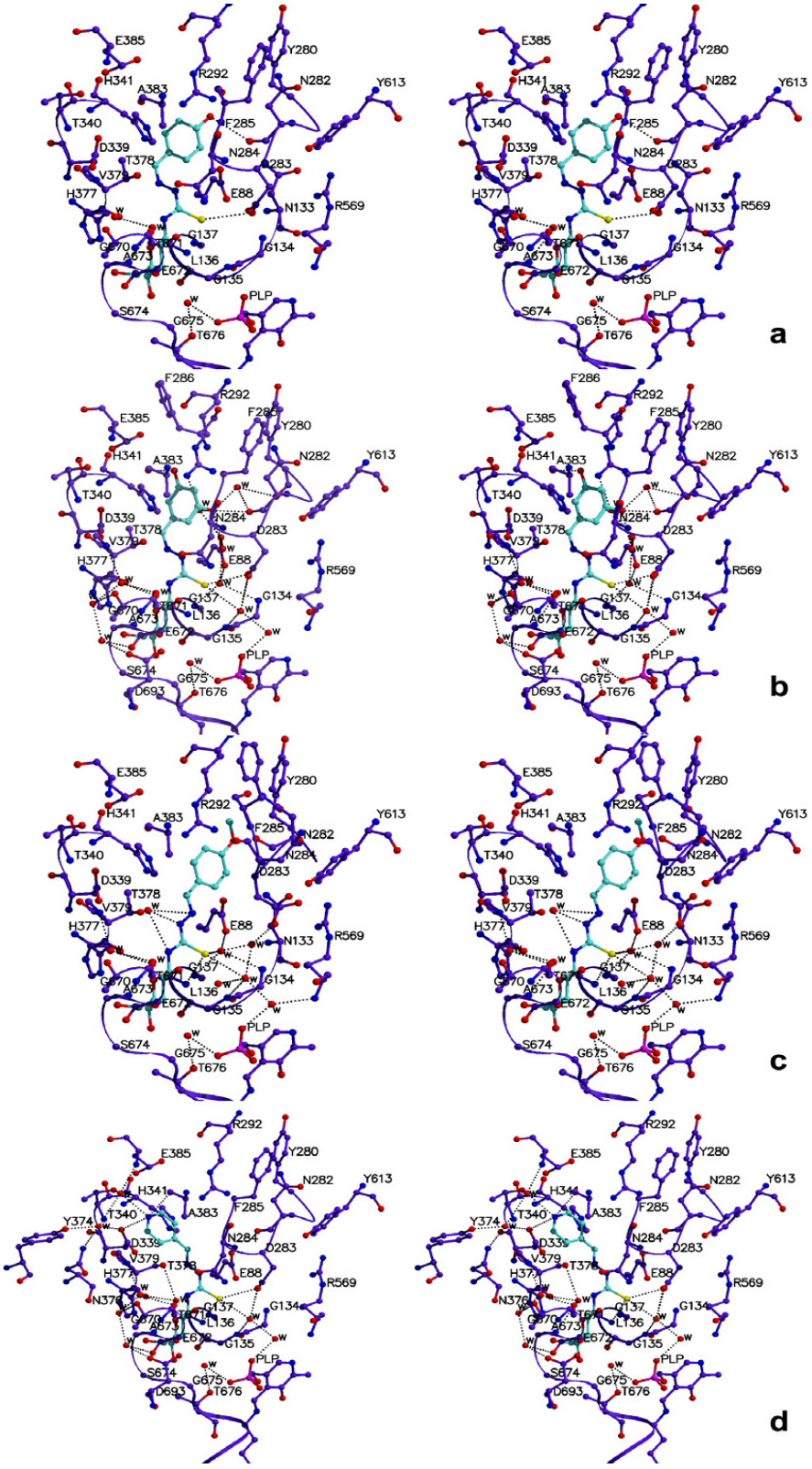

Figure 68 Stereo diagrams of the molecular interactions between GPb and inhibitors **L'$_{14}$** (a), **L'$_{13}$** (b), **L'$_{17}$** (c), **L'$_{22}$** and (d) when bound at the catalytic site. The side chains of protein residues involved in ligand binding are shown as ball-and-stick models. Hydrogen bond interactions between the inhibitors, protein residues and water molecules (w) are represented as dotted lines.

Thus, the torsion angle C9-C8-N1-C1 is −177° and 23° in the new allosteric site. As a result the hydroxybenzyl ring and the glycopyranose ring of the bound inhibitors are in line at the catalytic site but inclined by approximately 30°.

However, in both the catalytic site and the new allosteric site the hydroxybenzyl ring is coplanar to the plane of the thiosemicarbazone moiety. On the binding to the new allosteric site of GP*b* the inhibitos make a total of four hydrogen bonds and exploit 66 van der Waals interactions. The hydroxybenzyl ring is only involved in van der Waals interactions mainly with Arg60, Val64 and Val40' from the symmetry related protein subunit.

III.2.3.4. The methoxy/methyl group

The two inhibitors, 4-methoxy-benzaldehyde 4-(β-D-glucopyranosyl) thiosemicarbazone and the 4-methyl derivative (compounds **L'$_{17}$** and **L'$_{18}$** respectively), bind at both the catalytic site of GP*b* in a very similar manner and conformation. Upon binding to the catalytic site of GP*b*, each one form nine hydrogen bonds with protein residues and they exploit 107 and 101 van der Waals interactions with protein residues respectively (Fig. 68). Upon binding both inhibitors induce significant conformational changes to residues of the 280s loop and the largest shifts occur in residues Asp283 (1.0 Å at Cα positions) and Asn284 (1.7 Å at Cα positions). The methyl group of **L'$_{18}$** engages in 8 van der Waals interactions with GP*b* residues whereas the methoxy group **L'$_{17}$** in 15 (Table 12). The methyl derivative is almost two times more potent than the methoxy one and this cannot be explained from the structural point of view.

Upon binding to the new allosteric site of GP*b*, inhibitors **L'$_{17}$** and **L'$_{18}$** form three hydrogen bonds each and 79 and 81 van der Waals interactions, respectively. No other profound conformational changes were noted in the protein environment. Comparison with Bzurea that thiosemicarbazone moiety is 180° rotated with respect to the urea moiety, whereas the positions of the aromatic rings of the three inhibitors superimpose rather well. As a result the glucopyranose moiety is pointing in opposite directions in the **L'$_{17}$**, **L'$_{18}$**, and Bzurea complexes. In addition, in inhibitors **L'$_{17}$** and **L'$_{18}$** the aryl ring is coplanar to the thiosemicarbazone moiety whereas in Bzurea is inclined by 30°.

III.2.3.5. The pyridine group

The binding of 4-pyridinecarboxaldehyde 4-(β-D-glucopyranosyl) thiosemicarbazone (compound **L'$_{22}$**) at the catalytic and at the new allosteric site of GP*b* is not accompanied by any significant conformational changes of the enzyme including the 280s loop. Inhibitor **L'$_{22}$** forms 14 and 4 hydrogen bonds and 113 and 80 van der Waals interactions at the catalytic and the new allosteric site of GP*b* respectively. Structural comparison of the **L'$_{22}$** complex with the GP*b*-Bzurea complex [138] but also with the other 14 GP*b*-inhibitor complexes presented here, reveals that the aromatic ring of **L'$_{22}$** is positionated a different location compared to the rest of the inhibitors studied. Thus, the N2-N3 bond is rotated by 180° and as a result the pyridine bound in a new position within the β-pocket (shifted of 3.3 Å in C9 and 7.3 Å N4-C12 positions between **L'$_1$** and **L'$_{22}$**). In this new location the pyridine is engaged in hydrogen bond interactions with OD2 of Asp339 and the carbonyl oxygen of Ala383 and water mediated hydrogen bonds with Thr340 OG1 and Glu385 N (Fig. 68). Furthermore it is involved in van der Waals interactions with atoms from residues Asp339, His341, Thr378, and Ala383. In the new allosteric site, **L'$_{22}$** binds in a similar structural mode with the rest of the 14 inhibitors presented here.

III.3. Transtion metal complexes of β-D-glucopyranosyl-thiosemicarbazones and catalysis.

III.3.1. Overview

In the present work a variety of metal complexes (**II**, **III** and **IV**; Scheme 24) with glucose thiosemicarbazones (**I**) were prepared and characterized. In the palladium complexes the ligand is bound to the metal in a 1:1 ratio and constituted by the deprotonated ligand and two or one chlorine ions coordinated to the metal in **II** and **III**, respectively. In the platinum and nickel complexes, the ligand bound to the metal in a 1:2 ratio leading to structure **IV**. The structures proposed for these complexes is consistent with data obtained from ^{1}H and ^{13}C NMR spectra, FT-IR spectra, mass spectrometry and magnetic measurements.

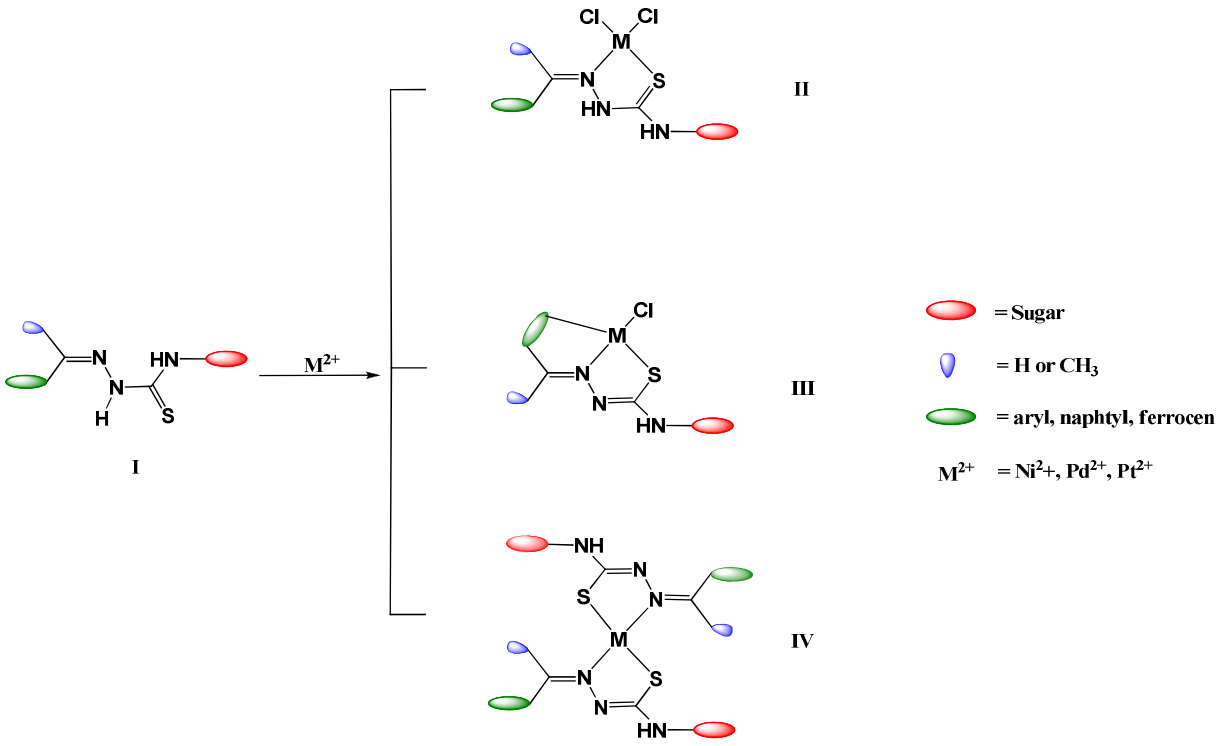

Scheme 24 The binding mode of thiosemicarbazones

Five-membered chelating ring formation (D) can take place, in principle starting from the free ligand (A), *via* rotation about the C-N (hydrazinic) single bond (B), followed by tautomerization to

the thiol form (C) and dissociation of the thiolate proton upon complexation (Scheme 25). In the solution thiosemicarbazones probabily consist of an equilibrium mixture of thione (A) and thiol (C) tautomers; Where ligand (A) asct as a neutral bidentate ligand while the loss of thiol proton from ligand (C) yields singly charged bidentate ligand. Therefore, depending upon preparative conditions (unspecially pH) the complex unit can be cationic, anionic, or neutral.

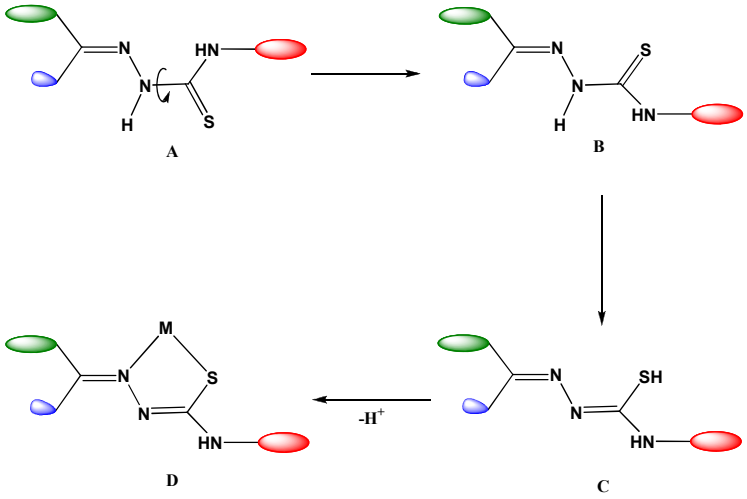

Scheme 25 Probable steps involved in the formation of five-membered chelating rings

Some of the metal complexes were evaluated in certain homogeneously catalysed reactions, and their catalytic activity is presented in the next sections.

III.3.2. Nickel(II) complexes

III.3.2.1. Synthesis

We have synthesized four nickel(II) complexes [Ni($\mathbf{L}_x$)$_2$] (Scheme 26) in yields 81-95% by treatment Ni(OAc)$_2$ hydrate with the appropriate acetyl-protected glucose-thiosemicarbazone derivative L in methanol in a 1:2 molar ratio. Synthesis was based on a literature procedure for the preparation of nickel complexes [307]. The complexes were recrystalyzed twice from dichloromethane/methanol. Unfortunately, all attempts to obtain crystals suitable for X-ray crystallography, were unsuccessful.

The colour of the complexes is brown-green ($\mathbf{C_1}$), brown-yellow ($\mathbf{C_2}$ and $\mathbf{C_4}$), and green ($\mathbf{C_3}$). Brown and green are common colours for the nickel(II) complexes involving thiosemicarbazone coordination due to the sulphur-to-metal charge transfer bands, which dominate their visible spectra [308].

The nickel(II) complexes were soluble in dichloromethane, chloroform, *N,N*-dimethylformamide, dimethyl sulfoxide, methanol, ethanol.

The molecular structure of the nickel(II) complexes are reported in Fig. 1. The nickel(II) ion is tetracoordinated by two ligand molecules acting as *N,S*-donor. In the literature, thiosemicarbazone ligands based on aldehyde form in general *trans* square planar complexes [309-311].

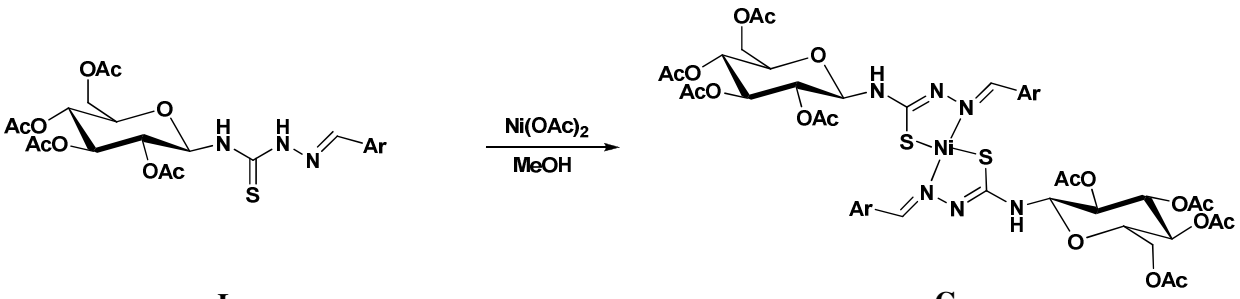

$\mathbf{L_x}$ $\mathbf{C_x}$

X = 1; Ar: -C_6H_4-F
X = 2; Ar: -C_6H_4-CF_3
X = 3; Ar: -C_6H_4-^{t}Bu-*p*
X = 4; Ar: -β–naphthyl

Scheme 26 Synthesis of nickel(II) complexes

Attempts to prepare the complex [Ni($\mathbf{L}_x$)Cl_2] by the reaction of nickel(II) chloride in aqueous methanol, at room temperature, in a ratio 1:1 metal-to-ligand were unsuccessful (Scheme 27). The ^{1}H NMR and IR spectral data indicate no reaction at all.

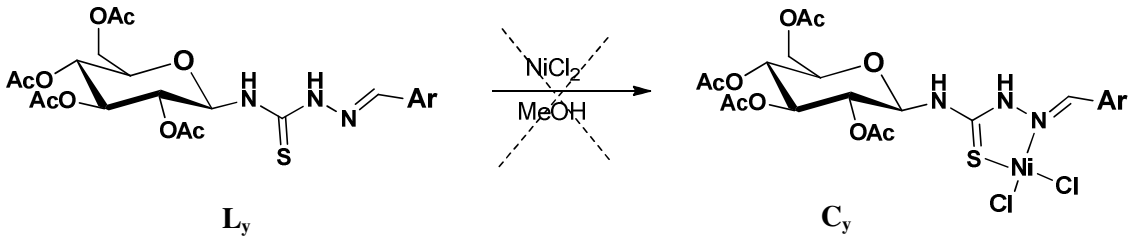

$\mathbf{L}_y$ $\mathbf{C}_y$

Y = 1; Ar: -C_6H_4-CF_3

Y = 2; Ar: -C_6H_4-^{t}Bu-*p*

Scheme 27 Unsuccessful attempt

III.3.2.2. Infrared spectra

The IR spectra of the complexes show the presence of υ(N-H) bands in the range 3322-3390 cm^{-1}. The free Schiff base showed a strong absorption at around 1529-1553 cm^{-1} due to the azomethine group υ(C=N). These absorption bands have been shifted to higher frequency (6-25 cm^{-1}) in all the nickel(II) complexes indicating the coordination of the azomethine nitrogen to nickel ion [312, 313].

Table 13 *Infrared spectra of thiosemicarbazones and their corresponding nickel(II) complexes*

Compound	*v*(N-H)	*v*(C=O)	*v*(N=C)	*v*(C-S)	
$\mathbf{L_1}$	3306	1746	1553	1039	840
Ni($\mathbf{L_1}$)$_2$	3390	1743	1578	1030	759
$\mathbf{L_8}$	3334	1750	1531	1031	830
Ni($\mathbf{L_8}$)$_2$	3412	1746	1535	1017	747
$\mathbf{L_{19}}$	3326	1749	1531	1047	826
Ni($\mathbf{L_{19}}$)$_2$	3354	1741	1541	1020	765
$\mathbf{L_{24}}$	3322	1753	1533	1035	830
Ni($\mathbf{L_{24}}$)$_2$	3368	1740	1539	1030	747

As a result of coordination of Ni(II) to thiol sulfur, the bands υ(C-S) in the free ligands (1031-1047 cm^{-1}) appeared at lower energies in all the complexes (1017-1030 cm^{-1}) [314]. Also, the υ(C-S) absorption band which may lays in the 826-840 cm^{-1} range in the spectra of the free Schiff bases disappeared completely and a new band appeared in the region 747-765 cm^{-1}. This observation may be attributed to the enolisation of NH-C=S group and subsequent coordination through the sulphur atom [315, 316]. Infrared spectrum of $\mathbf{C_3}$ and $\mathbf{C_4}$ complexes are showed in figures 69 and 70.

The infrared spectra of ligand $\mathbf{L_8}$ and nickel(II) complex $\mathbf{C_2}$ are given in figures 69 and 70, respectively.

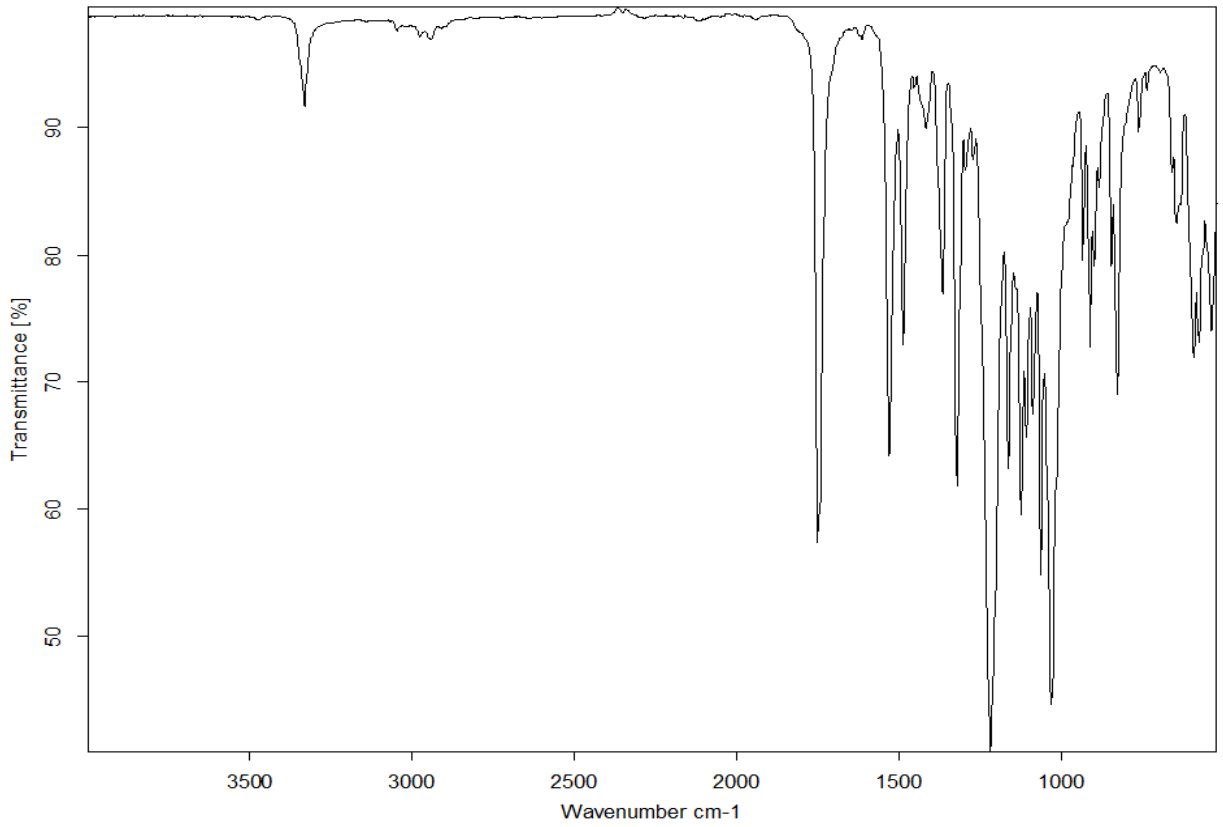

Figure 69 Infrared specrum of compound $\mathbf{L_8}$

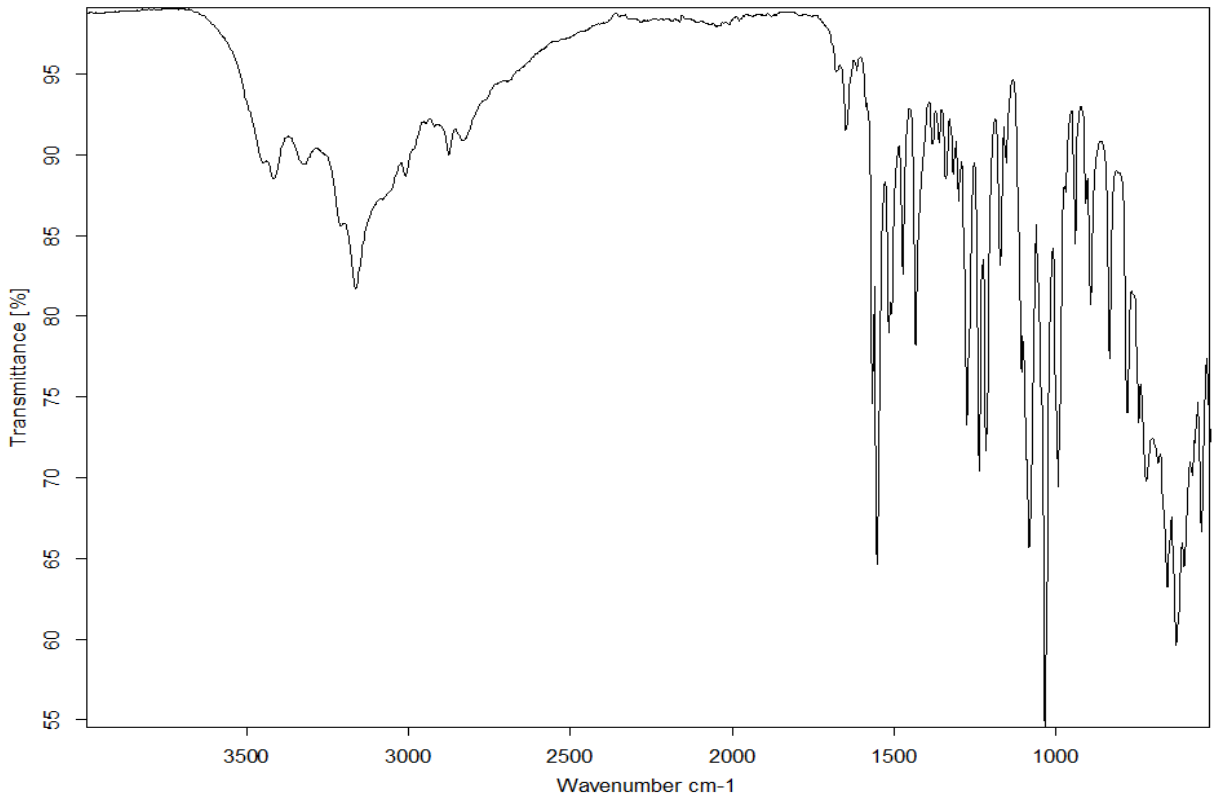

Figure 70 Infrared specrum of Ni($\mathbf{L_8}$)$_2$ ($\mathbf{C_2}$) complex

III.3.2.3. ^{1}H and ^{13}C NMR spectra – Magnetic susceptibility measurement

Various 2D NMR techniques including COSY, HMQC, and HMBC were used in order to assign the NMR spectra.

The deprotonation of the most characteristic proton N(2)H in all nickel(II) complexes was confirmed by the absence of ^{1}H NMR signals at δ 10.14−11.93 ppm due to the coordination through N(1)H, in accordance to literature information [317]. In the ^{1}H NMR spectra, the proton N(4)H is shifting from δ 8.29–8.80 in the free igands to δ 5.81−8.38 in the nickel complexes. The anomeric protons in the complexes at δ 5.10−5.54 ppm showed upfield shift with respect to the free ligands at δ 5.67−5.95 ppm, upon coordination with the azomethine nitrogen N(1)H, as mentioned also in the literature [318].

The ^{1}H NMR signals for the complex $\mathbf{C_3}$ are broad which can indicate a paramagnetic nickel(II) complex while for complexes $\mathbf{C_1}$ (showed in Fig. 71), $\mathbf{C_2}$ and $\mathbf{C_4}$ the signals indicate a diamagnetic nickel(II) complex [319]. An additional evidence for this consideration is provided by the magnetic measurements of the complexes in a magnetic balance at room temperature using the Gouy method.

The magnetic susceptibility (μ_{eff}) for the complex **C_3** was found to be 3.22 which is chracteristic for an octahedrtal paramagnetic complex, while complexes **C_1**, **C_2** and **C_4** were found to be diamagnetic with a probable square planar geometry. Perthaps, the octahedral geometry in complex **C_3** should be due to the participation of the solvent (MeOH) in the coordination sphere, and this coordination is possibly favored by the presence of the bulky *t*-Bu substituent.

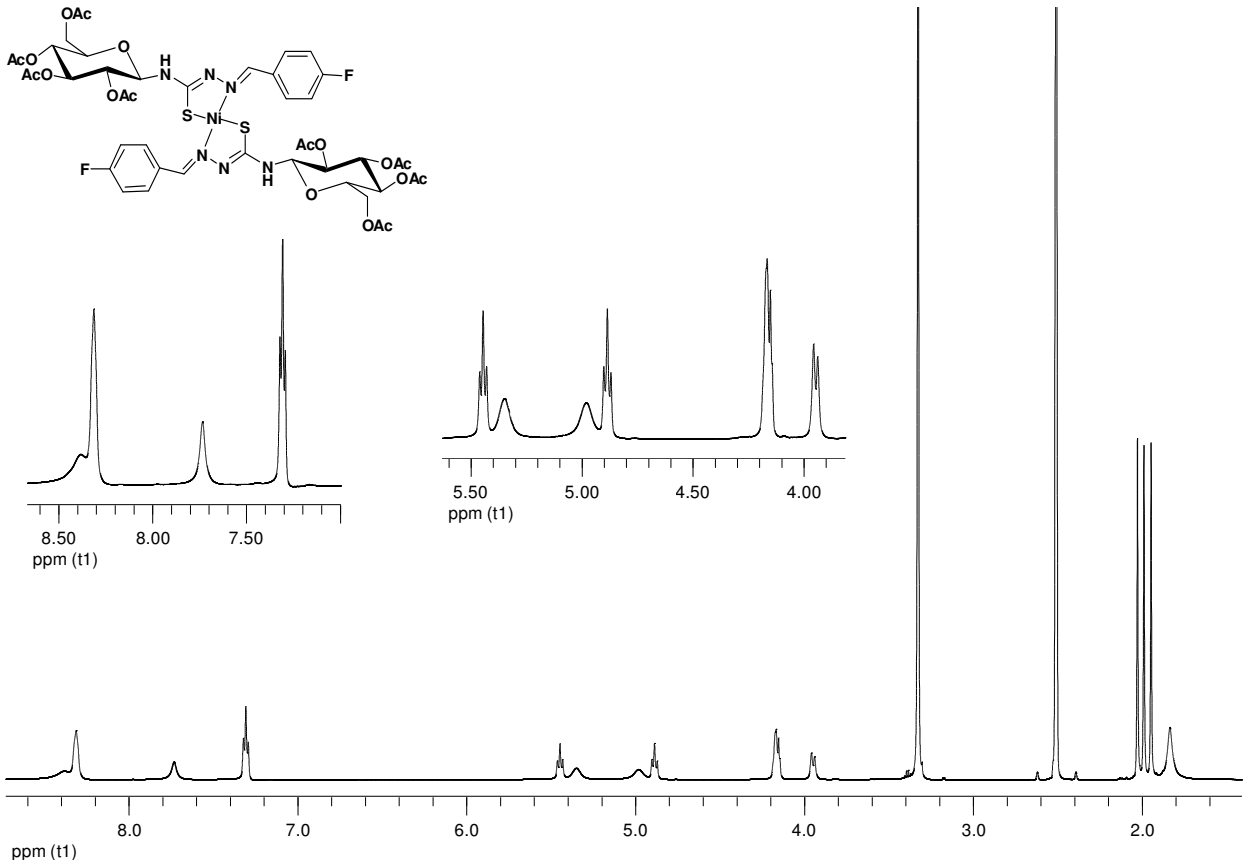

Figure 71 ^{1}H NMR spectrum of complex **C_1**

The C=S signal in the ^{13}C NMR spectra of complexes **C_1** and **C_4** is shifted upfield compared to the free ligands. In addition, the CH=N signal in these complexes is shifted downfield compared to the free ligands due to the coordination to the azomethine nitrogen. The anomeric carbons in the complexes were shiefted upfield for **C_1** (δ 82.2 ppm) and downfield for **C_4** (δ 83.9 ppm) compared to the free ligands (δ 82.3 ppm and δ 82.2 ppm, respectively).

Table 14 *^{1}H and ^{13}C NMR spectral data for some characteristics protons and carbons of thiosemicarbazones and their nickel(II) complexes*

	^{1}H NMR			^{13}C NMR	
Compound	N(2)H	N(4)H	CH=N	C=S	CH=N
L_1	11.93[a]	8.80	8.07	178.9	142.4
C_1	--	8.38	7.73	173.2	162.3
L_8	10.14[b]	8.38	7.84	179.0	141.9
C_2	--	6.00	7.53	175.0	158.0
L_{19}	10.26[b]	8.29	7.85	178.7	143.9
C_3	--	5.81	7.88	174.5	158.1
L_{24}	10.41[b]	8.38	7.82	178.9	144.3
C_4	--	5.90	7.69	175.0	158.5

[a] in DMSO-d_6, [b] in $CDCl_3$.

III.3.3. Palladium(II) complexes

III.3.3.1. Synthesis

Many areas of organic synthesis has been impacted by the versatile transitional metal palladium (Pd) (named due to the asteroid Pallas [320]).

The palladium(II) complexes **C_5** and **C_6** are prepared by a similar method reported by Mikata [22], by mixing the appropriate ligand with a K_2PdCl_4 solution in 1:1 metal-to-ligand molar ratio in a methanol/water for **C_5** and acetonitrile/water for **C_6** (Scheme 28 for complex **C_5** and Scheme 29 for **C_6**). The extremly low solubility of the complexes in most common solvents makes the separation difficult, and obtaining sufficient pure material to characterize the complexes is challenging. However, further purification was achieved by repeated recrystallizations from DMF/MeOH/ Et_2O (for complex **C_5**)and DMF/AcCN (for complex **C_6**).

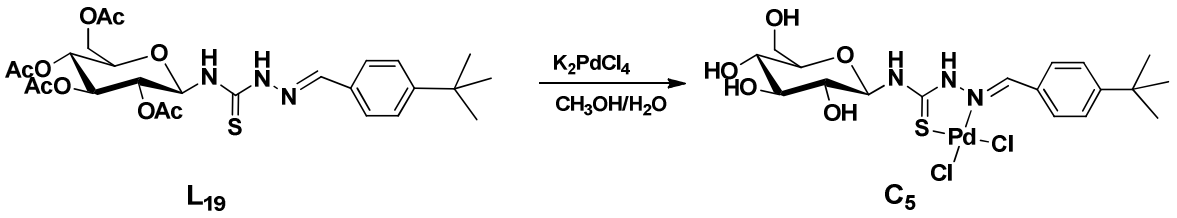

Scheme 28 Synthesis of palladium(II) complex **C_5**

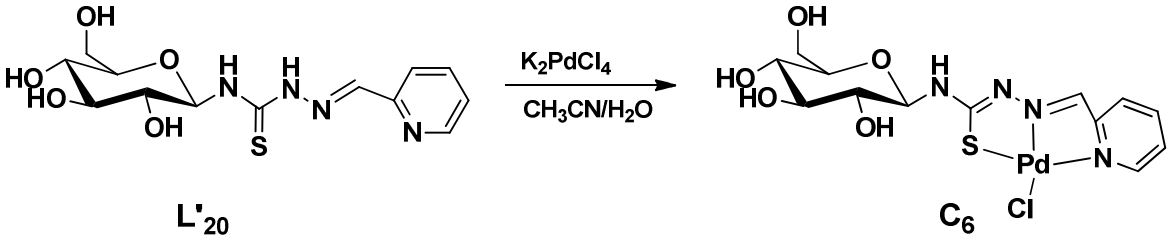

Scheme29 Synthesis of palladium(II) complex **C_6**

Scheme 28 represents one pot – two steps reaction in which the ligand is first bound to the metal, and subsequently, deprotection of the acetylated hydroxyl groups takes place. In scheme 29, the deprotected glucose derivative was used as starting material, and thus the reaction proceeds in one step.

The complex **C_5** exhibit *N,S*-bidentate behaviour while complex **C_6** exhibit *N,N,S*-terdentate behavior achieved by the coordination of the pyridine nitrogen atom, with a general formula $MLCl_2$ for complex **C_5** and MLCl for complex **C_6** as indicated by the IR spectra explained in details in the next section.

The palladium(II) complexes were obtained in good yields 62-78%. The color of the complex **C_5** is orange and for complex **C_6** is yellow-orange. The complexes are soluble in DMSO and DMF. Complex **C_6 is** also soluble in water. Attempts to obtain crystals for X-ray crystal structure determination were unsuccefull.

III.3.3.2. Infrared spectra

The IR spectra assignments of the corresponding ligands and the complexes are listed in Table 15. The bands corresponding to the ν(N-H) are present at 3324 and 3416 cm^{-1} for the ligands **L'$_{19}$** and **L'$_{20}$**, respectively, indicating that the ligands remain as the thione tautomers in the solid state [321]. The free ligands **L'$_{19}$** and **L'$_{20}$** show bands at 1541 and 1557 cm^{-1}, respectively, assigned to ν(C=N) moiety, which are higher shifted in the complexes **C_5** and **C_6** by 20 and 25 cm^{-1}, respectively, indicating the involvement of azomethine nitrogen in complexation [322]. The complexes **C_5** and **C_6**, containing the neutral ligand, show a second band corresponding to ν(N=C) at 1608 and 1655 cm^{-1}, respectively [323].

The most characteristic thioamide band due to ν(C=S) at 826 and 830 cm^{-1} for **L'$_{19}$** and **L'$_{20}$**, respectively, are appeared at 779 and 767 cm^{-1} in complexes **C_5** and **C_6**, respectively. The bands at 1365 and 1341 cm^{-1} in the spectra of ligands **L'$_{19}$** and **L'$_{20}$**, respectively, are assigned to the ν(N-C=S) stretching and bending modes of vibrations. These bands are shifted to higher energies (1368 and 1356 cm^{-1}) in the complexes showing sulfur coordinated to the metal [324]. In the case of complex **C_6** a negative shift corresponding to out-of-plane bending vibrations of the pyridine ring in the free ligand (629 cm^{-1}) to lower frequency (610 cm^{-1}) in the complex is confirmative of pyridine nitrogen coordination to the palladium(II) ion [325, 326]. Also, the band of the ligand (**L'$_{20}$**) at 993 cm^{-1} is assigned to the breathing motion of the pyridine ring, which is expected to shift to higher frequency when the pyridine nitrogen is involved in bonding with metal ions [327]. In the complex **C_6**, this band is found at 1016 cm^{-1} consistent with N coordination.

Based on the above spectral evidences, it is confirmed that the ligand **L'$_{19}$** in complex **C_5** is bidentate coordinating via the azomethine nitrogen and thiolate sulfur, and the ligand **L'$_{20}$** in

complex **C_6** is bonded in a tridenate mode, coordinating via azomethine nitrogen, the pyridyl nitrogen and thione sulfur.

Table 15 *Infrared spectra assignments (cm^{-1}) of glucose thiosemicarbazone derivatives and their palladium complexes*

Compound	*v*(C=N)	*v*(N=C)	*v*(C-S)
L'_{19}	1541	---	826
C_5	1561	1608	779
L'_{20}	1557	---	830
C_6	1580	1655	767

Infrared spectrums of ligands **L'_{19}** and **L'_{20}** and complexes **C_5** and **C_6** are given in figures 72-75.

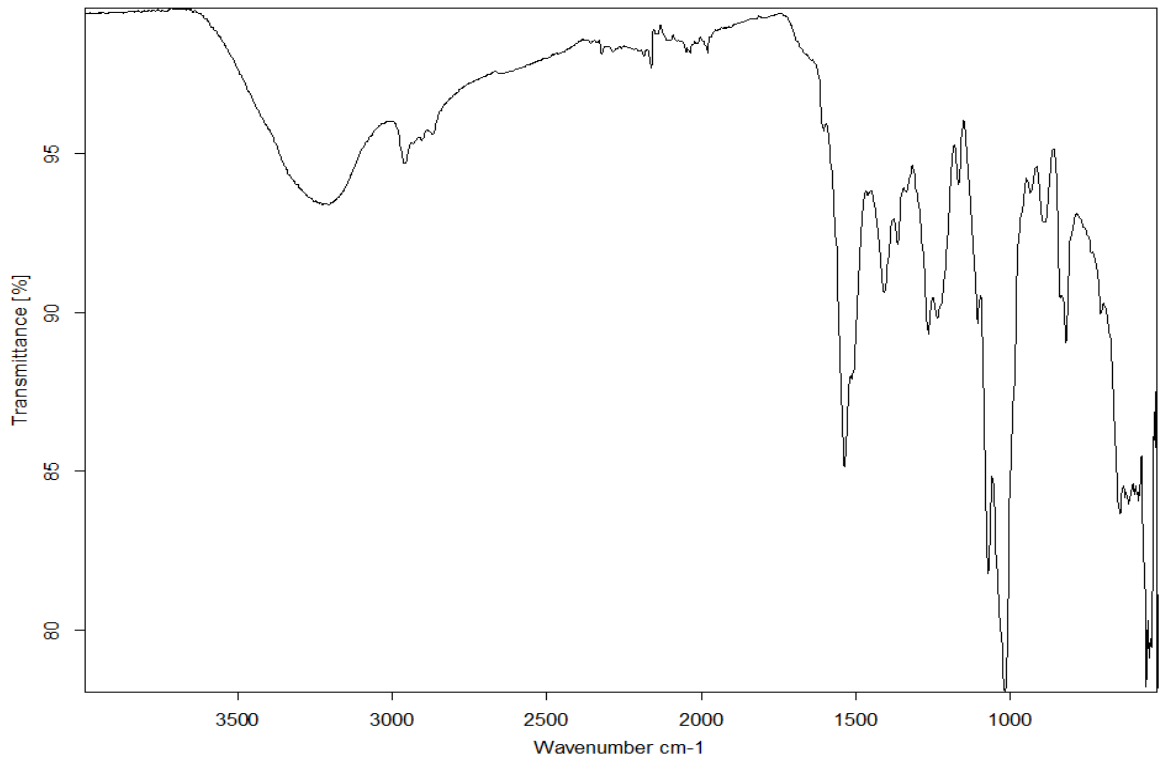

Figure 72 Infrared spectrum of **L'_{19}** ligand

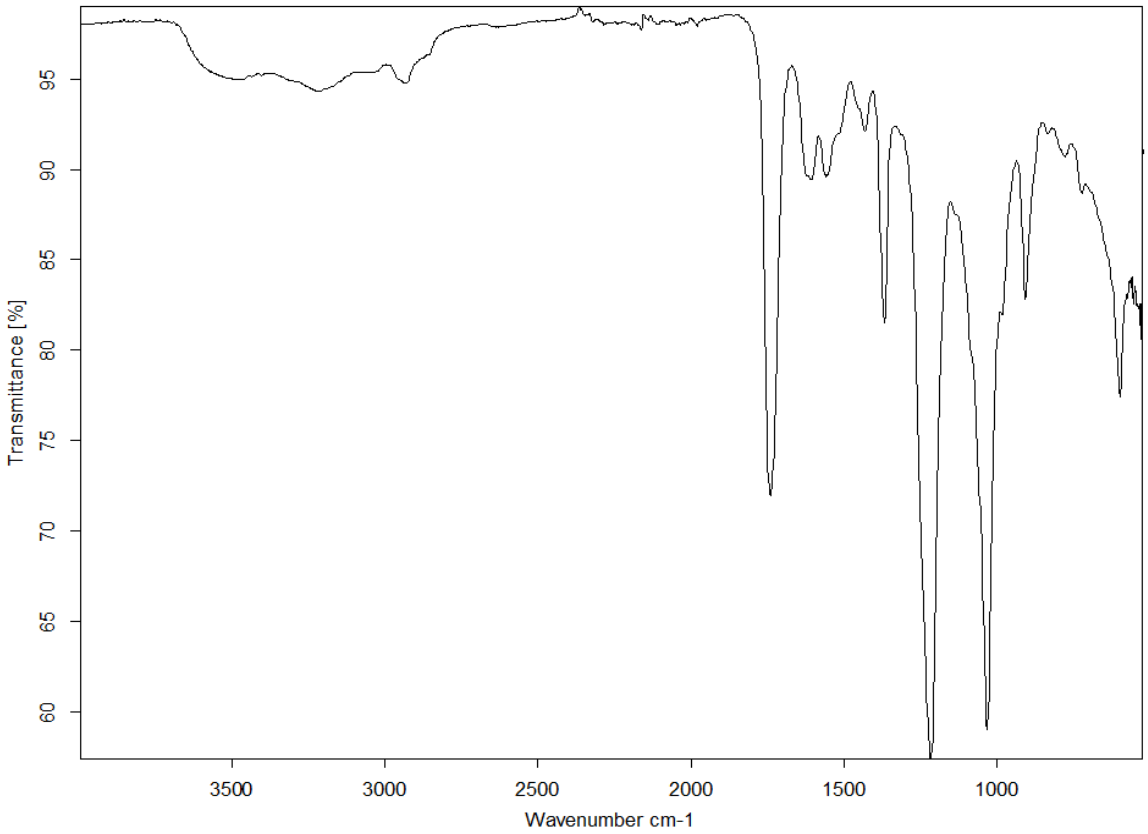

Figure 73 Infrared specrum of Pd**L'**$_{19}$$Cl_2$ (**C**$_5$) complex

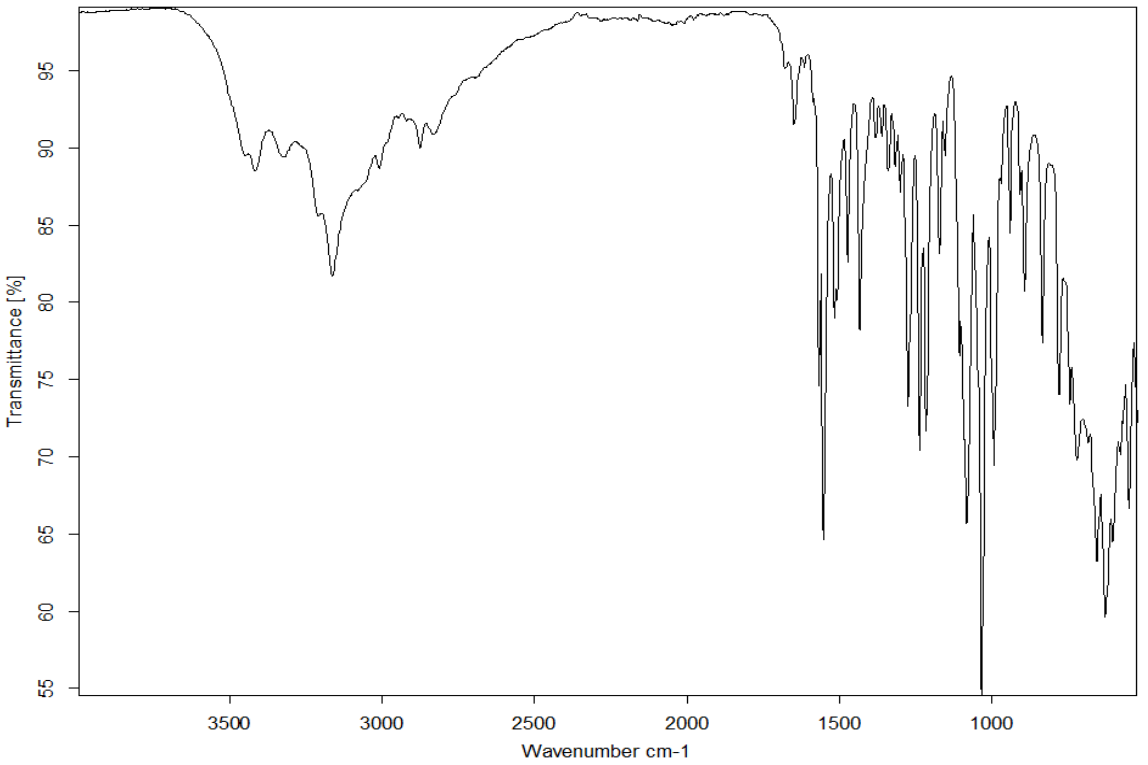

Figure 74 Infrared spectrum of **L'**$_{20}$ ligand

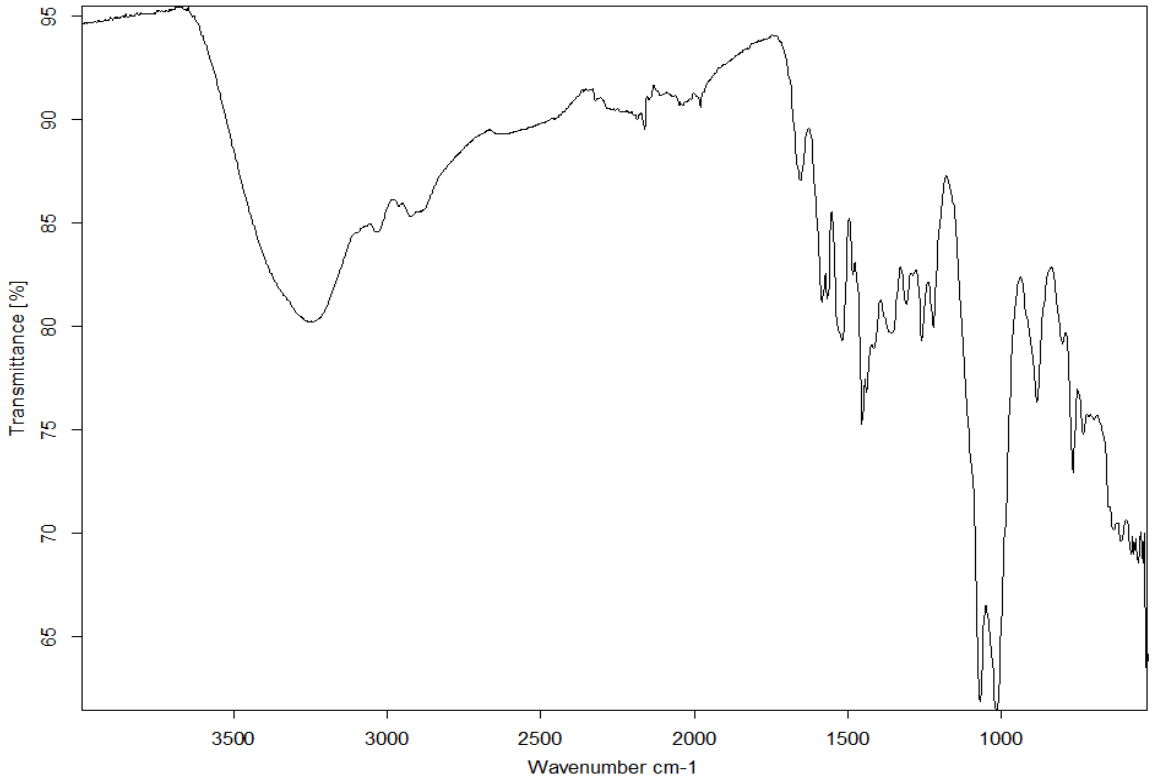

Figure 75 Infrared specrum of Pd**L'**$_{20}$Cl (**C**$_6$) complex

III.3.3.3. ^{1}H and ^{13}C NMR spectra

The d^8 square planar palladium(II) complexes are all diamagnetic and give well resolved NMR spectra which confirm the nature of the binding. The conformation of sugar and conectivity of the ligands in complexes **C**$_5$ and **C**$_6$ were confirmed by ^{1}H, ^{13}C, COSY and HMQC NMR spectroscopy. Asignments of the signals are based on the chemical shift and intensity pattems. The 600-MHz ^{1}H NMR spectra of the complexes in DMSO-d$_6$ show signals with the expected coupling pattern for the aryl and pyridine group (7.47-8.06 ppm for **C**$_5$ and 7.47-8.48 ppm for **C**$_6$).

The ^{1}H NMR spectra of ligands **L'**$_{19}$ and **L'**$_{20}$ (Table 16) exhibit a doublet at 8.48 and 8.73 ppm, respectively, due to the N(4)H proton. In the corresponding complexes **C**$_5$ (Fig. 76) and **C**$_6$, they turned to broad peaks at 8.21 and 8.72 ppm, respectively, which indicate that even in a polar solvent (DMSO) they remain in the thione form.

Resonances for the anomeric proton (1-H) occured at 5.38 ppm for **L'**$_{19}$ and 5.40 ppm for **L'**$_{20}$ in the free ligands, were shielded downfield in the complexes **C**$_5$ and **C**$_6$ (4.61 and 4.73 ppm, respectively). Therefore, H-2–H-6 protons were indentified from the 2D COSY and HSCQ NMR cross peaks starting from the anomeric proton resonance. Each peak shows the expected coupling

pattern. The peak (singlet) correspounding to methyl (from *tert*-butyl) was upfield shifted (from1.30 ppm to 1.29 ppm) in the spectrum of the complex **C_5**.

The ^{13}C NMR spectra of complexes **C_5** (Fig. 77) and **C_6** were recorded in DMSO-d_6 (Table 16) and the signals are in good agreement with the proposed structures. Variations occur in the ^{13}C NMR spectra for the signals of C=S and CH=N in acordance with the coordination of the sulfur and the imine nitrogen.

Another point worthy of note was the signals at 178.5 and 178.9 ppm assigned to C=S bond in compexes **C_5** and **C_6** respectively, which were shifted upfield for **C_5** (171.4 ppm) and downfield for **C_6** (181.4 ppm). In addition, the assigments for the carbons CH=N (155.2 ppm for **C_5** and 157.9 ppm for **C_6**) and 1-C (86.6 ppm for **C_5** and 86.3 ppm for **C_6**) are shifted downfield compared to the free ligands. Table 16 provides the most characteristic proton and carbon chemical shifts of ligands **L'$_{19}$** and **L'$_{20}$** and palladium(II) complexes **C_5** and **C_6**.

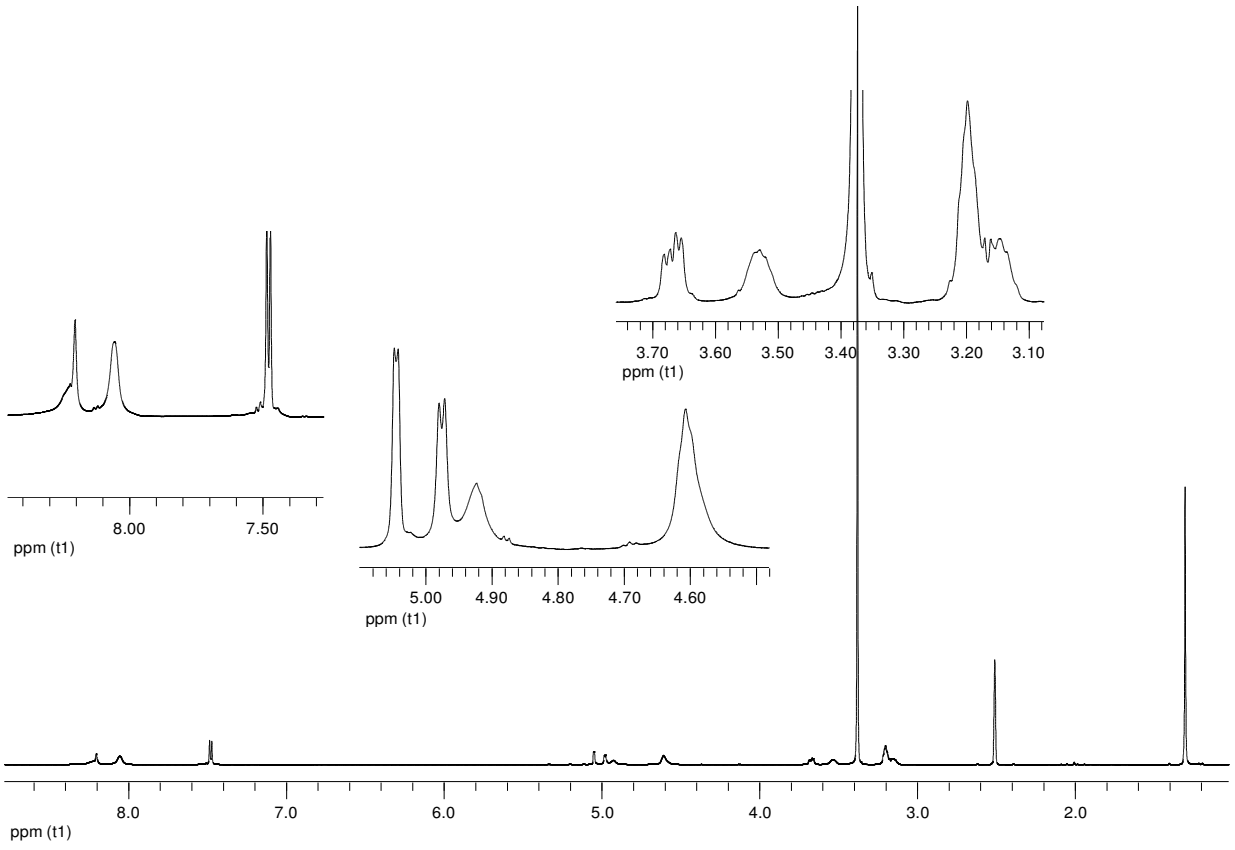

Figure 76 ^{1}H-NMR spectrum of **C_5** in DMSO-d_6 (600 MHz)

Table 16 *^{1}H and ^{13}C NMR spectral data for some characteristic protons and carbons of the ligands and their palladium complexes*

	^{1}H NMR			^{13}C NMR		
^{1}H NMR	N(4)H	CH=N	1-H	C=S	CH=N	1-C
L'$_{19}$	8.48	8.09	5.38	178.5	143.1	84.0
C$_5$	8.21	8.20	4.61	171.4	155.2	86.6
L'$_{20}$	8.73	8.15	5.40	178.9	143.3	84.1
C$_6$	8.72	8.08	4.73	181.4	157.9	86.3

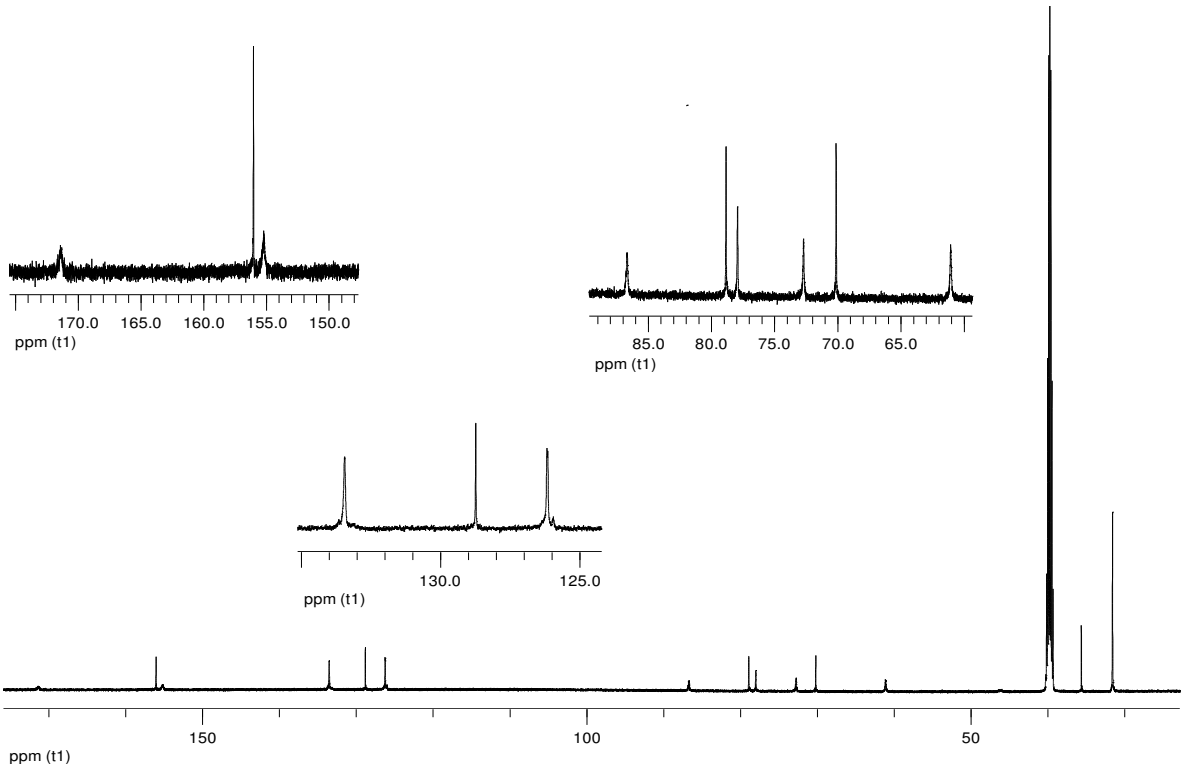

Figure 77 ^{13}C-NMR spectrum of **C$_5$** in DMSO-d$_6$ (75 MHz)

III.3.4. Platinum(II) complex

We have also synthesized the platinum complex of the ferrocene-containing β-D-glucose-thiosemicarbazone derivative **L'$_{23}$**.

III.3.4.1. Synthesis

The platinum complex **C$_7$** was prepared by mixing a methanolic solution of the ligand **L'$_{23}$** in an aqueous solution of K_2PtCl_4 (Scheme 32) [22]. The complex Pt(**L'$_{23}$**)$_2$ was obtained in a 68% yield and was found to be soluble in DMSO and DMF and insoluble in most organic solvents.

The ligand is deprotonated at the hydrazinic –N(2)H- group and forms the complex with the formula ML_2. The mass spectrum showed a peak at *m/z* 1117 for the molecular ion whose isotopic composition suggests a mononuclear complex of formula $C_{36}H_{44}Fe_2N_6O_{10}S_2Pt$. Additionally, IR and NMR spectral data given in the next sections indicates that the ligand is coordinating *via* nitrogen and sulfur donor atoms in a *N,S*-bidentate mode.

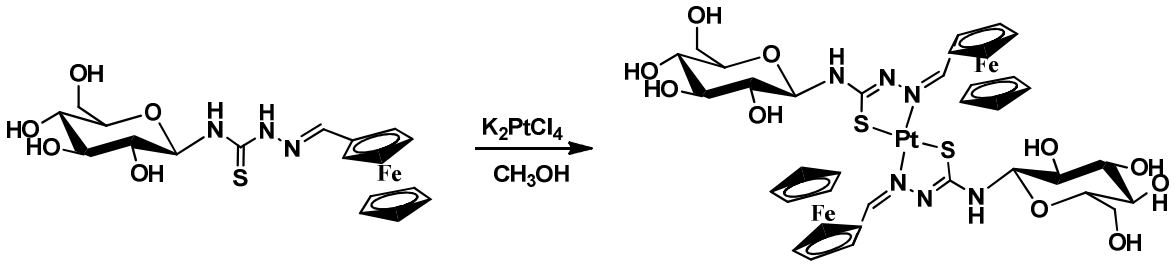

L'$_{23}$ **C$_7$**

Scheme 32 Synthesis of platinum(II) complex Pt(**L$_{23}$**)$_2$

III.3.4.2. Infrared spectra

The IR bands most useful for the determination of the mode of coordination are presented in table 18. The intense band 1535 cm^{-1}, assigned to ν(C=N) of the ligand is shifted to higher energy in the spectrum of the complex indicating azomethine nitrogen coordination [328, 329].

A strong band found at 1105 cm^{-1} in the the spectrum of the ligand, assigned to the *ν*(N-N), is negative shifted in the complex spectrum (1108 cm^{-1}). The two bands appeared at 1365 cm^{-1} and 1024 cm^{-1} [ν(CS)+ν(CN)] in the spectrum of the ligand have been shifted to lower frequency (1353 cm^{-1} and 1014 cm^{-1}, respectively) indicating coordination of the sulfur [330].

Also, the band attributed ν(N-C-S) in the spectrum of the ligand at 1222 cm^{-1} is lower shifted in the spectrum of the complex (1216 cm^{-1}). For the complex containing the anionic ligand, a second band due to the ν(C=N) and ν(N=C) modes is appeared [331] at 1591 cm-1.

Based on the above spectral data, it is confirmed that the ligand **L'$_{23}$** is coordinated to the metal in a bidentate mode *via* the azomethine nitrogen and thiolate sulfur. Figures 78 and 79 show the infrared spctra of ligand **L'$_{23}$** and complex **C$_7$**, respectively.

Table 18 *Infrared spectra (cm^{-1}) of the ligand* ***L'$_{23}$*** *and the complex* ***C$_7$***

Compound	*ν*(C=N)	*ν*(N=C)	*ν*(NCS)	*ν*(N-N)	*ν*(C-S)
L'$_{23}$	1535	---	1254	1024	822
C$_7$	1569	1592	1245	1014	798

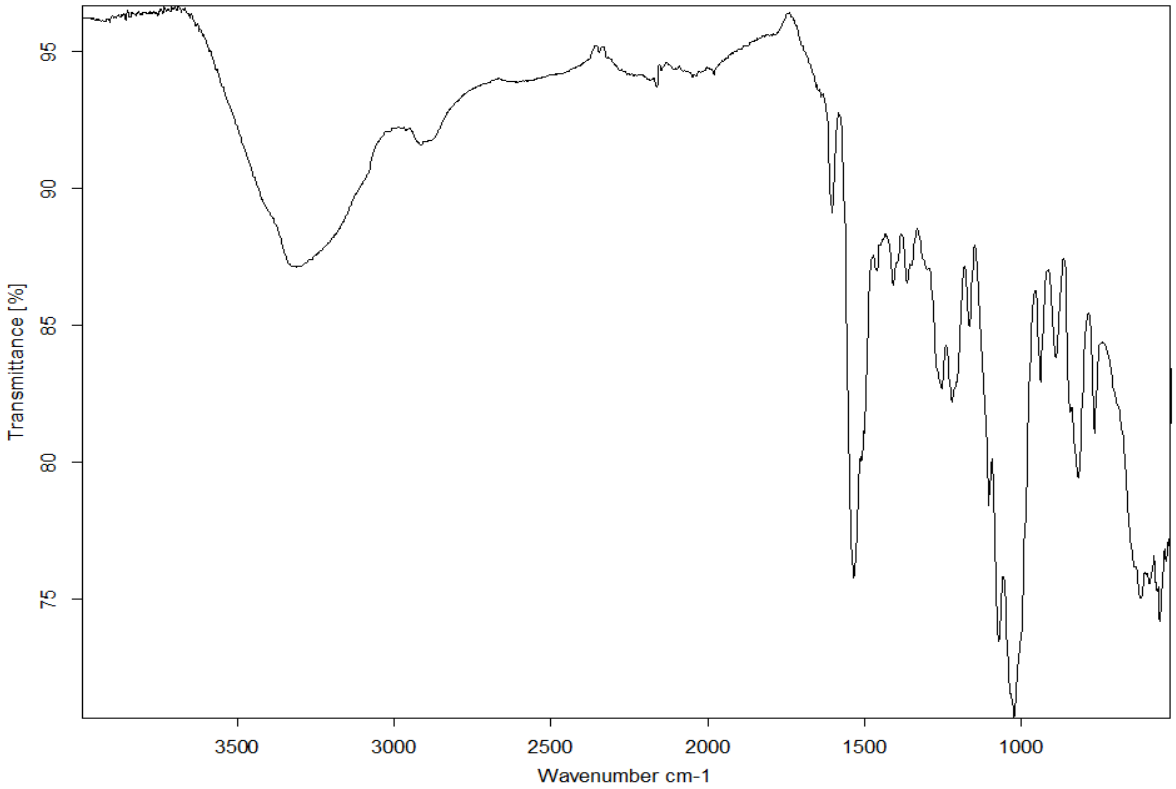

Figure 78 Infrared spectrum of **L'$_{23}$**

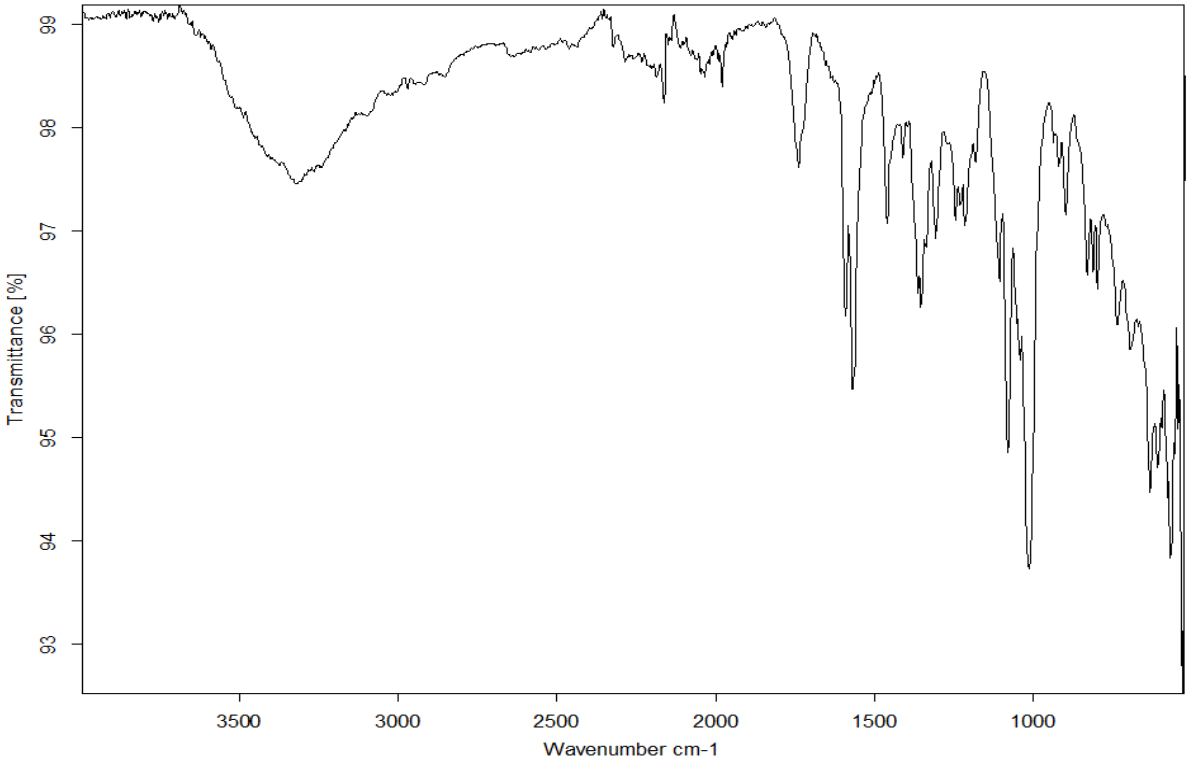

Figure 79 Infrared spectrum of complex **C$_7$**

III.3.4.3. ^{1}H and ^{13}C NMR spectra

Further evidence for the formation of the proposed structure for the complex was obtained from NMR spectroscopic studies as a diagnostic tool for the positional elucidation of the proton. The signal due to N(2)H proton which appears at δ 11.49 ppm in the free ligand was absent in the spectrum of its complex (**C$_7$**, Fig. 80), confirming that the ligand is behaving as an anion in the complex. It supports deprotonation during complexation. The N(4)H proton appears as a board singlet peak at δ 7.56 ppm in the platinum(II) complex and is upfield shifted comparing to the ligand. The proton CH=N in the free ligand appears at δ 7.95 ppm and was shielded during complexation. The doublet of doublets at δ 4.68 ppm, in the spectrum of the complex, is attributed to the anomeric proton which was upfield shifted from the free ligand (δ 5.34 ppm). The four picks assigned to the ferrocene ring in the free ligand at δ 4.81, 4.73, 4.44, 4.22 ppm are all down- or upshifted in the spectrum of the complex (δ 5.18, 4.42, 4.15, 4.12 ppm).

Table 19 *^{1}H NMR spectral data for some characteristic protons and carbons of the ligand* ***L'$_{23}$*** *and complex* ***C$_7$***

Compound	N(2)H	N(4)H	CH=N	1-H
L'$_{23}$	11.49	8.18	7.95	5.34
Pt(**L'$_{23}$**)$_2$	--	7.56	7.69	4.68

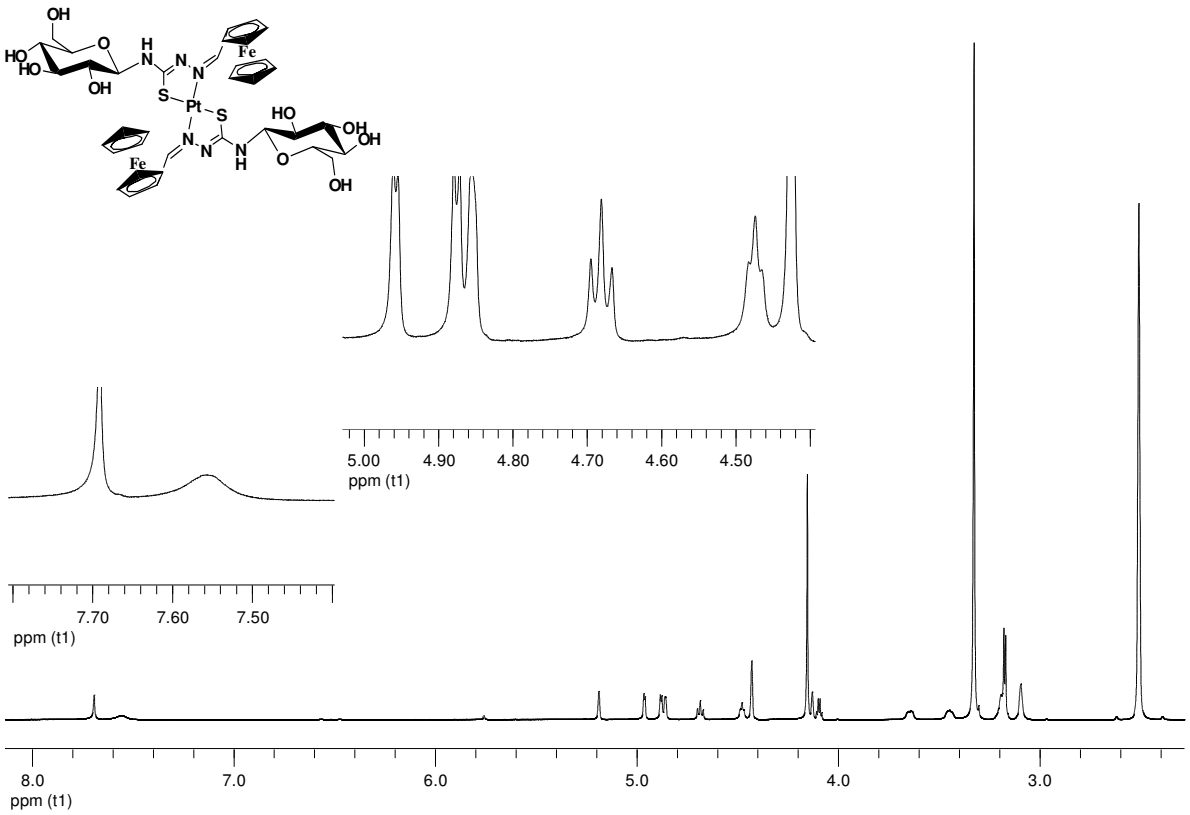

Figure 80 ^{1}H-NMR spectrum of $\mathbf{C_7}$ in DMSO-d_6 (600 MHz)

III.3.5. Catalysis

Our laboratory (Kostas et al.) has an important contribution in transition metal homogeneous catalysis (asymmetric or not) by phosphane or phosphane-free ligands, mainly in hydroformylation, hydrogenation, Heck and Suzuki reactions [105-107, 192, 332-337, 338-342].
As mentioned in the introduction (chapter II.4.5.4), the research teams of Kovala-Demertzi and Kostas reported for the **first time** the use of thiosemicarbazones in the palladium-catalyzed Heck and Suzuki reactions as efficient ligands under aerobic conditions [105-107], and one of these catalysts is currently **commercially available** by ALDRICH and SANTA CRUZ. Taking into considerations these achievements, in the present work, some of the above-mentioned complexes were evaluated in the Heck and Suzuki reactions, and the results are provided below.
In the present work, the activity of complex **C_5** as precatalyst in the Suzuki and Heck reactions was investigated.

III.3.5.1. Suzuki-Miyaura cross coupling reaction

Palladium complex **C_5** as a stock solution in DMF was applied to the Suzuki–Miyaura reaction of phenylboronic acid with some representative aryl halides (Scheme 30), from electron-rich to electron-poor, at room temperature or 100°C, using as a base K_2CO_3 or Na_2CO_3, without addition of free ligand or any promoting additive (Table 17). Since it is known that addition of water enhances the activity of the catalyst, [106, 339] catalysis was performed in the presence of a small amount of water (close to one equivalent with respect to the substrates). The solvent DMF was choosen due to the low solubility of palladium(II) complex in most organic solvents.
Catalyst is air stable at 100°C, and palladium black, which could indicate the degradation of the catalyst, was not observed. The reaction was performed using a 1:500, 1:1000 or 1:100,000 catalyst/aryl halide molar ratio. As expected, the catalytic activity depended on the halide, while electron withdrawing groups on the aryl ring increased the reaction rate. According to the GC analysis of the reaction mixtures resulting from the coupling of 4-subsituted aryl halides, homocoupling of phenylboronic acid to give unsubstituted biphenyl was observed in a low yield for the substrate with an electron-donating group (entry 1-3; Table 17).

In all cases, the conversion was quantitative or high. For the activated 1-bromo-4-nitrobenzene the conversion was acceptable just after 1 h at 100 ºC under argon or in air (entry 10 and 11), and the reaction could also be performed even at room temperature with however, a lower yield (entry 12). For the activated 1-bromo-4-nitrobenzene and 4-bromobenzonitrile, the conversion were usually very good (100%; entries 8 and 10), in air after 24 h. The results were also very good by using a very low Pd loading (1:100,000 catalyst: aryl halide molar ratio) leading to the coupling product with yields 62 and 100% for the 4-bromoanisole and 1-bromo-4-nitrobenzene, respectively (entries 3 and 13).

The results were good even for the deactivated 4-bromoanisole (entry 1). Analogous results were obtained, even in air as in argon, indicating the applicability of the catalyst which is active in air and thus no inert atmosphere is required (eg. entries 7 and 8).

The use of aryl chlorides as substrates remains the goal in cross-coupling reactions due to their low cost and convenient availability, but unfortunately, the oxidative addition in these cases is difficult due to the comparatively high C-Cl bond strength. In spite of this difficulty, complex **C_5** was applied to the cross-coupling of phenyl boronic acid with chlorobenzene and 4-nitro-chlorobenzene in air, under the above mentionated conditions, yielding the corresponding biaryls with TONs up to 740 and 210, respectively (entries 14 and 15).

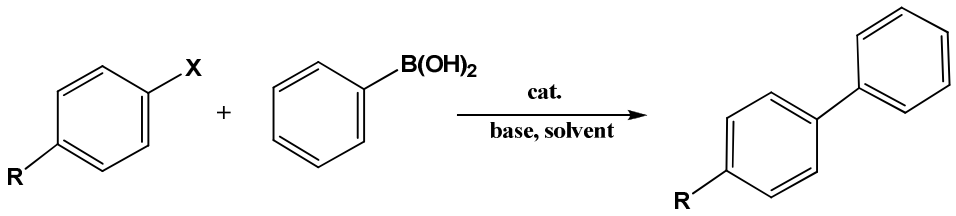

X = Cl, Br; R = OMe, H, CN, NO_2.

Scheme 30 Suzuki-Miyaura cross coupling of aryl halides with phenyl-boronic acid.

Suzuki coupling was also attempted by the nickel complex **C_3**, but unfortunately with too low conversions (<4%). The explanation may lie on the structure of the complex: the metal is bonded to two thiosemicarbazone moieties and as the metal space is very crowded, this results in an inhibition of the addition of the aryl halide to the metal during the catalytic cycle.

Table 17 *Suzuki−Miyaura cross-coupling of aryl halides with phenylboronic acid catalyzed by palladium complex* $\boldsymbol{C_5}$[a]

Entry	X	**R**	ArBr/Pd	T (ºC)	Time (h)	Conversion[b] (%)	TON
1[c]	Br	**OMe**	1000	100	24	90 (5)[d]	900
2	Br	**OMe**	500	100	4	37(18)[d]	185
3	Br	**OMe**	100,000	100	24	62 (6)[d]	62,000
4	Br	**H**	1000	100	24	90	900
5	Br	**H**	500	100	4	43	215
6	Br	**CN**	1000	100	24	100	1000
7	Br	**NO_2**	1000	100	24	100	1000
8[e]	Br	**NO_2**	1000	100	24	100	1000
9	Br	**NO_2**	500	100	4	77	385
10[e]	Br	**NO_2**	1000	100	1	70	700
11	Br	**NO_2**	1000	100	1	65	650
12[e]	Br	**NO_2**	1000	r.t.	24	30	300
13	Br	**NO_2**	100,000	100	24	100	100,000
14	Cl	**NO_2**	1000	100	24	74	740
15	Cl	**H**	1000	100	24	21	210

[a]Reaction conditions: ArBr or ArCl (1.0 mmol), $PhB(OH)_2$ (1.5 mmol), K_2CO_3 (2.0 mmol), H_2O (1.7 mmol), Pd complex in DMF (1 mL), in air; [b]Conversion to coupled product R-C_6H_4-Ph based on aryl bromide (GC); [c]Na_2CO_3 as a base; [d]Conversion to unsubstituted biphenyl due to homocoupling of phenylboronic acid; [e]Under Ar atmosphere.

III.3.5.2. Heck reaction

Palladium complex $\mathbf{C_5}$ was also applied to the Heck reaction of styrene with the de-activated 4-bromo anisole in DMF at 150°C for 24h under argon, using AcONa as a base, and in the absence

of any promoting additive (Scheme 31). The catalyst to bromide ration was 1:1700 and led to the formation of *trans*-stilbenes in 43% yield.

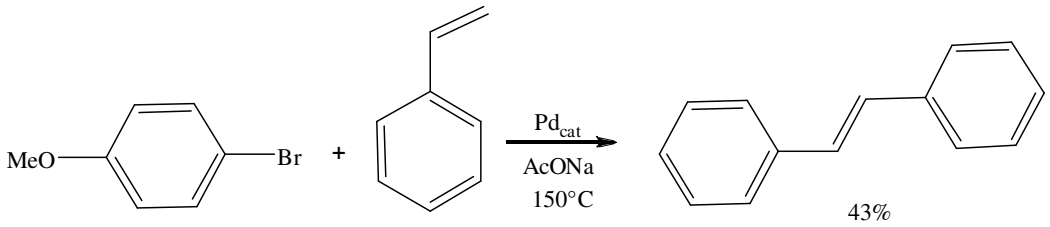

Reaction conditions: aryl halide (1.0 mmol), styrene (1.5 mmol), base (2.0 mmol) Pd complex in DMF (1 mL), 24h.

Scheme 31 Heck reaction of 4-bromo anisole with styrene

IV. Conclusions

IV. Conclusions

A systematic study led to the development of a library of twenty six β-D-glucopyranosyl-thiosemicarbazones derived from aldehydes (substituted benzaldehydes with NO_2, F, Cl, Br, OH, OMe, CF_3, *t*Bu or Me at the *ortho*-, *meta*- or *para*-position of the aromatic ring as well as a moiety derived from 2-, 3- or 4-pyridinecarboxaldehyde, 1-ferrocenecarboxaldehyde or β-naphthalenecarboxaldehyde) and ketones (4-methoxy-acetophenone or 2-acetonaphthanone). The spectroscopic data for all of them as well as the crystallographic studies for two derivatives clearly indicate the β configuration, and the *E* configuration pertaining to the stereochemistry of the C=N bond, and the reason for this should be that the *trans* arrangement places the amine and azomethine nitrogen atoms in relative positions more suitable for intramolecular hydrogen bonding. However, a partial conversion of the *E* into the *Z* form is possible in solution after several hours as shown by the ^{1}H NMR spectra.

Fifteen of these derivatives have been studied with kinetic and X-ray crystallography studies for binding to glycogen phosphorylase b (GP*b*). These inhibitors were found to be competitive inhibitors of the enzyme with respect to Glc-1-P and they all bind to the active site by anchoring their β-D-glucopyranose moiety at the α-D-glucose binding site and the thiosemicarbazone moiety at the hydrophobic β-pocket of the active site. In addition, these inhibitors with the exception of 2-nitro-benzaldehyde 4-(β-D-glucopyranosyl)-thiosemicarbazone, were also found bound at the new allosteric site of GP*b*. Binding at this site does not promote any significant conformational changes except for small shifts in the residues in the vicinity of the inhibitor (namely Arg60, Val64, Trp189 and Lys191), which undergo conformational changes in order to accommodate the ligand. However, it should be noted that the orientation of the aromatic group is maintained as observed previously in other compounds bound at this site. Comparing the binding of each compound at the catalytic site, it is interesting to see that there is a pattern emerging based on the electronegativity of the directing groups. Between the three compounds with the –Cl substituent, the one in the *ortho* position of the aromatic ring causes a moderate shift of the 280s loop upon binding. The one in the *meta* position causes a significant shift in the 280s loop, while the one in the *para* position causes a major shift in the 280s loop. However, between the three compounds with the –OH substituent the opposite effect is observed. The substituent in the *ortho* position of the aromatic ring causes the biggest shift of the 280s loop and the strongest destabilization of the protein. In the case of the –Br substituent the effect of a significant shift of the

280s loop is the same in both the *meta* and *para* positions of the aromatic ring. In addition, there is a similarity between the $–OCH_3$ and $–CH_3$ substituents. Both cause a significant shift of the 280s loop as mentioned above. Interestingly, the binding of the inhibitors with the $–NO_2$ triggers a negligible shift of the 280s loop. Finally, is it interesting to add that among these fifteen compounds, only that with the –OH substituent in the *ortho* position, changes the direction of the phenyl ring of Phe285 completely, compared to all the other cases where it is simply shifted. Out of the three inhibitors with the –OH substituent, the compound with the –OH group at the *ortho* position, also causes the biggest shift and destabilization of the 280s loop. It also has the lowest IC_{50} value between the three. These observations will be of value in the design of further potent and specific inhibitors of the enzyme. This study provides evidence that thiosemicarbazone derivatives of β-D-glucopyranose are potent inhibitors of glycogen phosphorylase with IC_{50} values in the low μM range (the best inhibitor with a fluorine substituent at the *para* position showed an IC_{50} of 5.7 μM) and could bind tightly at both the catalytic and new allosteric site of GP*b* as indicated by the high resolution structures of GP*b* determined in complex with fifteen aromatic substituted thiosemicarbazone derivatives of β-D-glucopyranose. Inhibition of GP has proven a promising approach in modulating the action of this enzyme, which is the main regulator of blood glucose level. The present study offers a new concept for fighting against type 2 diabetes, epidemically expanding metabolic disease.

Since the target β-D-glucopyranosyl thiosemicarbazones possess several potent donors sites for coordination with metals, and thus, they should be regarded as attractive ligands, some representative Ni(II), Pd(II) and Pt(II) complexes were synthesized by the treatment of these ligands with $Ni(OAc)_2$, K_2PdCl_4 and K_2PtCl_4, respectively, in methanol. In total, four Ni (three of them diamagnetic and one paramagnetic), two Pd and one Pt complexes were synthesized and fully characterized by spectroscopic techniques. All complexes exist as mononuclear species. The thiosemicarbazone ligands are coordinated to the metals upon deprotonation at the N(2) nitrogen in a bidentate *N*,*S*-mode forming five-membered chelating rings (except one palladium complex, the ligand is neutral), with the exception of a Pd complex with a ligand possessing a pyridine moiety, in which the pyridine nitrogen atom is also coordinated to the metal in a tridentate *N*,*N*,*S*-mode, forming two chelate rings. In contrast to the nickel(II) complexes possessing the sugar moiety with all hydroxyl group acetyl-protected, in the palladium(II) and platinum(II) complexes the sugar hydroxyl groups being unprotected. In the Ni and Pt complexes, two ligands are bound per metal forming complexes $\mathbf{ML_2}$, while the ligand to metal ratio in the Pd complexes is 1:1 with the formula $\mathbf{MLCl_2}$ or **MLCl**. The complexes are air-stable. It is of interest also to mention that the Pd

complex with a glucopyranosyl thiosemicarbazone possessing a pyridine moiety and free hydroxyl groups in the sugar ring is water-soluble.

The palladium complex of the phosphane-free system (4-*tert*-butyl-benzaldehyde *N*(4)-(β-D-glucopyranosyl)thiosemicarbazone) was found to be an efficient catalyst for the Suzuki coupling of aryl bromides and unactivated chlorides with phenylboronic acid under aerobic conditions. The catalyst seems to be air stable at 100°C, and palladium-black, which indicates the degradation of the catalyst, was not observed. As expected, the catalytic activity depended on the halide, while electron-withdrawing groups on the aryl ring increased the reaction rate. This palladium complex was also found to be an efficient catalyst for the Heck reaction of the de-activated 4-bromoanisole with styrene. For comparision purposes, Suzuki coupling was also attempted by the use of the Ni(II) complex of 4-*tert*-butyl-benzaldehyde *N*(4)-(β-D-glucopyranosyl)thiosemicarbazone under the same reaction conditions as the Pd complex, but unfortunately, it was found that it is an inefficient catalyst for this reaction.

V. Experimental part

V.1. General remarks

Reagents and solvents: D-Glucose pentaacetate **(1)**, KSCN, HBr/CH_3COOH, K_2PdCl_4, K_2PtCl_4, ($Ni(OAc)_2 \cdot 4H_2O$), $NiCl_2$, aldehydes and ketones were commercially available. All syntheses were carried out under an argon atmosphere with purified and dry reagents and solvents as indicated in Table 20.

Column chromatography was performed using silica gel and TLC on Kieselgel 60 F_{254} plates; the plates were visualized by charring after dipping in a solution EtOH (5% H_2SO_4) and heating at 150ºC or using a UV lamp.

Melting points were measured on a Büchi melting point apparatus and were not corrected.

Optical rotations were measured on a Perkin–Elmer polarimeter at room temperature.

IR measurements were made using a Bruker Tensor 27 instrument (400-3000cm^{-1}).

NMR measurements were made using a Varian 300 (300.13 MHz and 75.47 MHz for ^1H and ^{13}C, respectively) or 600 (599.83 MHz and 150.84 MHz for ^1H and ^{13}C, respectively). The assignment of the protons in the ^1H NMR spectra was performed by COSY and NOESY experiments, and distinction of the CH, CH_2 and CH_3 carbons in the ^{13}C NMR spectra was performed by DEPT NMR. Atom numbering used for the NMR spectra is as shown for $\mathbf{L_x}$ in Fig. 56.

ESI MS spectra were recorded on TSQ 7000 Finnigan MAT Mass Spectrometer operating either a positive or negative mode.

Elemental analyses for C, H, N were carried out on a Perkin–Elmer PE 2400 II instrument.

GC: Varian Star 3400 CX, with column 30 m × 0,53 mm DB5.

Initial temperature of column (Initial column temperature): 60 °C

Initial time of delay of column (Initial column hold time): 3,00 min

Final temperature of column (Final column temperature): 260 °C

Proportion of increase °C/min: 10,0

Time of delay of column (Column hold time): 27,0 min

Pressure of gas: 5 psi

Table 20 *Purification of solvents and reagents*

Solvents and Reagents	***Dryness and Distillation***
Acetone	stirred over K_2CO_3 for 24h then distilled (b.p. 56 ºC/1atm)
Acetonitrile	stirred over K_2CO_3 for 24h then fractional distillation (b.p. 81.6 ºC/1atm)
Chloroform	stirred over $CaCl_2$ for 24h then fractional distillation (b.p. 61.2 ºC/1atm)
Dichloromethane	refluxed over CaH_2(5% w/v) for 4h then distilled (b.p. 40ºC)
Dioxane	reflux over Na and benzophenone until the colore became blue then distilled (b.p. 101ºC)
N,N-Dimethylformamide	stirred over CaH_2(5% w/v) for 4h then distilled (b.p. 88ºC/100mmHg)
Ethanol	refluxed over CaO(250g/L) for 6h then distilled (b.p. 78.3ºC)
Ether	reflux over Na(1% w/v) and benzophenone(0.2% w/v) until the colore became blue freshly distilled (b.p. 34.6ºC)
Ethyl acetate	stirred over K_2CO_3 for 24h then distilled (b.p. 77.1ºC)
n-Hexane	stirred over $CaCl_2$ for 24h then distilled (b.p. 68.7ºC)
Hydrazine	refluxed over KOH(eq. weight) for 3h then distililled from fresh NaOH in a current of dry argon (b.p. 113.5ºC/1atm)
Methanol	refluxed over $CuSO_4$ for 6h then distilled (b.p. 64.5ºC)
Pyridine	stirred over KOH for 24h then fractional distillation (b.p. 115.6ºC)
Styrene	stirred over CaH_2 for 24h then distilled (b.p. 50-51ºC/25mmHg)
Toluene	dried over Na for 24 h then distilled (b.p. 110.6ºC)

V.2. (2,3,4,6-tetra-*O*-acetyl-α-D-glucopyranosyl) bromide (110) [267]

A solution of HBr in AcOH (112 mL; 33% HBr) was added drop wise, under argon, to a solution of pentaacetylglucose (20 g, 51.28 mmol) in AcOH (75 mL). The reaction mixture was stirred in the dark at 10-15°C until the reaction was completed (monitored by TLC EtOAC/hexane 1:1, R_f = 0.65). Then, ice-cold water (100 mL) was added and the mixture was extracted with $CHCl_3$ (3 × 75 mL). The combined organic layers were washed with a saturated $NaHCO_3$ solution, water, and brine, dried over Na_2SO_4, filtrated off, the filtrate was evaporated in vacuum to give a colorless syrupy mixture. Double recrystallization from dry ether yielded **110** as a white solid (12.65g, 30.8 mmol, 60%), sensitive to light and kept under argon in the fridge at −18ºC. M.p. 84-87°C (lit. 89°C). **^{1}H NMR**(500 MHz, $CDCl_3$, 25 ºC): δ 6.58 (d, $^3J_{H1\text{-}H2}$ = 4.1Hz, H1); 5.51 (dd, $^3J_{H3\text{-}H4}$ = 9.3Hz; $^3J_{H4\text{-}H5}$ 9.9Hz, 1H, H4); 5.12 (dd, $^3J_{H2\text{-}H3}$ = 9.9Hz, 1H, H3); 4.79 (dd, 1H, H2); 4.32-4.07 (m, 3H, H-5; H6; H-6 ‘) ; 2.06-1.99(4s, 12H, CH_3); **^{13}C NMR** (75.47 MHz, $CDCl_3$, 25 ºC): δ = 170.3, 169.7, 169. 7 and 169.3 (C=O), 86.5 (1-C), 72.3 (5-C), 70.7 (2-C), 70.3 (3-C), 67.3 (4-C), 61.1 (6-C), 20.5, 20.5, 20.5 and 20.4 (CH_3) ppm; Anal. Calcd for $C_{14}H_{19}BrO_9$.(411.21) C, 40.89; H, 4.66. Found(%): C, 41.05; H, 4.78.

V.3. (2,3,4,6-tetra-*O*-acetyl-β-D-glucopyranosyl) isothiocyanate (111) [268]

The glycosyl bromide **110** (41.1g, 0.1 mol) was mixed with KSCN (97g, 1 mol) homogenized in a mortar. The mixture was melted at 190°C using on oil bath under argon atmosphere. The reaction was stopped when TLC indicated a fully conversion of the bromide, and the mixture was then cooled at room temperature. Water and chloroform was added to dissolve the melt and the phases were separated. The aqueous phase was extracted with chloroform, and the combined organic phases were dried over Na_2SO_4. The crude product was recrystallized from ether/hexane 1:1 two times or by thin layer chromatography(as quickly you can in a dark place) using as eluent a mixture EtOAc/toluene 1:4 yielding **111** as a white solid, sensitive to light and moisture, kept in fridge (−4-0°C) (18.95, 0.049 mol, 45%). $C_{15}H_{19}NO_9S$ (389.08). M.p. 108-112°C (lit. 114ºC). $[\alpha]_D$ = -1.89(CH_3Cl; c = 1.1). **^{1}H NMR** (599.83 MHz, $CDCl_3$, 25 ºC): δ = 5.18 (t, J = 9.6 Hz, 1 H, 3-H), 5.09–5.06 (m, 2 H, 2-H, 4-H), 5.01 (d, J = 9.0 Hz, 1 H, 1-H), 4.20 (dd, $^3J_{5\text{-}H,6\text{-}H}$ = 4.8 Hz, $^2J_{6\text{-}H,6'\text{-}H}$ = 12.6 Hz, 1 H, 6-H), 4.10 (dd, $^3J_{5\text{-}H,6'\text{-}H}$ = 2.1 Hz, 1 H, 6´-H), 3.73 (ddd, $^3J_{4\text{-}H,5\text{-}H}$ = 10.2 Hz, 1 H, 5-H), 2.01 (s, 6 H, CH_3), 2.00 (s, 3 H, CH_3) 1.98 (s, 3 H, CH_3) ppm; **^{13}C NMR** (75.47 MHz, $CDCl_3$,

25 ºC): δ = 170.5, 170.0, 169.2 and 169.0 (C=O), 144.2 (C=S), 83.4 (1-C), 74.0 (3-C), 72.5 (2-C), 71.8 (5-C), 67.6 (4-C), 61.4 (6-C), 20.7 and 20.5 (CH_3).

V.4. 4-(2,3,4,6–tetra-*O*-acetyl-β-D-glucopyranosyl)thiosemicarbazide (112) [255]

To a solution of **111** (15 g, 38.6 mmol) in absolute ethanol (250 mL) was added dropwise dry hydrazine (15.2 g, 47.5 mmol) at 5−10°C under a vigorous stirring, and the reaction mixture was stirred for a few minutes until a white precipitated was formed. The precipitate was filtered off, washed with cold ethanol and ether and dried in desiccator. It was recrystallized twice from methanol in the freeze giving **112** as a white solid (10.48 g, 0.025 mol 65%). M.p. 162-165°C (170ºC). $[\alpha]_D$ = +34(CH_3Cl; c = 1.1). **IR** (KBr): *v* 3318, 3199 (NH), 1521 (NH), 1218, 1737 (C=O), 1382, 1035 (C–N), 900 (1-C–H), 818 (C=S) cm^{-1}; **^{1}H NMR** (300.13 MHz, DMSO-d_6, 25 ºC): δ = 9.27 (s, 1 H, N(2)H), 8.20 (br s, 1 H, N(4)H), 5.82 (br s, 1 H, 1-H), 5.36 (t, ^3J = 9.6 Hz, 1 H, 3-H), 5.08 (t, ^3J = 9.3 Hz, 1 H, 2-H), 4.92 (dd, $^3J_{3\text{-H},4\text{-H}}$ = 9.6 Hz, $^3J_{4\text{-H},5\text{-H}}$ = 9.9 Hz, 1 H, 4-H), 4.60 (br s, 2 H, NH_2), 4.17 (dd, $^3J_{5\text{-H},6\text{-H}}$ = 1.8 Hz; $^2J_{6\text{-H},6'\text{-H}}$ = 12.3 Hz, 1 H, 6-H), 4.01–3.92 (m, 2 H, 5-H, 6´-H), 2.00, 1.99 and 1.95 (3 × s, 12 H, CH_3) ppm; **^{13}C NMR** (75.47 MHz, DMSO-d_6, 25 ºC): δ = 182.0 (C=S), 170.0, 169.5 and 169.3 (C=O), 81.0 (1-C), 72.5 (3-C), 72.0 (2-C), 70.5 (5-C), 68.0 (4-C), 56.0 (6-C), 20.5, 20.4 and 18.5 (CH_3) ppm; Anal. calcd. $C_{15}H_{23}N_3O_9S$ (421.42): C, 42.75; H, 5.50; N, 9.97; Found C, 42.70; H, 5.79; N, 10.20.

V.5. Synthesis of aldehyde/ketone 4-(per-O-acetylated-β-D-glucopyranosyl) thiosemicarbazones $L_{1\text{-}26}$

General procedure: A solution of aldehyde or ketone (2.38 mmol) in ethanol (5 mL) was added dropwise to a solution of thiosemicarbazide **112** (1 g, 2.38 mmol) in ethanol (80 mL). For the synthesis of $\mathbf{L_{20}}$, $\mathbf{L_{21}}$, $\mathbf{L_{22}}$ and $\mathbf{L_{23}}$, methanol was used as solvent. After the addition of a catalytic amount of AcOH, the reaction mixture was stirred at room temperature or refluxed for 4-48 h. The solution was kept in fridge overnight to form a precipitate; in some cases the solution was concentrated to the half volume, and then water was added to precipitate a solid. The precipitate was filtered off, washed with cold ethanol and in some cases with ether, and recrystallized from ethanol or methanol ($\mathbf{L_{20}}$, $\mathbf{L_{21}}$, $\mathbf{L_{22}}$ and $\mathbf{L_{23}}$). The list of aldehyde/ketone 4-(per-*O*-acetylated-β-D-glucopyranosyl)thiosemicarbazones are given in Fig. 81.

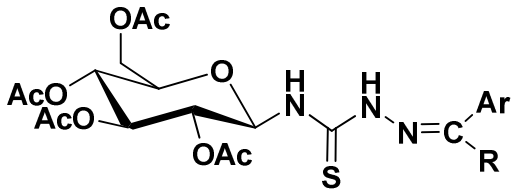

L_1 R = H, Ar = -C_6H_4-F-*p*;
L_2 R = H, Ar = -C_6H_4-Cl-*o*;
L_3 R = H, Ar = -C_6H_4-Cl-*m*;
L_4 R = H, Ar = -C_6H_4-Cl-*p*;
L_5 R = H, Ar = -C_6H_4-Br-*o*;
L_6 R = H, Ar = -C_6H_4-Br-*m*;
L_7 R = H, Ar = -C_6H_4-Br-*p*;
L_8 R = H, Ar = -C_6H_4-CF_3-*p*;
L_9 R = H, Ar = -C_6H_4-NO_2-*o*;
L_{10} R = H, Ar = -C_6H_4-NO_2-*m*;
L_{11} R = H, Ar = -C_6H_4-NO_2-*p;*
L_{12} R = H, Ar = -C_6H_4-OH-*o*;
L_{13} R = H, Ar = -C_6H_4-OH-*m*;
L_{14} R = H, Ar = -C_6H_4-OH-*p*;
L_{15} R = H, Ar = -C_6H_4-OMe-*o*;
L_{16} R = H, Ar = -C_6H_4-OMe-*m*;
L_{17} R = H, Ar = -C_6H_4-OMe_3-*p*;
L_{18} R = H, Ar = -C_6H_4-Me-*p*;
L_{29} R = H, Ar = -C_6H_4-*t*Bu-*p*;
L_{20} R = H, Ar = -2-pyridyl;
L_{21} R = H, Ar = -3-pyridyl;
L_{22} R = H, Ar = -4-pyridyl;
L_{23} R = H, Ar = -ferrocenyl;
L_{24} R = H, Ar = -β-naphthyl;
L_{25} R = CH_3, Ar = -C_6H_4-Me-*p*;
L_{26} R = CH_3, Ar = -β-naphthyl;

Figure 81 Aldehyde/ketone 4-(per-*O*-acetylated-β-D-glucopyranosyl)thiosemicarbazones

Table 21 below includes experimental details for the target molecules $\mathbf{L_{1\text{-}26}}$.

Table 21 *Aldehyde/ketone 4-(per-O-acetylated-β-D-glucopyranosyl)thiosemicarbazones – Reaction conditions and physical properties*

Compound	T [°C]	t [h]	Solvent	Recrystalization	Color	Yield (%)	M.p. [°C]
L_1	80°C	1.5	EtOH	MeOH	white	40	209-212
L_2	80°C	6	EtOH	MeOH	white	66	172-175
L_3	80°C	1	EtOH	MeOH	yellow	66	192-196
L_4	80°C	4	EtOH	EtOH	white	53	214-217
L_5	r.t.	1	EtOH	MeOH	white	71	171-175
L_6	80°C	24	EtOH	MeOH/H_2O	yellow	44	183-185
L_7	80°C	2	$EtOH_{dry}$	EtOH	white	64	210-212
L_8	80°C	20	EtOH	EtOH/Et_2O	colorless	73	223-225
L_9	r.t.	3	EtOH	MeOH/H_2O	yellow	92	136-140
L_{10}	80°C	8	EtOH	EtOH	yellow	79	191-195
L_{11}	80°C	3	$EtOH_{dry}$	EtOH	yellow	64	218-220
L_{12}	40°C	20	$EtOH_{dry}$	MeOH/H_2O	white	85	200(dec)
L_{13}	80°C	4	$EtOH_{dry}$	MeOH	white	50	201-204
L_{14}	80°C	72	$EtOH_{dry}$	MeOH/H_2O	colorless	82	200-202
L_{15}	r.t.	72	EtOH	MeOH/H_2O	white	81	208(dec)
L_{16}	80°C	1	EtOH	MeOH	white	78	175-179
L_{17}	80°C	4	EtOH	EtOH	white	88	213-216
L_{18}	80°C	20	EtOH	EtOH	white	69	198-201
L_{19}	80°C	14	$EtOH_{dry}$	EtOH	colorless	77	210-213
L_{20}	80°C	20	MeOH	EtOH	yellow	67	70-73
L_{21}	r.t.	2	MeOH	EtOH/H_2O	white	80	126-129
L_{22}	80°C	3	$EtOH_{dry}$	EtOH	white	64	196-200
L_{23}	80°C	3	EtOH	MeOH/H_2O	red	90	212-215
L_{24}	r.t.	72	EtOH	EtOH	white	94	212-215
L_{25}	80°C	6	MeOH	EtOH	white	78	192-198
L_{26}	80°C	3	EtOH	EtOH	white	72	182-185

Analytical data

4-Fluoro-benzaldehyde*N*(4)-(2,3,4,6-tetra-*O*-acetyl-β-D-glucopyranosyl) thiosemicarbazone (L_1)

IR(KBr) : *v* 3342, 3306, 3146, 2975, 1745, 1603, 1553, 1503, 1415, 1373, 1274, 1221, 1156, 1091, 1039, 916, 843, 714, 610, 574, 547 cm^{-1}; **^{1}H NMR**(300 MHz, DMSO-d_6, 25 ºC): δ = 11.93 (s, 1 H, N(2)H), 8.80 (d, $^3J_{N(4)H,1-H}$ = 9.0 Hz, 1 H, N(4)H), 8.07 (s, 1H, CH=N), 7.90 (dd, ^3J = 5.7 Hz, ^3J = 8.7 Hz, 2 H, H_{arom}), 7.27 (t, 3*J* = 8.7 Hz, 2 H, H_{arom}), 5.95 (dd, $^3J_{1-H,l2-H}$ = 9.3Hz, 1 H, 1-H), 5.43–5.27 (m, 2 H, 2-H, 4-H), 4.96 (t, ^3J = 9.6 Hz, 1 H, 3-H), 4.22 (dd, $^3J_{5-H,6-H}$ = 4.8 Hz; $^2J_{6-H,6´H}$ = 12.3 Hz, 1 H, 6-H), 4.07 (ddd, $^3J_{4-H,5-H}$ = 9.9 Hz, 1 H, 5-H), 3.98 (dd, $^3J_{5-H,6´-H}$ = 1.8 Hz; 1 H, 6´-H), 2.00, 1.99, 1.96 and 1.93 (4 × s, 12 H, CH_3) ppm; **^{13}C NMR**(75.47 MHz, $CDCl_3$, 25 ºC): δ = 178.9 (C=S), 171.1, 170.7, 169.9 and 169.6 (C=O), 142.4 (CH=N), 129.7, 129.4, 129.1, 129.1; 116.3 and 116.0 (C_{arom}), 82.3 (1-C), 73.5 (3-C), 72.6 (2-C), 70.6 (5-C), 68.4 (4-C), 61.6 (6-C), 20.8, 20.7, and 20.6 (CH_3) ppm; R_f (Hex/EtOAc 1:1) = 0.5. $[\alpha]_D$ = -72.9(CH_3Cl; c = 1). Anal. calcd. for $C_{22}H_{26}FN_3O_9S$. (509.15): C, 50.09; H, 4.97, N, 7.97. Found: C, 50.07; H, 5.29; N, 7.73.

2-Chloro-benzaldehyde 4-(2,3,4,6-tetra-*O*-acetyl-β-D-glucopyranosyl) thiosemicarbazone (L_2)

IR(KBr): *v* 3351, 3120, 2975, 1745 (C=O), 1592, 1533, 1504, 1470, 1433, 1367, 1216, 1141, 1066, 1039, 920, 830, 762, 708, 619, 574 cm^{-1}; **^{1}H NMR**(300.13 MHz, $CDCl_3$, 25 ºC): δ = 9.76 (s, 1 H, N(2)H), 8.29 (d, $^3J_{1-H,N(4)H}$ = 8.7 Hz 1 H, N(4)H), 8.26 (s, 1 H, CH=N), 8.09–8.06 (m, 1 H, H_{arom}) 7.37–7.30 (m, 3 H, H_{arom}), 5.72 (dd, $^3J_{1-H,2-H}$ = 9.3 Hz, 1 H, 1-H), 5.41 (t, $^3J_{2-H,3-H}$ = 9.6 Hz, 1 H, 3-H), 5.19–5.09 (m, 2 H, 2-H, 4-H), 4.37 (dd, $^3J_{5-H,6-H}$ = 4.5 Hz, $^2J_{6-H,6´H}$ = 12.6 Hz, 1 H, 6-H), 4.13 (dd, $^3J_{5-H,6´-H}$ = 2.1 Hz, 1 H, 6´-H), 3.89 (ddd, $^3J_{4-H,5-H}$ = 9.9 Hz, 1 H, 5-H), 2.07, 2.04, 2.03 and 2.02 (4 × s, 12 H, CH_3) ppm; **^{13}C NMR**(75.47 MHz, DMSO-d_6, 25 ºC): δ = 178.5 (C=S), 170.0, 169.5, 169.4 and 169.3 (C=O), 139.7 (CH=N), 133.4, 131.6, 131.1, 129.8, 127.6 and 127.3 (C_{arom}), 81.5 (1-C), 72.7 (3-C), 72.2 (2-C), 70.9 (5-C) 67.8 (4-C), 61.7 (6-C), 20.5, 20.4, 20.3 and 20.3 (CH_3) ppm. R_f (Hex/EtOAc 1:1) = 0.43. $[\alpha]_D$ = -103(CH_3Cl; c = 1.07). Anal. calcd. for $C_{22}H_{26}ClN_3O_9S{\cdot}H_2O$ (543.11): C, 47.02; H, 5.02; N, 7.48. Found: C, 47.54; H, 4.86; N, 7.03.

3-Chloro-benzaldehyde *N*(4)-(2,3,4,6-tetra-*O*-acetyl-β-D-glucopyranosyl) thiosemicarbazone (L_3)

IR(KBr): *v* 3322, 3138, 2995, 1749, 1549, 1509, 1475, 1431, 1367, 1237, 1093, 1063 1043, 931, 908, 830, 705, 679, 606, 553 cm^{-1}; **^{1}H NMR**(300.13 MHz, $CDCl_3$, 25 ºC): δ = 9.64 (s, 1 H, N(2)H), 8.35 (d, 1 H, $^3J_{1\text{-}H,N(4)H}$ = 8.7 Hz 1 H, N(4)H), 7.77 (s, 1 H, H_{arom}), 7.74 (s, 1 H, CH=N), 7.58 (d, ^3J = 6.9 Hz, 1 H, H_{arom}), 7.42–7.33 (m, 2 H, H_{arom}), 5.67 (dd, $^3J_{1\text{-}H,2\text{-}H}$ = 9.3 Hz, 1 H, 1-H), 5.42 (dd, $^3J_{3\text{-}H,4\text{-}H}$ = 9.6 Hz, 1 H, 3-H), 5.22–5.11 (m, 2 H, 2-H, 4-H), 4.38 (dd, $^3J_{5\text{-}H,6\text{-}H}$ = 4.5 Hz, $^2J_{6\text{-}H,6'H}$ = 12.6 Hz, 1 H, 6-H), 4.15 (dd, $^3J_{5\text{-}H,6'\text{-}H}$ = 2.1 Hz, 1 H, 6´-H), 3.92 (ddd, $^3J_{4\text{-}H,5\text{-}H}$ = 9.9 Hz, 1 H, 5-H), 2.09 and 2.04 (2 × s, 12 H, CH_3) ppm; **^{13}C NMR** (75.47 MHz, $CDCl_3$, 25 ºC): δ = 179.1 (C=S), 171.2, 170.7, 169.9 and 169.6 (C=O), 141.7 (CH=N), 135.0, 134.7, 130.7, 130.2, 127.3 and 126.0 (C_{arom}), 82.4 (1-C), 73.5 (3-C), 72.5 (2-C), 70.6 (5-C), 68.4 (4-C), 61.6 (6-C), 20.8, 20.7 and 20.6 (CH_3) ppm. R_f (Hex/EtOAc 1:1) = 0.60. $[\alpha]_D$ = -82.7(CH_3Cl; c = 1). Anal. calcd. for $C_{22}H_{26}ClN_3O_9S$ (543.97): C, 48.57; H, 4.82; N, 7.72. Found: C, 48.78; H, 5.11; N, 8.04.

4-Chloro-benzaldehyde 4-(2,3,4,6-tetra-*O*-acetyl-β-D-glucopyranosyl) thiosemicarbazone (L_4) [252]

IR(KBr): *v* 3295, 3122, 2983, 1745, 1594, 1549, 1507, 1492, 1371, 1088, 1039, 1013, 912, 830, 709, 628, 555 cm^{-1}; **^{1}H NMR**(300.13 MHz, $CDCl_3$, 25 ºC): δ = 9.40 (s, 1 H, N(2)H), 8.30 (d, $^3J_{1\text{-}H,N(4)H}$ = 8.7 Hz 1 H, N(4)H), 7.72 (s, 1 H, CH=N), 7.65 (d, ^3J = 8.4 Hz, 2 H, H_{arom}), 7.40 (d, ^3J = 8.4 Hz, 2 H, H_{arom}), 5.69 (dd, $^3J_{1\text{-}H,2\text{-}H}$ = 9.3 Hz, 1 H, 1-H), 5.41 (t, $^3J_{3\text{-}H,4\text{-}H}$ = 9.6 Hz, 1 H, 3-H), 5.20–5.10 (m, 2 H, 2-H, 4-H), 4.36 (dd, $^3J_{5\text{-}H,6\text{-}H}$ = 4.5 Hz, $^2J_{6\text{-}H,6'\text{-}H}$ = 12.3 Hz, 1 H, 6-H), 4.12 (dd, $^3J_{5\text{-}H,6'H}$ = 2.1 Hz; 1 H, 6´-H), 3.91 (ddd, $^3J_{4\text{-}H,5\text{-}H}$ = 10.2 Hz, 1 H, 5-H), 2.09, 2.05, 2.04 and 2.03 and (4 × s, 12 H, CH_3) ppm; **^{13}C NMR** (75.47 MHz, $CDCl_3$, 25 ºC): δ = 178.9 (C=S), 171.1, 170.7, 169.9 and 169.6 (C=O), 142.7 (CH=N), 137.0, 131.6 129.4 and 129.0 (C_{arom}), 82.3 (1-C), 73.7 (3-C), 72.8 (2-C), 70.7 (5-C), 68.6 (4-C), 61.8 (6-C), 20.7, 20.6, 20.6 and 20.6 (CH_3) ppm. R_f (Hex/EtOAc 1:1) = 0.58. $[\alpha]_D$ = -78(CH_3Cl; c = 1). Anal. calcd. for $C_{22}H_{26}ClN_3O_9S{\cdot}4H_2O$ (616.04): C, 42.89; H, 5.56; N, 6.82. Found: C, 43.12; H, 5.99; N, 6.44.

2-Bromo-benzaldehyde 4-(2,3,4,6-tetra-*O*-acetyl-β-D-glucopyranosyl) thiosemicarbazone (L_5)

IR(KBr): *v* 3350, 3134, 2975, 1753, 1730, 1529, 1504, 1466, 1437, 1219, 1142, 1119, 1097, 1066, 1039, 912, 883, 822, 752, 688, 575, 535 cm^{-1}; **^{1}H NMR**(300.13 MHz, $CDCl_3$, 25 ºC): δ = 9.61 (s, 1 H, N(2)H), 8.26 (d, $^3J_{1\text{-H,N(4)H}}$ = 8.7 Hz 1 H, N(4)H), 8.21 (s, 1 H, CH=N), 8.06 (d, ^3J = 7.8 Hz, 1 H, H_{arom}), 7.58 (d, ^3J = 7.8 Hz, 1 H, H_{arom}), 7.52 (d, ^3J = 7.8 Hz, 1 H, H_{arom}), 7.27 (d, ^3J = 7.8 Hz, 1 H, H_{arom}), 5.66 (dd, $^3J_{1\text{-H,2-H}}$ = 9.3 Hz, 1 H, 1-H), 5.41 (t, $^3J_{3\text{-H,4-H}}$ = 9.6 Hz, 1 H, 3-H), 5.21–5.09 (m, 2 H, 2-H, 4-H), 4.38 (dd, $^3J_{5\text{-H,6-H}}$ = 4.5 Hz, $^2J_{6\text{-H,6´-H}}$ = 12.6 Hz, 1 H, 6-H), 4.12 (dd, $^3J_{5\text{-H,6´H}}$ = 2.1 Hz; 1 H, 6´-H), 3.92 (ddd, $^3J_{4\text{-H,5-H}}$ = 10.2 Hz, 1 H, 5-H), 2.10, 2.09, 2.05 and 2.04 and (4 × s, 12 H, CH_3) ppm; **^{13}C NMR** (75.47 MHz, $CDCl_3$, 25 ºC): δ = 179.2 (C=S), 171.1, 170.7, 169.9 and 169.6 (C=O), 142.4 (CH=N), 133.3, 131.9, 131.8, 27.9, 127.8 and 124.7 (C_{arom}), 82.3 (1-C), 73.6 (3-C), 72.6 (2-C), 70.6 (5-C), 68.3 (4-C), 61.6 (6-C), 20.8, 20.8, 20.6 and 20.6 (CH_3) ppm. R_f (Hex/EtOAc 1:1) = 0.5**.** $[\alpha]_D$ = -62(CH_3Cl; c = 1). Anal. calcd. for $C_{22}H_{26}BrN_3O_9S\cdot 2H_2O$ (586.06): C, 42.31; H, 4.84; N, 6.73. Found: C, 42.88; H, 5.21; N, 6.66.

3-Bromo-benzaldehyde 4-(2,3,4,6-tetra-*O*-acetyl-β-D-glucopyranosyl) thiosemicarbazone (L_6)

IR(KBr): *v* 3370, 3326 , 2942, 1737, 1529, 1490, 1470, 1425, 1366, 1216, 1143, 1109, 1035, 900, 889, 843, 789, 683, 590, 572 cm^{-1}; **^{1}H NMR**(300.13 MHz, $CDCl_3$, 25 ºC): δ = 10.18 (s, 1 H, N(2)H), 8.35 (d, $^3J_{1\text{-H,N(4)H}}$ = 8.7 Hz 1 H, N(4)H), 7.92 (s, 1 H, CH=N), 7.83 (m, 1 H, H_{arom}), 7.60 (d, ^3J = 7.8 Hz, 1 H, H_{arom}), 7.53 (d, ^3J = 7.8 Hz, 1 H, H_{arom}), 7.29 (d, ^3J = 7.8 Hz, 1 H, H_{arom}), 5.66 (dd, $^3J_{1\text{-H,2-H}}$ = 9.3 Hz, 1 H, 1-H), 5.41 (t, $^3J_{3\text{-H,4-H}}$ = 9.6 Hz, 1 H, 3-H), 5.21–5.09 (m, 2 H, 2-H, 4-H), 4.38 (dd, $^3J_{5\text{-H,6-H}}$ = 4.5 Hz, $^2J_{6\text{-H,6´-H}}$ = 12.6 Hz, 1 H, 6-H), 4.15 (dd, $^3J_{5\text{-H,6´H}}$ = 1.5 Hz; 1 H, 6´-H), 3.91 (ddd, $^3J_{4\text{-H,5-H}}$ = 10.2 Hz, 1 H, 5-H), 2.08 and 2.04 and (2 × s, 12 H, CH_3) ppm. **^{13}C NMR**($CDCl_3$): δ δ = 178.9(C=S), 171.1, 170.7, 169.9 and 169.5 (C=O), 142.0 (CH=N), 135.0, 133.6, 130.4, 130.3, 126.4 and 123.1 (C_{arom}), 82.3 (1-C), 73.5 (3-C), 72.5 (2-C), 70.5 (5-C), 68.4 (4-C), 61.6 (6-C), 20.8, 20.8, 20.6 and 20.6 (CH_3) ppm. R_f (Hex/EtOAc 1:1) = 0.5. $[\alpha]_D$ = -72.5(CH_3Cl; c = 1). Anal. calcd. for $C_{22}H_{26}BrN_3O_9S\cdot 3H_2O$. (586.06): C, 41.13; H, 5.02; N, 6.54. Found: C, 41.78; H, 4.96; N, 6.21.

4-Bromo-benzaldehyde 4-(2,3,4,6-tetra-*O*-acetyl-β-D-glucopyranosyl) thiosemicarbazone (L_7)

IR(KBr): *v* 3304, 3134, 2983, 1741. 1590, 1545, 1506, 1488, 1370, 1228, 1096, 1067, 1035, 108, 920,822, 706, 626, 542, 572 cm^{-1}; **^{1}H NMR**(300.13 MHz, $CDCl_3$, 25 ºC): δ = 9.32 (s, 1 H, N(2)H), 8.30 (d, $^3J_{1\text{-H,N(4)H}}$ = 8.7 Hz 1 H, N(4)H), 7.69 (s, 1 H, CH=N), 7.55-7.52 (m, 4 H, H_{arom}), 5.68 (dd, $^3J_{1\text{-H,2-H}}$ = 9.3 Hz, 1 H, 1-H), 5.41 (t, $^3J_{3\text{-H,4-H}}$ = 9.6 Hz, 1 H, 3-H), 5.19–5.10 (m, 2 H, 2-H, 4-H), 4.39 (dd, $^3J_{5\text{-H,6-H}}$ = 4.5 Hz, $^2J_{6\text{-H,6´-H}}$ = 12.6 Hz, 1 H, 6-H), 4.11 (dd, $^3J_{5\text{-H,6´H}}$ = 2.1 Hz; 1 H, 6´-H), 3.90 (ddd, $^3J_{4\text{-H,5-H}}$ = 10.2 Hz, 1 H, 5-H), 2.09, 2.05, 2.04 and 2.03 and (4 × s, 12 H, CH_3) ppm; **^{13}C NMR**($CDCl_3$): δ δ = 179.5 (C=S), 171.6, 170.7, 169.9 and 169.6 (C=O), 140.5 (CH=N), 148.8, 134.8, 132.8, 130.0, 125.0 and 122.5 (C_{arom}), 82.4 (1-C), 73.6 (3-C), 72.5 (2-C), 70.7 (5-C), 68.4 (4-C), 61.6 (6-C), 20.8, 20.7 and 20.6 (CH_3) ppm. R_f (Hex/EtOAc 1:1) = 0.5. $[\alpha]_D$ = -79.8(CH_3Cl; c = 1). Anal. calcd. for $C_{22}H_{26}BrN_3O_9S \cdot 4H_2O$. (586.06): C, 40.01; H, 5.19; N, 6.36.. Found: C, 40.56; H, 5.68; N, 5.99.

4-Trifluoromethyl-benzaldehyde *N*(4)-(2,3,4,6-tetra-*O*-acetyl-β-D-glucopyranosyl) thiosemicarbazone (L_8)

IR(KBr): *v* 3334, 330, 2938, 1749, 1529, 1487, 1418, 1366, 1323, 1296, 1219, 1166, 1126, 1110, 1089, 1065, 1031, 936, 912, 847, 830, 649, 596, 580, 541 cm^{-1}; **^{1}H NMR**(300.13 MHz, $CDCl_3$, 25 ºC): δ = 10.14 (s, 1 H, N(2)H), 8.38 (d, $^3J_{1\text{-H,N(4)H}}$ = 8.7 Hz, 1 H, N(4)H), 7.84 (s, 1 H, CH=N), 7.83 (d, ^3J = 8.7 Hz, 2 H, H_{arom}), 7.67 (d, ^3J = 8.4 Hz, 2 H, H_{arom}), 5.67 (dd, $^3J_{1\text{-H,2-H}}$ = 9.0 Hz, 1 H, 1-H), 5.42 (t, $^3J_{2\text{-H,3-H}}$ = 9.3 Hz, 1 H, 3-H), 5.20-5.10 (m, 2 H, 2-H, 4-H), 4.40 (dd, $^3J_{5\text{-H,6-H}}$ = 4.5 Hz, $^2J_{6\text{-H,6´-H}}$ = 12.6 Hz, 1 H, 6-H), 4.15 (dd, $^3J_{5\text{-H,6´-H}}$ = 2.1 Hz, 1 H, 6´-H), 3.90 (ddd, $^3J_{4\text{-H,5-H}}$ = 10.2 Hz, 1 H, 5-H), 2.09, 2.05, 2.04 and 2.03 (4 × s, 12 H, CH_3) ppm; **^{13}C NMR**(75.47 MHz, $CDCl_3$, 25 ºC) δ = 179.0 (C=S), 171.1, 170.7, 169.9 and 169.6 (C=O), 141.9 (CH=N), 136.3, 132.3, 131.9, 127.8, 125.8, 125.8 and 121.9 (C_{arom} and CF_3), 82.2 (1-C), 73.5 (3-C), 72.5 (2-C), 70.5 (5-C5), 68.3 (4-C), 61.6 (6-C), 20.7, 20.6 and 20.6 (CH_3) ppm. R_f (Hex/EtOAc 1:1) = 0.42. $[\alpha]_D$ = -80.17(CH_3Cl; c = 1.17). Anal. calcd. for $C_{23}H_{26}F_3N_3O_9S$(577.53): C, 47.83; H, 4.54; N, 7.28. Found: C, 48.28; H, 4.37; N, 6.99.

2-Nitro-benzaldehyde *N*(4)-(2,3,4,6-tetra-*O*-acetyl-β-D-glucopyranosyl) thiosemicarbazone (L_9)

IR(KBr): *v* 3320, 3212, 2985, 1745, 1732, 1525, 1502, 1445, 1370, 1348, 1242, 1212, 1180, 1128, 1098, 1035, 965, 916, 862, 822, 808, 755, 695, 622, 580, 540 cm^{-1}; **^{1}H NMR**(300.13 MHz, $CDCl_3$, 25 ºC): δ = 9.69 (s, 1 H, N(2)H), 8.43 (s, 1 H, CH=N), 8.30 (d, $^3J_{1\text{-}H,N(4)H}$ = 9.0 Hz, 1 H, N(4)H), 8.21 (dd, *J* = 1.5 Hz, *J* = 7.8 Hz, 1 H, H_{arom}), 8.06 (dd, *J* = 1.2 Hz, *J* = 8.1 Hz, 1 H, H_{arom}), 7.75–7.69 (m, 1 H, H_{arom}), 7.61–7.55 (m, 1 H, H_{arom}), 5.73 (dd, $^3J_{1\text{-}H,2\text{-}H}$ = 9.3 Hz, 1 H, 1-H), 5.42 (dd, $^3J_{2\text{-}H,3\text{-}H}$ = 9.3 Hz; $^3J_{3\text{-}H,4\text{-}H}$ = 9.6 Hz, 1 H, 3-H), 5.18–5.09 (m, 2 H, 2-H, 4-H), 4.38 (dd, $^3J_{5\text{-}H,6\text{-}H}$ = 4.5 Hz, $^2J_{6\text{-}H,6'\text{-}H}$ = 12.6 Hz, 1 H, 6-H), 4.14 (dd, $^3J_{5\text{-}H,6'\text{-}H}$ = 2.16 Hz, 1 H, 6´-H), 3.92 (ddd, $^3J_{4\text{-}H,5\text{-}H}$ = 10.2 Hz, 1 H, 5-H), 2.09, 2.05, 2.04 and 2.03 (4 × s, 12 H, CH_3) ppm; **^{13}C NMR**(75.47 MHz, $CDCl_3$, 25 ºC): δ = 179.3 (C=S), 171.3, 170.7, 169.9 and 169.7 (C=O), 148.3 (C–NO_2), 138.8 (CH=N), 133.8, 130.8, 128.6 and 125.0 (C_{arom}), 82.3 (1-C), 73.6 (3-C), 72.6 (2-C), 70.7 (5-C), 68.3 (4-C), 61.6 (6-C), 20.8 and 20.6 (CH_3) ppm. R_f (Hex/EtOAc 1:1) = 0.46. $[\alpha]_D$ = -49.2(CH_3Cl; c = 1). Anal. calcd. for $C_{22}H_{26}N_4O_{11}S{\cdot}2H_2O$ (590.56): C, 44.74; H, 5.12; N, 9.49. Found C, 45.01; H, 5.48; N, 9.23

3-Nitro-benzaldehyde *N*(4)-(2,3,4,6-tetra-*O*-acetyl-β-D-gluco pyranosyl) thiosemicarbazone (L_{10})

IR(KBr): *v* 3328, 3127, 2979, 1746, 1737, 1613, 1529, 1510, 1440, 1365, 1352, 1237, 1209, 1177, 1123, 1091, 1035, 958, 920, 858, 820, 807, 735, 690, 672, 576, 554 cm^{-1}; **^{1}H NMR**(300.13 MHz, $CDCl_3$, 25 ºC): δ = 10.07 (s, 1 H, N(2)H), 8.57 (s, 1 H, CH=N), 8.43 (d, $^3J_{1\text{-}H,N(4)H}$ = 9.0 Hz, 1 H, N(4)H), 8.28 (d, *J* = 1.28 Hz, 1 H, H_{arom}), 8.08 (d, *J* = 7.8 Hz, 1 H, H_{arom}), 7.91 (s, 1 H, H_{arom}), 7.63 (t, *J* = 8.1 Hz, 1 H, H_{arom}), 5.65 (dd, $^3J_{1\text{-}H,2\text{-}H}$ = 9.3 Hz, 1 H, 1-H), 5.43 (t, $^3J_{2\text{-}H,3\text{-}H}$ = 9.3 Hz, 1 H, 3-H), 5.21–5.11 (m, 2 H, 2-H, 4-H), 4.39 (dd, $^3J_{5\text{-}H,6\text{-}H}$ = 4.5 Hz, $^2J_{6\text{-}H,6'\text{-}H}$ = 12.6 Hz, 1 H, 6-H), 4.12 (dd, $^3J_{5\text{-}H,6'\text{-}H}$ = 12.6 Hz, 1 H, 6´-H), 3.93 (ddd, $^3J_{4\text{-}H,5\text{-}H}$ = 10.2 Hz,1 H, 5-H), 2.09, 2.05, 2.04 and 2.03 (4 × s, 12 H, CH_3) ppm; **^{13}C NMR**($CDCl_3$(75.47 MHz, $CDCl_3$, 25 ºC): δ = 179.2 (C=S), 171.3, 170.7, 169.9 and 169.6 (C=O), 148.8 (C–NO_2), 140.5 (CH=N), 134.8, 132.8, 130.0, 125.0 and 122.5 (C_{arom}), 82.4 (1-C), 73.6 (3-C), 72.5 (2-C), 70.7 (5-C), 68.4 (4-C), 61.6 (6-C), 21.0 and 20.8 (CH_3) ppm. R_f (Hex/EtOAc 1:1) = 0.36. $[\alpha]_D$ = -84.8(CH_3Cl; c = 1). Anal. calcd. for $C_{22}H_{26}N_4O_9S{\cdot}3H_2O$(608.57): C, 43.42; H, 5.30; N, 9.21. Found.(%): C, 43.72; H, 5.68; N, 8.89.

4-Nitro-benzaldehyde *N*(4)-(2,3,4,6-tetra-*O*-acetyl-β-D-gluco pyranosyl) thiosemicarbazone (L_{11}) [251]

IR(KBr): *v* 3341, 3306, 2975, 1741, 1588, 1525, 1525, 1507, 1372, 1344, 1220, 1144, 1087, 1031, 981, 920, 844, 826, 750, 688, 578 cm^{-1}; **^{1}H NMR** (300.13 MHz, $CDCl_3$, 25 ºC): δ = 10.11 (s, 1 H, N(2)H), 8.42 (d, $^3J_{1\text{-H,N(4)H}}$ = 9.3 Hz, 1 H, N(4)H), 8.28 (d, J = 8.7 Hz, 2 H, H_{arom}), 7.91 (d, J = 9.0 Hz, 2 H, H_{arom}), 7.90 (s, 1 H, CH=N), 5.65 (dd, $^3J_{1\text{-H,2-H}}$ = 9.0 Hz, 1 H, 1-H), 5.43 (dd, $^3J_{2\text{-H,3-H}}$ = 9.3 Hz, $^3J_{3\text{-H,4-H}}$ = 9.6 Hz,1 H, 3-H), 5.20–5.11 (m, 2 H, 2-H, 4-H), 4.38 (dd, $^3J_{5\text{-H,6-H}}$ = 4.5 Hz, $^2J_{6\text{-H,6´-H}}$ = 12.6 Hz, 1 H, 6-H), 4.12 (dd, $^3J_{5\text{-H,6´-H}}$ = 1.8 Hz, 1 H, 6´-H), 3.92 (ddd, $^3J_{4\text{-H,5-H}}$ = 10.2 Hz, 1 H, 5-H), 2.09, 2.06 and 2.04 (3 × s, 12 H, CH_3) ppm; **^{13}C NMR**($CDCl_3$): (75.47 MHz, $CDCl_3$, 25 ºC): δ = 179.2 (C=S), 171.3, 170.7, 169.9 and 169.6 (C=O), 148.8 (C–NO_2), 140.4 (CH=N), 138.9, 128.2 and 124.2 (C_{arom}), 82.4 (1-C), 73.6 (3-C), 72.4 (2-C), 70.6 (5-C), 68.4 (4-C), 61.6 (6-C), 20.8, 20.7 and 20.6 (CH_3) ppm. R_f (Hex/EtOAc 1:1) = 0.42. $[\alpha]_D$ = -110(CH_3Cl; c = 1). Anal. calcd. for $C_{22}H_{26}N_4O_{11}S$(554.53): C, 47.65; H, 4.73; N, 10.10.Found.(%): C, 47.98; H, 5.12; N, 10.76.

2-Hydroxy-benzaldehyde *N*(4)-(2,3,4,6-tetra-*O*-acetyl-β-D-glucopyranosyl) thiosemicarbazone (L_{12})

IR(KBr): *v* 3330, 3269, 2948, 1745, 1664, 1618, 1533, 1459, 1366, 1214, 1153, 1022, 958, 920, 830, 758, 599, 542 cm^{-1}; **^{1}H NMR**(300.13 MHz, $CDCl_3$, 25 ºC): δ = 9.81 (s, 1 H, N(2)H), 8.90 (s, 1 H, CH=N); 7.99 (s, 1 H, CH_{arom}), 7.81 (d, $^3J_{1\text{-H,N(4)H}}$ = 8.7 Hz, 1 H, N(4)H), 7.33 (t, J = 7.8 Hz, 1 H, CH_{arom}) 7.06 (d, J = 8.1 Hz, 1 H, CH_{arom}), 6.69 (t, J = 7.2 Hz, 1 H, CH_{arom}), 5.68 (dd, $^3J_{1\text{-H,2-H}}$ = 9.3 Hz, 1 H, 1-H), 5.42 (t, $^3J_{3\text{-H,4-H}}$ = 9.6 Hz, 1 H, 3-H), 5.15–5.09 (m, 2 H, 2-H, 4-H), 4.33 (dd, $^3J_{5\text{-H,6-H}}$ = 4.5 Hz, $^2J_{6\text{-H,6´-H}}$ = 12.6 Hz, 1 H, 6-H), 4.12 (dd, $^3J_{5\text{-H,6´-H}}$ = 2.1 Hz, 1 H, 6´-H), 3.90 (ddd, $^3J_{4\text{-H,5-H}}$ = 10.2 Hz, 1 H, 5-H), 2.09, 2.08, 2.05 and 2.04 (4 × s, 12 H, CH_3) ppm; **^{13}C NMR**(75.47 MHz, $CDCl_3$, 25 ºC): δ = 177.7 (C=S), 172.1, 170.7, 169.9 and 169.6 (C=O), 157.2 (C–OH), 148.3 (CH=N), 132.8, 132.0, 120.2, 117.4 and 116.6 (C_{arom}), 82.5 (1-C), 73.4 (3-C), 72.3 (2-C), 71.0 (5-C), 68.2 (4-C), 61.5 (6-C), 20.7, 20.6 and 20.5 (CH_3) ppm. R_f (Hex/EtOAc 1:1) = 0.37. $[\alpha]_D$ = -147 (CH_3Cl; c = 1). Anal. calcd. for $C_{22}H_{27}N_3O_{10}S{\cdot}5H_2O$ (615.61): C, 50.28; H, 5.18; N, 8.00. Found.(%): C, 42.88, H, 6.43, N, 7.12.

3-Hydroxy-benzaldehyde *N*(4)-(2,3,4,6-tetra-*O*-acetyl-β-D-glucopyranosyl) thiosemicarbazone (L_{13})

IR(KBr): *v* 3379, 3320, 3249, 2950, 1745, 1588, 1537, 1487, 1453, 1367, 1217, 1110, 1089, 1065, 1035, 982, 920, 826, 793, 688, 640, 601, 549 cm^{-1}; **^{1}H NMR**(300.13 MHz, DMSO-d_6, 25 ºC): δ = 9.87 (s, 1 H, N(2)H), 8.23 (d, $^3J_{1\text{-H,N(4)H}}$ = 8.7 Hz, 1 H, N(4)H), 7.74 (s, 1 H, CH=N), 7.29–7.24 (m, 2 H, H_{arom}), 7.07 (d, *J* = 7.8 Hz, 1 H, H_{arom}), 6.92 (dd, *J* = 1.5 Hz, *J* = 8.1 Hz, 1 H, H_{arom}), 5.71 (dd, $^3J_{1\text{-H,2-H}}$ = 9.3 Hz, 1 H, 1-H), 5.41 (t, $^3J_{3\text{-H,4-H}}$ = 9.6 Hz, 1 H, 3-H), 5.24–5.11 (m, 2 H, 2-H, 4-H), 4.37 (dd, $^3J_{5\text{-H,6-H}}$ = 4.5 Hz, $^2J_{6\text{-H,6´-H}}$ = 12.6 Hz, 1 H, 6-H), 4.13 (dd, $^3J_{5\text{-H,6´-H}}$ = 2.1 Hz, 1 H, 6´-H), 3.92 (ddd, $^3J_{4\text{-H,5-H}}$ = 10.2 Hz, 1 H, 5-H), 2.08, 2.06, 2.05 and 2.04 (4 × s, 12 H, CH_3) ppm; **^{13}C NMR** (75.47 MHz, DMSO-d_6, 25 ºC): δ = 178.3 (C=S), 172.1, 170.1, 169.5 and 169.4 (C=O), 157.7 (C–OH), 144.3 (CH=N), 135.0, 129.7, 118.8, 117.5 and 114.0 (C_{arom}), 81.5 (1-C), 72.8 (3-C), 72.3 (2-C), 71.0 (5-C), 68.0 (4-C), 61.8 (6-C), 21.0, 20.6, 20.4 and 20.3 (CH_3) ppm. R_f (Hex/EtOAc 1:1) = 0.22. $[\alpha]_D$ = -115.3(CH_3Cl; c = 1.33). Anal. calcd. for $C_{22}H_{27}N_3O_{10}S$(525.53): C, 50.28; H, 5.18; N, 8.00. Found.(%): C, 49.72; H, 5.39; N, 8.02.

4-Hydroxy-benzaldehyde *N*(4)-(2,3,4,6-tetra-*O*-acetyl-β-D-glucopyranosyl) thiosemicarbazone L_{14} [251, 253, 255]

IR(KBr): *v* 3562, 3404, 3220, 3314, 2960, 1741, 1601, 1536, 1514, 1452, 1371, 1218, 1169, 1039, 920, 835, 639, 600, 534 cm^{-1}; **^{1}H NMR**(300.13 MHz, $CDCl_3$, 25 ºC): δ = 9.84 (s, 1H, N(2)H), 8.20 (d, $^3J_{1\text{-H,N(4)H}}$ = 8.7 Hz, 1 H, N(4)H), 7.69 (s, 1 H, CH=N), 7.51 (d, *J* = 8.7 Hz, 2 H, H_{arom}), 6.68 (d, *J* = 8.7 Hz, 2 H, H_{arom}), 5.77 (br s, 1 H, OH), 5.74 (dd, $^3J_{1\text{-H,2-H}}$ = 9.0 Hz, 1 H, 1-H), 5.41 (t, $^3J_{3\text{-H,4-H}}$ = 9.6 Hz, 1 H, 3-H), 5.23–5.10 (m, 2 H, 2-H, 4-H), 4.36 (dd, $^3J_{5\text{-H,6-H}}$ = 4.5 Hz, $^2J_{6\text{-H,6´-H}}$ = 12.6 Hz, 1 H, 6-H), 4.14 (dd, $^3J_{5\text{-H,6´-H}}$ = 2.1 Hz, 1 H, 6´-H6), 3.92 (ddd, $^3J_{4\text{-H,5-H}}$ = 10.2 Hz, 1 H, 5-H), 2.08, 2.05, 2.04 and 2.02 (4 × s, 12 H, CH_3) ppm; **^{13}C NMR**(DMSO-d_6): (75.47 MHz, DMSO-d_6, 25 ºC): δ = 177.8 (C=S), 170.2, 169.7, 169.7 and 169.5 (C=O), 159.8 (C–OH), 144.3 (CH=N), 129.6, 124.8 and 115.8 (C_{arom}), 81.5 (1-C), 72.9 (3-C), 72.3 (2-C), 71.0 (5-C), 68.1 (4-C), 61.9 (6-C), 20.7, 20.6, 20.6 and 20.5 (CH_3) ppm. R_f (Hex/EtOAc 1:2) = 0.46. $[\alpha]_D$ = -104.8(CH_3Cl; c = 1). Anal. calcd. for $C_{22}H_{27}N_3O_{10}S{\cdot}2H_2O$(561.56): C, 47.05; H, 5.56; N, 7.48. Found.(%): C, 47.46, H, 5.36, N, 7.67.

2-Methoxy-benzaldehyde *N*(4)-(2,3,4,6-tetra-*O*-acetyl-β-D-glucopyranosyl) thiosemicarbazone (L_{15})

IR(KBr): *v* 3328, 3270, 2946, 1745, 1600, 1529, 1485, 1438, 1366, 1215, 1039, 956, 910, 826, 757, 598, 544 cm^{-1}; **^{1}H NMR**(300.13 MHz, $CDCl_3$, 25 ºC): δ = 9.43 (s, 1 H, N(2)H), 8.25 (d, $^3J_{1\text{-}H,N(4)H}$ = 8.7 Hz, 1 H, N(4)H), 8.21 (s, 1 H, CH=N), 7.97 (d, *J* = 7.8 Hz, 1 H, H_{arom}), 7.39 (t, *J* = 7.8 Hz, 1 H, H_{arom}), 7.02 (t, *J* = 7.5 Hz, 1 H, H_{arom}), 6.90 (d, *J* = 8.4 Hz, 1 H, H_{arom}), 5.78 (dd, $^3J_{1\text{-}H,2\text{-}H}$ = 9.3 Hz, 1 H, 1-H), 5.40 (t, $^3J_{2\text{-}H,3\text{-}H}$ = 9.3 Hz, 1 H, 3-H), 5.20–5.09 (m, 2 H, 2-H, 4-H), 4.38 (dd, $^3J_{5\text{-}H,6\text{-}H}$ = 4.5 Hz, $^2J_{6\text{-}H,6'\text{-}H}$ = 12.6 Hz, 1 H, 6-H), 4.10 (dd, $^3J_{5\text{-}H,6'\text{-}H}$ = 2.1 Hz, 1 H, 6´-H), 3.88 (ddd, $^3J_{4\text{-}H,5\text{-}H}$ = 10.2 Hz, 1 H, 5-H), 3.86 (s, 3 H, OCH_3); 2.09, 2.04, 2.03 and 2.02 (4 × s, 12 H, CH_3CO) ppm; **^{13}C NMR**(75.47 MHz, $CDCl_3$, 25 ºC): δ = 178.8 (C=S), 170.9, 170.7, 169.9 and 169.6 (C=O), 158.4 (*C*–OMe), 139.8 (CH=N), 132.2, 126.6, 121.2, 121.1 and 111.0 (C_{arom}), 82.3 (1-C), 73.5 (3-C), 72.7 (2-C), 70.5 (5-C), 68.3 (4-C), 61.6 (6-C), 55.6 (OCH_3), 20.8, 20.7 and 20.6 (*C*H_3CO) ppm. R_f (Hex/EtOAc 1:1) = 0.32. $[\alpha]_D$ = -83.7 (CH_3Cl; c = 0.7). Anal. calcd. for $C_{23}H_{29}N_3O_{10}S{\cdot}7H_2O$ (561.56): C, 41.50; H, 6.51; N, 6.31. Found.(%): C, 41.89; H, 7.02; N, 6.44.

3-Methoxy-benzaldehyde *N*(4)-(2,3,4,6-tetra-*O*-acetyl-β-D-glucopyranosyl) thiosemicarbazone (L_{16})

IR(KBr): *v* 3338, 3135, 2995, 1737, 1581, 1545, 1505, 1433, 1368, 1217, 1156, 1113, 1072, 1035, 910, 830, 779, 754, 679, 638, 573, 540 cm^{-1}; **^{1}H NMR**(300.13 MHz, DMSO-d_6, 25 ºC): δ = 10.22 (s, 1 H, N(2)H), 8.30 (d, $^3J_{1\text{-}H,N(4)H}$ = 8.7 Hz, 1 H, N(4)H), 7.77 (s, 1 H, CH=N), 7.36 (s, 1 H, H_{arom}), 7.28–7.21 (m, 1 H, H_{arom}), 7.11 (d, *J* = 7.5 Hz, 1 H, H_{arom}), 6.92 (d, *J* = 8.1 Hz, 1 H, H_{arom}) 5.61 (dd, $^3J_{1\text{-}H,2\text{-}H}$ = 9.3 Hz, 1 H, 1-H), 5.36 (t, $^3J_{3\text{-}H,4\text{-}H}$ = 9.6 Hz, 1 H, 3-H), 5.16–5.04 (m, 2 H, 2-H, 4-H), 4.31 (dd, $^3J_{5\text{-}H,6\text{-}H}$ = 4.5 Hz, $^2J_{6\text{-}H,6'\text{-}H}$ = 12.6 Hz, 1 H, 6-H), 4.06 (dd, $^3J_{5\text{-}H,6'\text{-}H}$ = 2.1 Hz, 1 H, 6´-H), 3.88 (ddd, $^3J_{4\text{-}H,5\text{-}H}$ = 10.2 Hz, 1 H, 5-H), 3.84 (s, 3 H, OCH_3), 2.00, 1.99, 1.97 and 1.94 (4 × s, 12 H, CH_3CO) ppm; **^{13}C NMR**(75.47 MHz, DMSO-d_6, 25 ºC): δ = 178.4 (C=S), 170.0, 169.6, 169.5 and 169.3 (C=O), 159.6 (*C*–OMe), 143.5 (CH=N), 135.1, 129.8, 120.8, 116.5 and 111.5 (C_{arom}), 81.4 (1-C), 72.6 (3-C), 72.1 (2-C), 70.7 (5-C), 67.9 (4-C), 61.7 (6-C), 20.6, 20.4, 20.4 and 20.3 (*C*H_3CO) ppm. R_f (Hex/EtOAc 1:1) = 0.47. $[\alpha]_D$ = -102(CH_3Cl; c = 1.07). Anal. calcd. for $C_{23}H_{29}N_3O_{10}S{\cdot}5H_2O$ (629.63): C, 43.87; H, 6.24; N, 6.67. Found.(%): C, 44.14; H, 6.66; N, 6.93.

4-Methoxy-benzaldehyde *N*(4)-(2,3,4,6-tetra-*O*-acetyl-β-D-glucopyranosyl) thiosemicarbazone (L_{17})

IR(KBr): *v* 3312, 3272, 2975, 1749, 1602, 1541, 1514, 1502, 1371, 1301, 1229, 1169, 1192, 1035, 977, 920, 822, 773, 629, 609, 564, 534 cm^{-1}; **^{1}H NMR**($CDCl_3$): (300.13 MHz, $CDCl_3$, 25 ºC): δ = 9.78 (s, 1 H, N(2)H), 8.26 (d, $^3J_{1\text{-H,N(4)H}}$ = 8.7 Hz, 1 H, N(4)H), 7.70 (s, 1 H, CH=N), 7.65 (d, *J* = 9.0 Hz, 2 H, H_{arom}), 6.95 (d, *J* = 8.7 Hz, 2 H, H_{arom}), 5.72 (dd, $^3J_{1\text{-H,2-H}}$ = 9.3 Hz, 1 H, 1-H), 5.40 (dd, $^3J_{3\text{-H,4-H}}$ = 9.6 Hz, 1 H, 3-H), 5.21–5.10 (m, 2 H, 2-H, 4-H), 4.38 (dd, $^3J_{5\text{-H,6-H}}$ = 4.5 Hz, $^2J_{6\text{-H,6´-H}}$ = 12.6 Hz, 1 H, 6-H), 4.14 (dd, $^3J_{5\text{-H,6´-H}}$ = 1.8 Hz, 1 H, 6´-H), 3.90 (ddd, $^3J_{4\text{-H,5-H}}$ = 10.2 Hz, 1 H, 5-H), 3.84 (s, 3 H, OCH_3), 2.08, 2.04, 2.03 and 2.02 (4 × s, 12 H, CH_3CO) ppm; **^{13}C NMR**(75.47 MHz, $CDCl_3$, 25 ºC): δ = 178.3 (C=S), 170.9, 170.7, 169.9 and 169.5 (C=O), 161.8 (*C*–OMe), 143.9 (CH=N), 129.6, 125.5 and 114.4 (C_{arom}), 82.2 (1-C), 73.5 (3-C), 72.7 (2-C), 70.5 (5-C), 68.3 (4-C), 61.6 (6-C), 20.7, 20.6 and 20.6 (*C*H_3CO) ppm. R_f (Hex/EtOAc 1:1) = 0.34. $[\alpha]_D$ = -83(CH_3Cl; c = 1). Anal. calcd. for $C_{23}H_{29}N_3O_{10}S$(539.56): C, 51.20; H, 5.42; N, 7.79. Found.(%): C, 50.94; H, 5.67; N, 8.02.

4-Methyl-benzaldehyde *N*(4)-(2,3,4,6-tetra-*O*-acetyl-β-D-glucopyranosyl) thiosemicarbazone (L_{18})

IR(KBr): *v* 3314, 3291, 2991, 1741, 1607, 1553, 1501, 1370, 1224, 1093, 1043, 978, 933, 830 771, 700, 629, 599, 534 cm^{-1}; **^{1}H NMR** (300.13 MHz, $CDCl_3$, 25 ºC): δ = 9.73 (s, 1 H, N(2)H), 8.25 (d, $^3J_{1\text{-H,N(4)H}}$ = 8.7 Hz, 1 H, N(4)H), 7.77 (s, 1 H, CH=N), 7.60 (d, *J* = 8.1 Hz, 2 H, H_{arom}), 7.25 (d, *J* = 7.8 Hz, 2 H, H_{arom}), 5.72 (dd, $^3J_{1\text{-H,2-H}}$ = 9.3 Hz, 1 H, 1-H), 5.41 (t, $^3J_{3\text{-H,4-H}}$ = 9.6 Hz, 1 H, 3-H), 5.21–5.10 (m, 2 H, 2-H, 4-H), 4.34 (dd, $^3J_{5\text{-H,6-H}}$ = 4.5 Hz, $^2J_{6\text{-H,6´-H}}$ = 12.3 Hz, 1 H, 6-H), 4.11 (dd, $^3J_{5\text{-H,6´-H}}$ = 1.8 Hz, 1 H, 6´-H), 3.89 (ddd, $^3J_{4\text{-H,5-H}}$ = 10.2 Hz, 1 H, 5-H), 2.38 (s, 3 H, CH_3–Ar), 2.10, 2.08, 2.04 and 2.03 (4 × s, 12 H, CH_3CO) ppm; **^{13}C NMR**(75.47 MHz, DMSO-d_6, 25 ºC): δ = 178.1 (C=S), 170.0, 169.5, 169.5 and 169.4 (C=O), 143.9 (*C*H_3–Ar), 140.2 (CH=N), 131.0, 129.3 and 127.6 (C_{arom}), 81.4 (1-C), 72.7 (3-C), 72.2 (2-C), 69.9 (5-C), 67.9 (4-C), 61.8 (6-C), 20.5, 20.4 20.4 and 20.4 (*C*H_3CO) ppm. R_f (Hex/EtOAc 1:1) = 0.43. $[\alpha]_D$ = -77.6(CH_3Cl; c = 1.03). Anal. calcd. for $C_{23}H_{29}N_3O_9S{\cdot}2H_2O$: C, 49.37; H, 5.94; N, 7.51. Found.(%): C, 48.88; H, 6.24; N, 7.87.

4-*tert*-Buthyl-benzaldehyde *N*(4)-(2,3,4,6-tetra-*O*-acetyl-β-D-glucopyranosyl) thiosemicarbazone (L_{19})

IR(KBr): *v* 3343, 3326, 2958, 1749, 1609, 1533, 1485, 1425, 1364, 1218, 1110, 1093, 1047, 916, 826 708, 628, 559, 530 cm^{-1}; **^{1}H NMR** (300.13 MHz, $CDCl_3$, 25 ºC): δ = 10.26 (s, 1 H, N(2)H), 8.29 (d, $^3J_{1\text{-H,N(4)H}}$ = 8.7 Hz, 1 H, N(4)H), 7.85 (s, 1 H, CH=N), 7.65 (d, J = 8.1 Hz, 2 H, H_{arom}), 7.44 (d, J = 8.4 Hz, 2 H, H_{arom}), 5.71 (dd, $^3J_{1\text{-H,2-H}}$ = 9.0 Hz, 1 H, 1-H), 5.40 (dd, $^3J_{3\text{-H,4-H}}$ = 9.6 Hz, 1 H, 3-H), 5.21–5.09 (m, 2 H, 2-H, 4-H), 4.37 (dd, $^3J_{5\text{-H,6-H}}$ = 4.5 Hz, $^2J_{6\text{-H,6´-H}}$ = 12.6 Hz, 1 H, 6-H), 4.12 (dd, $^3J_{5\text{-H,6´-H}}$ = 2.1 Hz, 1 H, 6´-H), 3.92 (ddd, $^3J_{4\text{-H,5-H}}$ = 10.2 Hz, 1 H, 5-H), 2.07, 2.04, 2.03 and 2.01 (4 × s, 12 H, CH_3CO), 1.32 (s, 9 H, CH_3(*t*Bu)) ppm; **^{13}C NMR**($CDCl_3$): (75.47 MHz, $CDCl_3$, 25 ºC): δ = 178.7 (C=S), 170.9, 170.7, 169.9 and 169.6 (C=O), 154.4 (C_{arom}–*t*Bu), 143.9 (CH=N), 130.1, 127.5 and 125.9 (C_{arom}), 82.2 (1-C), 73.4 (3-C), 72.7 (2-C), 70.4 (5-C), 68.3 (4-C), 61.6 (6-C), 34.9 (*C*Me_3), 31.1 (*C*H_3(*t*Bu)), 20.8, 20.6 and 20.6 (*C*H_3CO) ppm. R_f (Hex/EtOAc 1:1) = 0.64. $[\alpha]_D$ = -77.7(CH_3Cl; c = 1.27). Anal. calcd. for $C_{26}H_{35}N_3O_9S$(565.64): C, 55.21; H, 6.24; N, 7.43. Found.(%): C, 55.35; H, 6.66; N, 7.84.

2-Pyridinecarboxaldehyde *N*(4)-(2,3,4,6-tetra-*O*-acetyl-β-D-glucopyranosyl) thiosemicarbazone (L_{20})

IR(KBr): *v* 3555, 3328, 3279, 2967, 1741, 1631 1591, 1529, 1482, 1414, 1366, 1214, 1116, 1035, 901, 839, 704, 648, 610 cm^{-1}; **^{1}H NMR**(599.83 MHz, $CDCl_3$, 25 ºC): δ = 10.14 (s, 1 H, N(2)H), 8.60 (d, J = 4.2 Hz, 1 H, 3'-H), 8.45 (d, $^3J_{1\text{-H,N(4)H}}$ = 8.7 Hz, 1 H, N(4)H), 8.04 (d, J = 7.8 Hz, 1 H, 6'-H), 7.96 (s, 1 H, CH=N), 7.79-7.74 (m, 1 H, 5'-H), 7.33-7.28 (m, 1 H, 4'-H), 5.72 (dd, $^3J_{1\text{-H,2-H}}$ = 9.0 Hz, 1 H, 1-H), 5.41 (t, $^3J_{3\text{-H,4-H}}$ = 9.6 Hz, 1 H, 3-H), 5.21–5.10 (m, 2 H, 2-H, 4-H), 4.37 (dd, $^3J_{5\text{-H,6-H}}$ = 4.5 Hz, $^2J_{6\text{-H,6´-H}}$ = 12.6 Hz, 1 H, 6-H), 4.12 (dd, $^3J_{5\text{-H,6´-H}}$ = 1.8 Hz, 1 H, 6´-H), 3.90 (ddd, $^3J_{4\text{-H,5-H}}$ = 10.2 Hz, 1 H, 5-H), 2.11, 2.08, 2.04 and 2.03 (4 × s, 12 H, CH_3)ppm; **^{13}C NMR**(150.84 MHz, $CDCl_3$, 25 ºC): δ = 179.4 (C=S), 171.1, 170.7, 169.9 and 169.6 (C=O), 152.2 and 149.5 (C_{arom}), 140.5 (CH=N), 136.9, 124.6 and 121.1 (C_{arom}), 82.2 (1-C), 73.5 (3-C), 72.7 (2-C), 70.6 (5-C), 68.3 (4-C), 61.6 (6-C), 20.8, 20.7, 20.6 and 20.6 (CH_3) ppm. R_f (Hex/EtOAc 1:3) = 0.17; ΔH = 27.69J/g. $[\alpha]_D$ = -66.9(CH_3Cl; c = 1.23). Anal. calcd. for $C_{21}H_{26}N_4O_9S$(510.52): C, 49.41; H, 5.13; N, 10.97. Found.(%): C, 49.82; H, 5.45; N, 11.12.

3-Pyridinecarboxaldehyde *N*(4)-(2,3,4,6-tetra-*O*-acetyl-β-D-glucopyranosyl) thiosemicarbazone (L_{21})

IR(KBr): *v* 3320, 3261, 2950, 1745, 1533, 1467, 1434, 1364, 1152, 1007, 1211, 1031, 951, 928, 826, 743, 678, 601, 537 cm^{-1}; **^{1}H NMR**(300.13 MHz, $CDCl_3$, 25 ºC): δ = 10.49 (s, 1 H, N(2)H), 8.81 (d, *J* = 1.8 Hz, 1 H, H_{arom}), 8.64 (dd, *J* = 1.5 Hz, *J* = 4.8 Hz, 1 H, H_{arom}), 8.34 (d, $^3J_{1\text{-}H,N(4)H}$ = 9.0 Hz, 1 H, N(4)H), 8.16 (dt, *J* = 1.8 Hz, *J* = 7.8 Hz, 1 H, H_{arom}), 7.89 (s, 1 H, CH=N), 7.37 (dd, *J* = 1.8 Hz, *J* = 7.8 Hz, 1 H, H_{arom}), 5.68 (dd, $^3J_{1\text{-}H,2\text{-}H}$ = 9.3 Hz, 1 H, 1-H), 5.41 (t, $^3J_{3\text{-}H,4\text{-}H}$ = 9.6 Hz, 1 H, 3-H), 5.18–5.09 (m, 2 H, 2-H, 4-H), 4.37 (dd, $^3J_{5\text{-}H,6\text{-}H}$ = 4.5 Hz, $^2J_{6\text{-}H,6'\text{-}H}$ = 12.6 Hz, 1 H, 6-H), 4.14 (dd, $^3J_{5\text{-}H,6'\text{-}H}$ = 1.8 Hz, 1 H, 6´-H), 3.90 (ddd, $^3J_{4\text{-}H,5\text{-}H}$ = 10.2 Hz, 1 H, 5-H), 2.09, 2.07, 2.04 and 2.02 (4 × s, 12 H, CH_3) ppm; **^{13}C NMR**((75.47 MHz, $CDCl_3$, 25 ºC): δ = 179.1 (C=S), 171.1, 170,7, 169.9 and 169.6 (C=O), 151.3 and 149.5 (C_{arom}), 140.3 (CH=N), 133.7, 129.2 and 124.0 (C_{arom}), 82.2 (1-C), 73.5 (3-C), 72.5 (2-C), 70.6 (5-C), 68.3 (4-C), 61.6 (6-C), 20.7, 20.7 and 20.6 (CH_3) ppm. R_f (Hex/EtOAc 1:3) = 0.16. $[\alpha]_D$ = -82.2(CH_3Cl; c = 1). Anal. calcd. for $C_{21}H_{26}N_4O_9S$(510.52): C, 49.41; H, 5.13; N, 10.97. Found.(%): C, 49.86; H, 4.98; N, 11.15.

4-Pyridinecarboxaldehyde *N*(4)-(2,3,4,6-tetra-*O*-acetyl-β-D-glucopyranosyl) thiosemicarbazone (L_{22})

IR(KBr): *v* 3589, 3329, 3296, 2962, 1737, 1612, 1525, 1421, 1369, 1216, 1144, 1110, 1085, 1031, 896, 830, 736, 671, 602, 574, 534 cm^{-1}; **^{1}H NMR**(300.13 MHz, $CDCl_3$, 25 ºC): δ = 10.56 (s, 1 H, N(2)H), 8.69 (d, *J* = 5.4 Hz, 2 H, H_{arom}), 8.39 (d, $^3J_{1\text{-}H,N(4)H}$ = 8.7 Hz, 1 H, N(4)H), 7.81 (s, 1 H, CH=N), 7.62 (d, *J* = 5.4 Hz, 2 H, H_{arom}), 5.64. (dd, $^3J_{1\text{-}H,2\text{-}H}$ = 9.0 Hz, 1 H, 1-H), 5.41 (t, $^3J_{3\text{-}H,4\text{-}H}$ = 9.6 Hz, 1 H, 3-H), 5.19–5.09 (m, 2 H, 2-H, 4-H) 4.35 (dd, $^3J_{5\text{-}H,6\text{-}H}$ = 4.5 Hz, $^2J_{6\text{-}H,6'\text{-}H}$ = 12.6 Hz, 1 H, 6-H), 4.10 (dd, $^3J_{5\text{-}H,6'\text{-}H}$ = 2.1 Hz, 1 H, 6´-H), 3.90 (ddd, $^3J_{4\text{-}H,5\text{-}H}$ = 10.2 Hz, 1 H, 5-H), 2.09, 2.08, 2.04 and 2.03 (4 × s, 12 H, CH_3) ppm; **^{13}C NMR**(75.47 MHz, $CDCl_3$, 25 ºC): δ = 179.4 (C=S), 171.3, 170.7, 169.9 and 169.6 (C=O), 150.0 (C_{arom}), 140.7 (CH=N), 140.5 and 121.4 (C_{arom}), 82.2 (1-C), 73.5 (3-C), 72.5 (2-C), 70.6 (5-C), 68.3 (4-C), 61.6 (6-C), 20.8, 20.7, 20.7 and 20.6 (CH_3) ppm. R_f (Hex/EtOAc 1:2) = 0.14. $[\alpha]_D$ = -93(CH_3Cl; c = 1.07). Anal. calcd. for $C_{21}H_{26}N_4O_9S{\cdot}3H_2O$(564.56): C, 44.68; H, 5.72; N, 9.92.Found.(%): C, 45.09; H, 5.83; N, 10.14.

1-Ferrocenecarboxaldehyde *N*(4)-(2,3,4,6-tetra-*O*-acetyl-β-D-glucopyranosyl) thiosemicarbazone (L_{23})

IR(KBr): *v* 3322, 3089, 1725, 1604, 1525, 1508, 1434, 1365, 1299, 1248, 1214, 1107, 1035, 961, 912, 820, 765, 657, 643, 597, 577, 561, 547 cm^{-1}; **^{1}H NMR**(300.13 MHz, DMSO-d_6, 25 ºC): δ = 11.72 (s, 1 H, N(2)H), 8.38 (d, $^3J_{1\text{-}H,N(4)H}$ = 9.0 Hz, 1 H, N(4)H), 7.93 (s, 1 H, CH=N), 5.87 (dd, $^3J_{1\text{-}H,2\text{-}H}$ = 9.3 Hz, 1 H, 1-H), 5.42 (t, $^3J_{3\text{-}H,4\text{-}H}$ = 9.6 Hz, 1 H, 3-H), 5.26 (t, *J* = 9.3 Hz, 1 H, 2-H), 4.96 (dd, $^3J_{3\text{-}H,4\text{-}H}$ = 9.6 Hz, $^3J_{4\text{-}H,5\text{-}H}$ = 9.9 Hz, 1 H, 4-H), 4.84 (s, 1 H, Fc), 4.73 (s, 1 H, Fc), 4.49–4.45 (m, 2 H, Fc), 4.22 (s, 5 H, Fc), 4.20 (dd, $^3J_{5\text{-}H,6'\text{-}H}$ = 4.2 Hz, 1 H, 6´-H), 4.06 (ddd, $^3J_{5\text{-}H,6\text{-}H}$ = 1.8 Hz, 1 H, 5-H), 3.97 (dd, $^2J_{6\text{-}H,6'\text{-}H}$ = 12.3 Hz, 1 H, 6-H), 2.01, 2.00, 1.97 and 1.96 (4 × s, 12 H, CH_3) ppm; **^{13}C NMR**(75.47 MHz, DMSO-d_6, 25 ºC): δ = 177.0 (C=S), 170.0, 169.6, 169.5 and 169.3 (C=O), 145.0 (CH=N), 81.2 (1-C), 78.3 (*C*(Fc)–CH=N), 72.5 (3-C), 72.1 (2-C), 70.7 (5-C), 70.3 (Fc), 69.0 (Fc), 68.1 (4-C), 67.9, 67.6 and 64.4 (Fc), 61.7 (6-C), 20.6, 20.4, 20.4 and 20.3 (CH_3) ppm. R_f (Hex/EtOAc 1:1) = 0.5. Anal. calcd. for $C_{26}H_{31}FeN_3O_9S$(617.45): C, 50.58; H, 5.06; N, 6.81. Found.(%): C, 50.78; H, 4.65; N, 7.03.

β-Naphthalenecarboxaldehyde *N*(4)-(2,3,4,6-tetra-*O*-acetyl-β-D-glucopyranosyl) thiosemicarbazone (L_{24})

IR(KBr): *v* 3450, 3322, 2950, 1753, 1533, 1500, 1428, 1357, 1214, 1111, 1100, 1035, 915, 904, 843, 830, 819, 741, 652, 589, 521 cm^{-1} **^{1}H NMR**(300.13 MHz, $CDCl_3$, 25 ºC): δ = 10.41 (s, 1 H, N(2)H), 8.38 (d, $^3J_{1\text{-}H,N(4)H}$ = 8.7 Hz, 1 H, N(4)H), 7.98 (d, *J* = 5.4 Hz, 3 H, H_{naphth}), 7.83 (d, *J* = 9.3 Hz, 2 H, H_{naphth}), 7.82 (s, 1 H, CH=N), 7.49-7.52 (m, 2 H, H_{naphth}), 5.72 (dd, $^3J_{1\text{-}H,2\text{-}H}$ = 9.3 Hz, 1 H, 1-H), 5.41 (t, $^3J_{2\text{-}H,3\text{-}H}$ = 9.3 Hz, 1 H, 3-H), 5.25–5.10 (m, 2 H, 2-H, 4-H), 4.37 (dd, $^3J_{5\text{-}H,6\text{-}H}$ = 4.5 Hz, $^2J_{6\text{-}H,6'\text{-}H}$ = 12.6 Hz, 1 H, 6-H), 4.12 (dd, $^3J_{5\text{-}H,6'\text{-}H}$ = 1.8 Hz, 1 H, 6´-H), 3.91 (ddd, $^3J_{4\text{-}H,5\text{-}H}$ = 10.2 Hz, 1 H, 5-H), 2.08, 2.06 and 2.04 and 2.03 (4 × s, 12 H, CH_3) ppm; **^{13}C NMR**(75.47 MHz, $CDCl_3$, 25 ºC): δ = 178.9 (C=S), 171.0, 170.8, 170.0 and 169.7 (C=O), 144.3 (CH=N), 134.5, 133.0, 130.7, 129.9, 128.8, 128.4, 127.9, 127.4, 126.7 and 122.8 (C_{naphth}), 82.2 (1-C), 73.4 (3-C), 72.7 (2-C), 70.5 (5-C), 68.4 (4-C), 61.7 (6-C), 20.7, 20.7, 20.6 and 20.6 (CH_3) ppm. R_f (Hex/EtOAc 1:1) = 0.4. $[\alpha]_D$ = -116.7(CH_3Cl; c = 1.05). Anal. calcd. for $C_{26}H_{29}N_3O_9S{\cdot}2H_2O$ (595.62): C, 52.43; H, 5.58; N, 7.05. Found.(%): C, 52.12; H, 5.97; N, 6.65.

4-Methoxy-acetophenone *N*(4)-(2,3,4,6-tetra-*O*-acetyl-β-D-glucopyranosyl) thiosemicarbazone (L_{25})

IR(KBr): *v* 3330, 3282, 2950, 1741, 1603, 1529, 1479, 1417, 1367, 1219, 1182, 1098, 1035, 916, 856, 830, 805, 726, 652, 601, 571, 537 cm^{-1}; **^{1}H NMR**(300.13 MHz, $CDCl_3$, 25 ºC): δ = 8.81 (s, 1 H, N(2)H), 8.38 (d, $^3J_{1\text{-H,N(4)H}}$ = 9.0 Hz, 1 H, N(4)H), 7.78 (d, J = 9.0 Hz, 2 H, H_{arom}), 6.95 (d, J = 9.0 Hz, 2 H, H_{arom}), 5.76 (dd, $^3J_{1\text{-H,2-H}}$ = 9.3 Hz, 1 H, 1-H), 5.40 (t, $^3J_{3\text{-H,4-H}}$ = 9.6 Hz, 1 H, 3-H), 5.21–5.09 (m, 2 H, 2-H, 4-H), 4.36 (dd, $^3J_{5\text{-H,6-H}}$ = 4.5 Hz, $^2J_{6\text{-H,6´-H}}$ = 12.6 Hz, 1 H, 6-H), 4.14 (dd, $^3J_{5\text{-H,6´-H}}$ = 2.1 Hz, 1 H, 6´-H), 3.90 (ddd, $^3J_{4\text{-H,5-H}}$ = 10.2 Hz, 1 H, 5-H), 3.85 (s, 3 H, OCH_3), 2.23 (s, 3 H, CH_3C=N), 2.08, 2.04 and 2.02 (3 × s, 12 H, CH_3CO) ppm; **^{13}C NMR**(75.47 MHz, DMSO-d_6, 25 ºC): δ = 179.1 (C=S), 170.1, 169.9, 169.7 and and 169.5 (C=O), 160.7 (C_{arom}–O), 149.9 (C=N), 130.6, 129.8, 128.6, 113.6 and 113.5 (C_{arom}), 81.4 (1-C), 72.6 (3-C), 72.3 (2-C), 71.0 (5-C), 68.2 (4-C), 61.9 (6-C), 55.3 (OCH_3), 20.7, 20.7, 20.6 and 20.5 (CH$_3$CO), 14.5 (CH$_3$C=N) ppm. R_f (Hex/EtOAc 1:2) = 0.64. $[\alpha]_D$ = -48.1(CH_3Cl; c = 1.05). Anal. calcd. for $C_{24}H_{31}N_3O_{10}S{\cdot}3H_2O$(607.63): C, 47.44; H, 6.14; N, 6.92. Found.(%): C, 47.12; H, 5.98; N, 6.55.

2-Acetonaphthanone *N*(4)-(2,3,4,6-tetra-*O*-acetyl-β-D-glucopyranosyl) thiosemicarbazone (L_{26})

IR(KBr): *v* 3325, 3302, 2950, 1741, 1529, 1483, 1368, 1218, 1147, 1094, 1035, 942, 916, 857, 835, 750, 718, 665, 593, 565 cm^{-1}; **^{1}H NMR**(300.13 MHz, $CDCl_3$, 25 ºC): δ = 9.18 (s, 1 H, N(2)H), 8.50 (d, 1 H, $^3J_{1\text{-H,N(4)H}}$ = 8.7 Hz, 1 H, N(4)H), 8.17 (s, 1 H, H_{naphth}), 8.05 (dd, J = 1.8 Hz, J = 8.7 Hz, 1 H, H_{naphth}), 7.93–7.83 (m, 3 H, H_{naphth}), 7.53–7.50 (m, 2 H, H_{naphth}), 5.76 (dd, $^3J_{1\text{-H,2-H}}$ = 9.0 Hz, 1 H, 1-H), 5.43 (t, $^3J_{2\text{-H,3-H}}$ = 9.6 Hz, 1 H, 3-H), 5.26–5.11 (m, 2 H, 2-H, 4-H), 4.34 (dd, $^3J_{5\text{-H,6-H}}$ = 4.5 Hz, $^2J_{6\text{-H,6´-H}}$ = 12.6 Hz, 1 H, 6-H), 4.12 (dd, $^3J_{5\text{-H,6´-H}}$ = 2.1 Hz, 1 H, 6´-H), 3.92 (ddd, $^3J_{4\text{-H,5-H}}$ = 10.2 Hz, H, 5-H), 2.38 (s, 3 H, CH_3C=N), 2.08, 2.06 and 2.05 (3 × s, 12 H, CH_3CO) ppm; **^{13}C NMR**(75.47 MHz, $CDCl_3$, 25 ºC): δ = 179.6 (C=S), 171.0, 170.8, 169.9 and 169.6 (C=O), 148.0 (C=N), 134.1, 134.0, 133.0, 128.7, 128.3, 127.6, 127.2, 126.9, 126.5 and 123.4 (C_{naphth}), 82.3 (1-C), 73.5 (3-C), 72.7 (2-C), 70.5 (5-C), 68.4 (4-C), 61.6 (6-C), 20.7, 20.7 and 20.6 (CH$_3$CO), 13.2 (CH$_3$C=N) ppm. R_f (Hex/EtOAc 1:2) = 0.42. $[\alpha]_D$ = -61.5(CH_3Cl; c = 1.07). Anal. calcd. for $C_{27}H_{31}N_3O_9S{\cdot}3H_2O$ (627.66): C, 51.67; H, 5.94; N, 6.69. Found.(%): C, 52.01; H, 6.23; N, 6.67.

V.6. Synthesis of β-D-glucopyranosyl-modified thiosemicarbazones L'$_{1\text{-}26}$

General procedure: Sodium methoxide as a powder (7.5 mmol) was added to a solution of **L$_{1\text{-}26}$** (1.5 mmol) in dry methanol (20 mL). The reaction mixture was stirred at room temperature for 3 h and kept in fridge overnight. Then, the solution was neutralized with Amberlist-15 (or acetic acid for the compounds **L'$_6$**, **L'$_{21}$**, **L'$_{22}$** and **L'$_{23}$**) to remove the sodium ions, and the solvent was evaporated by vacuum at a temperature below 40 °C. Purification was carried out by recrystallization (methanol, methanol/water 1:1 or acetonitrile/water 1:1). The N–H stretching vibration in the FT-IR spectra of **L'$_{1\text{-}26}$** has not been determined as it was obscured by the broad absorption band of the hydroxyl group. The list of aldehyde/ketone 4-(β-D-glucopyranosyl)thiosemicarbazones are given in Fig. 82.

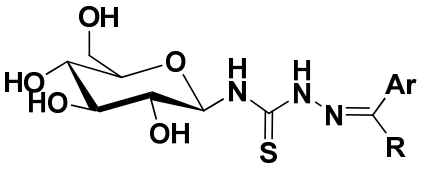

L'$_1$ R = H, Ar = -C_6H_4-F-*p*;
L'$_2$ R = H, Ar = -C_6H_4-Cl-*o*;
L'$_3$ R = H, Ar = -C_6H_4-Cl-*m*;
L'$_4$ R = H, Ar = -C_6H_4-Cl-*p*;
L'$_5$ R = H, Ar = -C_6H_4-Br-*o*;
L'$_6$ R = H, Ar = -C_6H_4-Br-*m*;
L'$_7$ R = H, Ar = -C_6H_4-Br-*p*;
L'$_8$ R = H, Ar = -C_6H_4-CF_3-*p*;
L'$_9$ R = H, Ar = -C_6H_4-NO_2-*o*;
L'$_{10}$ R = H, Ar = -C_6H_4-NO_2-*m*;
L'$_{11}$ R = H, Ar = -C_6H_4-NO_2-*p;*
L'$_{12}$ R = H, Ar = -C_6H_4-OH-*o*;
L'$_{13}$ R = H, Ar = -C_6H_4-OH-*m*;
L'$_{14}$ R = H, Ar = -C_6H_4-OH-*p*;
L'$_{15}$ R = H, Ar = -C_6H_4-OMe-*o*;
L'$_{16}$ R = H, Ar = -C_6H_4-OMe-*m*;
L'$_{17}$ R = H, Ar = -C_6H_4-OMe_3-*p*;
L'$_{18}$ R = H, Ar = -C_6H_4-Me-*p*;
L'$_{19}$ R = H, Ar = -C_6H_4-*t*Bu-*p*;
L'$_{20}$ R = H, Ar = -2-pyridyl;
L'$_{21}$ R = H, Ar = -3-pyridyl;
L'$_{22}$ R = H, Ar = -4-pyridyl;
L'$_{23}$ R = H, Ar = -ferrocenyl;
L'$_{24}$ R = H, Ar = -β-naphthyl;
L'$_{25}$ R = CH_3, Ar = -C_6H_4-Me-*p*;
L'$_{26}$ R = CH_3, Ar = -β-naphthyl;

Figure 82 Aldehyde/ketone 4-(β-D-glucopyranosyl)thiosemicarbazones

Table 22 below includes experimental details for the target molecules **L'$_{1\text{-}26}$**.

Table 22 *Aldehyde/ketone 4-(β-D-glucopyranosyl)thiosemicarbazones – Reaction conditions and physical properties.*

Ligand	t [h]	Recrystalization	Color	Yield (%)	M.p. [°C][a]
L_1	4	MeOH/H_2O (1:1)	white	74	171-175
L_2	3	MeOH/H_2O (1:1)	white	50	204-208
L_3	2	MeOH/H_2O (1:1)	colorless	71	190-193
L_4	0.5	MeOH/H_2O (1:1)	white	53	169-171
L_5	2	MeOH/H_2O (1:1)	white	78	216-217
L_6	3	MeOH/H_2O (1:1)	white	70	190-192
L_7	4	MeOH/H_2O (1:1)	white	78	202-206
L_8	3	acetone/H_2O (1:1)	white	76	160-165
L_9	2	MeOH	yellow	55	194-198
L_{10}	4	MeOH/Et_2O (1:1)	yellow	70	201-205
L_{11}	4	MeOH/Et_2O (1:1)	yellow	39	213-215
L_{12}	2	MeOH/H_2O (1:2)	white	92	hygroscopic
L_{13}	3	MeOH	white	74	188-194
L_{14}	3	$MeOH_{hot}$	white	76	163-168
L_{15}	2	MeOH/H_2O (1:1)	yellow	63	172-175
L_{16}	3	MeOH/H_2O (1:1)	white	77	184-187
L_{17}	4	MeOH/acetone	white	68	187-190
L_{18}	3	MeOH/H_2O (1:1)	creme	62	182-185
L_{19}	3	THF/H_2O (5:1)	white	72	123-125
L_{20}	2	MeOH/acetone (1:1)	white	85	179-182
L_{21}	3	AcCN/H_2O (1:1)	yellow	86	199-201
L_{22}	2	MeOH/Et_2O (1:1)	yellow	33	201-205
L_{23}	4	iso-Pr/H_2O (2:1)	red	74	85-91
L_{24}	3	MeOH	white	67	218-222
L_{25}	2½	MeOH	yellow	60	127-131
L_{26}	2	MeOH/H2O (1:1)	white	77	182-185

[a] with descomposition

Analytical data

4–Fluorobenzaldehyde *N*(4)-(β-D-glucopyranosyl)thiosemicarbazone) (L'$_1$)

IR(KBr): *v* 3596, 3299, 3222, 2877, 1601, 1545, 1504, 1417, 1377, 1322, 1233, 1207, 1161, 1117, 1096, 1072, 1022, 986, 904, 888, 830, 785,745, 623 cm^{-1}; **^{1}H NMR**(300.13 MHz, DMSO-d_6, 25 ºC): δ = 11.75 (s, 1 H, N(2)H), 8.60 (d, $^3J_{1\text{-H,N(4)H}}$ = 9.0 Hz, 1 H, N(4)H), 8.10 (s, 1 H, CH=N), 7.96-7.91 (m, 2 H, H_{arom}), 7.29–7.23 (m, 2 H, H_{arom}), 5.39 (dd, $^3J_{1\text{-H,2-H}}$ = 9.0 Hz, 1 H, 1-H), 5.03–4.94 (m, 2 H, OH), 4.50 (s, 1 H, OH), 3.65 (dd, $^3J_{5\text{-H,6-H}}$ = 5.4 Hz, $^2J_{6\text{-H,6´-H}}$ = 11.4 Hz, 1 H, 6-H), 3.53–3.14 (m, 5 H, 2-H, 3-H, 4-H, 5-H, 6´-H) ppm; **^{13}C NMR**(75.47 MHz, DMSO-d_6, 25 ºC): δ = 178.6 (C=S), 141.8 (CH=N), 164.8, 161.5, 130.6, 129.8, 115.9 and 115.6 (C_{arom}), 84.0 (1-C), 78.7 (3-C), 77.6 (2-C), 71.9 (5-C), 69.8 (4-C), 60.8 (6-C) ppm. R_f ($CHCl_3$/MeOH 5:1) = 0.45. $[\alpha]_D$ = +52.9(MeOH; c = 1.1). Anal. calcd. for $C_{14}H_{18}FN_3O_5S{\cdot}5H_2O$ (359.37): C, 37.41; H, 6.28; N, 9.35. Found.(%): C, 37.87; H, 5.98; N, 9.56.

2–Chlorobenzaldehyde *N*(4)-(β-D-glucopyranosyl)thiosemicarbazone) (L'$_2$)

IR(KBr): *v* 3525, 3388, 3249, 2873, 1595, 1537,1469, 1444, 1376, 1287, 1261, 1206, 1170, 1112, 1081, 1039, 987, 949, 916, 883, 830, 752, 710, 604, 556 cm^{-1}; **^{1}H NMR** (300.13 MHz, DMSO-d_6, 25 ºC): δ = 11.93 (s, 1 H, N(2)H), 8.66 (d, $^3J_{1\text{-H,N(4)H}}$ = 9.0 Hz, 1 H, N(4)H), 8.53 (s, 1 H, CH=N), 8.36 (d, *J* = 7.5 Hz, 1 H, H_{arom}), 7.52–7.36 (m, 3 H, H_{arom}), 5.39 (dd, $^3J_{1\text{-H,2-H}}$ = 9.0 Hz, 1 H, 1-H), 5.03–5.00 (m, 2 H, OH), 4.91 (s, 1 H, OH), 4.50 (t, ^3J = 5.6 Hz, 1 H, OH), 3.66 (dd, $^3J_{5\text{-H,6-H}}$ = 5.4 Hz, $^2J_{6\text{-H,6´-H}}$ = 11.4 Hz, 1 H, 6-H), 3.55–3.14 (m, 5 H, 2-H, 3-H, 4-H, 5-H, 6´-H) ppm; **^{13}C NMR**(75.47 MHz, DMSO-d_6, 25 ºC): δ = 178.8 (C=S), 138.9 (CH=N), 133.2, 131.4, 131.2, 129.8, 127.7 and 127.3 (C_{arom}), 84.1 (1-C), 78.7 (3-C), 77.6 (2-C), 71.9 (5-C), 69.8 (4-C), 60.8 (6-C) ppm. R_f ($CHCl_3$/MeOH 5:1) = 0.40. $[\alpha]_D$ = +41.4(MeOH; c = 1). Anal. calc. for $C_{14}H_{18}ClN_3O_5S$(447.89): C, 37.54; H, 5.85; N, 9.38. Found.(%): C, 37.68, H, 5.46, N, 9.03.

3–Chlorobenzaldehyde *N*(4)-(β-D-glucopyranosyl)thiosemicarbazone) (L'$_3$)

IR(KBr): *v* 3359, 3209, 3032, 2926, 1644, 1537, 1508, 1471, 1431, 1376, 1295, 1237, 1168, 1112, 1075, 1035, 981, 930, 892, 830, 784, 705, 681, 661, 602, 554 cm^{-1}; **^{1}H NMR**(300.13 MHz,

DMSO-d_6, 25 ºC): δ = 11.82 (s, 1 H, N(2)H), 8.75 (d, $^3J_{1\text{-H,N(4)H}}$ = 8.7 Hz, 1 H, N(4)H), 8.08 (s, 2 H, CH=N and H_{arom}), 7.71 (s, 1 H, H_{arom}), 7.46 (s, 2 H, H_{arom}), 5.40 (dd, $^3J_{1\text{-H,2-H}}$ = 9.0 Hz, 1 H, 1-H), 5.02 (s, 2 H, OH), 4.90 (s, 1 H, OH), 4.49 (s, 1 H, OH), 3.65 (dd, $^3J_{5\text{-H,6-H}}$ = 3.9 Hz, $^2J_{6\text{-H,6´-H}}$ = 11.4 Hz, 1 H, 6-H), 3.56–3.15 (m, 5 H, 2-H, 3-H, 4-H, 5-H, 6´-H) ppm; **^{13}C NMR**(75.47 MHz, DMSO-d_6, 25 ºC): δ = 178.8 (C=S), 141.4 (CH=N), 136.2, 133.7, 130.5, 129.6, 126.8 and 126.3 (C_{arom}), 84.1 (1-C), 78.7 (3-C), 77.6 (2-C), 71.8 (5-C), 69.9 (4-C), 60.9 (6-C) ppm. R_f ($CHCl_3$/MeOH 5:1) = 0.45. $[\alpha]_D$ = +54.8(MeOH; c = 1.33). Anal. calcd. for $C_{14}H_{18}ClN_3O_5S{\cdot}5H_2O$ (465.90): C, 36.09; H, 6.06; N, 9.02. Found.(%): C, 35.78, H, 5.89, N, 8.95.

4–Chlorobenzaldehyde *N*(4)-(β-D-glucopyranosyl)thiosemicarbazone) (L'$_4$) [252]

IR(KBr): *v* 3371, 3340, 3295, 2885, 1595, 1537, 14482, 1405, 1326, 1293, 1227, 1202, 1167, 1144, 1099, 1077, 1031, 976, 900, 886, 830, 810, 712, 649, 624, 595, 567 cm^{-1}; **^{1}H NMR**(300.13 MHz, DMSO-d_6, 25 ºC): δ = 11.78 (s, 1 H, N(2)H), 8.62 (d, $^3J_{1\text{-H,N(4)H}}$ = 9.0 Hz, 1 H, N(4)H), 8.09 (s, 1 H, CH=N), 7.90 (d, *J* = 8.4 Hz, 2 H, H_{arom}), 7.48 (d, *J* = 8.4 Hz, 2 H, H_{arom}), 5.38 (dd, $^3J_{1\text{-H,2-H}}$ = 9.3 Hz, 1 H, 1-H), 5.01–4.99 (m, 2 H, OH), 4.90–4.88 (m, 1 H, OH), 4.50–4.46 (m, 1 H, OH), 3.65 (dd, $^3J_{5\text{-H,6-H}}$ = 5.4 Hz, $^2J_{6\text{-H,6´-H}}$ = 11.4 Hz, 1 H, 6-H), 3.50–3.14 (m, 5 H, 2-H, 3-H, 4-H, 5-H, 6´-H) ppm; **^{13}C NMR**(75.47 MHz, DMSO-d_6, 25 ºC): δ = 178.5 (C=S), 142.6 (CH=N), 135.0, 132.7, 129.3 and 129.0 (C_{arom}), 83.9 (1-C), 78.4 (3-C), 77.2 (2-C), 71.8 (5-C), 69.7 (4-C), 60.8 (6-C) ppm. R_f ($CHCl_3$/MeOH 5:1) = 0.51. $[\alpha]_D$ = +55.5(MeOH; c = 1). Anal. calcd. for $C_{14}H_{18}ClN_3O_5S$(375.83): C, 44.74; H, 4.83; N, 11.18. Found.(%): C, 44.34; H, 5.12; N, 11.67.

2–Bromobenzaldehyde-(β- D-glucopyranosyl]thiosemicarbazone) L'$_5$

IR(KBr): *v* 3547, 3275, 2881, 1593, 1545, 1469, 1350, 1315, 1270, 1200, 1169, 1126, 1097, 1078, 1026, 994, 896, 830, 758, 649,555 cm^{-1}; **^{1}H NMR**(DMSO-d_6 δ 11.95 (s, 1 H, N(2)H), 8.69 (d, $^3J_{1\text{-H,N(4)H}}$ = 9.0 Hz, 1 H, N(4)H), 8.50 (s, 1 H, CH=N), 8.33 (d, *J* = 7.5Hz, 1 H, H_{arom}), 7.66 (d, *J* = 7.8Hz, 1 H, H_{arom}), 7.43 (t, *J* = 7.8Hz, 1 H, H_{arom}), 7.43 (t, *J* = 7.8Hz, 2 H, H_{arom}), 5.38 (dd, $^3J_{1\text{-H,2-H}}$ = 9.0 Hz, 1 H, 1-H), 5.00–4.90 (m, 2 H, OH), 4.50 (s, 1 H, OH), 3.64 (dd, $^3J_{5\text{-H,6-H}}$ = 3.9 Hz, $^2J_{6\text{-H,6´-H}}$ = 11.4 Hz, 1 H, 6-H), 3.51–3.14 (m, 5 H, 2-H, 3-H, 4-H, 5-H, 6´-H); **^{13}C NMR**(DMSO-d_6): δ = 179.2 (C=S), 141.8 (CH=N), 133.5; 133.2; 132.1; 128.5; 128.2; and 124.1 (C_{arom}), 84.5 (1-C), 79.1 (3-C), 78.0 (2-C), 72.3 (5-C), 70.3 (4-C), 61.3 (6-C) ppm. R_f ($CHCl_3$/MeOH 5:1) = 0.53. $[\alpha]_D$ =

+32(MeOH; c = 1). Anal. calcd**.** for $C_{14}H_{18}BrN_3O_5S\cdot 3H_2O$ (419.02): C, 35.45; H, 5.10; N, 8.86. Found: C, 35.42; H, 4.87; N, 8.45.

3–Bromobenzaldehyde-(β -D-glucopyranosyl]thiosemicarbazone) (L'_6)

IR(KBr): 3547, 3361, 3206, 2869, 1644, 1613, 1533, 1468, 1426, 1295, 1265, 1236, 1167, 1111, 1079, 1031, 980, 916, 890, 839, 782, 681, 659, 603, 554 cm^{-1}; **^{1}H NMR**(DMSO-d_6): δ 11.80 (s, 1 H, N(2)H), 8.72 (d, $^3J_{1\text{-H,N(4)H}}$ = 9.0 Hz, 1 H, N(4)H), 8.18 (s, 1 H, H_{arom}), 8.06 (s, 1 H, CH=N), 7.76 (d, J = 7.5Hz, 1 H, H_{arom}), 7.58 (d, J = 7.8Hz, 1 H, H_{arom}), 7.38 (dd, J = 7.5Hz, 7.8Hz, 1 H, H_{arom}), 5.39 (dd, $^3J_{1\text{-H,2-H}}$ = 9.3 Hz, 1 H, 1-H), 5.00; 4.90, 4.49 (3s, 3 H, OH), 3.67 (dd, $^3J_{5\text{-H,6-H}}$ = 5.4 Hz, $^2J_{6\text{-H,6´-H}}$ = 11.4 Hz, 1 H, 6-H), 3.58–3.14 (m, 5 H, 2-H, 3-H, 4-H, 5-H, 6´-H) ppm; **^{13}C NMR**(DMSO-d_6): δ = 179.2 (C=S), 141.8 (CH=N), 136.9; 133.0; 132.2; 129.6; 127.6; and 122.7 (C_{arom}), 84.6 (1-C), 79.2 (3-C), 78.1 (2-C), 72.2 (5-C), 70.3 (4-C), 61.3 (6-C) ppm. R_f ($CHCl_3$/MeOH 5:1) = 0.51. $[\alpha]_D$ = +49.5(MeOH; c = 1). Anal. calcd. for $C_{14}H_{18}BrN_3O_5S\cdot 3H_2O$ (419.02): C, 35.45; H, 5.10; N, 8.86. Found: C, 35.42; H, 4.87; N, 8.45.

4–Bromobenzaldehyde-(β- D-glucopyranosyl]thiosemicarbazone) (L'_7)

IR(KBr): *v* 3540, 3305, 3192, 2897, 1641, 1606, 1553, 1511, 1465, 1422, 1401, 1359, 1303, 1251, 1202, 1171, 1103, 1075, 1035, 989, 900, 882, 822, 721, 653, 629, 578, 554 cm^{-1}; **^{1}H NMR**(DMSO-d_6): δ 11.80 (s, 1 H, N(2)H), 8.62 (d, $^3J_{1\text{-H,N(4)H}}$ = 8.7 Hz, 1 H, N(4)H), 8.06 (s, 1 H, CH=N), 7.81 (d, 2 H, H_{arom}), 7.61 (d, 2 H, H_{arom}), 5.36 (dd, $^3J_{1\text{-H,2-H}}$ = 9.0 Hz, 1 H, 1-H), 5.02; 4.90, 4.49 (3s, 3 H, OH), 3.64 (dd, $^3J_{5\text{-H,6-H}}$ = 5.4 Hz, $^2J_{6\text{-H,6´-H}}$ = 11.4 Hz, 1 H, 6-H), 3.52–3.14 (m, 5 H, 2-H, 3-H, 4-H, 5-H, 6´-H) ppm; **^{13}C NMR**(DMSO-d_6): δ = 179.2 (C=S), 144.8 (CH=N), 153.3; 136.0; 130.9; 120.1; 118.5; and 114.3 (C_{arom}), 84.7 (1-C), 79.3 (3-C), 78.1 (2-C), 72.8 (5-C), 70.6 (4-C), 61.6 (6-C) ppm. R_f ($CHCl_3$/MeOH 5:1) = 0.46. $[\alpha]_D$ = +86.3(MeOH; c = 1). Anal. calcd. for $C_{14}H_{18}BrN_3O_5S$ (419.02): C, 40.01; H, 4.32; N, 10.00. Found(%): C, 39.78; H, 4.85; N, 10.03.

4–Trifluoromethyl-benzaldehyde *N*(4)-(β-D-glucopyranosyl)thiosemicarbazone) (L'$_8$)

IR(KBr): *v* 3546, 3322, 3300, 2893, 1636, 1541, 1501, 1415, 1322, 1267, 1230, 1167, 1111, 1066, 1035, 989, 900, 880, 826, 766, 723, 654, 594, 538 cm^{-1}; **^{1}H NMR**(300.13 MHz, DMSO-d_6, 25 ºC): δ = 11.92 (s, 1 H, N(2)H), 8.73 (d, $^3J_{1\text{-H,N(4)H}}$ = 9.0 Hz, 1 H, N(4)H), 8.16 (s, 1 H, CH=N), 8.09 (d, *J* = 8.1 Hz, 2 H, H_{arom}), 7.76 (d, *J* = 8.1 Hz, 2 H, H_{arom}), 5.40 (dd, $^3J_{1\text{-H,2-H}}$ = 9.0 Hz, 1 H, 1-H), 5.08 (br s, 2 H, OH), 4.96 (br s, 1 H, OH), 4.52 (br s, 1 H, OH), 3.66 (dd, $^3J_{5\text{-H,6-H}}$ = 5.4 Hz, $^2J_{6\text{-H,6´-H}}$ = 11.4 Hz, 1 H, 6-H), 3.51–3.17 (m, 5 H, 2-H, 3-H, 4-H, 5-H, 6´-H) ppm; **^{13}C NMR** (75.47 MHz, DMSO-d_6, 25 ºC): δ = 178.9 (C=S), 141.1 (CH=N), 138.0, 129.7, 129.3, 128.1, 125.5, 125.4 and 125.4 (C_{arom} and CF_3), 84.1 (1-C), 78.7 (3-C), 77.6 (2-C), 71.9 (5-C), 69.8 (4-C), 60.8 (6-C) ppm. R_f ($CHCl_3$/MeOH 5:1) = 0.44. $[\alpha]_D$ = +48.3(MeOH; c = 1). Anal. calcd. for $C_{15}H_{18}FN_3O_5S2H_2O$(445.41): C, 40.45; H, 4.98; N, 9.43. Found.(%): C, 40.22; H, 4.73; N, 9.83.

2–Nitrobenzaldehyde *N*(4)-(β-D-glucopyranosyl)thiosemicarbazone) (L'$_9$)

IR(KBr): *v* 3355, 3309, 2918, 1655, 1537, 1499, 1471, 1350, 1310, 1270, 1219, 1173, 1035, 1000, 896, 852, 822, 791, 748, 699, 663, 563, 540 cm^{-1}; **^{1}H NMR**(300.13 MHz, DMSO-d_6, 25 ºC): δ = 12.03 (s, 1 H, N(2)H), 8.68 (d, $^3J_{1\text{-H,N(4)H}}$ = 9.0 Hz, 1 H, N(4)H), 8.53 (s, 1 H, CH=N), 8.47 (dd, *J* = 1.5 Hz, *J* = 8.1 Hz, 1 H, H_{arom}), 7.79–7.74 (m, 1 H, H_{arom}), 7.68–7.62 (m, 1 H, H_{arom}), 5.39 (dd, $^3J_{1\text{-H,2-H}}$ = 9.3 Hz, 1 H, 1-H), 5.02–5.00 (m, 2 H, OH), 4.90–4.88 (m, 1 H, OH), 4.49 (t, ^3J = 5.8 Hz, 1 H, OH), 3.65 (dd, $^3J_{5\text{-H,6-H}}$ = 5.4 Hz, $^2J_{6\text{-H,6´-H}}$ = 11.7 Hz, 1 H, 6-H), 3.53–3.15 (m, 5 H, 2-H, 3-H, 4-H, 5-H, 6´-H) ppm; **^{13}C NMR**(75.47 MHz, DMSO-d_6, 25 ºC): δ = 179.0 (C=S), 148.3 (C–NO_2), 138.0 (CH=N), 133.3, 130.5, 128.5, 128.2 and 124.5 (C_{arom}), 84.1 (1-C), 78.7 (3-C), 77.5 (2-C), 71.9 (5-C), 69.8 (4-C), 60.8 (6-C) ppm. R_f ($CHCl_3$/MeOH 5:1) = 0.51. $[\alpha]_D$ = +42.5(MeOH; c = 1.06). Anal. calcd. for $C_{14}H_{18}N_4O_7S{\cdot}4H_2O$ (458.44): C, 36.68; H, 5.72; N, 12.22. Found.(%): C, 36.42; H, 6.01; N, 11.95.

3–Nitrobenzaldehyde *N*(4)-(β-D-glucopyranosyl)thiosemicarbazone) (L'$_{10}$)

$C_{14}H_{18}N_4O_7S$ (386.09). Yield: 70%. M.p. 201-205ºC(decomp.) R_f(($CHCl_3$/MeOH 5:1) = 0.52. $[\alpha]_D$ = +54(MeOH/DMF 3:1; c = 0.75).

IR(KBr): *v* 3416, 3304, 3172, 2987, 1545, 1514, 1412, 1352, 1266, 1211, 1168, 1035, 996, 910, 889, 810, 736, 708, 677, 591, 533 cm^{-1}; **^{1}H NMR**(300.13 MHz, DMSO-d_6, 25 ºC): δ = 11.91 (br s, 1 H, N(2)H), 8.80 (d, $^3J_{1\text{-}H,N(4)H}$ = 8.7 Hz, 1 H, N(4)H), 8.62 (s, 1 H, H_{arom}), 8.34 (d, *J* = 7.5 Hz, 1 H, H_{arom}), 8.25–8.21 (m, 2 H, H_{arom} and CH=N), 7.72 (dd, *J* = 7.5 Hz, *J* = 8.1 Hz, 1 H, H_{arom}), 5.40 (dd, $^3J_{1\text{-}H,2\text{-}H}$ = 9.3 Hz, 1 H, 1-H), 5.05 (s, 2 H, OH), 4.95 (s, 1 H, OH), 4.53 (s, 1 H, OH), 3.68 (dd, $^3J_{5\text{-}H,6\text{-}H}$ = 5.4 Hz, $^2J_{6\text{-}H,6'\text{-}H}$ = 11.7 Hz, 1 H, 6-H), 3.53–3.15 (m, 5 H, 2-H, 3-H, 4-H, 5-H, 6´-H) ppm; **^{13}C NMR** (75.47 MHz, DMSO-d_6, 25 ºC): δ = 179.0 (C=S), 148.4 (C–NO_2), 141.0 (CH=N), 136.0, 133.7, 130.3, 124.3 and 121.9 (C_{arom}), 84.3 (1-C), 78.8 (3-C), 77.7 (2-C), 71.9 (5-C), 69.9 (4-C), 60.9 (6-C) ppm. R_f ($CHCl_3$/MeOH 5:1) = 0.52. $[\alpha]_D$ = +54(MeOH/DMF 3:1; c = 0.75). Anal. calcd. for $C_{14}H_{18}N_4O_7S{\cdot}5H_2O$ (476.46): C, 35.29; H, 5.92; N, 11.76. Found.(%): C, 34.96; H, 5.34; N, 12.06.

4–Nitrobenzaldehyde *N*(4)-(β-D-glucopyranosyl)thiosemicarbazone)L'$_{11}$ [251]

IR(**KBr**): ν 3405, 3359, 3304, 2873, 1583, 1537, 1511, 1499, 1332, 1293, 1225, 1202, 1166, 1096, 1035, 976, 892, 822, 750, 648, 599 (C=S) cm^{-1}; **^{1}H NMR**(300.13 MHz, DMSO-d_6, 25 ºC): δ = 11.97 (s, 1 H, N(2)H), 8.79 (d, $^3J_{1\text{-}H,N(4)H}$ = 9.0 Hz, 1 H, N(4)H), 8.26–8.14 (m, 5 H, H_{arom} and CH=N), 5.40 (dd, $^3J_{1\text{-}H,2\text{-}H}$ = 9.0 Hz, 1 H, 1-H), 5.03–5.01 (m, 2 H, OH), 4.91–4.90 (m, 1 H, OH), 4.50 (t, ^3J = 5.7 Hz, 1 H, OH), 3.65 (dd, $^3J_{5\text{-}H,6\text{-}H}$ = 5.4 Hz, $^2J_{6\text{-}H,6'\text{-}H}$ = 11.7 Hz, 1 H, 6-H), 3.54–3.15 (m, 5 H, 2-H, 3-H, 4-H, 5-H, 6´-H) ppm; **^{13}C NMR**(75.47 MHz, DMSO-d_6, 25 ºC): δ = 179.0 (C=S), 147.7 (C–NO_2), 140.4 and 140.3 (CH=N and C_{arom}), 128.5 and 123.8 (C_{arom}), 84.1 (1-C), 78.7 (3-C), 77.6 (2-C), 71.9 (5-C), 69.9 (4-C), 60.8 (6-C) ppm. R_f ($CHCl_3$/MeOH 5:1) = 0.34. $[\alpha]_D$ = +61.3(MeOH/DMF 3:1; c = 0.75). Anal. calcd. for $C_{14}H_{18}N_4O_7S{\cdot}4H_2O$ (458.44): C, 36.68; H, 5.72; N, 12.22. Found.(%): C, 36.98; H, 5.58; N, 12.84.

2–Hydroxybenzaldehyde *N*(4)-(β-D-glucopyranosyl)thiosemicarbazone) (L'$_{12}$)

IR(**KBr**): *v* 3233, 3203, 2864, 1553, 1409, 1266, 1228, 1156, 1073, 1035, 910, 889, 843, 753, 648, 568, 543 cm^{-1}; **^{1}H NMR**(300.13 MHz, DMSO-d_6, 25 ºC): δ = 11.99 (s, 1 H, N(2)H), 8.47 (d, $^3J_{1\text{-}H,N(4)H}$ = 8.7 Hz, 1 H, N(4)H), 8.43 (s, 1 H, CH=N), 7.99(d, *J* = 7.5 Hz, 1 H, H_{arom}), 7.26–7.21 (m, 1 H, H_{arom}), 6.88–6.80 (m, 2 H, H_{arom}), 5.37 (dd, $^3J_{1\text{-}H,2\text{-}H}$ = 9.3 Hz, 1 H, 1-H), 5.02–5.01 (m, 2 H, OH), 4.91–4.90 (m, 1 H, OH), 4.51–4.47 (m, 1 H, OH), 3.64 (dd, $^3J_{5\text{-}H,6\text{-}H}$ = 5.4 Hz, $^2J_{6\text{-}H,6'\text{-}H}$ = 11.7

Hz, 1 H, 6-H), 3.48–3.12 (m, 5 H, 2-H, 3-H, 4-H, 5-H, 6´-H) ppm; **^{13}C NMR** (75.47 MHz, DMSO-d_6, 25 ºC): δ = 178.3 (C=S), 156.6 (C–OH), 140.0 (CH=N), 131.4, 126.7, 120.3, 119.2 and 116.1 (C_{arom}), 83.9 (1-C), 78.6 (3-C), 77.6 (2-C), 72.0 (5-C), 69.8 (4-C), 60.8 (6-C) ppm. R_f ($CHCl_3$/MeOH 5:1) = 0.22. $[\alpha]_D$ = +43(MeOH; c = 1).

3–Hydroxybenzaldehyde *N*(4)-(β-D-glucopyranosyl)thiosemicarbazone) L'$_{13}$

IR(KBr): *v* 3217, 3208, 2950, 1612, 1582, 1553, 1504, 1417, 1366, 1315, 1259, 1226, 1168, 1091, 1076, 1031, 986, 892, 832, 788, 687, 620, 553 cm^{-1}; **^{1}H NMR**(300.13 MHz, DMSO-d_6, 25 ºC): δ = 11.69 (s, 1 H, N(2)H), 9.61(s, 1 H, OH), 8.44 (d, $^3J_{1\text{-H,N(4)H}}$ = 9.3 Hz, 1 H, N(4)H), 8.02 (s, 1 H, CH=N), 7.22–7.21 (m, 3 H, H_{arom}), 6.84–6.81 (m, 1 H, H_{arom}), 5.37 (dd, $^3J_{1\text{-H,2-H}}$ = 9.0 Hz, 1 H, 1-H), 5.06–5.02 (m, 2 H, OH), 4.92–4.91 (m, 1 H, OH), 4.51 (t, ^3J = 5.7 Hz, 1 H, OH), 3.64 (dd, $^3J_{5\text{-H,6-H}}$ = 5.7 Hz, $^2J_{6\text{-H,6´-H}}$ = 11.4 Hz, 1 H, 6-H), 3.48–3.14 (m, 5 H, 2-H, 3-H, 4-H, 5-H, 6´-H) ppm. **^{13}C NMR** (75.47 MHz, DMSO-d_6, 25 ºC): δ = 178.7 (C=S), 157.8 (C–OH), 144.3 (CH=N), 135.5, 130.4, 119.6, 118.0 and 113.8 (C_{arom}), 84.2 (1-C), 78.8 (3-C), 77.6 (2-C), 72.3 (5-C), 70.1 (4-C), 61.1 (6-C) ppm. R_f ($CHCl_3$/MeOH 5:1) = 0.30. $[\alpha]_D$ = +58.7(MeOH; c = 1). Anal. calcd. for $C_{14}H_{19}N_3O_6S{\cdot}2H_2O$ (393.41): C, 42.74; H, 5.89; N, 10.68. Found.(%): C, 42.74; H, 5.89; N, 10.98.

4–Hydroxybenzaldehyde *N*(4)-(β-D-glucopyranosyl)thiosemicarbazone) (L'$_{14}$) [251, 253, 255]

IR(KBr): *v* 3297, 3206, 2909, 1609, 1521, 1512, 1434, 1373, 1230, 1162, 1162, 1070, 1018 909, 839, 648, 607, 560, 530 cm^{-1}; **^{1}H NMR**(300.13 MHz, DMSO-d_6, 25 ºC): δ = 11.56 (s, 1 H, N(2)H), 9.92 (br s, 1 H, OH), 8.38 (d, $^3J_{1\text{-H,N(4)H}}$ = 9.0 Hz, 1 H, N(4)H), 8.00 (s, 1 H, CH=N), 7.62 (d, J = 9.0 Hz, 2 H, H_{arom}), 6.78 (d, J = 9.0 Hz, 2 H, H_{arom}), 5.35 (dd, $^3J_{1\text{-H,2-H}}$ = 9.6 Hz, 1 H, 1-H), 5.00 (s, 2 H, OH), 4.88 (s, 1 H, OH), 4.45 (s, 1 H, OH), 3.64 (dd, $^3J_{5\text{-H,6-H}}$ = 5.7 Hz, $^2J_{6\text{-H,6´-H}}$ = 11.4 Hz, 1 H, 6-H), 3.49–3.10 (m, 5 H, 2-H, 3-H, 4-H, 5-H, 6´-H) ppm; **^{13}C NMR**(75.47 MHz, DMSO-d_6, 25 ºC): δ = 178.0 (C=S), 160.3 (C–OH), 143.6 (CH=N), 129.3, 124.3 and 115.8 (C_{arom}), 83.9 (1-C), 79.2 (3-C), 78.6 (2-C), 72.0 (5-C), 69.8 (4-C), 60.8 (6-C) ppm. R_f ($CHCl_3$/MeOH 5:1) = 0.12. $[\alpha]_D$ = +65.3(MeOH; c = 1). Anal. calc. for $C_{14}H_{19}N_3O_6S$(357.38): C, 47.05; H, 5.36; N, 11.76. Found.(%): C, 46.98; H, 5.64; N, 11.55.

2–Methoxybenzaldehyde *N*(4)-(β-D-glucopyranosyl)thiosemicarbazone) (L'_{15})

IR(KBr): ν 3559, 3324, 3212, 2897, 1602, 1537, 1505, 1487, 1436, 1320, 1289, 1248, 1171, 1099, 1071, 1026, 993, 892, 830, 752, 590, 545 cm^{-1}; **^{1}H NMR**(300.13 MHz, DMSO-d_6, 25 ºC): δ = 11.73 (s, 1 H, N(2)H), 8.51 (d, $^3J_{1\text{-H,N(4)H}}$ = 9.0 Hz, 1 H, N(4)H), 8.47 (s, 1 H, CH=N), 8.14 (dd, J = 1.8 Hz, J = 7.8 Hz, 1 H, H_{arom}), 7.43–7.37 (m, 1 H, H_{arom}), 7.08–6.95 (m, 2 H, H_{arom}), 5.37 (dd, $^3J_{1\text{-H,2-H}}$ = 9.0 Hz, 1 H, 1-H), 5.02–4.99 (m, 2 H, OH), 4.89–4.88 (m, 1 H, OH), 4.47 (t, ^3J = 5.8 Hz, 1 H, OH), 3.84 (s, 3 H, OCH_3), 3.66 (dd, $^3J_{5\text{-H,6-H}}$ = 5.7 Hz, $^2J_{6\text{-H,6´-H}}$ = 11.4 Hz, 1 H, 6-H), 3.51–3.43 (m, 2 H) and 3.25–3.13 (m, 3 H) (2-H, 3-H, 4-H, 5-H, 6´-H) ppm; **^{13}C NMR**(75.47 MHz, DMSO-d_6, 25 ºC): δ = 178.4 (C=S), 157.9 (*C*–OMe), 138.6 (CH=N), 131.6, 126.3, 121.9, 120.5 and 111.7 (C_{arom}), 83.9 (1-C), 78.6 (3-C), 77.6 (2-C), 72.0 (5-C), 69.8 (4-C), 60.8 (6-C), 55.7 (OCH_3) ppm. R_f ($CHCl_3$/MeOH 5:1) = 0.42. $[\alpha]_D$ = +37.8(MeOH; c = 1). Anal. calcd. for $C_{15}H_{21}N_3O_6S{\cdot}3H_2O$ (425.45): C, 42.35; H, 6.40; N, 9.88. Found.(%): C, 41.97, H, 6.67, N, 10.03.

3–Methoxybenzaldehyde *N*(4)-(β-D-glucopyranosyl)thiosemicarbazone) (L'_{16})

IR(KBr): *v* 3498, 3320, 3198, 2905, 1616, 1579, 1557, 1526, 1480, 1441, 1362, 1320, 1289, 1202, 1162, 1091, 1076, 1031, 994, 896, 851, 783, 648, 618, 593, 562, 547 cm^{-1}; **^{1}H NMR**(300.13 MHz, DMSO-d_6, 25 ºC): δ = 11.76 (s, 1 H, N(2)H), 8.59 ((d, $^3J_{1\text{-H,N(4)H}}$ = 9.0 Hz, 1 H, N(4)H), 8.08 (s, 1 H, CH=N), 7.43–7.34 (m, 3 H, H_{arom}), 6.99 (d, J = 7.5 Hz, 1 H, H_{arom}), 5.37 (dd, $^3J_{1\text{-H,2-H}}$ = 9.0 Hz, 1 H, 1-H), 5.02 (br s, 2 H, OH), 4.91 (br s, 1 H, OH), 4.47 (br s, 1 H, OH), 3.81 (s, 3 H, OCH_3), 3.66 (d, J = 11.4 Hz, 1 H, 6-H), 3.53–3.14 (m, 5 H, 2-H, 3-H, 4-H, 5-H, 6´-H) ppm; **^{13}C NMR**(75.47 MHz, DMSO-d_6, 25 ºC): δ = 178.6 (C=S), 159.6 (*C*–OMe), 143.0 (CH=N), 135.3, 129.8, 120.4, 115.9 and 112.2 (C_{arom}), 84.0 (1-C), 78.6 (3-C), 77.6 (2-C), 71.9 (5-C), 69.8 (4-C), 60.8 (6-C), 55.3 (OCH_3) ppm. R_f ($CHCl_3$/MeOH 5:1) = 0.41. $[\alpha]_D$ = +50.7(MeOH; c = 1.14). Anal. calcd. for $C_{15}H_{21}N_3O_6S{\cdot}4H_2O$ (443.47): C, 40.63; H, 6.59; N, 9.48. Found (%): C, 40.17; H, 7.01; N, 9.12.

4–Methoxybenzaldehyde *N*(4)-(β-D-glucopyranosyl)thiosemicarbazone) (L'_{17})

IR(KBr): *v* 3547, 3308, 3188, 2893, 1603, 1549, 1512, 1464, 1422, 1359, 1304, 1251, 1171, 1031 1003, 990, 888, 839, 720 cm^{-1}; **^{1}H NMR**(300.13 MHz, DMSO-d_6, 25 ºC): δ = 11.63 (s, 1 H,

N(2)H), 8.46 (d, $^3J_{1\text{-H,N(4)H}}$ = 9.0 Hz, 1 H, N(4)H), 8.06 (s, 1 H, CH=N), 7.78 (d, *J* = 7.8 Hz, 2 H, H_{arom}), 6.98 (d, *J* = 7.8 Hz, 2 H, H_{arom}), 5.37 (dd, $^3J_{1\text{-H,2-H}}$ = 9.3 Hz, 1 H, 1-H), 5.01–4.99 (m, 2 H, OH), 4.89–4.88 (m, 1 H, OH), 4.47 (t, ^3J = 5.8 Hz, 1 H, OH), 3.80 (s, 3 H, OCH_3), 3.63 (dd, $^3J_{5\text{-H,6-H}}$ = 5.7 Hz, $^2J_{6\text{-H,6´-H}}$ = 11.4 Hz, 1 H, 6-H), 3.50–3.44 (m, 2 H) and 3.26–3.12 (m, 3 H) (2-H, 3-H, 4-H, 5-H, 6´-H) ppm; **^{13}C NMR**(75.47 MHz, DMSO-d_6, 25 ºC): δ = 178.2 (C=S), 160.8 (*C*–OMe), 143.0 (CH=N), 129.2, 126.4 and 114.2 (C_{arom}), 84.0 (1-C), 78.6 (3-C), 77.6 (2-C), 72.0 (5-C), 69.8 (4-C), 60.8 (6-C), 55.3 (OCH_3) ppm. R_f ($CHCl_3$/MeOH 5:1) = 0.33. $[\alpha]_D$ = +68.5(MeOH; c = 1). Anal. calcd. for $C_{15}H_{21}N_3O_6S{\cdot}5H_2O$ (461.49): C, 39.04; H, 6.77; N, 9.11. Found(%): C, 38.79; H, 6.34; N, 8.95.

4–Methyl-benzaldehyde *N*(4)-((β-D-glucopyranosyl)thiosemicarbazone) (L'$_{18}$)

IR(KBr): *v* 3322, 3304, 3186, 2979, 1645, 1605, 1553, 1503, 1413, 1360, 1273, 1174, 1104, 1076, 1035, 989, 904, 882, 830, 772, 711, 579, 561 cm^{-1}; **^{1}H NMR**(300.13 MHz, DMSO-d_6, 25 ºC): δ = 11.67 (s, 1 H, N(2)H), 8.48 (d, $^3J_{1\text{-H,N(4)H}}$ = 9.3 Hz, 1 H, N(4)H), 8.06(s, 1 H, CH=N), 7.72 (d, *J* = 8.1 Hz, 2 H, H_{arom}), 7.23 (d, *J* = 7.8 Hz, 2 H, H_{arom}), 5.37 (dd, $^3J_{1\text{-H,2-H}}$ = 9.6 Hz, 1 H, 1-H), 5.00–4.99 (m, 2 H, OH), 4.88–4.87 (m, 1 H, OH), 4.46 (t, ^3J = 5.7 Hz, 1 H, OH), 3.63 (dd, $^3J_{5\text{-H,6-H}}$ = 5.7 Hz, $^2J_{6\text{-H,6´-H}}$ = 11.4 Hz, 1 H, 6-H), 3.50–3.43 (m, 2 H) and 3.23–3.12 (m, 3 H) (2-H, 3-H, 4-H, 5-H, 6´-H), 2.32 (s, 3 H, CH_3) ppm; **^{13}C NMR** (75.47 MHz, DMSO-d_6, 25 ºC): δ = 178.4 (C=S), 143.1 (CH=N), 139.9, 131.2, 129.3 and 127.5 (C_{arom}), 83.9 ((1-C), 78.6 (3-C), 77.6 (2-C), 72.0 (5-C), 69.8 (4-C), 60.8 (6-C) ppm. R_f ($CHCl_3$/MeOH 5:1) = 0.40. $[\alpha]_D$ = +63.1(MeOH; c = 1). Anal. calcd. for $C_{15}H_{21}N_3O_5S{\cdot}2H_2O$ (391.44): C, 46.03; H, 6.44; N, 10.73. Found(%): C, 46.85; H, 6.29; N, 11.11.

4–*tert*-Butyl-benzaldehyde *N*(4)-(β-D-glucopyranosyl)thiosemicarbazone) (L'$_{19}$)

IR(KBr): *v* 3324, 3204, 2864, 1541, 1408, 1365, 1266, 1169, 1109, 1072, 1018, 900, 826, 646, 561, 533 (C=S) cm^{-1}; **^{1}H NMR**(599.83 MHz, DMSO-d_6, 25 ºC): δ = 11.71 (s, 1 H, N(2)H), 8.48 (d, $^3J_{1\text{-H,N(4)H}}$ = 9.0 Hz, 1 H, N(4)H), 8.09 (s, 1 H, CH=N), 7.75 (d, *J* = 8.4 Hz, 2 H, H_{arom}), 7.44 (d, *J* = 7.2 Hz, 2 H, H_{arom}), 5.38 (dd, J = 9.0 Hz, 1 H, 1-H), 5.03 (br s, 2 H, OH), 4.90 (br s, 1 H, OH), 4.48 (br s, 1 H, OH), 3.65 (d, *J* = 11.4 Hz, 1 H, 6-H), 3.49–3.10 (m, 5 H, 2-H, 3-H, 4-H, 5-H, 6´-H), 1.30 (s, 9 H, CH_3(*t*Bu)) ppm; **^{13}C NMR**(75.47 MHz, DMSO-d_6, 25 ºC): δ = 178.5 (C=S), 152.9

(C_{arom}–*t*Bu), 143.1 (CH=N), 131.3, 127.4 and 125.5 (C_{arom}), 84.0 (1-C), 78.7 (3-C), 77.6 (2-C), 72.1 (5-C), 69.9 (4-C), 60.9 (6-C), 34.6 (CMe_3), 31.0 (CH_3(*t*Bu)) ppm. R_f ($CHCl_3$/MeOH 5:1) = 0.53. $[\alpha]_D$ = +66.2(MeOH; c = 1.14).

2–Pyridinecarboxaldehyde *N*(4)-(β-D-glucopyranosyl)thiosemicarbazone) (L'_{20})

IR(KBr): *v* 3416, 3324, 3163, 2832, 1678, 1557, 1518, 1474, 1434, 1340, 1278, 1238, 1155, 1108, 1083, 1039, 896, 830, 780, 629 cm^{-1}; **^{1}H NMR**(300.13 MHz, DMSO-d_6, 25 ºC): δ = 11.94 (s, 1 H, N(2)H), 8.73 (d, $^3J_{1\text{-}H,N(4)H}$ = 9.0 Hz, 1 H, N(4)H), 8.59–8.56 (m, 1 H, H_{arom}), 8.35 (d, *J* = 8.1 Hz, 1 H, H_{arom}), 8.15 (s, 1 H, CH=N), 7.87–7.82 (m, 1 H, H_{arom}), 7.41–7.37 (m, 1 H, H_{arom}), 5.40 (dd, $^3J_{1\text{-}H,2\text{-}H}$ = 9.3 Hz, 1 H, 1-H), 5.05 (br s, 3 H, OH), 4.51 (br s, 1 H, OH), 3.66 (d, *J* = 11.4 HZ, 1 H, 6-H), 3.55–3.43 (m, 2 H) and 3.27–3.15 (m, 3 H) (m, 5 H, 2-H, 3-H, 4-H, 5-H, 6´-H) ppm; **^{13}C NMR**(75.47 MHz, DMSO-d_6, 25 ºC): δ = 178.9 (C=S), 153.0 and 149.4 (C_{arom}), 143.3 (CH=N), 136.5, 124.3 and 120.6 (C_{arom}), 84.1 (1-C), 78.7 (3-C), 77.6 (2-C), 71.9 (5-C), 69.8 (4-C), 60.8 (6-C) ppm. R_f ($CHCl_3$/MeOH 9:1) = 0.60. Anal. calcd. for $C_{13}H_{18}N_4O_5S{\cdot}3H_2O$ (396.42): C, 39.39; H, 6.10; N, 14.13. Found(%): C, 39.78; H, 6.45; N, 14.15.

3–Pyridinecarboxaldehyde *N*(4)-((β-D-glucopyranosyl)thiosemicarbazone) (L'_{21})

IR(KBr): *v* 3574, 3399, 3211, 3075, 2873, 1597, 1537, 1489, 1421, 1338, 1257, 1211, 1165, 1094, 1073, 1043, 904, 828, 811, 703, 624 cm^{-1}; **^{1}H NMR**(300.13 MHz, DMSO-d_6, 25 ºC): δ = 11.86 (br s, 1 H, N(2)H), 8.97 (d, *J* = 1.5 Hz, 1 H, H_{arom}), 8.69 (d, $^3J_{1\text{-}H,N(4)H}$ = 9.0 Hz, 1 H, N(4)H), 8.56 (dd, *J* = 4.8 Hz, *J* = 1.8 Hz, 1 H, H_{arom}), 8.29 (dt, *J* = 8.1 Hz, *J* = 1.8 Hz, 1 H, H_{arom}), 8.11 (s, 1 H, CH=N), 7.43 (dd, *J* = 8.1 Hz, *J* = 4.8 Hz, 1 H, H_{arom}), 5.37 (dd, $^3J_{1\text{-}H,2\text{-}H}$ = 9.0 Hz, 1 H, 1-H), 5.04 (br s, 2 H, OH), 4.94 (br s, 1 H, OH), 4.53 (t, ^3J = 5.6 Hz, 1 H, OH), 3.65 (dd, $^3J_{5\text{-}H,6\text{-}H}$ = 5.7 Hz, $^2J_{6\text{-}H,6'\text{-}H}$ = 11.4 Hz, 1 H, 6-H), 3.56–3.45 (m, 2 H) and 3.27–3.14 (m, 3 H) (2-H, 3-H, 4-H, 5-H, 6´-H) ppm; **^{13}C NMR**(75.47 MHz, DMSO-d_6, 25 ºC): δ = 178.8 (C=S), 150.5 and 149.0 (C_{arom}), 140.1 (CH=N), 134.2, 129.9 and 123.7 (C_{arom}), 84.1 (1-C), 78.7 (3-C), 77.6 (2-C), 71.9 (5-C), 69.9 (4-C), 60.9 (6-C) ppm. R_f ($CHCl_3$/MeOH 9:1) = 0.90. Anal. calcd. for $C_{13}H_{18}N_4O_5S{\cdot}2H_2O$ (378.40): C, 41.26; H, 5.86; N, 14.81. Found(%): C, 41.84; H, 5.53; N, 14.74.

4–Pyridinecarboxaldehyde *N*(4)-(β-D-glucopyranosyl)thiosemicarbazone) (L'$_{22}$)

IR(KBr): *v* 3597, 3323, 3193, 2848, 1610, 1541, 1493, 11442, 1411, 1354, 1320, 1269, 1213, 1168, 1115, 1079, 1035, 896, 830, 772, 652, 609 cm^{-1}; **^{1}H NMR**(300.13 MHz, DMSO-d_6, 25 ºC): δ = 11.99 (s, 1 H, N(2)H), 8.75 (d, $^3J_{1\text{-H,N(4)H}}$ = 8.7 Hz, 1 H, N(4)H), 8.61 (dd, *J* = 5.7 Hz, 2 H, H_{arom}), 8.07 (s, 1 H, CH=N), 7.84 (d, *J* = 5.7 Hz, 2 H, H_{arom}), 5.40 (dd, $^3J_{1\text{-H,2-H}}$ = 9.0 Hz, 1 H, 1-H), 5.03 (br s, 2 H, OH), 4.91 (br s, 1 H, OH), 4.49 (m, 1H, OH), 3.65 (dd, $^3J_{5\text{-H,6-H}}$ = 4.8 Hz, $^2J_{6\text{-H,6´-H}}$ = 11.4 Hz, 1 H, 6-H), 3.54–3.45 (m, 2 H) and 3.27–3.14 (m, 3 H) (2-H, 3-H, 4-H, 5-H, 6´-H) ppm; **^{13}C NMR** (75.47 MHz, DMSO-d_6, 25 ºC): δ = 179.0 (C=S), 150.1 (C_{arom}), 141.4 (CH=N), 140.7 and 121.6 (C_{arom}), 84.1 (1-C), 78.7 (3-C), 77.4 (2-C), 71.8 (5-C), 69.8 (4-C), 60.9 (6-C) ppm. R_f ($CHCl_3$/MeOH 5:1) = 0.23. $[\alpha]_D$ = +49.6(MeOH/DMF 3:1; c = 0.8). Anal. calcd. for $C_{13}H_{18}N_4O_5S$ (342.37): C, 45.61; H, 5.30; N, 16.36. Found(%): C, 45.02; H, 5.67; N, 16.78.

1–Ferrocenecarboxaldehyde *N*(4)-(β-D-glucopyranosyl)thiosemicarbazone) (L'$_{23}$)

IR(KBr): *v* 3326, 3309, 1605, 1535, 1410, 1365, 1254, 1105, 1073, 1024, 940, 891, 822, 770, 622, 560 cm^{-1}; **^{1}H NMR**(300.13 MHz, DMSO-d_6, 25 ºC): δ = 11.49 (s, 1 H, N(2)H), 8.18 (d, $^3J_{1\text{-H,N(4)H}}$ = 9.0 Hz, 1 H, N(4)H), 7.95 (s, 1 H, CH=N), 5.34 (dd, $^3J_{1\text{-H,2-H}}$ = 9.3 Hz, 1 H, 1-H), 4.81 (d, *J* = 1.8 Hz, 1 H, Fc), 4.73 (d, *J* = 2.4 Hz, 1 H, Fc), 4.44 (m, 2 H, Fc), 4.22 (s, 5 H, Fc), 3.90 (br s, 4 H, OH), 3.65 (d, *J* = 11.1 Hz, 1 H, 6-H), 3.50–3.38 (m, 3 H), and 3.24–3.09 (m, 2 H) (2-H, 3-H, 4-H, 5-H, 6´-H) ppm; **^{13}C NMR**(75.47 MHz, DMSO-d_6, 25 ºC): δ = 177.5 (C=S), 144.3 (CH=N), 83.7 (1-C), 78.6 (*C*(Fc)–CH=N), 78.5 (3-C), 77.6 (2-C), 72.0 (5-C), 70.2 (Fc), 70.1 (Fc), 69.8 (4-C), 68.9 (Fc), 68.2 (Fc), 67.3 (Fc), 60.7 (6-C) ppm. R_f ($CHCl_3$/MeOH 9:1) = 0.90. $[\alpha]_D$ = +40(DMF; c = 1). Anal. calcd. for $C_{18}H_{23}FeN_3O_5S$ (449.30): C, 48.12; H, 5.16; N, 9.35. Found(%): C, 48.11; H, 5.68; N, 9.12.

β–Naphthalenecarboxaldehyde *N*(4)-(β-D-glucopyranosyl) thiosemicarbazone)] (L'$_{24}$)

IR (KBr): *v* 3399, 3330, 3301, 1525, 1356, 1307, 1264, 1210, 1162, 1094, 1078, 1043, 998, 900, 868, 843, 759, 677, 622, 533 cm^{-1}; **^{1}H NMR** (599.83 MHz, DMSO-d_6): δ 11.84 (s, 1H, N(2)H),

8.64 (d, $^{3}J_{1\text{-}H,N(4)H}$ 9.0 Hz, 1H, N(4)H), 8.28 (s, 1H, H_{naphth}), 8.24 (d, *J* 8.4 Hz, 1H, H_{naphth}), 8.15 (s, 1H, CH=N), 7.99–7.97 (m, 1H, H_{naphth}), 7.94 (d, *J* 7.8 Hz, 2H, H_{naphth}), 7.56–7.55 (m, 2H, H_{naphth}), 5.42 (dd, $^{3}J_{1\text{-}H,2\text{-}H}$ 9.3 Hz, 1H, 1-H), 5.05–5.03 (m, 2H, OH), 4.92–4.91 (m, 1H, OH), 4.50 (t, ^{3}J 6.0 Hz, 1 H, OH), 3.66 (dd, $^{3}J_{5\text{-}H,6\text{-}H}$ 5.4 Hz, $^{2}J_{6\text{-}H,6'\text{-}H}$ 11.4 Hz, 1H, 6-H), 3.57–3.54 (m, 1H), 3.51–3.47 (m, 1H) and 3.28–3.16 (m, 3H) (2-H, 3-H, 4-H, 5-H, 6´-H) ppm; **^{13}C NMR** (75.47 MHz, DMSO-d_6): δ 178.6 (C=S), 143.2 (CH=N), 133.7, 132.8, 131.7, 129.3, 128.3, 127.8, 127.1, 126.7 and 123.2 8 (C_{naphth}), 84.1 (1-C), 78.7 (3-C), 77.6 (2-C), 71.9 (5-C), 69.9 (4-C), 60.9 (6-C). R_f ($CHCl_3$/MeOH 5:1) 0.40; $[\alpha]_D$ = +60.5 (*c* 1, MeOH). Anal. calcd. for $C_{18}H_{21}N_3O_5S$ (391.44): C, 55.23; H, 5.41; N, 10.73. Found(%): C, 55.57; H, 5.12; N, 11.02.

4-Methoxy-acetophenone *N*(4)-(β-D-glucopyranosyl)thiosemicarbazone) (L'$_{25}$)

IR (KBr): *v* 3330, 3297, 2915, 1600, 1510, 1414, 1302, 1251, 1177, 1072, 1018, 891, 835, 804, 537 cm^{-1}; **^{1}H NMR** (599.83 MHz, DMSO-d_6, 25 ºC): δ = 10.47 (br s, 1 H, N(2)H), 8.35 (d, $^{3}J_{1\text{-}H,N(4)H}$ = 8.4 Hz, 1 H, N(4)H), 7.85 (d, *J* = 8.4 Hz, 2 H, H_{arom}), 6.96 (d, *J* = 8.4 Hz, 2 H, H_{arom}), 5.38 (dd, $^{3}J_{1\text{-}H,2\text{-}H}$ = 9.0 Hz, 1 H, 1-H), 5.01 (br s, 3 H, OH), 4.52 (br s, 1 H, OH), 3.79 (s, 3 H, OCH_3), 3.63 (d, *J* = 11.4 Hz, 1 H, 6´-H), 3.48 (dd, *J* = 4.2 Hz, *J* = 12.0 Hz, 1 H, 6-H), 3.39 (t, *J* = 9.0 Hz, 1 H), 3.25 (t, *J* = 8.4 Hz, 1 H), 3.17 (dd, *J* = 9.0 Hz, *J* = 9.6 Hz, 1 H) and 3.15–3.12 (m, 1 H) (2-H, 3-H, 4-H, 5-H), 2.30 (s, 3 H, CH_3C=N) ppm; **^{13}C NMR** (150.84 MHz, DMSO-d_6, 25 ºC): δ = 179.3 (C=S), 160.4 (C_{arom}–O), 149.1 (C=N), 130.5, 129.9, 128.2, 113.8 and 113.7 (C_{arom}), 83.8 (1-C), 78.6 (3-C), 77.4 (2-C), 72.3 (5-C), 69.8 (4-C), 60.8 (6-C), 55.2 (OCH_3), 14.3 (CH$_3$C=N) ppm. R_f ($CHCl_3$/MeOH 5:1) = 0.60. $[\alpha]_D$ = +45.6(MeOH; c = 1). Anal. calcd. for $C_{16}H_{23}N_3O_6S{\cdot}3H_2O$ (439.48): C, 43.73; H, 6.65; N, 9.56. Found(%): C, 43.57; H, 6.98; N, 10.01.

2–Acetophenone *N*(4)-(β-D-glucopyranosyl)thiosemicarbazone) (L'$_{26}$)

IR (KBr): *v* 3374, 3311, 3237, 1600, 1525, 1508, 1429, 1363, 1266, 1209, 1173, 1116, 1055, 956, 900, 865, 843, 750, 652, 607, 570, 557 cm^{-1}; **^{1}H NMR** (599.83 MHz, DMSO-d_6, 25 ºC): δ = 11.84 (s, 1 H, N(2)H), 8.64 (d, $^{3}J_{1\text{-}H,N(4)H}$ = 9.0 Hz, 1 H, N(4)H), 8.28 (s, 1 H, H_{naphth}), 8.24 (d, *J* = 8.4 Hz, 1 H, H_{naphth}), 8.15 (s, 1 H, CH=N), 7.99–7.97 (m, 1 H, H_{naphth}), 7.94 (d, *J* = 7.8 Hz, 2 H, H_{naphth}), 7.56–7.55 (m, 2 H, H_{naphth}), 5.42 (dd, $^{3}J_{1\text{-}H,2\text{-}H}$ = 9.3 Hz, 1 H, 1-H), 5.05–5.03 (m, 2 H, OH), 4.92–4.91 (m, 1 H, OH), 4.50 (t, ^{3}J = 6.0 Hz, 1 H, OH), 3.66 (dd, $^{3}J_{5\text{-}H,6\text{-}H}$ = 5.4 Hz, $^{2}J_{6\text{-}H,6'\text{-}H}$ = 11.4 Hz, 1

H, 6-H), 3.57–3.54 (m, 1 H), 3.51–3.47 (m, 1 H) and 3.28–3.16 (m, 3 H) (2-H, 3-H, 4-H, 5-H, 6´-H) ppm; **^{13}C NMR** (75.47 MHz, DMSO-d_6, 25 ºC): δ = 178.6 (C=S), 143.2 (CH=N), 133.7, 132.8, 131.7, 129.3, 128.3, 127.8, 127.1, 126.7 and 123.2 8 (C_{naphth}), 84.1 (1-C), 78.7 (3-C), 77.6 (2-C), 71.9 (5-C), 69.9 (4-C), 60.9 (6-C) ppm. R_f ($CHCl_3$/MeOH 5:1) = 0.44. $[\alpha]_D$ = +60.5(MeOH; c = 1). Anal. calcd. for $C_{19}H_{23}N_3O_5S{\cdot}2H_2O$ (441.50): C, 51.69; H, 6.16; N, 9.52. Found(%): C, 51.12; H, 5.98; N, 9.32.

V.7. X-Ray crystallography for L_9 and L'_{15}

Slow crystallization from ethanol yielded colourless crystals of **L_9** (0.25 x 0.30 x 0.75 mm) which were mounted in air. Diffraction measurements were made on Crystal Logic Dual Goniometer diffractometer using graphite monochromated Mo radiation. Unit cell dimensions were determined and refined by using the angular setting of 25 automatically centred reflections in the range $11° < 2\theta < 23°$ and they appear in Table 23. Intensity data were recorded using a $\theta-2\theta$ scan. Three standard reflections monitored every 97 reflexion showed less than 3% variation and no decay. Lorentz, polarization and absortion corrections were applied using Crystal Logic software. Slow crystallization from methanol yielded colorless crystals of **L'_{15}** (0.26 x 0.50 x 0.50 mm), which were taken from the mother liquor and immediately cooled to −93°C. Diffraction mesuraments were made it on a Rigaku R-AXIS SPIDER Image Plate diffactometer using graphite monochromated Cu Kα radiation. Data collection (x-scans) and prossesing (cell refinement, data reduction and empirical absorption correction) were performed using the CRYSTALCLEAR program package [343]. The structure were solved by direct methods using SHELXS-97 [344] and refined by full-matrix least-squeares method on F2 with SHELXS-97 [345]. All non-hydrogen atoms were refined anisotropically. Hydrogen atoms were located by difference maps and were refined isotropically (expect those of the methyl group in 2d which were introduced at calculated positions as riding on bonded atoms.

Table 23

X-ray experimental data for compounds **L_9** and **L'_{15}**

	L_9	**L'_{15}**
Empirical formula	$C_{23}H_{26}F_3N_3O_9S$	$C_{14}H_{19}N_3O_6S$
Formula mass	577.54	357.39
Crystal system	Orthorhombic	Orthorhombic
Space group	$P2_12_12_1$	$P2_12_12_1$
α(Å)	17.608(4)	7.5232(1)
b(Å)	9.325(2)	12.6624(2)
c(Å)	17.738(4)	17.4260(3)
V(Å^3)	2912.5(11)	1660.03(4)
Z	4	4
D_{calcd}(gcm^3)	1.317	1.430
F(0 0 0)	1200	752
μ(mm^{-1})	0.181	2.068
T(K)	298	180
λ(Å)	0.71073	1.54178
Radiation	Mo Kα	Cu Kα
θ limits	2.3/25.0	6.8/65.0
No. of data with $I > 2\sigma(I)$	3891	2781
No. of variables	440	293
R	0.0418	0.0243
Rw	0.1191	0.0626
Gof	1.01	1.07
Largest difference in final difference map (e Å^{-3})	0.19, –0.14	0.18, –0.20

V.8. Synthesis of metal complexes

V.8.1. Nickel(II) complexes

A typical procedure: To a suspension of the appropriate ligand (105.4 mg (**L_1**), 115.4 mg (**L_8**), 113 mg (**L_{19}**), 112 mg (**L_{24}**); 0.2 mmol), in methanol (4 mL), a solution of the nickel acetate ($Ni(OAc)_2 \cdot 4H_2O$) (38 mg; 0.15 mmol) in methanol (6 mL) was added drop wise, at room temperature, with stirring [346]. The solution was allowed to on overnight stirring. Then it was kept in the fridge until a solid was formed. The separated product was filtered, washed with cold ether and dried in the desiccator. The complexes were recrystalized from dichloromethane/methanol.

Analytical data

Nickel(2+) bis[4-fluoro-benzaldehyde 4-(2,3,4,6-tetra-*O*-acetyl-β-D-glucopyranosyl)thiosemicarbazone, *N*, *S*] (C_1)

$C_{40}H_{50}F_6N_6O_{18}S_2Ni$ (1139.7). Yield 81%; m.p. 180 ºC; R_f (Hex/EtOAc 1:1) = 0.21; diamagnetic. **IR (KBr)**: *v* 3390, 3348, 2944, 1743, 1598, 1578, 1536, 1500, 1417, 1366, 1208, 1159, 1092, 1030, 906, 889, 759, 697, 550 cm^{-1}; **^{1}H NMR** (600 MHz, DMSO-d_6, 25 ºC): δ = 8.38 (sb, 1H, N(4)H), 8.31 (s, 2 H, H_{arom}), 7.73 (d, *J* = 7.8 Hz, 2 H, CH=N), 7.30 (t, *J* = 8.4 Hz, 1 H, H_{arom}), 5.44 (t, $^3J_{1\text{-}H,2\text{-}H}$ = 9.6, 1 H, 1-H), 5.34 (sb, 1 H, 3-H), 4.97 (sb, 1 H, 4-H), 4.88 (dd, $^3J_{2\text{-}H,3\text{-}H}$ = 9.0, 1 H, 2-H), 4.16-4.15 (m, 2 H, 5-H and 6-H), 3.94 (d, $^3J_{5\text{-}H,6'\text{-}H}$ = 10.8 Hz, 1 H, 6'-H), 2.02, 1.98, 1.94 (3s, 9H, CH_3), 1.82 (sb, 3H, CH3) ppm; **^{13}C NMR** (150 MHz, DMSO-d_6, 25 ºC): δ =173.2 (C=S), 169.9, 169.6, 169.4, 168.9 (C=O), 164.0, 162.3 (CH=N), 136.3, 126.4, 115.6, 115.4 (C_{arom}), 82.2 (1-C), 73.1 (3-C), 71.8 (2-C), 70.8 (5-C), 67.9 (4-C), 61.9 (6-C), 20.5, 20.4, 20.3 (CH_3) ppm. ESI MS: *m/z* = 1111.2047(1111.2017 calcd.)

Nickel(2+) bis[4-trifluoro-benzaldehyde 4-(2,3,4,6-tetra-*O*-acetyl-β-D-glucopyranosyl)thiosemicarbazone, *N*, *S*] (C_2)

$C_{46}H_{50}F_6N_6O_{18}S_2Ni$(1211.7). Yield 95%; m.p. 250–253 ºC; R_f (Hex/EtOAc 1:1) = 0.45; diamagnetic. **IR (KBr)**: *ν* 3412, 3358, 2884, 1762, 1746, 1535, 1502, 1438, 1416, 1372, 1313, 1225, 1205, 1173, 1132, 1094, 1066, 1017, 982, 907, 888, 874, 747, 696, 603 cm^{-1}; **^{1}H NMR** (600 MHz, $CDCl_3$, 25 ºC): δ = 8.01 (d, 2 H, H_{arom}), 7.61 (d, J = 7.8 Hz, 2 H, H_{arom}), 7.53 (s, 1 H, CH=N), 6.00 (brs, 1H, N(4)H), 5.35 (dd, $^3J_{2\text{-}H,3\text{-}H}$ = 9.0, $^3J_{3\text{-}H,4\text{-}H}$ 9.6 Hz, 1 H, 3-H), 5.10-5.05 (m, 1 H, 2-H and 4-H), 5.00 (dd, $^3J_{N(4)H,1\text{-}H}$ = 9.0, $^3J_{1\text{-}H,2\text{-}H}$ = 9.6 Hz, 1 H, 1-H), 4.32 (dd, $^3J_{5\text{-}H,6\text{-}H}$ = 4.8, $^3J_{6\text{-}H,6'\text{-}H}$ = 12.0 Hz, 1 H, 6-H), 4.11(d, 1 H, 6'-H), 3.82(d, $^3J_{5\text{-}H,6'\text{-}H}$ = 6.6 Hz, 1 H, 5-H), 2.11, 2.07, 2.04(3s, 9H, CH_3), 1.98(s, 3H, CH_3) ppm; **^{13}C NMR** (150 MHz, $CDCl_3$, 25 ºC): δ =175.0 (C=S), 171.0, 170.5, 170.0, 169.5 (C=O), 158.0 (CH=N), 136.1, 134.7, 132.4, 125.3, 121.7 (C_{arom}), 83.8 (1-C), 73.4 (3-C), 72.5 (2-C), 70.7 (5-C), 68.5 (4-C), 62.0 (6-C), 20.8, 20.7, 20.6, 20.6 (CH_3) ppm. ESI MS: *m/z* = 1121.1973 (1121.1953 calcd.)

Nickel(2+) bis[4-*tert*-butyl-benzaldehyde 4-(2,3,4,6-tetra-*O*-acetyl-β-D-glucopyranosyl)thiosemicarbazone, *N*, *S*] (C_3)

$C_{52}H_{68}N_6O_{18}S_2Ni$(1187.9). Yield 88%(105 mg); m.p. 183–188 ºC; R_f (Hex/EtOAc 1:1) = 0.63; paramagnetic (μ_{eff} = 3.22). **IR (KBr)**: *ν* 3354, 3320, 2960, 1741, 1605, 1560, 1522, 1498, 1433, 1382, 1345, 1202, 1150, 1095, 1020, 960, 906, 765, 670, 590, 565 cm^{-1}; **^{1}H NMR** (600 MHz, $CDCl_3$, 25 ºC): 7.88 (brs, 2 H, CH=N, H_{arom}), 7.43 (sb, 3 H, H_{arom}), 5.81 (s. br.1 H, 1-H), 5.35-5.03 (m, 4 H), 4.30-3.85 (m, 3 H), 2.06; (s, 6 H, CH_3), 1.99 (s, 6 H, CH_3), 1.35 (s, 9 H, CH_3(*t*Bu)) ppm; **^{13}C NMR** (150 MHz, $CDCl_3$, 25 ºC): δ =174.5 (C=S), 170.9, 170.6, 170.0, 169.5 (C=O), 158.1 (CH=N), 155.4, 132.4, 129.4, 125.3 (C_{arom}), 83.9 (1-C), 73.3 (3-C), 72.7 (2-C), 70.6 (5-C), 68.5 (4-C), 61.9 (6-C), 35.1, 31.0 (C-^{t}Bu) 20.8, 20.7, 20.6, 20.6 (CH_3) ppm. ESI MS: *m/z* = 1187.3479(1187.3458 calcd.)

Nickel(2+) bis[β-naphtylbenzaldehyde 4-(2,3,4,6-tetra-*O*-acetyl-β-D-glucopyranosyl)thiosemicarbazone, *N*, *S*] (C_4)

$C_{52}H_{56}N_6O_{18}S_2Ni$ (1175.9). Yield 86%; more than 250ºC (stable). R_f (Hex/EtOAc 1:1) = 0.17; diamagnetic. **IR (KBr)**: *v* 3410, 3368, 1740, 1539, 1497, 1432, 1366, 1234, 1207, 1091, 1030, 905, 884, 812, 747, 645, 600 cm^{-1}; **^{1}H NMR** (600 MHz, $CDCl_3$, 25 ºC): δ = 8.28 (s, 1 H, H_{arom}), 8.19 (d, J = 7.8 Hz, 1 H, H_{arom}), 7.87-7.83 (m, 2 H, H_{arom}), 7.77 (d, J = 8.4 Hz, 1H, H_{arom}), 7.69 (s, 1 H, CH=N), 7.58 (t, J = 7.2 Hz, 1 H, H_{arom}), 7.52 (t, J = 7.2 Hz, 1 H, H_{arom}), 5.90 (sb, 1H, N(4)H), 5.38(dd, $^3J_{2\text{-}H,3\text{-}H}$ = 9.0 $^3J_{3\text{-}H,4\text{-}H}$ 9.3 Hz, 1 H, 3-H), 5.21 (dd, 1 H, 2-H), 5.11 (dd, $^3J_{N(4)H,2\text{-}H}$ = 8.4. $^3J_{1\text{-}H,2\text{-}H}$ = 9.6 Hz, 1 H, 1-H), 5.04 (dd, $^3J_{4\text{-}H,5\text{-}H}$ = 9.6 Hz, 1H, 4-H), 4.34 (dd, $^3J_{5\text{-}H,6\text{-}H}$ = 4.2 $^3J_{6\text{-}H,6'\text{-}H}$ = 12.0 Hz, 1 H, 6-H), 4.15(d, $^3J_{5\text{-}H,6'\text{-}H}$ = 6.6 Hz, 1 H, 6'-H), 3.88(d, 1 H, 5-H), 2.11, 2.07, 2.05(3s, 9H, CH_3), 1.97(s, 3H, CH_3)ppm; **^{13}C NMR** (150 MHz, $CDCl_3$, 25 ºC): δ =175.0 (C=S), 170.9, 170.7, 170.0, 169.5 (C=O), 158.5 (CH=N), 134.3, 134.1, 132.5, 129.7, 129.2, 128.4, 127.8, 127.7, 127.6, 126.8 (C_{arom}), 83.9 (1-C), 73.4 (3-C), 72.7 (2-C), 70.8 (5-C), 68.4 (4-C), 61.9 (6-C), 20.8, 20.7, 20.6, 20.6 (CH_3) ppm. ESI MS: *m/z* = 1174.2

V.8.2. Palladium(II) complexes

Palladium(2+) dichloro[4-*tert*-butyl-benzaldehyde 4-(β-D-glucopyranosyl) thiosemicarbazone), *N*, *S*] (C_5)

Ligand **L_{19}** (282.5 mg; 0.5 mmol) in methanol (8 mL) and a solution of potassium tetrachloropalladate(II) (162.3 mg; 0.5 mmol) in degassed water (1.5 mL) were stirred under argon at room temperature for a weekend (the color of the solution turned from red to yellow). A precipitate was formed which was filtared, washed many times with water and then with cold methanol and ether. A double recrystallization from DMF/MeOH/Et_2O yielded a yellow solid (175 mg, 62%), m.p. >260 ºC.

$C_{18}Cl_2H_{26}N_3O_5SPd$ (573.8); **IR (KBr)**: *v* 3515, 3221, 2990, 1742, 1608, 1561, 1432, 1368, 1217, 1034, 908, 779, 599, 531 cm^{-1}; **^{1}H NMR** (600 MHz, DMSO-d_6, 25 ºC): δ = 8.21 (br s, 1 H, N(4)H), 8.20 (s, 1 H, CH=N), 8.06 (br s, 2 H, H_{arom}), 7.47 (d, J = 8.4 Hz, 2 H, H_{arom}), 5.04 (d, J = 3.6 Hz, 1 H, OH), 4.97 (d, J = 5.4 Hz, 1 H, OH), 4.92 (br s, 1 H, OH), 4.61 (s br, 2 H, 1-H and OH), 3.67 (dd, $^3J_{6\text{-}H,6'\text{-}H}$ = 13.2 Hz, $^3J_{5\text{-}H,6\text{-}H}$ = 6.0 Hz, 1 H, 6-H), 3.54–3.52 (m, 1 H, 6'-H), 3.22–3.14 (m, 4 H, 2-H, 3-H, 4-H, 5-H), 1.29 (s, 9 H, CH_3(*t*Bu)) ppm; **^{13}C NMR** (150 MHz, DMSO-d_6, 25 ºC): δ = 171.4 (C=S), 156.0 (CH=N), 155.2 (C_{arom}–*t*Bu), 133.4, 128.7, 126.1, and 126.0 (C_{arom}),

86.6 (1-C), 78.7 (3-C), 77.8 (2-C), 72.6 (5-C), 70.0 (4-C), 61.0 (6-C), 35.4 (CMe$_3$), 31.3 (CH$_3$(tBu)) ppm. ESI MS: m/z = 572.0

Palladium(2+) chloro[2-Pyridinecarboxaldehyde 4-(β-D-glucopyranosyl) thiosemicarbazone, N,N,S] (C_6)

The ligand **L'$_{20}$** (171.2 mg; 0.5 mmol) was added in portions to a solution of potassium tetrachloropalladate(II) (163.2 mg; 0.5 mmol) in water/acetonitrile 1:1 (8 mL) under argon. The mixture was stirred at room temperature for 72 h. The red mixture turned to orange. An orange solid was filtered off and washed a few times with dichloromethane and acetonitrile. The solid was recystallized twice from DMF/AcCN and dried in desiccator yielding a yellow-orange solid (202 mg, 78%), m.p. 146 ºC (dec.).

$C_{13}Cl_2H_{16}N_4O_5SPd$ (482.2); **IR (KBr)**: v 3521, 3246, 3217, 2932, 1580, 1552, 1484, 1439, 1355, 1313, 1259, 1221, 1071, 1030, 886, 767, 610, 540 cm^{-1}; **^{1}H NMR** (600 MHz, DMSO-d_6, 25 ºC): δ = 8.72 (d, $^3J_{1\text{-H,N(4)H}}$ = 9.0 Hz 1 H, N(4)H), 8.48 (d, ^3J = 4.8 Hz, 1 H, H$_{Py}$), 8.15 7.47 (t, J = 7.8 Hz, 1 H, H$_{Py}$), 8.08 (s, 1H, CH=N), 7.77 (d, J = 7.8 Hz, 1 H, H$_{Py}$), 7.47 s br, 1 H, H$_{Py}$), 4.73 (s br, 1 H, 1-H), 4.90 (s br, 4 H, OH), 3.63 (d, $^3J_{6\text{-H,6'-H}}$ = 11.4 Hz, 1 H, 6-H), 3.44–3.42 (m, 1 H, 6'-H), 3.15–3.02 (m, 4 H, 2-H, 3-H, 4-H, 5-H) ppm; **^{13}C NMR** (150 MHz, DMSO-d_6, 25 ºC): δ = 181.4 (C=S), 157.9 (CH=N), 149.6, 148.7, 141.5, 126.5, and 126.3 (C$_{Py}$), 86.3 (1-C), 78.8 (3-C), 77.5 (2-C), 72.6 (5-C), 69.9 (4-C), 61.1 (6-C) ppm. ESI MS: m/z = 480.9

V.8.3. A platinum(II) complex

Platinum(2+) [bis(1-ferrocenecarboxaldehyde 4-(β-D-glucopyranosyl) thiosemicarbazone), *N*, *S*] (C_7)

A solution of potassium tetrachloroplatinate(II) (50 mg; 0.12 mmol) in degassed water (1 mL) was added to a solution of **L'$_{23}$** (90 mg; 0.2 mmol) in methanol (9 mL), and the solution was stirred at room temperature for 12 h under argon. After 10 min. the solution became cloudy and a red precipitate was formed. The precipitate was filtered off, washed with methanol and ether and dried, yielding **C$_7$** as a red solid (74.2 mg, 68%), m.p. 210 ºC (dec.).

$C_{36}H_{44}Fe_2N_6O_{10}S_2Pt$ (1091.1); **IR (KBr)**: *v* 3317, 3247, 2990, 1740, 1591,1569, 1460, 1412, 1353, 1309, 1245, 1216, 1108, 1014, 899, 798, 736, 695, 545 cm^{-1}; **^{1}H NMR** (600 MHz, $CDCl_3$, 25 ºC): δ = 7.69 (sb, 1 H, CH=N), 7.56 (s br, 1 H, N(4)H), 5.18 (s, 1 H, Fc), 4.95 (d, 1H, OH), 4.87 (d, 1H, OH), 4.86 (s, 1H, OH), 4.68 (dd, $^3J_{1\text{-H,N(4)H}}$ = 8.4 Hz, $^3J_{1\text{-H,2-H}}$ = 9.0 Hz, 1 H, 1-H), 4.48 (t, 1H, OH), 4.42 (m, 2 H, Fc), 4.15 (s, 5 H, Fc), 4.12 (s, 1 H, Fc) 3.65-3.63 (m, 1H, 6-H), 3.45-3.43 (m, 1H, 4-H), 3.19-3.08 (m, 5 H, 2-H, 3-H, 5-H, 6'-H) ppm. ESI MS: *m/z* = 1091.7

V.9. Catalysis

V.9.1. Suzuki reaction

General Procedure: A mixture of aryl bromide (2 mmol), PhB(OH)2 (0.366 g, 3.0 mmol), potassium carbonate (0.553 g, 4.0 mmol), water (60μL, 3.3 mmol) and a stock solution of palladium(II) complex in DMF (1 mL). The solution was stirred under argon or air, at room temperature or 100°C, for 1-24h and then cooled at room temperature. After addition of water and extraction with dichloromethane, the organic phase was washed with brine, dried under Na_2SO_4, filtered, passed through Celite and analyzed by GC and GC-MS. All the biaryls prepared were known compounds.

V.9.2. Heck reaction

A Schlenk flask equipped with reflux condenser, was charged under argon or in air with 4-bromo-anisole (1.0 mmol), styrene (0.17 mL, 1.5 mmol), base (2.0 mmol), a stock solution of palladium(II) complex in DMF (**C_5,** 1 mg, 1.7 μmol in 1 mL DMF), stirred in a preheated bath for 24 h, and then allowed to cool at room temperature. After addition of aqueous NaOH and extraction with dichloromethane, the organic phase was washed with brine, dried over Na_2SO_4, filtered, passed through Celite, and analyzed by GC and GC-MS.

V.10. Glycogen phosphorylase (GP) preparation / kinetic experiments and X-ray crystallography for GP complexes

(*collaboration with the structural biology and chemistry group of IOPC/NHRF*)

All reagents were purchased from Fluka, Sigma Aldrich or Merck. Were used UV-Visible Spectrophotometer CARY 100 Conc. The water bath was regulated at 30°C.

Glycogen phosphorylase (GP*b*) was isolated from rabbit skeletal muscle and purified as described previously [347].

Kinetic studies were performed in the direction of glycogen synthesis in the presence of various concentrations of inhibitors. All kinetic experiments were carried out in the presence of 30 mM imidazole/HCl buffer 60 mM KCl, 0.6 mM EDTA, and 0.6 mM dithiothreitol (pH 6.8), 0.2% (w/v) glycogen, 1mM AMP and various concentrations of glucose-1-phosphate (Glc-1-P). Experiments were performed in the presence of 1% DMSO and K_m of the enzyme for Glc-1-P was 2.2-3.0 mM. Enzyme activity was measured at pH 6.8 by the release of inorganic phosphate as described by Saheki et al [348].

Six solutions were prepared each containing G1P at various concentrations, AMP (50 mM), which acts as an activator of the reaction, and distilled water. In more detail, the final solutions contained AMP (1mM), H_2O and the following G1P concentrations: 2 mM, 4 mM, 5 mM, 10 mM, 15 mM and 20 mM. The low concentrations of G1P are needed in order to determine the K_m of the enzyme, while the higher concentrations are needed in order to determine the V_{max} of the reaction.

After deducting the "blank" values from the recorded assay absorbance values, data were processed with the program Grafit using non-linear regression and explicit weighting. Absorbance values were converted to specific activity, which is the amount of product formed by the enzyme in a given amount of time under given conditions per milligram of enzyme. It is also a measure of the purity of the enzyme. The curve obtained from a GP*b* assay are given in Fig. 83 and the equation used in order to calculate the specific activities is the following:

$$v = \frac{1}{t} \times ln\left(\frac{limit}{limit - \mu molPi}\right) \times limit$$

The K_m and V_{max} values were calculated based on the Michaelis-Menten equation:

$$v = \frac{vmax \times [S]}{Km + [S]}$$

v: initial rate of reaction; *[S]:* substrate concentration; v_{max}*:* maximum rate of reaction

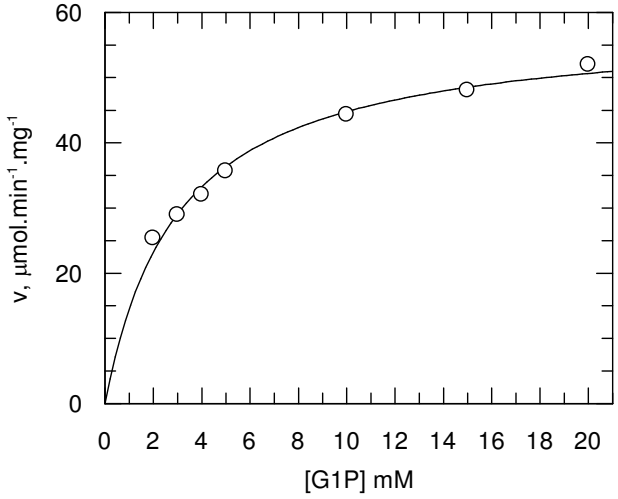

Figure 83 A curve obtained from a GP*b* assay: K_m: 2.0 ± 0.2 mM & V_{max}:50.2 ± 2.8 µmol.min^{-1}.mg^{-1}

Crystallographic binding studies were performed by diffusion of a solution of β-D-glucopyranosyl thiosemicarbazones in the crystallization media with 20% w/v of DMSO into freshly prepared GPb crystals, grown in the tetragonal lattice, space group $P4_32_12$, as previously described [349]. Experiment conditions for the formation of the GPb-inhibitor complexes were as follows: 20 mM of **L'$_2$** (13 hrs), or **L'$_8$** (16 hrs), or **L'$_3$** (11.5 hrs), or **L'$_4$** (16 hrs), or **L'$_5$** (21 hrs), or **L'$_{13}$** (21 hrs), or **L'$_{14}$** (3.5 hrs), or **L'$_{15}$** (21hrs), or **L'$_{19}$** (3.5 hrs), or **L'$_{23}$** (7 hrs), 10 mM **L'$_9$** (7 hrs), 5 mM **L'$_{10}$** (18 hrs), 6.7 mM **L'$_{12}$** (3 hrs), or **L'$_{18}$** (3 hrs), and 10 mM **L'$_7$** (7 hrs). Diffraction data were collected at EMBL-Hamburg outstation (Beamline X13), Daresbury Synchrotron Laboratory, UK (Beamline PX 10.1) and Max-Lab, Lund (Beamline ID9111-2). Crystal orientation, integration of reflections, inter-frame scaling, partial reflection summation, data reduction and post-refinement were all performed using the HKL programme suite [350].

Crystallographic refinement of the complexes was performed by maximum-likelihood methods using REFMAC [351]. The starting model employed for the refinement of the complexes was the structure of the native T state GPb complex determined at 1.9 Å resolutions (Leonidas et al., unpublished results). Ligand models of the compounds were fitted to the electron density maps after adjustment of their torsion angles. Alternate cycles of manual rebuilding with 'COOT' and refinement with REFMAC improved the quality of the models. The stereochemistry of the protein residues was validated by PROCHECK [352]. Hydrogen bonds and van der Waals interactions

were calculated with the program CONTACT as implemented in CCP4 [353] applying a distance cut off 3.3 Å and 4.0 Å, respectively. Protein structures were superimposed using LSQKAB. The figures were prepared with the programs MolScript [354], Bobscript [355] and rendered with Raster3D [356]. The coordinates of the new structures have been deposited with the RCSB Protein Data Bank (http://www.rcsb.org/pdb) with codes 3MQF (**L'$_2$**), 3MTA (**L'$_7$**), 3MT7 (**L'$_8$**), 3MS7 (**L'$_3$**), 3MTB (**L'$_4$**), 3MT8 (**L'$_5$**), 3MS4 (**L'$_9$**), 3MSC (**L'$_{10}$**), 3MT9 (**L'$_{12}$**), 3NC4 (**L'$_{13}$**), 3MRV (**L'$_{14}$**), 3MTD (**L'$_{15}$**), 3MRX (**L'$_{18}$**), 3MS2 (**L'$_{19}$**) and 3MRT (**L'$_{23}$**).

VI. Abstract

VI.1. Abstract

A series of twenty six aromatic aldehyde/ketone 4-(β-D-glucopyranosyl)thiosemicarbazones (βGluTSC) have been synthesized by condensation of 4-(per-O-acetylated-β-D-glucopyranosyl)thiosemicarbazide with an aldehyde or ketone, and then, deacetylation of the resulting product. The thiosemicarbazone part of the studied glucosyl thiosemicarbazones possess a moiety derived from substituted benzaldehydes with NO_2, F, Cl, Br, OH, OMe, CF_3, *t*Bu or Me at the *ortho*-, *meta*- or *para*-position of the aromatic ring as well as a moiety derived from 2-, 3- or 4-pyridinecarboxaldehyde, 1-ferrocenecarboxaldehyde, β-naphthalenecarboxaldehyde, 4-methoxy-acetophenone or 2-acetonaphthanone. The compounds were fully characterized by spectroscopic techniques, elemental analysis, and for two derivatives by X-ray analysis. The data indicate the β configuration, and the *E* configuration pertaining to the stereochemistry of the C=N bond. However, a partial conversion of the *E* into the *Z* form is possible in solution after several hours.

Since glycogen phosphorylase (GP) is a promising target for the treatment of type 2 diabetes, in the process of structure based drug design for GP, fifteen of the above-mentioned aromatic aldehyde 4-(β-D-glucopyranosyl)thiosemicarbazones were evaluated as inhibitors of rabbit muscle glycogen phosphorylase b (GP*b*) by kinetic studies. These compounds are competitive inhibitors of GP*b* with respect to α-D-glucose-1-phosphate with IC_{50} values ranging from 5.7 to 524.3 μM. In order to elucidate the structural basis of their inhibition, the crystal structures of these compounds in complex with GP*b* at 1.95-2.23 Å resolution were determined. The complex structures reveal that the inhibitors are accommodated at the catalytic site with the glucopyranosyl moiety at approximately the same position as α-D-glucose and stabilize the T conformation of the 280s loop. The molecules fit tightly into the β-pocket, a side channel from the catalytic site with no access to the bulk solvent. The differences in their inhibitory potency can be interpreted in terms of variations in the interactions of the aldehyde-derived moiety with protein residues in the β-pocket. In addition, fourteen out of the fifteen studied inhibitors were found bound at the new allosteric site of the enzyme.

Mononuclear Ni(II) (diamagnetic as well as paramagnetic), Pd(II) and Pt(II) complexes with βGluTSC derivatives have also been prepared. The structures features of the complexes have been characterized by NMR, FT-IR and mass spectroscopy. A palladium(II) complex was found to be an efficient catalyst for the Suzuki and Heck reactions even in air atmosphere.

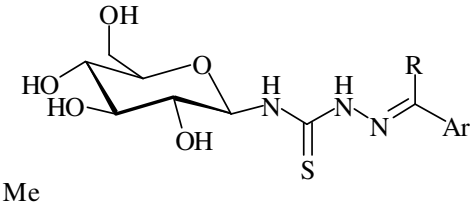

R = H, Me

Ar = -C_6H_4-X (*o*,*m*,*p*), pyridyl (2-,3-,4-), ferrocenyl, β-naphthyl

X = F, Cl, Br, CF_3, NO_2, OH, OMe, Me, *t*Bu

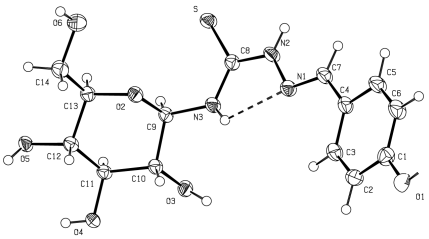

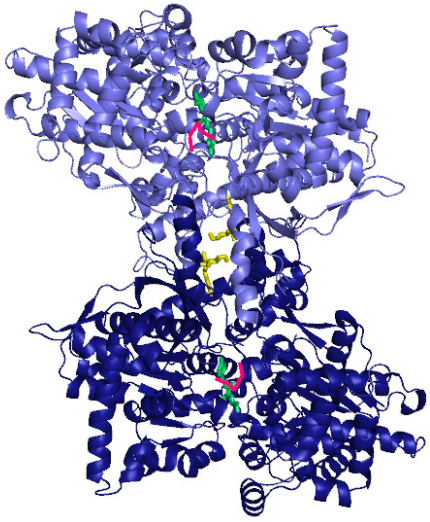

VI.2. Περίληψη

Μια σειρά από 26 αρωματικές αλδεΰδες/κετόνες 4-(β-D-γλυκοπυρανοζυλο)θειοημικαρβαζόνες (βGluTSC) έχουν παρασκευασθεί κατά την συμπύκνωση 4-(περ-O-ακετυλιωμένου-β-D-γλυκοπυρανοζυλο)θειοημικαρβαζιδίου με μια αλδεΰδη ή κετόνη και στη συνέχεια αποακετυλίωση. Το τμήμα της θειοημικαρβαζόνης των προς μελέτη παραγώγων προέρχεται από υποκατεστημένες βενζαλδεΰδες με NO_2, F, Cl, Br, OH, OMe, CF_3, *t*Bu ή Me στην *ορθο*-, *μετα*- ή *παρα*-θέση του αρωματικού δακτυλίου καθώς επίσης και από 2-, 3- ή 4-πυριδινο-καρβοξαλδεΰδη, 1-φερροκενο-καρβοξαλδεΰδη, β-ναφθαλενο-καρβοξαλδεΰδη, 4-μεθοξυ-ακετοφαινόνη ή 2-ακετοναφθόνη. Οι ενώσεις χαρακτηρίσθηκαν πλήρως με φασματοσκοπικές τεχνικές, στοιχειακές αναλύσεις και για δύο από αυτές με ανάλυση ακτίνων X. Τα δεδομένα υποδεικνύουν την β-διαμόρφωση καθώς και την *E*-διαμόρφωση για την στερεοχημεία του δεσμού C=N. Εντούτοις, μερική μετατροπή της δομής *E* σε *Z* είναι δυνατή σε διάλυμα μετά από μερικές ώρες.

Δεδομένου ότι η φωσφορυλάση του γλυκογόνου (GP) είναι ένας υποσχόμενος στόχος για την θεραπεία του διαβήτη τύπου 2, στην διαδικασία του σχεδιασμού φαρμάκων με βάση την δομή, 15 από τις παραπάνω αρωματικές αλδεΰδες 4-(β-D-γλυκοπυρανοζυλο)θειοημικαρβαζόνες αξιολογήθηκαν ως αναστολείς της φωσφορυλάσης του γλυκογόνου b (GPb) μυών κουνελιού με κινητικές μελέτες. Οι παραπάνω ενώσεις ανταγωνίζονται ως αναστολείς της GPb την 1-φωσφορική α-D-γλυκόζη με τιμές IC_{50} από 5,7 έως 524,3 μM. Προκειμένου να διευκρινισθεί η σχέση της δομής τους με την ανασταλτική τους δραστικότητα, προσδιορίστηκαν οι κρυσταλλικές δομές των συμπλόκων αυτών των ενώσεων με την GPb σε ευκρίνεια 1,95-2,23 Å. Οι κρυσταλλικές δομές αποκάλυψαν ότι αναστολείς αυτοί προσδένονται στο καταλυτικό κέντρο του ενζύμου με το γλυκοπυρανόζυλο τμήμα περίπου στην ίδια θέση με την α-D-γλυκόζη και σταθεροποιούν την T-διαμόρφωση του 280s βρόχου. Τα μόρια δένονται σφικτά στο β-θυλάκιο, ένα πλευρικό κανάλι από το καταλυτικό κέντρο χωρίς πρόσβαση στον διαλύτη. Οι διαφορές στην ανασταλτική τους ικανότητα μπορούν να ερμηνευτούν με βάση την ποικιλία των αλληλεπιδράσεων των διαφορετικών αλδεϋδικών τμημάτων με πρωτεϊνούχα κατάλοιπα στο β-θυλάκιο. Επιπρόσθετα, 14 από τις 15 ενώσεις που μελετήθηκαν δένονται επίσης και στο νέο αλλοστερικό κέντρο του ενζύμου.

Έχουν παρασκευασθεί επίσης μονοπυρηνικά σύμπλοκα Ni(II) (διαμαγνητικά καθώς και παραμαγνητικά), Pd(II) και Pt(II) με βGluTSC. Ο τρόπος συναρμογής στα σύμπλοκα αυτά

μελετήθηκε με φασματοσκοπία NMR, FT-IR και MS. Ένα σύμπλοκο του παλλαδίου αποδείχθηκε δραστικός καταλύτης στις αντιδράσεις Suzuki και Heck ακόμη και στον αέρα.

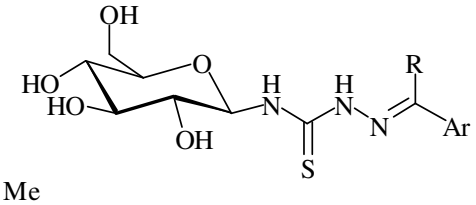

R = H, Me
Ar = -C_6H_4-X (*o*,*m*,*p*), pyridyl (2-,3-,4-), ferrocenyl, β-naphthyl
X = F, Cl, Br, CF_3, NO_2, OH, OMe, Me, *t*Bu

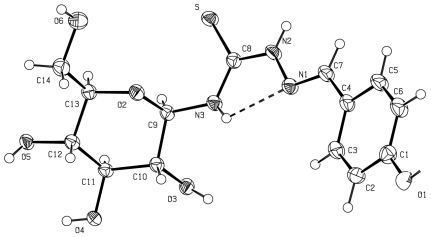

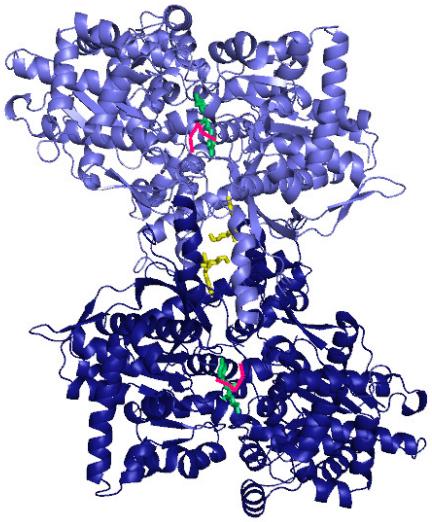

VI. References

1. R. J. Linhardt, T. Toidam *Carbohydrates in drug design 1997,* Marcel Dekker: New York.

2. K. L. Goa, P. Benfield *Drugs* **1994**, *47*, 536.

3. H. Sashiwa, S. Tripathy, R. Roy *Biomacromolecules* **2000**, *1*, 303.

4. T. E. McAlindon, M. P. LaValley, J. P. Gulin, D. T. Felson *J. Am. Med. Assoc.* **2000,** *283*, 1469.

5. C. E. Matthews, K. E. van Holder, K. G. Ahern *Biochemistry* **1999**, (3rd Ed.), Benjamin Cummins.

6. L. C. Maillard *C. R. Acad. Sci., Ser. 2* **1912**, *154*, 66.

7. F. Ledl, E. Schleicher *Angew. Chem.* **1990**, *102*, 597.

8. J. J. Turner, N. Wilschut, H. S. Overkleeft, W. Klaffke, G. A. Van Der Marel, J. H. Van Boom *Tetrahedron Lett.* **1999**, *40*, 7039.

9. E. Fisher *Berichte der deutschen chemischen Gesellschft* **1980**, 23, 799.

10. J. Fuentes, J. Moreda, C. Ortiz, I. Robina, C. Welsh *Tetrahedron* **1992**, 31, 6413.

11. I. Bokor, T. Docsa, P. Gergely, L. Somsak *Bioorg. Med. Chem.* **2010**, 18, 1171.

12. M. Jacobsson, J. Malmberg, U. Ellervik *Carbohydr. Res.* **2006**, 341, 1266.

13. J. M. Langenhan, J. S. Thorson *Current Organis Synthesis* **2005**, 2, 59.

14. A. P. Rauter, N. M. Xavier, S. D. Lucas, M. Santos *Adv. Carbohydr. Chem. And Biochem.* **2010,** 63, 29.

15. P. M. Dewick *Medicinal Natural Products: A Byosynthetic Approch* (2nd Ed.) **2002** UK.

16. I. Brudziñska, Y. Mikata, M. Obata, C. Ohtsuki, S. Yano *Bioorg. Med. Chem.* **2004**, 14, 2533.

17. G. Pratviel, J. Bernadou, and B. Meunier *Angew. Chem., Int. Ed. Engl*. **1995**, 34, 746.

18. M. R. Hansen, and L. H. Hurley *Acc. Chem. Res*., **1996**, 29, 249.

19. S. Hemmerich *Drug Discovery Today* **2001**, 6, 27.

20. F. Wimmer, S. Wimmer, P. Castan, S. Cros, N. Johnson, E. Colacio-Rodigez *Anticancer Res*. **1989**, 9, 791.

21. H. Kunz *Angew. Chem. Int. Ed. Engl.* **1987**, 26, 294.

22. Y. Mikata, Y. Shinohara, K. Yoneda, Y. Nakamura, I. Brudziñska, T. Tanase, T. Kitayama, R. Takagi, T. Okamota, I. Kinoshita, M. Doe, C. Ovrig, S. Yano *Bioorg. Med. Chem. Lett.* **2001**, 11, 3045.

23. L. M. Likhosherstov, O. S. Novikova, V. A Derevitskaja, N. K. Kochelkov *Carbohydr. Res.* **1986**, 146, C1–C5.

24. L. Lalegerie, J. Yon, *Biochimie* **1982**, 64, 977.

25. D. E. Walker, B. Axelrod *Arch. Biochem. Biophys.***1978**, 187, 102.

26. E. Truscheit, W. Frommer, B. Junge, L. Müllerd, D. Schmidt, W. Wingender *Angew. Chem. Znt. Ed. Engl*., **1981**, 20, 744.

27. H. Y. L. Lai, B. Axelrod *Biochem. Biophys. Res. Commun.* **1973**, 54, 462.

28. A. Lubineau, J. Auge, B. Drouillat *Carbohydr. Res.* **1995**, 266, 211. I.

29. S. Kamiya, H. Minamikawa, J. H. Jung, B. Yang, M. Masuda, T. Shimizu *Langmuir* **200**5, 21, 743.

30. F. Cateni, P. Boniveto, G. Procida, M. Zacchigna, L. G. Favretto, G. Scialino, E. Banfi *Bioorg. Med. Chem.* **2007**, 15, 815.

31. V. M. Díaz Pérez, C. Ortiz Mellet, J. Fuentes, J. M. García Fernández *Carbohydr. Res.* **2000**, 326, 161.

32. P. Allevi, M. anastasia, P. Ciuffreda *Tetrahedron Letts.* **1993**, 34, 7313.

33. N. A. Al-Masoudi, Y. A. Al-Soud *Tetrahedron Letts.* **2002**, 43, 4021.

34. V. H. Lillelund, H. H. Jensen, X. Liang, M. Bols *Chem. Rev.* **2002**, 102, 515.

35. A. A.-H. Abdel, E. S. H. Al Ashry, R. R. Schmidt *Carbohydr. Res.* **1999**, 315, 106.

36. L. Kiss, L. Somsák *Carbohydr. Res.* **1996**, 291, 43.

37. W. Lai, O. R. Martin *Carbohydr. Res.* **1993**, 250, 185.

38. G. Legler, M. Herrchen *Carbohydr. Res.* **1983**, 116, 95.

39. Z. Györgydeák, Z. Hadady, N. Felföldi, A. Krakomperger, V. Nagy, M. Tóth, A. Brunyánszki, T. Docsa, P. Gergely, L. Somsák *Bioorg. Med. Chem.* **2004**, 12, 4861.

40. S. Hanessian, *Preparative Carbohydrate Chemistry* **1996**.

41. E. Schmitz, I. Eichorn *The Chemistry of the Ether Linkage* (S. Patai, Ed.) Interscience, New York **1967**, 309.

42. F. A. Carey, R. J. Sundberg *Advanced Organic Chemistry: Part A Structure and mechanism* (4^{th} Ed.) University of Virginia Published New York **2000**, 70.

43. J. March *Advanced Organic Chemistry*: Wiley, 4th Ed. **1992**.

44. IUPAC *Compendium of Chemical Terminology*, 2nd Ed. (the "Gold Book") **1997**.

45. R. A. Sheldon *Chirotechnology* **1993**, Dekker, New York. (INTRODUCERE)

46. R. D.Gillard, J. A.McCleverty *Comprehensive Coordination Chemistry*, Eds. Wilkinson, Pergamon Press, Oxford, **1987**.

47. F. E. Anderson, J. C. Duca, J. W. Scudi *J. Chem. Soc.* **1951**, 4967.

48. B. A. Gingras, R. W. Hornal, C. H. Bayleycan. *J. Chem.* **1960**, 38, 712.

49. P. Guerreiro, S. Tamburini, V. A.Vigato *Coord. Chem. Rev*. **1995**, 139, 17.

50. S. Padhye, G.B. Kauffman *Coord. Chem. Rev.* **1985**, 63, 127.

51. T. S. Lobana, R. Sharma, G. Bawa, S. Khanna *Coord. Chem. Rev.* **2009**, 253, 977.

52. D. L. Klayman, J. E. Bartosevich, T. S. Griffin, C. J. Mason, J. P. Scovill *J. Med. Chem.* **1979**, 22, 855.

53. D. L. Klayman, A. J. Lin *Org. Prep. Proced. Int.* **1984**, 16, 79.

54. J. P. Scovill, *Phosphorous, Sulfer, Silicone* **1991**, 60, 15.

55. J. J. Blanksma *Rs. Trav. Chim.* **1910**, 29, 408.

56. D. L. Klayman, J. P. Scovill, J. F. Bartosevich, J. Bruce *J. Med. Chem.* **1983**, 26, 35.

57. S. Halder *Polyhedron* **2007**, 26, 2741.

58. G. D. Andreetti, P. Domiano, G. Gasparri Fava, M. Nardeli, P. Sgarabotto *Acta Crystallogr. Sect. B* **1970**, 26, 1005.

59. T. P Stanojkovic, D. Kovala-Demertzi, A. Primikyri, I. Garcia-Santos, A. Catineiras, Z. Juranic, M. A. Demertzis *J. Inorg. Biochem*. **2010**, 104, 467.

60. C. K. Bhaskare, P. P. Hankare, R. S., Ranpure *J. Indian Chem. Soc.* **1988**, 65, 121.

61. D. X. West, R. M. Makeever, J. P. Scovill, D. L. Klayman *Polyhedron* **1984**, 3, 947.

62. M. D. Timken, S. R. Wilson, D. N. Hendrickson *Inorg. Chem*. **1985**, 24, 3450.

63. D. X. West, J. P. Scovill, J. Silverton, A. Bavoso *Transition Met. Chem.* **1986**, 11, 123.

64. D. X. West, A. E Liberta, S. B. Padhye, R C. Chikate, P. B Sonawane, A. S. Kumbhar, R. G. Yerande *Coord. Chem. Rev.* **1993**, 123, 49.

65. D. Chattopadhyay, S. K. Mazumdar, T. Banerjee, W. S. Sheldrick *Acta Crystallogr. Sect. C* **1989**, 45, 314.

66. J. N. Brown, K. C. Agrawal *Acta Crystallogr. Sect. B* **1978**, 34, 2038.

67. G. J. Palenik, D. F. Rendle, W. S. Carter *Acta Crystallogr. Sect B* **1974**, 30, 2390.

68. F. H. Allen, O. Kennard, D. G. Watson, L. Brammer, A. G. Orpen, R. Taylor *J. Chem. Soc. Dalton Trans* **1987** S1.

69. J. S. Casas, M. S. García-Tasente, J. Sordo *Coord. Chem. Rev.* **2000**, 209, 197.

70. L. A. Saryan, E. Ankel, C. Krishnamurti, D. H. Petering, H. J. Elford*, J. Med. Chem.* **1979**, 22, 1218.

71. N. C. Desai, H. K. Shukla, B. R. Parekh, K. A. Thaker *J. Indian Chem. Soc.* **1984**, 455.

72. B. Rosenberg, L. Van Camp, T. Krigas *Nature* **1965**, 205, 698.

73. J. L. Butour, S. Wimmer, F. Wimmer, P. Castan *Chem. Biol. Inter.* **1997**, 104, 165.

74. M. Das, S. E. Livingstone *Br. J. Cancer* **1978**, 37, 466.

75. S. Ghosh, A. K. Misra, G. Bhatia, M. M. Khan, A. K. Khanna *Bioorg. Med. Chem. Lett.* **2009**, 19, 386.

76. D. R. Richardson, K. Milnes *Blood* **1997**, 89, 3025.

77. A. Garoufis, S. K. Hadjikakou, N. Hadjilliadis *Coor. Chem. Rev.* **2009**, 253, 1384.

78. N.Takahashi, Y. Fujibayashi, Y. Yonekura, M. J. Welch, A.Waki, T. Tsuchida, N. Sadato, K. Sugimoto, H. Itoh *Ann. Nucl. Med.* **2000**, 323.

79. M. D. Yu, M. A. Green, B. H. Mock, S. M. Shaw *J. Nucl. Med.* **1989**, 920.

80. C. J. Anderson, M. J. Welch *J. Chem. Rev.* **1999**, 2219.

81. J. P. Holland, F. I. Aigbirhio, H. M. Betts, P. D. Bonnitcha, Paul Burke, Martin Christlieb, G. C. Churchill, A. R. Cowley, J. R. Dilworth, P. S.Donnelly, J. C. Green, J. M. Peach, S. R. Vasudevan, J. E. Warren *Inorg. Chem.*, **2007**, 46, 465.

82. J. S. Lewis, T. L. Sharp, R. Laforest, Y. Fujibayashi, M. J. Welch *J. Nucl. Med.* **2001**, 42, 655.

83. D. J. Bauer, L. St. Vincent, C. H. Kempe, A. W. Downie *The Lancet* **1963**, 282, 494.

84. A.-M. Tsimberidou, Y. Alvarado, Y. Alvarado *Expert Rev. Anticancer Ther.* **2002**, 2, 437.

85. J. G. Tojal, A. G. Orad, J. L. Serra, J. L. Pizarro, L. Lezama, Arriortua, T. Rojo *J. Inorg. Biochem.* **1999***,* 75, 45.

86. M. Joseph, M. Kuriakose, M. R. P. Kurup, E. Suresh, A. Kishore, S. G. Bhat *Polyhedron* **2006**, 25, 61

87. S. K. Jain, B. S. Garg, Y. K. Bhoon *Spectrochim. Acta A* **1986***,* 42, 959.

88. M. E. Hossain, M. N. Alam. J. Begum, M. A. Ali, M. Nazimudhin, F. E. Smith, R. C. Hynes *Inorg. Chim. Acta* **1996**, 249, 207.

89. W.-Hu, W. Zhou, C.-Xia, X. Wen *Bioorg. Med. Chem. Lett.* **2006**, 16, 2213.

90. D. Kovala-Demertzi, A. Domopoulou, M. A. Demertzis, G. Valle, A. Papageorgiou *J. Inorg. Biochem* **1997**, 68, 148.

91. J. S. K. Chen, N. Agarwal, K. Mehta *Breast Cancer Res. Treat.* **2002**, 71, 237.

92. S. Padhye, Z. Afrasiabi, E. Sinn, J. Fok, K. Mehta, N. Rath *Inorg.Chem*. **2005**, 44, 1154.

93. D. Kovala-Demertzi, M. A. Demertzis, J. R. Miller, C. Papadopoulou, C. Dodorou, G. Filousis *J. Inorg. Biochem*. **2001**, 86, 555.

94. Z. Iakovidou, A. Papageorgiou, M. A. Demertzis, E. Mioglou, D. Mourelatos, A. Kotsis, P. N. Yadav, D. Kovala-Demertzi *Anti-Cancer Drugs* **2001**, 12, 65.

95. D. Singh, R. V. Singh, R. B. Goyal *Appl. Organomet. Chem*. **2004**, 5, 45.

96. D. Kovala-Demertzi, P. N. Yadav, J. Wiecek, S. Skoulika, T. Varadinova, M. A. Demertzis *J. Inorg. Biochem*. **2006**, 100, 1558.

97. D. Kovala-Demertzi, P. N. Yadav, M. A. Demertzis, M. Coluccia *J. Inorg. Biochem.* **2000**, 78, 347.

98. D. Kovala-Demertzi, A. Papageorgiou, L. Papathanasis, A. Alexandratos, P. Dalezis, J. R. Miller, M. A. Demertzis *European J. Med. Chem.* **2009**, 44, 1296.

99. T. Atalay, E. G. Akgemci *Tr. J. Chem.* **1998**, 22, 123.

100. R. B. Singh, B. S. Garg, R.P. Singh *Talanta.* **1978**, 25, 619.

101. J. E. J. C. Graudo, C. A. L. Filgueiras, A. M-Netto, A. Batista *J. Braz. Chem. Soc.* **2000**, 11, 237.

102. Y. Khuhawar, Z.P. Memon, S.N. Lanjwani *Chromatographia* **1995**, 41, 236.

103. P. C. Okafor, E. E. Ebenso, U. J. Ekpe *Bull. Chem.Soc. Ethiopia* **2004**, 18, 181.

104. A. R. Cowley, J. Davis, J. R. Dilworth, P. S. Donnelly, R. Dobson, A. Nightingale, J. P. Peach, B. Shore, D. Kerr, L. Seymour *Chem. Comm.* **2005**, 845.

105. D. Kovala-Demertzi, P. N. Yadav, M. A. Demertzis, J. P. Jasinski, F. J. Andreadaki, I. D. Kostas *Tetrahedron Lett.* **2004**, 45, 2923.

106. I. D. Kostas, F. J. Andreadaki, D. Kovala-Demertzi, C. Prentjas, M. A. Demertzis *Tetrahedron Lett*. **2005**, 46, 1967.

107. I. D. Kostas, G. A. Heropoulos, D. Kovala-Demertzi, P. N. Yadav, J. P. Jasinski, M. A. Demertzis, F. J. Andreadaki, G. Vo-Thanh, A. Petit, A. Loupy *Tetrahedron Lett.* **2006**, *47*, 4403.

108. Moller, D.E. *Nature,* **2001**, *414*, 821.

109. N. G. Oikonomakos, *Curr. Protein Pept. Sci.* **2002**, 5, 561.

110. P. Zimmet, K.G.M.M. Albert, J. Shaw *Nature* **2001**, 414, 782-787.

111. B. R. Henke, *J. Med. Chem.* **2004**, 47, 4118.

112. B. B. Zhang, D. E. Moller *Cur. Opin. Chem. Biol.* **2000**, 4, 461.

113. L. N. Johnson *FASEB J*. **1992**, 6, 2274.

114. M. Board, M. Hadwen, L. N. Johnson *Eur. J. Biochem.* **1995**, 228, 753.

115. N. G. Oikonomakos, L. Somsák *Curr Opin Investig Drugs* **2008**, 9, 379.

116. M. N. Kosmopoulou, D. D. Leonida, E. D. Chrysina, N. Bischler, G. Eisenbrand, C. E. Sakarellos, R. Pauptit, N. G. Oikonomakos *Eur. J. Biochem.* **2004**, 271, 2280.

117. N. G. Oikonomakos, J. B. Schnier, S. E. Zographos, V. T. Skamnaki, K. E. Tsitsanou, L. N. Johnson *J. Biol. Chem.* **2000**, 275, 34566.

118. L. N. Johnson, J. Hajdu, K. R. Achatya, D. I. Stuard, P. J. McLaughlin, N. G. Oikonomakos, D. Bardford *Allosteric Enzyme*(G. Herve, Ed.) **1989**, 81.

119. L. Somsak, K. Czifrak, M. Toth, E. Bokor, E. D. Chrysina, K. M. Alexacou, J. M. Hayes, C. Tiraidis, E. Lazoura, D. D. Leonidas, S. E. Zographos, N. G. Oikonomakos *Curr. Med. Chem.* **2008,** *15*, 2933.

120. L. N. Johnson, J. Cheetham, P. J. McLaughlin, K. R. Acharya, D. Bardford, D. C. Phillips *Curr. Top. Microbiol. Immunol.* **1988**, 139, 81.

121. N. Pinotsis, D. D. Leonida, E. D. Chrysina, N. G. Oikonomakos, I. M. Mavvridis *Protein Sci.* **2003**, 12, 1914.

122. S. E. Zographos , N.G. Oikonomakos, K. E. Tsitsanou, D. D. Leonida, E. D. Chrysina, V. T. Skamnaki, H. Bischoff, S. Goldmann, K. A. Watson, L. N. Johnson *Structure* **1997**, 5, 1413.

123. N.G. Oikonomakos, K. E. Tsitsanou, S. E. Zographos, V. T. Skamnaki, S. Goldmann, H. Bischoff *Protein Sci.* **1999**, 8, 1930.

124. K. E. Tsitsanou, V. T. Skamnaki, N.G. Oikonomakos *Arch. Biochem. Biophys*. **2000**, 384, 245.

125. N. G. Oikonomakos, V. T. Skamnaki, K. E. Tsitsanou, N. G. Gavalas, L. N. Johnson *Structure* **2000**, 8, 575.

126. V. L. Rath, M. Ammirati, D. E. Danley, J. L. Ekstrom, E. M. Gibbs, T. R. Hynes, A. M. Mathiowetz, R. K. mcPherson, T. V. Olson, J. L. Treadway, D. J. Hoover *Chem. Biol.* **2000**, 7, 677.

127. L. Somsak, V. Nagy, Z. Hadady, T. Docsa, P. Gergely *Current Pharmaceutical Design* **2003**, 9, 1177.

128. S. Alemany, P. Cohen *FEBS Lett.* **1986**, 198, 194.

129. M. Bollen, W. Stalmans *Crit. Rev. Biochem. Mol. Biol.* **1992**, 27, 227.

130. D. J. Baker, J. A. Timmons, P. L. Greenhaff *Diabetes* **2005,** *54*, 2453.

131. W. Stalmans,H. De Wulf, L. Hue, H. G. Hers *Eur. J. Biochem*. **1974**, 41, 127.

132. J. Monod, J. P. Changeux, F. Jacob *J. Mol Biol.* **1965***,* 2, 88.

133. J. I. Martin, L. N. Johnson, S. G. Withers *Biochemistry* **1990***,* 29, 10745.

134. N. K. Vyas, M. N. Vyas, F. A. Quiocho, *Science* **1988**, 242, 1290.

135. F. A. Quiocho, *Pure Appl. Chem.* **1989**, 61, 1293.

136. L. Somsák, N. Felfö, B. Kónya, C. Hüse, K. Telepó, É. Bokor, K. Czifrák, *Carbohydr. Res.*, **2008**, 343, 2083.

137. N. G. Oikonomakos, M. Kontou, S. E. Zographos, K. A. Watson, L. N. Johnson, C. J. F. Bichard, G. W. J. Fleet, K. R. Achrya *Protein Sci.* **1995**, 4, 2469.

138. N. G. Oikonomakos, M. N. Kosmopoulou, S. E. Zographos, D. D. Leonida, E. D. Chrysina, L. Somsák, V. Nagy, J.-P. Praly, T. Docsa, B. Ttoth, P. Gergely *European J. Biochem.* **2002**. 269, 1684.

139. C. J. F. Bichard, E. P. Mitchell, M. R. Wormald, K. A. Watson, L. N. Johnson, S. E. Zographos, D. D. Koutra, N. G. Oikonomakos, G. W. J. Fleet *Tetrahedron Lett.* **1995**, 36, 2145.

140. Z. Györgydeák, Z. Hadady, N. Felföldi, A. Krakomperger, V. Nagy, M. Tóth, A. Brunyánszky, T. Docsa, P. Gergely, L. Somsák, *Bioorg. Med. Chem.* **2004**, 12, 4861.

141. E. I. Petsalakis, E. D. Chrysina, C. Tiraidis, T. Hadjiloi, D. D. Leonida, N. G. Oikonomakos, U. Aich, B. Varghese, D. Loganathan *Bioorg. Med. Chem.* **2006**, 14, 5316.

142. E. Bokor, T. Docsa, P. Gergely, L. Somsák *Bioorg. Med. Chem.* **2010**, 18, 1171.

143. J. L. Martin, K. Veluraja, K. Ross, L. N. Johnson, G. W. J. Fleet, N. G. Ramsden, I. Bruce, M. G. Orchard, N. G. Oikonomakos, A. C. Papageorgiou, D. D. Leonida, H. S. Tsitoura *Biochemistry* **1991**, 30, 10101.

144. K. A. Watson, E. P. Mitchell, L. N. Johnson, J. C. Son, C. J. F. Bichard, M. G. Orchard, G. W. J. Fleet, N. G. Oikonomakos, D. D. Leonida, M. Kontou, A. C. Papageorgiou *Biochemistry* **1994**, 33, 5745.

145. N. G. Oikonomakos, V. T. Skamnaki, E. Ösz, L. Szilágyi, L. Somsák, T. Docsa, B. Tóth, P. Gergely *Bioorg. Med Chem.* **2002**, 10, 261.

146. T. M. Krülle, C. De la Fuente, K. A. Watson, M. Gregoriou, L. N. Johnson, K. E. Tsitsanou, S. E. Zographos, N. G. Oikonomakos, G. W. J. Fleet *Synlett* **1997**, 211.

147. K. E. Tsitsanou, N. G. Oikonomakos, S. E. Zographos, V. T. Skamnaki, M.Gregoriou, K. A. Watson, L. N. Johnson, G. W. J. Fleet *Protein Sci.* **1999**, 8, 741.

148. N. Felföldy, M. Tóth, E. D. Chrysina, M.-C. Charavgi, K.-M. Alexacou, L. Somsák *Carbohydr .Res.* **2010**, 345, 208.

149. P. J. Goodford *J. Med. Chem.* **1985**, 28, 849.DIABETES

150. K. J. Laidler, J. H. Meiser, *Physical Chemistry*, Benjamin/Cummings, **1982**, 423.

151. M. W. Roberts, *Catalysis Letters,* **2000**, 67, 1, 1-4.

152. L.R. MacGillivray, J. L. Reid, J. A. Ripmeester, *J. Am. Chem. Soc.* **2000**, 122, 32, 7817.

153. X. Cai, X. Dong, W. Lin, *J. Natural Gas Chem.* **2006**, 15, 122.

154. P. G. Cozzi, A. Mignona, and P. Vicennati *Adv. Synth. Catal.* **2008**, 350, 975.

155. H. Goa, R. J. Angelici, *J. Molec. Catal. A; Chemical* **1999**, 149, 63.

156. L.-G. Qiu, A.-j. Xie, Y.-H. Shen, *J. Molec. Catal. A; Chemical* **2006**, 244, 58.

157. D. P. Allen, C. M. Crudden, L. A. Calhoun, R. Wang, *J. Organomett. Chem.* **2004**, 689, 3203.

158. O. Roelen Chemische Verwertungsgesellschaft Oberhausen m.b.H. DE **1943**, 849.548 (1938/1952) and US 2.327.066.

159. D. Evans, J. A. Osborn, F. H. Jardine, G. Wilkinson *Nature* **1965**, 208, 1203.

160. M. Beller, C. Bolm *Transition Metals for Organic Synthesis* 2nd Ed.; Wiley-VCH: Weinheim **2004**.

161. S. Bhaduri, D. Mukesh *Homogeneous Catalysis: Mechanisms and Industrial Applications*; John Wiley & Sons, Inc.: New York, **2000**.

162. G. Rothenberg *Catalysis: Concepts and green applications* **2008**, 1.

163. T. Yanagisawa, T. Shimizu, K. Kuroda, C. Kato *Bull. Chem. Soc. Jpn*. **1990**, 63, 988.

164. R. Shirt, M. Garland, D. W. T. Rippin *Analytica Chimica Acta* **1998**, 374, 67

165. F. Ullman *Chem. Berichte* **1901**, 34, 2174.

166. P. E. Fanta *Synthesis* **1974**, 9.

167. P. W. Van Leeuwen *Homogeneous Catalysis: Understang the Art 1st Ed.* **2005**.

168. D. M. Chisholm, J. S. McIonde *Dalton Trans* **2008**, 3933.

169. N. Miyaura, T. Yanagi, A. Suzuki *Synth. Commun.* **1981**, 11, 513.

170. N. T. S. Phan, M. Van Der Sluys, C. W. Jones, *Adv. Synth. Catal.* **2006**, 348, 609.

171. A. K. Diallo, C. Ornelas, L. Salmon, J. R. Aranzaes, D. Astruc, *Angew. Chem. Int. Ed.* **2007**, 46, 8644.

172. A. V. Gaikwad, A. Holuigue, M. B. Thathagar, J. E. ten Elshof, G. Rothenberg, *Chem. Eur. J.* **2007**, 13, 6908.

173. J. M. Richardson, C. W. Jones, *J. Catal.* **2007**, 251, 80.

174. G. Budroni, A. Corma, H. García, A. Primo, *J. Catal.* **2007**, 251, 345.

175. J. S. Chen, A. N. Vasiliev, A. P. Panarello, J. G. Khinast, *Appl. Catal. A: General* **2007**, 325, 76.

176. J. P. Simeone, J. R. Sowa Jr., *Tetrahedron* **2007**, 63, 12646.

177. D. Zim, S. M. Nobre, A. L. Monteiro, *J. Mol. Catal. A: Chem*. **2008**, 287, 16.

178. K. Köhler, R. Heidenreich, S. S. Soomro, S. S. Pröckl, *Adv. Synth. Catal.* **2008**, 350, 2930.

179. I. P. Beletskaya, A. N. Kashin, I. A. Khotina, A. R. Khokhlov, *Synlett* **2008**, 10, 1547.

180. A. Gniewek, J. J. Ziółkowski, A. M. Trzeciak, M. Zawadzki, H. Grabowska, J. Wrzyszcz, *J. Catal*. **2008**, 254*,* 121.

181. J. Durand, E. Teuma, F. Malbosc, Y. Kihn, M. Gormez, *Catal. Commun*. **2008**, 9, 273.

182. D.-H. Lee, J.-H. Kim, B.-H Jun, H. Kang, J. Park, Y.-S. Lee, *Org. Lett*. **2008**, 10, 1609.

183. J. D. Webb, S. MacQuarrie, K. McEleney, C. M. Crudden, *J. Catal*. **2007**, 252, 97.

184. M. L. Kantam, M. Roy, S. Roy, B. Sreedhar, S. S. Madhavendra, B. M.Choudary, R. L. De *Tetrahedron* **2007**, 63, 8002.

185. M. R. Badger, G. D. Price *Annu. Rev. Plant Physiol. Plant Mol. Bio*. **1994**, 45, 369.

186. N. Miyaura, A. Suzuki *Chem. Rev.* **1995**, 95, 2457.

187. N. Miyaura, K. Yamada, A. Suzuki *Tetrahedron Lett.,* **1979**, 20, 3437.

188. N. Miyaura, and A. Suzuki *Chem. Commun.,* **1979**, 866.

189. J. H. Kirchhoff, M. R. Netherton, I. D. Hills, and G. C. Fu *J. Am. Chem. Soc.,* **2002**, 124, 13662.

190. A. Suzuki *Pure Appl. Chem.* **1991**, 63, 419.

191. A. Suzuki *J. Organometallic Chem*. **1999**, 576, 147.

192. I. Kostas, B. Steele, A, Terzis, S. Amosova, A. Martynov, and N. Makhaeva *Eur. J. Inorg. Chem.* **2006**, 2642.

193. J. E. Milne, S. L. Buchwald *J. Am. Chem. Soc.* **2004**, 126, 13028

194. C. M. Crudden, D. P. Allen *Coord. Chem. Rev.* **2004**, 248, 2247

195. H.M. Lee, J. Y. Zeng, C. H. Hu, M. T. Lee *Inorg. Chem*. **2004**, 43, 6822

196. R. Chincilla, C. Nájera, M. Yus *Chem. Rev.* **2004**, 104, 2667

197. N. T. S. Phan, M. Van Der Sluys, C. W. Jones *Adv. Synth. Catal.* **2006**, *348*, 609.

198. V. Farina *Adv. Synth. Catal*. **2004**, *346*, 1553.

199. F. Alonso, I. P. Beletskaya, M. Yus *Tetrahedron* **2005**, *61*, 11771.

200. K. Köhler, W. Kleist, S. S. Pröckl *Inorg. Chem*. **2007**, *46*, 1876.

201. A. F. Schmidt, A. Al Halaiqa V. V. Smirnov *Synlett* **2006**, *18*, 2861.

202. J. M. Richardson, C. W. Jones *Adv. Synth. Catal*. **2006**, *348*, 1207.

203. M. B. Thathagar, J. E. ten Elshof G. Rothenberg *Angew. Chem. Int. Ed*. **2006**, *45*, 2886.

204. S. L. Broadwater, D. T. McQuade *J. Org. Chem*. **2006**, *71*, 2131.

205. Y. Ji, S. Jain, R. J. Davis *J. Phys. Chem. B* **2005**, *109*, 17232.

206. A. Biffis, M. Zecca, M. Basato *Eur. J. Inorg. Chem*. **2001**, *5*, 1131

207. R. F. Heck, J. P. Nolley *Journal Organic Chemistry,* **1972**, *37*, 2320.

208. L. Kurti, B. Czako, Burlington *MA: Elsevier, Inc.* **2005**, 196.

209. A. F. Littke, G. C. Fu *Angew. Chem. Int. Ed.* **2002**, 41, 4176.

210. J. Gong, G. Liu, C. Du, Y. Zhu, Y. Wu *J. Organomet. Chem.* **2005**, 690, 3963.

211. C. Bianchini, G. Lenoble, W. Oberhauser, S. Parisel, F. Zanobini *Eur. J. Inorg. Chem.* **2005**, 125.

212. K. W. Anderson, S. L. Buchwald *Angew. Chem. Int. Ed.* **200**5, 44, 6173.

213. T. E. Barder, S. D. Walker, J. R. Martinelli, S. L. Bucchwald *J. Am. Chem. Soc.* **2005**, 127, 4685.

214. A. Schnyder, A. F. Indolese, M. Stunder, H.-U. Blaser *Angew. Chem. Int. Ed.* 2002, 41. 3668.

215. R. Imbos, A. J. Minnaard, B. L. Feringa *J. Am. Chem. Soc*. **2002**, 124, 184.

216. D. Morales-Morales, R. Redón, Y. Zheng, J. R. Dilworth *Inorg. Chem. Acta* **2002**, 328, 39.

217. I. Kondolff, H. Doucet, M. Santelli *Tetrahedron Lett*. **2003**, 44, 8487.

218. A. A. D. Tulloch, A. A. Danopoulos, R. P. Tooze, S. M. Cafferkey, S. Kleinhenz, M. B. Hursthouse *Chem. Commun.* **2000**, 1247.

219. E. Peris, J. A. Loch, J. Mata, R. H. Crabtree *Chem. Commun*. **2001**, 201.

220. C. Mazet, L. H. Gade *Eur. J. Inorg. Chem*. **2003**, 1161.

221. S. B. Park, H. Alper *Org. Lett.* **2003**, 5. 3209.

222. Q. Yao, E. P. Kinney, Z. Yang *J. Org. Chem*. **2003**, 68, 7528.

223. D. A. Alonso, C. Nájera, M. C. Pacheco *J. Org. Chem.* **2002**, 67, 5588.

224. C.-L. Chen, Y. -H. Liu, S.-M. Peng, S.-T. Liu *Tetrahedron Lett.* **2005**, 46, 521.

225. H. B. Kagan *L'actualité chimique* **2003**, 10.

226. W. S. Knowles, M. J. Sabacky *Chem. Commun.* **1968**, 1445.

227. H. Nozaki, H. Takaya, S. Moriuti, R. Noyori *Tetrahedron* **1968**, 24, 3655.

228. W. S. Knowles, M. J. Sabacky, B. D. Vineyard, D. J. Weinkauff *J. Am. Chem. Soc.* **1975**, *97*, 2567.

229. R. Noyori *Angew. Chem. Int. Ed.* **2002**, *41*, 2008.

230. K. B. Sharpless *Angew. Chem. Int. Ed.* **2002**, *41*, 2024.

231. G. J. Boons, K. J. Hale *Organic Synthesis with Carbohydrates*, **2000.**

232. M. M. K. Boysen *Chem. Eur. J.* **2007**, *13*, 8648.

233. M. Diéguez, O. Pámiez, C. Claver *Chem. Rev*. **2004**, 104, 3189

234. M. Beller, J. G. E. Krauter, A. Zapf *Angew. Chem. Int. Ed.* **1997**, 36, 772.

235. S. Parisot, R. Kolodziuk, C. Goux-Henry, A. Iourtchenko, D. Sinou *Tetrahedron Lett.* **2002**, 43, 7397.

236. R. Selke, M. Ohff, A. Riepe *Tetrahedron* **1996**, 52, 15079.

237. T. V. Rayanbabu, A. L. Casalnuovo *J. Am. Chem. Soc* **1992**, 114, 6265.

238. O. Pàmies, G. Net, A. Ruiz, C. Claver *Tetrahedron: Asymmetry* **1999**, 10, 2007

239. O. Pàmies, G. Net. A. Ruiz, C. Claver *Eur. J. Inorg. Chem.* **2000**, 1287;

240. P. Barbaro, A. Currao, J. Herrmann, R. Nesper, P. S. Pregosin, R. Salzmann *Organometallics* **1996**, 15, 1879.

241. M. Tschoerner, G. Trabesinger, A. Albinati, P. S. Pregosin *Organometallics* **1997**, 16, 3447.

242. K. Selvakumar, M. Valentini, P. S. Pregosin, A. Albinati *Organometallics* **1999**, 18, 4591.

243. P. Klüfers, T. Kunte *Angew. Chem.* **2001**, 113, 4356

244. M. L. Ferrara, I. Orabona, F. Ruffo, M. Funicello, A. Panunzi *Organometallics* **1998,** 17, 3832.

245. M. L. Ferrara, F. Giordano, I. Orabona, A. Panunzi, F. Ruffo *Eur. J. Inorg. Chem.***1999***,* 1939.

246. M. Beller, J. G. E. Krauter, A. Zapf, S. Bogdanovici *Catal. Today*. **1999**, 48, 279.

247. S. Kobayashi, W. W.-L. Lam, K. Manabe *Tetrahedron Lett.* **2000**, 41, 6115.

248. T. Hashizume, K. Yonehara, R. Ohe, S. Uemura *J. Org. Chem.,* **2000**, 65, 5197.

249. C. Rabeyrin, D. Sinou *Tetrahedron Lett.* **2000**, 41, 7461.

250. D. Sinou, C. Rabeyrin, C. Nguefack *Adv. Synth. Catal.* **2003**, 345, 357.

251. F.-P. van de Kamp, F. Micheel *Chem. Ber.* **1956**, 89, 133.

252. R. Bognár, L. Somogyi, L. Szilágyi, Z. Györgydeák *Carbohydr. Res.* **1967**, 5, 320.

253. M. Wójtowicz, C. Gmernicka-Haftek, W. Wieniawski. *Acta Pol. Pharm.* **1975**, 32, 49.

254. A. A. Tashpulatov, V. A. Afanas'ev, M. Y. Lidak, N. M. Sukhova, Y. Y. Popelis, I. Rakhmatullaev *Chem. Heterocycl. Compd.* **1983**, 137.

255. S.-S. Zhang, S.-J. Ye, X.-M. Li, S.-S. Gu, Q. Liu *Chem. Res. Chinese U.* **2005**, 21, 545.

256. A. A. Tashpulatov, V. A. Rakhmatullaev, N. Ismailov *Zh. Org. Khim.* **1988**, 24, 1893.

257. K. Cao, Z. Wang, X. Zhao *Jingxi Shiyou Huagong* **2003**, 42.

258. K. Cao, Z. Wang, X. Zhao *Shiyou Daxue Xuebao, Ziran Kexueban* **2004**, 28, 100.

259. H. S. Isbell, H. L. Frush *J. Org. Chem.* **1958**, 21, 1309.

260. L. M. Likhosherstov, O. S. Novikova, and V. N. Shibaev, *Doklady Chemistry* **2002**, 383, 89-92.

261. O. López, I. Maya, J. Fuentes, and J. G. Fernández-Balaños *Tetrahedron* **2004**, 60, 61-72.

262. J.-L. Montero, J.-Y. Winum, A. Leydet, M. Kamal, A. A. Pavia, J.-P. Roque *Carbohydr. Res.* **1997**, 297, 175.

263. S. Koto, N. Morishima, T. Irisawa, Y. Hashimoto, M. Yamazaki *S. Zen Nippon Kakagaku Kaishi* **1982**, 1615.

264. M. Hunsen, D. A. Long, C. R. D'Ardenne, A. L. Smith *Carbohydr. Res*. **2005**, 340, 2670.

265. P. G. Scheurer, F. Smith *J. Am. Chem. Soc.* **1954**, 76, 3224.

266. F. Catani, P. Boniveto,G. Procida, M. Zacchigna, L. G. Favretto, G. Scilino, E. Banfi *Bioorg. and Med. Chem.* **2007**, 15, 815.

267. M. Schönherr*, Dissertation thesis, Chemie und Pharmazie der Universität Regensburg* **2002**.

268. T. K. Lindhorst, C. Kieburg *Synthesis* **1995**, 1228.

269. B. Young , S.-S. Zhang, H. X. Li, J. Z. Li, K. Jiao *Chem. Res. Chinese. U***. 2005**, 21, 457.

270. A. A. Tashpulatov, V. A. Afanasev, M. Y. Lidak, N. M. Sukhova, Y. Y. Popelis, I. Rakhmatullaev *Chem. Heterocycl. Comp.* **1983**, 137.

271. R. P. John, A. Sreekanth, M. R. P. Kurup, H.-K. Fun *Polyhedron* **2005**, 24, 601.

272. S. A. Khan, M. Yusuf *European J. Med. Chem.* **2009**, 44, 2270.

273. J. M. Vila, T. Pereira, A. Amoedo, M. Granã, J. Martínez, M. López-Torres, A. Fernández *J. Organometalic Chem*., **2001**, 623, 176.

274. A. Pérez-Rebolledo, I. C. Mendes, N. L. Speziali, P. Bertani, J. M. Resende, A. F. de Carvalho Alcântara, H. Beraldo *Polyhedron* **2007**, 26, 1449.

275. M. J. M. Campbell *Coord. Chem. Rev.* **1975**, 15, 279.

276. P. Bindu, M. R. P. Kurup, T. R. Satyakeerty *Polyhedron,* **1999**, 18, 321.

277. E. Bermejo, A. Casteneiras, R. Dominguez, R. Carballo, C. M.-Mossmer, J. Strahle, D. X. West *Z. Anorg. Allg. Chem.* **1999,** 625, 961**.**

278. H. Booth *Tetrahedron Lett.* **1965**, 411.

279. P. R. Ashton, V. Balzani, M. Clemente-León, B. Colonna, A. Credi, N. Jayaraman, F. M. Raymo, J. F. Stoddart, M. Venturi *Chem. Eur. J.* **2002**, 8, 673.

280. J.R. Dimmock, S. S. Jonnalagadda, S. Husein, S. Tewari, J. W. Quail, R. S. Reid, L. T. J. Delbaere, L. Prasad *Eur. J. Med. Chem*. **1990**, 25, 581.

281. D. X. West, J. S. Ives, J. Krejci, M. M. Salberg, T. L. Zumbahlen, G. A. Bain, A. E. Liberta *Polyhedron* **1995**, 14, 2189.

282. P. Pelagatti, A. Venturini, A. Leporati, M. Carcelli, A. Bacchi, G. Pelizzi, C. Pelizzi *J. Chem Soc. Dalton Trans.* **1998**, 2715.

283. J. Martínez, L. A. Adrio, J. M. Antelo, J. M. Ortigueria, M. T. Pereira, J. J. Fernández, A. Fernández, J. M. Vila *J. Organomet. Chem.* **2006**, 691, 2721.

284. A. E. Graminha, A. A. Batista, I. C. Mendez, L. R. Teixeira, H. Beraldo *Spectrochimica Acta, Part A* **2008**, 69, 1277.

285. K. Linek, J. Alföldi, Š. Kučár, T. Sticzay, Z. Novotaná *Carbohydr. Res.* **1983**, 115, 259.

286. L. Szilágyi, Z. Györgydeák, H. Duddeck *Crabohydr. Res.* **1986**, 158, 67.

287. I. Antonini, F. Claudi, P. Franchetti, M. Gnifantini, S. Marteli *J. Med. Chem.* **1977**, 20, 447.

288. J. Easmon, G. Heimisch, W. Holzer *Heterocycles* **1989**, 29, 1399.

289. D. Sriram, H. Sreenivasan, S. Srinivasan, K. Priya, M. V. Thirtha, D. Loganathan *Acta Crystallogr., Sect.* ***C*** **1997**, 53, 1075.

290. F. H. Allen, O. Kennard, D. G. Waston, L. Brammer, A. G. Orpen, R. Taylor *J. Chimie. Soc., Perkin Trans.2* **1987**, S1−S19.

291. L. Brammer, F. H. Allen, O. Kennard, D. G. Waston, R. Taylor *J. Chem. Soc., Dalton Trans.* **1980**, S1−S83.R.D.

292. **A.-C. Tenchiu (Deleanu)**, I. D. Kostas, D. Kovala-Demertzi, A. Terzis *Carbohydr. Res.* **2009**, 344, 1352.

293. K.-M. Alexacou, **A.-C. Tenchiu (Deleanu)**, E. D. Chrysina, M.-D. Charavgi, I. D. Kostas, S. E. Zographos, N. G. Oikonomakos, D. D. Leonida *Bioorg. Med. Chem.* **2010**, 18, 7911.

294. H. Beraldo, D. Gambino *Mini Rev Med Chem* **2004**, 4, 31.

295. M. Belicchi-Ferrari, F. Bisceglie, C. Casoli, S. Durot, I. Morgenstern-Badarau, G. Pelosi, E. Pilotti, S. Pinelli, P. Tarasconi *J Med Chem* **2005**, 48, 1671.

296. D. Kovala-Demertzi, A. Papageorgiou, L. Papathanasis, A. Alexandratos, P. Dalezis, J. R. Miller, M. A. Demertzis *Eur. J. Med. Chem.* **2009**, 44, 1296.

297. D. Kovala-Demertzi, P. N. Yadav, J. Wiecek, S. Skoulika, T. Varadinova, M. A. Demertzis *J. Inorg. Biochem.* **2006**, 100, 1558.

298. L. Somsak, K. Czifrak, M. Toth, E. Bokor, E. D. Chrysina, K. M. Alexacou, J. M. Hayes, C. Tiraidis, E. Lazoura, D. D. Leonidas, S. E. Zographos, N. G. Oikonomakos *Curr. Med. Chem.* **2008**, 15, 2933.

299. M. OReilly, K. A. Watson, R. Schinzel, D. Palm, L. N. Johnson *Struct. Biol.* **1997**, 4, 405.

300. K. A. Watson, R. Schinzel, D. Palm, L. N. Johnson *EMBO J*. **1997**, 16, 1.

301. D. Barford, L. N. Johnson *Nature* **1989**, 340, 609.

302. K. M. Alexacou, J. M. Hayes, C. Tiraidis, S. E. Zographos, D. D. Leonida, E. D. Chrysina, G. Archontis, N. G. Oikonomakos, J. V. Paul, B. Varghese, D. Loganathan *Protein* **2008**, 71, 1307.

303. J. A. K. Howard, V. J. Hoy, D. Ohagan, G. T. Smith *Tetrahedron* **1996**, 52, 12613.

304. V. G. Tsirkone, E. Tsoukala, C. Lamprakis, S. Manta, J. M. Hayes, S. T. Skamnaki, C. Drakou, S. E. Zographos, D. Komiotis, D. D. Leonida *Bioorg. Med. Chem.* **2010**, 18, 3414.

305. P. Auffinger, F. A. Hays, E. Westhof, P. S. Ho *Proc. Natl. Acad. Sci. U.S.A*. **2004**, 101, 16789.

306. P. Politzer, P. Lane, M. C. Concha, Y. G. Ma, J. S. J. Murray *Mol. Model.* **2007**, 13, 305.

307. T. S. Lobana, S. Khanna, R. J. Butcher *Inorg. Chem. Comm* **2008**, 11, 972.

308. J. K. Swearingen, D. X. West *Transition Met. Chem.* **2001**, 26, 252.

309. J. L. Garcia-Trojal, A. Pizarro, A. R. Garcia-Orad, M. Perez-Sanz, A. A. Ugalde, J. L. Diaz, M. I. Serra, T. Arriortura, J. Rojo *J. Inorg. Biochem*. **2001**, 86, 627.

310. R. Alonso, E. Bermejo, A. Castineiras, T. Perez, R. Carballo *Z. Anorg. Allg. Chem.* **1997**, 623, 818.

311. R. Alonso, E. Bermejo, R. Carballo, A. Castineiras, T. Perez Z. Natureforsch *B. Chem. Sci.* **2001**, 56, 219.

312. L. J. Baucher *J. Ionrg. Nucl. Chem.* **1974**, 36, 531.

313. J. Uttamachanadani, R. K. Kapoor *Trans. Met. Chem.* **1978**, 3, 79.

314. F. M. Iskander, M. A.E. Shaban, S. M. El-Badry *Carbohydr. Res.***2003**, 338, 2341.

315. N. Dharmaraj, P. Viswanathamurthi, K. Natarajan *Trans. Met. Chem.* **2001**, 26, 105.

316. M. B. Ferrari, S. Cappacchi, F. Bisceglie, G. Pelosi, P. Tarasconi *Inorg. Chem. Acta* **2001**, 302, 81.

317. D. X. West, A. M. Stark, G. Bain, A. E. Liberta *Trans. Met. Chem.* **1996**, 21, 289.

318. D. Kovala-Demertsi, A. Domopoulou, A. Demertzis, J. Valdez-Martines, S. Hernandez-Ortega, G. Espinosa-Perez, D. X. West, M. Salberg, G. Bain, P. D. Bloom *Polyhedron* **1996**, 15, 2587.

319. R. L. de Lima, L. R. de Souza Teixeira, T. M. G. Carneiro, H. Beraldo *J. Braz. Chem. Soc.* **1999**, 10, 184.

320. E. M. Beccalli, G. Broggini, M. Martinelli, S. Sottocornola *Chem. Rev.* **2007**, 107, 5318.

321. Y-P. Tian, W-T. Yu, C-Y. Zhao, M-H. Jiang, Z-G. Cal, H.- K. Fun *Polyhedron* **2002**, 21, 1217.

322. B. Neelam,M. Mannar, N. Fehmida, B. Alok, B. Sudha, A. Amir *E. J. Med. Chem.* **2004**, 39, 459.

323. A. Sreekanth, H.-K. Fun, M. R. P. Kurup *J. Mol. Struct.* **2005**, 737, 61.

324. D. X. West, A. C.Whyte, F. D. Sharif, H. Gebremedhin, A. E. Liberta *Transition Met. Chem.* **1993**, 18, 238.

325. B. S. Garg, M. R. P. Kurup, S. K. Jain, Y. K. Bhoon *Transition Met. Chem.* **1991**, 16, 111.

326. D. Kovala-Demertzi, A. Domopoulou, M. Demertzis *Polyhedron* **1994**, 13, 1917.

327. P. Sinya *Spectrochim. Acta* **1964**, 20, 879.

328. R. P. John, A. Sreekanth, M. R. P. Kurup, A. Usman, I. A. Razak, H.-K. Fun *Spectrochimica Acta* **2003**, 59A, 1349.

329. M. Joseph, V. Suni, M. R. P. Kurup, M. Nethaji, A. Kishore, S. G. Bhat *Polyhedron* **2004**, 23, 3029.

330. R. P. John, A. Sreekanth, M. R. P. Kurup, S. M. Mobin *Polyhedron* **2002**, 21, 2515.

331. A. Sreekanth, H.-K. Fun, M. R. P. Kurup *J. Mol. Struct.* **2005**, 737, 61.

332. I. D. Kostas, A. G. Coutsolelos, G. Charalambidis, A. Skondra *Tetrahedron Let.* **2007**, 48, 6688.

333. I. D. Kostas, B. R. Steele, A. Terzis, S. V. Amosova *Tetrahedron* **2003**, 59, 3467.

334. I. D. Kostas, B. R. Steele, F. J. Andreadaki, V. A. Potapov *Inorg. Chim. Acta* **2004**, 357, 2850.

335. I. D. Kostas, K. A. Vallianatou, P. Kyritsis, J. Zedník, J. Vohlídal *Inorg. Chim. Acta* **2004**, 357, 3084.

336. K. A. Vallianatou, I. D. Kostas, J. Holz, A. Börner *Tetrahedron Lett.* **2006**, 47, 7947.

337. I. D. Kostas, K. A. Vallianatou, J. Holz, A. Börner *Tetrahedron Lett.* **2008**, 49, 331.

338. M. an der Heiden, H. Plenio *Chem. Eur. J.* **2004**, *10*, 1789.

339. I.D. Kostas *J. Organomet. Chem.* **2001**, *626*, 221.

340. I.D. Kostas *J. Organomet. Chem.* **2001**, *634*, 90.

341. I.D. Kostas *Curr. Org. Synth.* **2008**, *5*(3), 227-249.

342. I.D. Kostas "Other P/N-Ligands" (Chiral Bidentate Monophosphorus Ligands: Hybrid Monophosphorus Ligands – Bidentate P/NR2 Ligands – Other P/N-Ligands). In *Phosphorus Ligands in Asymmetric Catalysis – Synthesis and Applications*, A. Börner (Ed.), Wiley-VCH, Weinheim, **2008**, Vol. 2, part IV, chapter 1.2, pp. 596-632.

343. Rigaku/MSC CRYSTALCLEAR; Rigaku/MSC: The Woodlands, TX, USA, **2005**.

344. G. M. Sheldrick, SHELS-97: *Structure Solving Program*; University of Grötingen: Grötingen, germany, **1997**.

345. G. M. Sheldrick, SHELXS-97: Crystal Structure Refinement; University of Grötingen: Grötingen, germany, **1997**.

346. M. Belicchi-Ferrari, F. Bisceglie, G. Pelosi, S. Pinelli, P. Tarasconi *Polyhedron* **2007**, 26, 5150.

347. A. E. Melpidou, N. G. Oikonomakos *FEBS Lett.* **1983,** *154*, 105.

348. S. Saheki, A. Takeda, T. Shimazu *Anal. Biochem.* **1985,** *148*, 277.

349. N. G. Oikonomakos, A. E. Melipidou, L. N. Johnson *Biochim. Biophys. Acta* **1985**, 832, 248.

350. Z. Z. Otwinowski, W. *Minor Methods Enzymol*; C. W. J. Carter, R. M. Sweet, Eds.; Academic Press: New York **1997**, 276, 307.

351. G. N. Murshudov, A. A. Vagin, E. J. Dodson *Acta Crystallogr*. **1997**, D53, 240.

352. R. A. Laskowski, M. W. MacArthur, D. S. Moss, J. M. Thornton *J. Appl. Crystallog*. **1993**, 26, 283.

353. CCP4. *Acta Crystallog*. **1994**, D50, 760.

354. P. J. Kraulis *J. Appl.Crystallog*. **1991**, 24, 946.

355. R. M. Esnouf *J. Mol. Graphics and Model*. **1997**, 15, 132.

356. E. A. Merritt, D. J. Bacon *Macromol. Crystallog*. **1997**, B277, 505.